Plastid Terminal oxidase (PTOX) and its physiological roles in carotenoid biosynthesis and in response eo stress in tomato

Maryam Shahbazi

UNIVERSITE JOSEPH FOURIER
SCIENCES TECHNOLOGIE MEDECINE

Ecole Doctorale Chimie et Science du Vivant

THÈSE

pour obtenir le grade de **DOCTEUR DE L'UNIVERSITE JOSEPH FOURIER**

Spécialité : *Biologie Végétale*

L'oxydase terminale plastidiale (PTOX) et ses fonctions physiologiques dans la biosynthèse des caroténoïdes et dans la réponse au stress chez la tomate

Présentée et soutenue publiquement par :

Maryam SHAHBAZI

Le 16 juin 2008

Composition de jury :

Pierre Carol	Professeur, Université Pierre et Marie Curie, Paris	Rapporteur
Dominique Rumeau	Chargée de Recherche CNRS, Cadarache	Rapporteur
Norbert Rolland	Directeur de Recherche CNRS, Grenoble	Président
Marcel Kuntz	Directeur de recherche CNRS, Grenoble	Directeur de thèse

Laboratoire Plastes et Différenciation Cellulaire
Unité Mixte de Recherche UJF- CNRS 5575

A mon mari Hamid,
à mes fils Ahmad et Behzad,
et à tous ceux que je
porte dans mon coeur

Il n'y a pas de

plus belle pensée que celle

que l'on fait partager

Remerciements

Je tiens tout d'abord à exprimer ma reconnaissance à Madame Dominique Rumeau et Monsieur Pierre Carol pour avoir accepté de prendre de leur temps pour juger mon travail et d'être les rapporteurs de mon travail. Je tiens à remercier également Monsieur Norbert Rolland qui m'a fait l'honneur de présider ce jury.

Je remercie tout particulièrement et sincèrement mon directeur de thèse, Monsieur Marcel Kuntz pour son soutien, son apport scientifique, sa disponibilité, sa patience et aussi pour m'avoir fait confiance tout au long de ces années.

Je tiens ensuite à remercier Monsieur Michel Herzog, directeur du Laboratoire, qui m'a accueilli au Laboratoire Plastes et Différenciation cellulaire.

Un grand merci à notre équipe, Eliane Charpentier, pour son aide régulière, Joël Gaffé qui m'a guidée et aidée notamment lors des premières manips au CERMO, et Stéphane Labroux pour son aide et ses conseils. Mention particulière pour Anne-Marie Labouré pour toute son humanité, sa chaleur et ses compétences, et pour Jean-Pierre Alcaraz pour sa bonne humeur et son expérience, et à tous les deux pour leur présence à nos côtés qui chaque jour contribue largement à ce que la journée soit agréable, même dans les pires moments.

Je remercie également l'ensemble des membres du laboratoire encore présents ou partis, pour leur sympathie et leur attitude, je pense notamment à Livia, Gabrielle, Florence, Régis, Christiane, Frank, Yec'han, Jacinthe, Jean Jacques, Emilie, Abder et Jean Marc. Encore à Livia et Florence, je voudrais adresser mes sincères remerciements, pour leurs conseils et tout ce que j'ai appris grâce à elles. Je remercie tous les thésards et étudiants, et en particulier Abir, Wafa, Hannane, Iga, Mohamed, Moustafa, Sumaira, Claudia, Edouard et Florian pour la bonne ambiance au travail. Un grand merci à France pour sa disponibilité et sa gentillesse dès les premiers jours de mon travail au CERMO et jusqu'à maintenant.

Merci à Monsieur Philippe Choler, à Monsieur Serge Aubert et à Florence Baptist, pour leur gentillesse et leurs conseils. Je témoigne également ici ma reconnaissance et un grand merci à Monsieur Mathias Gilbert pour son aimable collaboration et pour nos discussions scientifiques.

J'exprime toute ma gratitude à Gaynor pour ses corrections anglaises et ses suggestions pour ce mémoire.

Je souhaiterais également remercier, très chaleureusement, mes amis, notamment Shokooh, Bahar, Shadi, Parvin, Arezou, Atefeh, Roya, Nazi, Mohsen, Mohammad, ainsi que Carole, Christian et Patrik pour leur amitié et leur soutien si important pendant ces années. Je remercie tous les autres que je ne peux pas citer, mais ils sont tous dans mes pensées.

Je finis en remerciant les personnes qui ont certainement le plus contribué à ce travail et qui m'ont permis d'en arriver là, en particulier mon mari, Hamid, je le remercie d'être à mes côtés pour tant de choses que je ne peux pas énumérer ici, et mes fils, Ahmad et Behzad, pour leur patience et leur joie de vivre, ainsi que ma chère famille en Iran, ma mère, mon père, mes soeurs et mes frères pour m'avoir encouragée en particulier durant toutes ces années.

Contents

List of Tables

List of Figures

Abbreviations

A	antheraxanthin
AA	antimycin A
AL	actinic light
AOX	mitochondrial alternative oxidase
APX	ascorbate peroxydase
At	*Arabidopsis thaliana*
ATP	adenosine 5'-triphosphate
BN	blue native gel electrophoresis
bp	base pairs
BSA	bovine serum albumin
cDNA	complementary DNA
CET	cyclic electron transfer
Chl	chlorophyll
Cyt	cytochrome
DCMU	dichlorophenyl dimethylurea
DM	dedecyl maltoside
DMSO	dimethyl sulfoxide
DNase	deoxyribonuclease I
DNA	deoxyribonucleic acid
DPB	days post breaker
DPI	diphenyleneiodonium
EDTA	ethylenediamine tetraacetic acid
ELIP	early light-inducible proteins
$\mathbf{F}_0$	dark initial fluorescence
Fd	ferredoxin
$\mathbf{F}_m$	maximum fluorescence
FNR	Fd-NAD^+ oxydoreductase
FQR	Fd-plastoquinone oxydoreductase
$\mathbf{F}_v$	variable fluorescence
$\mathbf{F}_s$	steady-state fluorescence
gh	*ghost*
Hepes	N-(2-hydroxyethyl)piperazine N'-(2-ethanesulfonic acid)
HPLC	high pressure liquid chromatography
HTL	high temperature thermoluminescence
im	*immutans*
IPTG	isopropyl thio-b-D-galactoside
KCN	potassium cyanide
kDa	kilo Dalton
LHC	light harvesting complex
MDA	malondialdehyde
ML	measuring light
MOPS	4-morpholinopropansulfonacid

ms	miliseconds
MT	tomato dwarf MicroTom type
NADH	nicotinamide-adenine dinucleotide
NADH-dH	NADH deshydrogenase
NADPH	nicotinamide-adenosine di nucleotidephosphate
NDH complex	NAD(P)H-plastoquinone oxydoreductase complex
NPQ	nonphotochemical quenching
OD	optical density
OEC	oxygen-evolving complex
OG	n-octyl gallate
PC	plastocyanin
PCR	polymerase chain reaction
PDS	phytoene desaturase
PGR5	proton gradient regulation
Pheo	pheophytine of PSII
PI	photoinhibition
PMSF	phenylmethylsulfonyl fluoride
PQ	plastoquinone
PSI	photosystem I
PSII	photosystem II
PTOX	plastid terminal oxidase or *immutans*
QA/QB	quinons sites of PSII
qE	pH-dependant quenching
qP	photochemical quenching
RC	reaction center
ROS	reactive oxygen species
RNA	ribonucleic acid
RNase	ribonuclease
PFD	photon flux densities
SDS	sodium dodecylsulfate
SDS-PAGE	SDS polyacrylamide gelelectrophoresis
SM	San Marzano
SOD	superoxyde dismutase
TBE	Tris-borate-EDTA buffer
TBS	Tris buffered saline
TE	Tris-EDTA buffer
TL	thermoluminescence
Tris	tris (hydroxymethyl) aminomethane
Tween 20	polyoxyethylensorbitanmonolaurat
V	violaxanthine
WWC	water-water cycle
ZDS	ζ-carotene desaturase

Chapter 1

Introduction

Our laboratory is interested in molecular and cellular mechanisms involved in plastid differenciation with particular emphasis on chromoplasts, and carotenoid biosynthesis, especially under stress conditions. As a part of this general project, a nucleus-encoded plastid-localized terminal oxidase (PTOX) was characterized. This enzyme participates in the carotenoid desaturation steps as a redox component. As PTOX appears to play a more global role in plastid metabolism (as a plastoquinol oxidase in chlororespiration), and also functions as a light stress protein, we decided to study the different roles of PTOX which have in common the modulation of plastoquinone redox states.

Therefore, prior to presenting and discussing the results, some basic information about plastids, carotenoid biosynthesis, linear and non-linear photosynthetic electron transfer fluxes, a number of protective mechanisms for photosynthetic apparatus, and finally identification of PTOX are introduced.

1.1 Plastids

1.1.1 Origin of plastids

Plastids are major organelles found only in plant and algal cells. According to the endosymbiotic theory, chloroplasts were derived from an endosymbiosis between a eucaryote cell and a primitive cyanobacterium (review by Gray, 1992; Reyes-Prieto *et al.*, 2007; Deschamps *et al.*, 2008). This organelle is genetically semi-autonomous. It contains its own genome of around 120 to 160 kbp called "plastome" whose size is species-dependent. This conserved plastid genome is required for the synthesis of a few plastid proteins (Peltier *et al.*, 2002; Kleffmann *et al.*, 2006). During evolution, a large part of the cyanobacterial genome has been transferred to the nucleus and most of the plastid protein are encoded by the nucleus. Hence, plastids were converted to an organelle in host cells, keeping some of its ancestral characters, whilst also acquiring certain new properties (Martin *et al.*, 2002). Plastids are surrounded by a double membrane, the internal envelope being directly inherited from the endosymbiont and the external membrane being of a mixed origin, indicating a co-evolution of the host cell and its endosymbiont (Cavalier-Smith, 2000). Plastids reproduce solely by division, independently of cell division (review in Aldridge *et al.*, 2005).

Although they contain similar genetic information, plastids vary in size, shape, content, internal structure and function. These characteristics are influenced by cellular development and external conditions. Plastids are responsible for photosynthesis, for the storage of certain products including starch, as well as carrying out a wide variety of metabolic processes such as biosynthesis of chlorophylls, carotenoids, fatty acids, amino acids, vitamines and secondary metabolites. Plastids also participate in the assimilation of some inorganic nutrients (nitrate and sulfate). The different plastid types identifying by their size, their developmental stages or their fonctions are presented here.

1.1.2 Plastid classification

Proplastids represent an undifferentiated form of plastids, the precursors of all types of plastids, located in meristematic regions. In proplastids, the internal membrane system remains poorly developed (Thomson and Whatley, 1980).

Amyloplasts are non-pigmented and starch-storing plastids, commonly found in storage organs such as root tubers. They are similar to proplastids but contain starch granules. In root tips, amyloplasts serve also as statoliths for the gravity-sensing apparatus (Morita and Tasaka, 2004).

Oleoplasts are plastids which are transitory and synthesize and accumulate fatty acids and lipids from pyruvate imported from the cytosol (Eastmond and Rawsthorne, 2000).

Leucoplasts are colorless plastids which are involved in the synthesis of volatile compounds, such as monoterpenes which are constituants of essential oils. Their synthesis is carried out by specialized secretory gland cells associated specifically with leaf and stem trichomes (Cheniclet and Carde, 1988). Leucoplasts can also be found in floral organs.

Etioplasts are plastids of etiolated plants whose development from proplastids to chloroplasts has been arrested by the absence of light. Etioplasts lack chlorophyll, but produce a large amount of the colorless chlorophyll precursor, proto-chlorophyllide. They contain membrane lipids in a typical prominent form, the quasicrystalline membranous structure called the prolamellar body which, in addition, contains carotenoids and different components (Reinbothe *et al.*, 1999), and which can rapidly differentiate into thylakoids upon exposure to light.

Chloroplasts are green photosynthetic plastids found in leaf, stem and green fruits, which are responsible for light energy capture and its transformation into chemical energy. The conversion of proplastids to chloroplasts is accompanied by high transcription levels of plastid and

nuclear-encoded genes involved in the transcription/translation apparatus. Chloroplasts are surrounded by a double-membrane system consisting of an outer and inner envelope. They also contain a complex internal membrane system, known as the thylakoid membrane and which contains distinct regions. Some thylakoid segments (granal thylakoids) are organized in grana, stacks of appressed membranes; whereas others (stromal thylakoids) are unstacked and thus are exposed to the surrounding fluid medium, the stroma (Fig. 1.1). The thylakoid membranes contain lipids and carotenoids associated with chlorophylls and reaction center proteins (reviewed by Vothknecht and Westhoff, 2001). Screening for *Arabidopsis* photosynthetic pigment mutants has confirmed the importance of carotenoids in chloroplast development (Gutierrez-Nava *et al.*, 2004). Thylakoids are all interconnected and enclose an internal space, the lumen (Fig. 1.1). In higher plants, chlorophyll biosynthesis (conversion of protochlorophyllides to chlorophylls) and chlorophyll-protein complex formation are light-dependent. In higher plants and algae, chloroplasts contain starch granules and small plastoglobules. Chloroplasts also participate in the biosynthesis of amino acids and fatty acids.

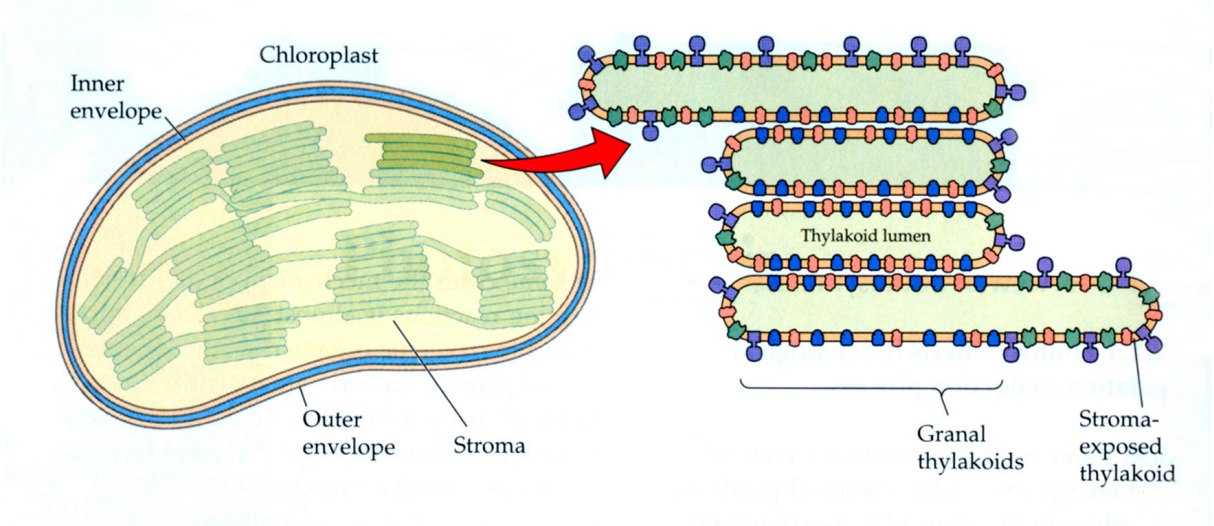

FIGURE 1.1 – **Schematic diagram of plant chloroplast, showing compartmentation of the organelle. In a typical plant chloroplast, the internal membranes (thylakoids) include stacked membrane regions (granal thylakoids), and unstacked membrane regions (stromal thylakoid, adapted from Buchanan *et al.*, 2000).**

Chloroplasts contain large amounts of DNA, RNA and plastid ribosomes. In Cyanobacteria, more than thousand proteins of chloroplast and in higher plants only around 100 proteins are encoded by the plastidial genome (Schmitz-Linneweber *et al.*, 2001). The nuclear-encoded proteins of chloroplast are synthesized in the cytoplasm as immature forms containing transit

peptides necessary for their import into chloroplasts. During protein import, the mature forms of proteins are obtained by cleavage of the transit peptide. The proteomic analysis or informatic estimation has shown that around 2000 nuclear-encoded proteins are imported into chloroplasts (Peltier *et al.*, 2002; Kleffmann *et al.*, 2006).

Plastids have morphological plasticity and possess a remarkable capacity to differentiate, de-differentiate, and re-differentiate. For example, chloroplasts in green fruits lose gradually their photosynthetic properties due to certain metabolic changes during fruit ripening and they re-differentiate into **chromoplasts** (Camara *et al.*, 1995). Chromoplasts are responsible for the color of many fruits, flowers and some roots. Chromoplast development is accompanied by activation or accumulation of enzymes that catalyze carotenoid biosynthesis. Chromoplasts frequently contain many plastoglobules, often of large size, which serve for lipid storage during thylakoid disorganization (Kessler *et al.*, 1999). In some red fruits and in certain mutants of sweet pepper lacking chloroplasts at all developmental stages, chromoplasts can be directly formed from proplastids or amyloplasts. Based on the internal structures visualized by electron microscopy, chromoplasts are classified as globular, membranous, crystalline or fibrillar (Camara *et al.*, 1995). These structures are considered as storage structures for the accumulating carotenoids.

1.1.3 Carotenoids

1.1.3.1 Carotenoids and their roles

Carotenoids are the most abundant pigments in nature and more than 700 different carotenoids and geometrical isomers have been identified in plants, algae, fungi and certain bacteria (EFSA FEEDAP Panel, 2005). Plant carotenoids accumulate in plastids and play a fundamental role in photosynthesis as accessory pigments and in the xanthophyll cycle, where they prevent photo-oxidative damage. They accumulate in chromoplasts in senescent or stressed leaves, in flowers and fruits, making these organs attractive to insects and other animals, thus facilitating pollination and seed dispersal.

In addition to their color properties, 50 carotenoids are also known to have provitamin A activity and are fundamental for animals (including humans), which cannot synthesize this vitamin. β-carotene, in particular, has the greatest provitamin A activity. Lycopene has been shown to possess a strong antioxidant action, while lutein and zeaxanthin are deposited in the eyes

and protect retinal cells of the macula against "phototoxic" damage caused by short-wavelength high-energy light radiation (Finley, 2005).

Since carotenoids are very important for plants and animals, it has been attempted to enhance carotenoid levels in crop plants. Some examples of genetically modified crops with altered carotenoid levels, *e.g.* tomato, canola and rice, are given in Fraser and Bramley (2004).

1.1.3.2 Biosynthesis of carotenoids

Carotenoids belong to the isoprenoid family which has extraordinary diversity *e.g.*, monoterpenes such as menthol or rubber. The carotenoid branch of the isoprenoid metabolism is synthesized within plastids. The basic chemical structure consists of eight isoprenoid units joined end to end to form a C_{40} hydrocarbon skeleton that includes a system of conjugated double bonds (the chromophore) and linear or cyclic end groups. These characteristics account for their physical, chemical and biological properties. Carotenoids are divided into two groups: carotenes (containing only carbon and hydrogen atoms) and xanthophylls (containing oxygen atoms in various chemical forms; keto, hydroxyl, epoxy, *etc.*). The biosynthesis of carotenoids and xanthophylls is summarized in figure 1.2 and is reviewed by Fraser and Bramley (2004).

The five carbon building blocks that serve as precursors for all isoprenoids, namely isopentenyl diphosphate (IPP) and dimethylallyl diphosphate (DMAPP), are produced by two pathways: from acetyl-CoA by the mevalonate (MVA) pathway in the cytosol/endoplasmic reticulum (Bach *et al.*, 1999), or by the methylerythritol (MEP) pathway which occurs in plant plastids (Rohmer *et al.*, 1996; Rodriguez-Concepcion and Boronat, 2002).

For the synthesis of carotenoids, the MEP pathway is used. The C_5 building blocks, (IPP and DMAPP) via a C_{20} intermediate, geranylgeranyl diphosphate (GGPP) (Kuntz *et al.*, 1992), generate phytoene, a C_{40} acyclic precursor and the first and non-colored carotenoid (Bramley *et al.*, 1992; Romer *et al.*, 1993). The enzymes IPP isomerase, GGPP synthase and phytoene synthase (PSY) are soluble and localized in the stroma (Sandmann, 1994). The condensation of two molecules of GGPP to phytoene by phytoene synthase is the first specific step of the carotenoid biosynthesis pathway.

Phytoene is subjected to successive desaturation (dehydrogenation) reactions catalyzed by phytoene desaturase (PDS, Bartley *et al.*, 1992) and then by ζ-carotene desaturase (ZDS, Albrecht *et al.*, 1995), which lead to the formation of lycopene (Cunningham and Gantt, 1998). Phytofluene, ζ-carotene (the first colored carotenoid), and neurosporene are intermediates in

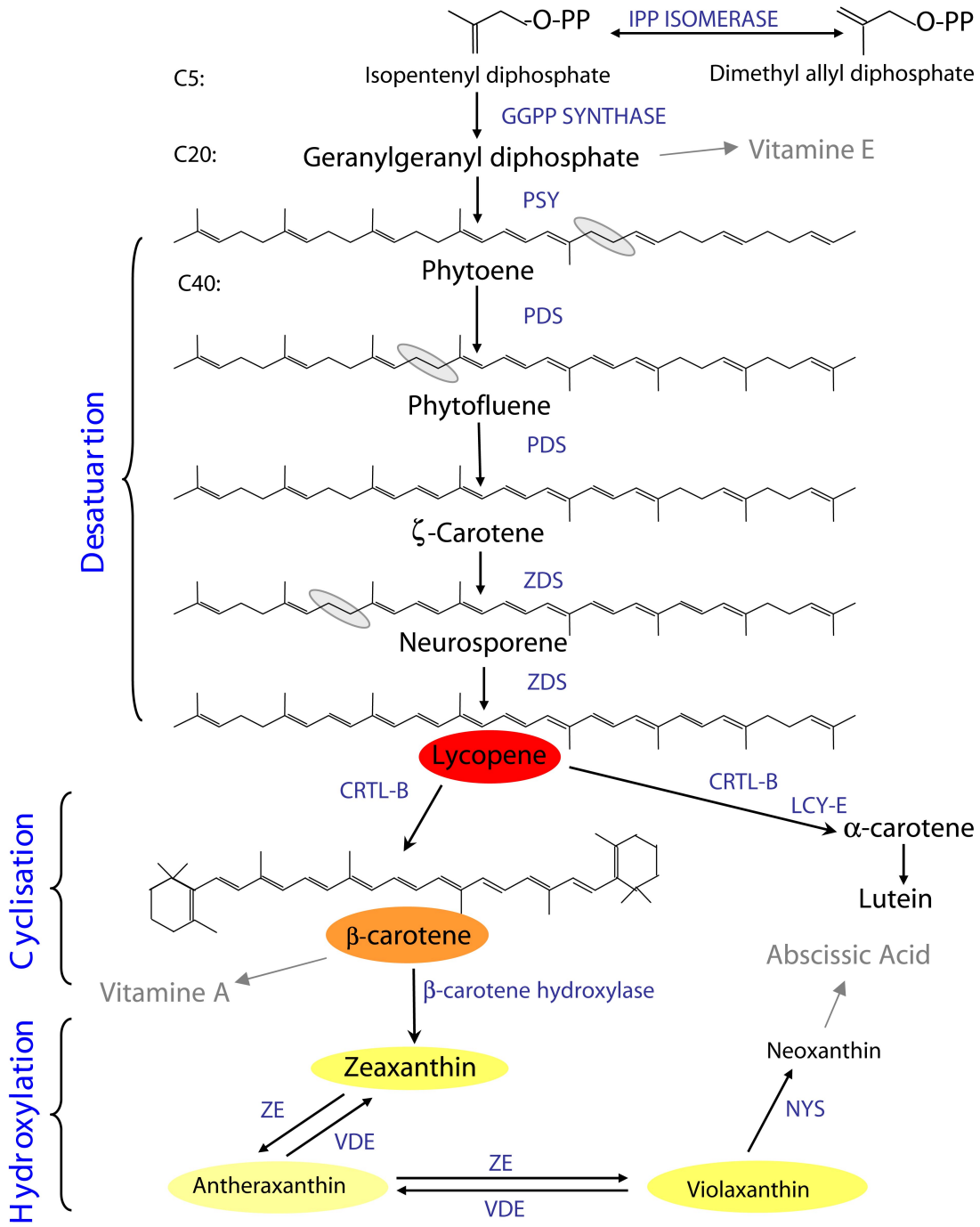

FIGURE 1.2 – **Biosynthesis of carotenoids in plants. The pathway for conversion of geranyl diphosphate to phytoene, followed by desaturation, cyclisation (on both ends of the chain), and finally hydroxylation steps to generate xanthophylls. PSY, phytoene synthase; PDS, phytoene desaturase ; ZDS, ζ carotène desaturase; CRTL-B, lycopene β-cyclase; LCY-E, lycopene epsilon-cyclase; ZE: zeaxanthin epoxidase; VDE, violaxanthin de-epoxidase; NYS, neoxanthin synthase (adapted from Simkin, 2002).**

these reactions. These reactions require flavine adenine dinucleotide (FAD) and oxidized quinones. The removal of two hydrogen atoms during each desaturation step and the fact that these reactions need to be driven by redox mechanisms suggest the involvement of an electron transport chain for an efficient desaturation reaction. The role of this electron transport chain has been elucidated via characterization of *Arabidopsis* and tomato mutants which accumulate phytoene (Carol *et al.*, 1999; Josse *et al.*, 2000, *cf.* § 1.5.2) which accumulate phytoene. The phenotype of these mutants is a consequence of a non-functional plastid terminal oxidase (PTOX) in the redox chain (see below), which inhibits desaturation. PDS and ZDS are membrane enzymes which catalyse similar reactions and share significant amino acid sequence homology (Fraser and Bramley, 2004).

Lycopene is the main pigment that accumulating in red tomato fruits. However, in most other plant tissues, lycopene is further converted into other carotenoid molecules with cyclic end groups, such as β-carotene, whose formation is catalyzed by lycopene β-cyclase (CRTL-B, Cunningham *et al.*, 1996), or α-carotene whose formation is catalyzed by the action of both lycopene β-cyclase and lycopene epsilon-cyclase (LCY-E, Ronen *et al.*, 1999).

Hydroxylation of α-carotene produces lutein, the most abundant xanthophyll in chloroplasts. Hydroxylation of β-carotene results in formation of zeaxanthin (Sandmann, 1994). Epoxidation of zeaxanthin by zeaxanthin epoxidase yields violaxanthin (Marin *et al.*, 1996; Bouvier *et al.*, 1996). Violaxanthin can be converted to neoxanthin, which contains a single allenic end group (Bouvier *et al.*, 2000). Zeaxanthin can be formed back from violaxanthin by violaxanthin de-epoxidase via the so-called xanthophyll cycle, which is especially important at high light intensity (*cf.* § 1.3.2.2).

1.2 Chloroplast and photosynthesis

Photosynthesis is a process where light energy is directly used to synthesize organic compounds. In eucaryotes, particularly in higher plants, the biophysical and biochemical reactions of photosynthesis occur in chloroplasts. In photosynthetic procaryotes including cyanobacteria, photosynthetic and respiratory oxido-reduction reactions are located in the same membranes and use the same electron carriers (Martin and Herrmann, 1998).

Photosynthesis requires the coordination of two phases: light reactions and carbon-linked reactions. The two phases of photosynthesis occur in different regions of the chloroplast. The

thylakoid membranes contain the photosynthetic pigments and reaction centers which are responsible for capture and conversion of light energy into chemical bond energy via a photosynthetic electron transfer chain. In contrast, the carbon-linked Calvin cycle reactions occur in the stroma (Buchanan *et al.*, 2000).

1.2.1 Light absorption

Light energy is absorbed by pigment molecules, including chlorophylls. Carotenoids are accessory light-harvesting pigment molecules. This energy absorption results in the conversion from the lowest-energy (ground) state to an excited state (pigment*). Once excited, an electron can return to the more stable state by releasing energy as heat (relaxation), fluorescence or energy transfer through a charge separation event, in which the excited pigment reduces an acceptor molecule. The latter, called photochemistry, converts light energy into chemical products (Buchanan *et al.*, 2000).

1.2.1.1 Chlorophyll

Chlorophyll (Chl) has unique and essential roles in photosynthesis light-harvesting and energy transduction. Chlorophyll molecules contain a tetrapyrrol ring (porphyrin; a heme-like structure) with a magnesium atom bound in the center of this ring (instead of an iron atom in heme). The precursor of Chl biosynthesis is 5-aminolevulinic acid (ALA). Most genes required in Chl biosynthesis show a light-induced and developmental-dependent expression profile (Eckhardt *et al.*, 2004). The diverse forms of chlorophyll include an altered side chain on the ring or different degrees of saturation of the ring system. Chlorophyll has two major peaks in the visible absorption spectra at 430 nm (blue) and 680 nm (red) wavelengths. It absorbs less effectively green light, and non-absorbed green light can be reflected as chlorophyll color (Buchanan *et al.*, 2000).

1.2.1.2 Carotenoids and photosynthesis

Carotenoids absorb light between 400 and 500 nm, a range in which absorption by chlorophyll a is relatively weak. Carotenoids present in photosynthetic membranes are associated with the light harvesting complex (LHC) and reaction center (RC) of photosystems (Cunningham and Gantt, 1998). Carotenoids play a minor role as accessory light-harvesting pigments, absorbing and transferring light energy to Chl molecules. They play an important structural role in the

assembly of the LHC through membrane lipid stabilisation (Havaux *et al.*, 2004), and function as photo-protective agents for photosystems from photooxidative damage (Frank and Cogdell, 1996; Niyogi, 2000, *cf.* § 1.3.2.1)

1.2.2 Energy conversion

Photosystems contain a photochemical reaction center (RC) where charge separation occurs involving multiple light harvesting pigment-protein complexes. Two photosystems, I and II, are present in oxygenic photosynthetic organisms. The electron transfer and the positive charge accumulation at the donor side of photosystem (PS) II (producing a strong oxidant, $P680^+$) permit water photolysis and producing oxygen. At the acceptor side of PSII, the electrons are transferred via a chain of membrane electron carriers, including plastoquinones (PQ), the cytochrome (Cyt) b_6f complex and plastocyanin (PC).

In PSI, the charge separation produces a strong reductant, $P700^+$ which can oxidize PC. After charge separation, reduced ferredoxin (Fd) serves as an electron donor for reduction of $NADP^+$ by ferredoxin-$NADP^+$-reductase.

This interaction of PSI and PSII in the transfer of electrons from water to $NADP^+$ in the light is called the Z-scheme (Hill and Bendall, 1960). Electrons are transferred from water to $NADP^+$; and a proton gradient is established across the membrane. This electrochemical gradient is utilized ultimately for the synthesis of ATP by ATP synthase (see Albertsson, 2001, for a review). The membrane organization of the Z-scheme is presented in figure 1.3.

1.2.3 Electron transfer chain components

1.2.3.1 Thylkoid membrane organization

The main fraction of PSII and LHCII are concentrated in the stacked grana core, whereas PSI (with LHCI), a minor fraction of PSII and the ATPase are mainly localized in grana margins and stroma lamellae. It is assumed that the Cyt b_6f complex is equally distributed. The physical separation of the photosystems requirs mobile electron carriers such as PQ and PC, which shuttle electrons between the spatially separated membrane complexes (Albertsson, 2001).

Photosystem II (PSII) mediates electron transfer from water to PQ as a result of the light-induced charge separation between the primary chlorophyll donor P680 and a pheophytin acceptor molecule. The reaction center of PSII comprises the D1 and D2 trans-membrane proteins

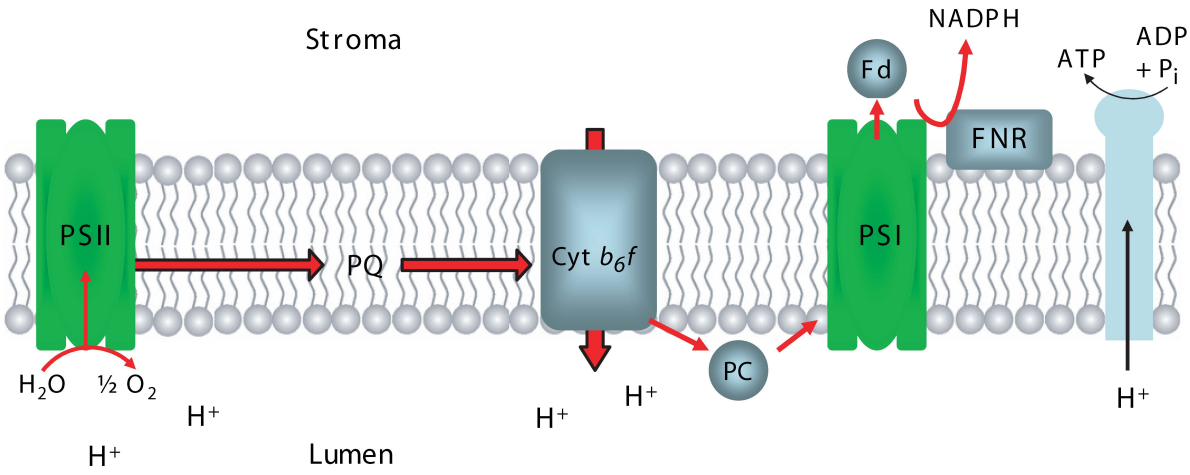

FIGURE 1.3 – **. Membrane organization of Z-scheme. The electrons from photosystems II are transferred via a chain of membrane electron carriers, including plastoquinones (PQ), the cytochrome (Cyt) b_6f complex and plastocyanin (PC), photosystems I, and finally ferredoxin (Fd) (red lines). The proton gradient is utilized for the synthesis of ATP by the ATP synthase.**

(encoded by the *psbA* and *psbB* plastid genes, respectively) containing two tyrosine residues as electron donors to $P680^+$ (Debus *et al.*, 1988). D1 and D2 are bound to two pheophytin *a* molecules and plastoquinones Q_A and Q_B. In the primary photochemical reaction, one electron is transferred from the pigment P680 in the first excited singlet state (P680) to pheophytin *a*. The electron is then transferred to the primary quinone-type acceptor Q_A, then to the quinone Q_B. After receiving two electrons, Q_B binds two protons from the lumen side of the thylakoid membrane (Q_BH_2) and in turn dissociates from the RC of PSII and diffuses into the lipid bilayer of the membrane to merge into the plastoquinone (PQ) pool (Krause and Weis, 1991).

Most LHC pigments are associated to Chl *a*/*b* binding proteins (CAB) in PSII and form chlorophyll-protein complex. Analysis of excited-state dynamics in PSII from X-ray crystallography studies has revealed a crucial role in energy transfer from the antenna to the RC complex of the two inner-antenna CP43 and CP47 proteins (encoded by *psbC* and *psbD*, respectively) associated to chlorophyll molecules (Vasil'ev *et al.*, 2001).

Cyt b_{559} is located in the RC complex and comprises two subunits α and β (encoded by *PsbE* and *PsbF*, respectively). Cyt b_{559} is involved in different roles including PSII assembly and cyclic electron transfer flux around PSII (Kruk and Strzalka, 2001). In addition, under stress conditions affecting the water oxidizing complex and Q_B function, the redox reactions of Cyt b_{559} play a significant protective role (Kaminskaya *et al.*, 2003). Recently, a novel quinone-

binding site (Q_C) in PSII has been identified that regulates Cyt b_{559} function (Kaminskaya *et al.*, 2007).

The function of many of the other structural low-molecular mass subunits (PsbH, J, K, L, M, N, R) remains unknown. PsbS has been shown to play a key role in nonphotochemical quenching (NPQ, Li *et al.*, 2002; Kiss *et al.*, 2008).

The oxygen-evolving complex (OEC) contributes to water oxidation at the lumenal side of PSII. In plants, OEC contains three peripheral subunits OE33, OE23 and OE17. The OEC contains the Mn-cluster as well as calcium and chloride, which are essential for catalytic activity. The reaction pattern and mechanism of water oxidation has been reviewed recently (Renger and Kuhn, 2007).

In all, the PSII consists of more than 25 polypeptide subunit species, 200 - 250 chlorophyll molecules per P680 and a chlorophyll *a*/*b* ratio of 2-3 (Albertsson, 2001).

Plastoquinones are located in a pool of quinone molecules which can diffuse freely in the membrane due to their long carbonated chain (around 7 PQ molecules per PSII). After receiving two electrons and two protons, PQ is fully reduced (plastoquinol) and serves as an electron donor to the Cyt b_6f complex. The PQ pool plays a role in linear electron transport, the Q-cycle, cyclic electron transport around PSI, and chlororespiration (Joët *et al.*, 2002a). The PQ pool forms a buffer between PSII and the rest of the electron transport chain. It has been suggested that the occupancy state of the Q_B site (that depends directly on the redox state of the PQ pool) may play a role in the determination of the Chl *a* fluorescence yield (Schreiber *et al.*, 2002). The redox state of PQ plays a role in the regulation of several processes, consisting of:

-The activation of a kinase responsible for the phosphorylation of several PSII subunits (reviewed by Allen, 2003).

-The activation of another kinase capable of phosphorylating a part of the PSII light-harvesting complex (LHCII) (reviewed by Rochaix, 2007).

-The participation in signaling for the regulation of the expression of several genes related to photosynthetic electron transport functions (Foyer and Noctor, 2003).

The **Cyt b_6f** complex, like the mitochondrial Cyt bc_1 complex, belongs to the *bc*-type family of cytochromes, which couple electron transfer and proton translocation across the membrane. The Cyt b_6f complex transfers electrons from plastoquinol to a soluble electron carrier located in the thylakoid lumen, PC. The electron transfer is accompanied by formation of a proton gradient across the thylakoid membrane, which is used by the ATP synthase to generate ATP.

The Cyt b_6f complex is formed by the Rieske protein (containing a [2Fe-2S] cluster; PetC), the cytochroms f (PetA) and b_6 (PetB), subunit IV (PetD), and several small subunit species (PetG, PetL, PetM, PetN) including the newly described subunit V encoded by the nuclear gene *petO* (Hamel *et al.*, 2000). PetD is implicated in PQH_2 binding. Two quinol/quinone binding sites are located on opposite sites of the membrane. Firstly, there is the Q_o site on the lumenal side of the membrane, which is involved in PQH_2 oxidation and Rieske protein reduction (Cramer *et al.*, 1996). Secondly, there is the Q_i site on the stromal side of the membrane, which is implicated in a cyclic electron flux called the "Q-cycle" as proposed by Mitchell (1975). Recent knowledge of this mechanism suggests that it contributes to the generation of the proton gradient that drives ATP synthesis. Beside its role in photosynthetic electron transfer, the Cyt complex is also involved in the avoidance of deleterious side reactions via the semiquinone radical intermediates that can lead to oxidative stress (reviewed by Cape *et al.*, 2006).

Plastocyanin (PC) is a water-soluble protein located in the lumen (encoded by the nuclear genome), which as a reduced form is the electron donor to PSI. PC contains an atom of copper and it diffuses freely in the lumen.

Photosystem I (PSI) is formed by a core complex with an attached light harvesting complex (LHCI). It drives the electron transfer from plastocyanin at the lumenal side to ferredoxin located in the chloroplast stroma. The electron transfer within PSI occurs via the primary electron donor P700, which is a chlorophyll *a* dimer, and the electron acceptors, a chlorophyll *a* monomer (A_0), two vitamin K molecules (A_1) and the three 4Fe-4S clusters (F_X, F_A and F_B).

The integral core of PSI is formed by PsaA and B (encoded by the plastidial genome) and several small transmembrane subunits. The low-molecular-mass PsaC binds to the Fe-S center F_X. PsaF is implicated in the binding of PC to this complex. PsaG, H, and K proteins have been shown to be involved in the interaction between LHCI and the PSI core (Jensen *et al.*, 2000). PsaI and J subunits appear to be responsible for the organization of peripheral proteins; PsaL stabilizes the PSI trimer. PsaJ is an important subunit that, together with PsaF and PsaN, is required for the formation of the plastocyanin-binding domain of PSI (Jordan *et al.*, 2001; Hansson *et al.*, 2007). The peripheral subunits PsaD and E, located at the stromal face of PSI, form a ferredoxin-docking pocket (Jordan *et al.*, 2001) and these subunits and probably the PsaM subunit play a role in cyclic electron flow around PSI reviewed by (Chitnis, 1996). PsaO is involved in balancing the excitation pressure between the two photosystems (Jensen *et al.*, 2004).

Ferredoxin (Fd), a small [2Fe-2S] protein encoded by the nuclear genome, is the terminal electron acceptor for PSI. Structure and function of plant-type ferredoxins are reviewed in Fukuyama (2004).

Antenna proteins (LHC) The common ancestor of the LHC proteins is believed to be a cyanobacterial high-light inducible protein with one membrane-spanning helix. After endosymbiotic chloroplast formation, the *Lhc* gene progenitor was transferred to the nuclear genome, where subsequent duplication and deletion events took place, eventually leading to the large *Lhc* gene family existing today (Jansson, 1999). The protein precursors contain an N-terminal transit peptide that is cleaved off during import into the chloroplast, after which the mature proteins are inserted into the thylakoid membrane (Cline and Henry, 1996). LHCII is divided into the minor LHCII (CP24, CP26 and CP29; these apoproteins are encoded by the nuclear genes *Lhcb4*, *Lhcb5* and *Lhcb6*, respectively) which is monomeric and associated with the core of PSII, and the major LHCII which is a trimer, Lhcb1, 2, and 3. Lhcb1 and 2 are believed to exist as a mobile complex migrating to PSI during the mechanism known as state transition (Depege *et al.*, 2003, *cf.* § 1.3.1). PSII in stacked grana thylakoids is mainly organized as a so-called PSII-LHCII supercomplex, which is a core dimer with minor LHCII and two major LHCII trimers. The specificity of the LHCII-binding sites plays a key role in the organization of the protein arrangement in grana thylakoids (Kirchhoff *et al.*, 2007). LHCII also appears to bind to a specific site on PSI (subunit H) during state transitions (*cf.* § 1.3.1), and if this site is nonfunctional (as in mutants lacking PsaH) LHCII tends to remain associated with PSII (Zhang and Scheller, 2004). LHCI is composed of four different subunits, Lhca1 to Lhca4. All LHC-related proteins have been shown to bind chlorophylls and carotenoids (Kirchhoff *et al.*, 2007).

Two additional groups of proteins showing homology to the LHC family, PsbS and early light-inducible proteins (ELIPs), have been identified in higher plants. The PsbS protein appears to control the organization of LHC in thylakoid (grana) membranes (Kiss *et al.*, 2008). ELIPs are the light stress-responsive proteins which are immediately induced in plants exposed to light stress (Kimura *et al.*, 2003).

Ferredoxin NADP$^+$ reductase (FNR) is a flavine adenine dinucleotide (FAD)-containing enzyme. It is soluble and encoded by the nuclear genome. Electrons from PSI are transferred to NADP$^+$ in the stroma via Fd and the intermediate FNR enzyme. FNR can be reduced in two single electron steps. It has been recently shown in wheat that a FNR isoform bound to the

membrane is mainly involved in cyclic electron transfer. However, FNR isoforms participating in linear electron transport can also efficiently bind to membranes. This suggests that the mechanism directing the enzyme to one of the two possible electron pathways involves pH-dependent protein conformational changes (Grzyb *et al.*, 2008).

FNR enzymes may modulate the partition between linear and cyclic photosynthetic electron pathways. Such a view is in accordance with kinetic measurements (Breyton *et al.*, 2006). In *A. thaliana* mutants deficient in chloroplast FNR isoforms, the linear and cyclic electron transfer capacities are lowered, with a significant decrease in CO_2 fixation (Lintala *et al.*, 2007). FNR is proposed to reduce PQ through cyclic photosynthetic electron and chlororespiration (Bojko *et al.*, 2003). Higher tolerance to oxidative stress in FNR overexpressing lines also suggests an antioxidant role for free FNR (Rodriguez *et al.*, 2007).

The chloroplast **ATP synthase** belongs to the family of F_1-type ATPases that is also present in bacteria and mitochondria. It generates ATP from ADP and inorganic phosphate using energy derived from a *trans*-thylakoid electrochemical proton gradient. The plastid ATP synthase complex consists of nine different subunits, four of which (I - IV) are localized in the membrane integral CF_0 subcomplex (which is responsible for proton translocation), and five stromal subunits (α_3, β_3, γ, δ and ε), which constitute the extrinsic CF_1 subcomplex forming the catalytic entity. X-ray crystallography studies have shown that α and β subunits are arranged alternatively in a circle (Menz *et al.*, 2001). The ATP formation is known as the "binding change mechanism". As protons move from the lumen to stromal region through the CF_0 channel, the energy released results in a rotation of the ring of subunits III and of the associated γ/ε stalk (CF_1). This rotation causes conformational changes and then affinity changes in the three nucleotide binding sites of $\alpha_3\beta_3$ subunits. These changes are associated with substrate binding (ADP and inorganic phosphate), ATP formation, then the release of the product (ATP). The membrane-embedded ring formed by subunits III of CF_0 sector has been proposed to be a part of a rotary motor, converting electrochemical energy into chemical energy stored in ATP (Choquet and Vallon, 2000).

1.3 Acclimation of the photosynthetic apparatus against stress conditions

The photosynthesis complex machinery is liable to light-induced damage caused by the inevitable generation of reactive intermediates and by-products. Short and long term fluctuations in light intensity, as well as environmental stresses such as cold, drought, salinity, and nutrient deficiency, that limit CO_2 fixation, can result in the absorption of more light energy than can be utilized productively by photosynthesis. One of the striking features of thylakoid membranes and the photosynthetic apparatus is their flexibility to acclimate to changing environmental conditions. The time required for adaptation processes can range from seconds or minutes (short-term), to days or even longer periods (long-term). Under light stress conditions, safe dissipation of excess photons and electrons is activated to protect the photosynthetic apparatus from light-induced damage. These regulatory mechanisms may not be efficient enough and photoinhibition of PSII can occurs. However, after a relatively rapid turnover of PSII, recovery is possible.

The long-term acclimation may normally involve the regulation of nuclear and chloroplast gene expression by quinone redox potential (Mullineaux *et al.*, 2000). Plastoquinone, thioredoxin and reactive oxygen have all been shown to have signalling functions (Foyer and Noctor, 2003). These acclimation responses to excess light include increasing the capacity for photosynthetic electron transport and CO_2 fixation, as well as decreasing the size of the LHC associated with the photosystems.

Some important adaptation and safe dissipation of excess photons and electrons mechanisms are discussed below.

1.3.1 Redistribution of excitation energy from PSII to PSI

In linear electron transport, PSI and PSII must operate at the same rate, but natural environmental conditions, such as the quality and quantity of light, are constantly fluctuating, which may alter the balance between the two photosystems. The two photosystems have different absorption spectra, and therefore a change in light quality may favor one photosystem over the other. One of the key processes of short-term adaptation is the redox-controlled kinase/phosphatase system operating in the energy spill-over between the two photosystems. This process also known as state 1/state 2 transitions (Gal *et al.*, 1997; Allen, 2003; Rochaix, 2007). As it shown

in figure 1.4, if PSII is overexcited relative to PSI, the PQ pool becomes overreduced. Binding of plastoquinol at the Q_o site and subsequent reduction of Cyt b_6f complex triggers a kinase activation that phosphorylates a mobile pool of LHCII, leading to the lateral movement of LHCII in favor of PSI and redistribution of energy from PSII (state 1) to PSI (state 2, Zito *et al.*, 1999; Allen, 2003; Bellafiore *et al.*, 2005). In addition, it has been proposed that LHCII phosphorylation helps the rearrangement of the PSII-LHCII complex and thylakoids to optimize the dynamic property and flexibility of the thylakoids during the dark-light transition (Su and Shen, 2005).

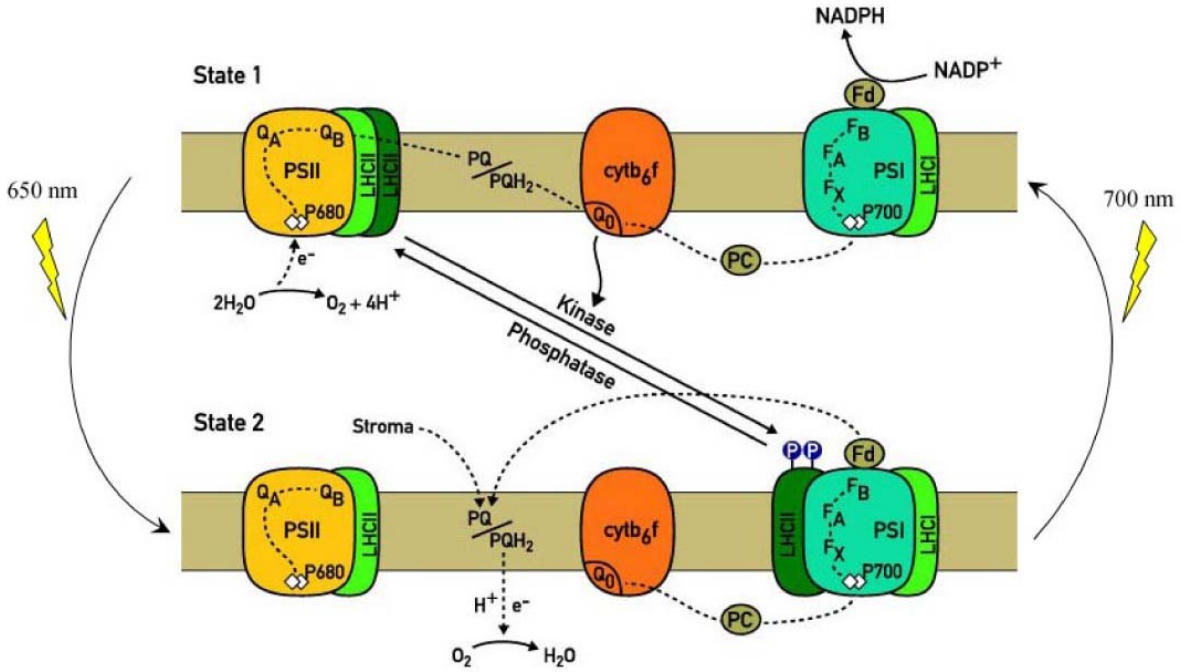

FIGURE 1.4 – **Scheme of photosynthetic complexes in the thylakoid membrane and state transitions. State transitions are determined to a large extent by the redox state of the PQ pool. Preferential excitation of PSI leads to the oxidation of the PQ pool and to form state 1. In state 1 the mobile LHCII is bound to PSII and the photosynthetic electron transport chain acts mostly in a linear mode generating NADPH and ATP. Preferential excitation of PSII relative to PSI leads to a reduced state of the PQ pool and thus to the docking of plastoquinol to the Q_o site of the Cyt b_6f complex. This activates the LHCII kinase and leads to the displacement of phosphorylated LHCII from PSII to PSI (state 2). State 2 can also be induced in the dark through the chlororespiratory electron transport chain under anaerobic conditions which prevent the oxidation of the PQ pool or in response to reduced levels of ATP. Electron transfer chains are represented as dotted lines. Q_A, Q_B, primary and secondary electron acceptors of PSII; F_X, F_A, F_B, 4Fe-4S centers acting as electron acceptors within PSI; PQ, plastoquinone pool; PC, plastocyanin; Fd, ferredoxin (adapted from Rochaix, 2007).**

Two models have been proposed to explain the movement of LHCII. According to one model, LHCII moves in state transitions not because phospho-LHCII has higher affinity for

PSI but because this phosphorylation causes structural changes in the thylakoid membranes, promoting movement of LHCII, *i.e.* both in its phosphorylated and unphosphorylated form (Zhang and Scheller, 2004). According to the other model, the net movement of LHCII toward PSI in state 2 is caused by PSII with higher affinity for unphosphorylated LHCII and PSI with higher affinity for phospho-LHCII (Allen and Forsberg, 2001). Activation of an LHCII kinase therefore decreases the absorption of light by PSII and increases that by PSI. This adaptation typically occurs in the range of a few seconds (Gal *et al.*, 1997). Much research to identify kinases involved in the phosphorylation of thylakoid proteins has been carried out. A family of proteins, thylakoid-associated kinases, has been identified as good candidates for LHCII kinases (Snyders and Kohorn, 2001). In addition, a protein kinase Stt7 recently identified in *chlamydomonas* (Depege *et al.*, 2003) and a thylakoid-associated Ser-Thr regulatory kinase, Stn7, in *Arabidopsis* (Bellafiore *et al.*, 2005), have been shown to be required for state transition.

In *Chlamydomonas reinhardii*, the transition from state 1 to state 2 induces a switch from linear to cyclic electron flow and reveals a relationship between the redistribution of antenna complexes during state transition and the onset of cyclic electron flux (Finazzi *et al.*, 2002). The phosphorylation is regulated by the light intensity leading to the conformational change of LHCII (Vink *et al.*, 2004).

1.3.2 Energy dissipation as the protection mechanism against photo-oxidation

Light is essential for photosynthesis, but high light intensity can cause serious damage to the reaction centers and other cellular constituents through overreduction of the electron carriers and production of reactive oxygen species (ROS). Plants may dissipate excess photons and electrons by photoprotective mechanisms via carotenoids and in particular the xanthophyll cycle for quenching excited chlorophylls, as well as other nonphotochemical mechanisms (Niyogi, 2000). These processes is the pathway to the fully photoinhibited reaction center of PSII are normally reversible (for review, see Baker and Rosenqvist, 2004).

In general, the term "photoinhibition" (PI) is used in the literature to describe a reaction in which the electron transport activity of PSII is lost in such a manner that re-synthesis of the D1 protein is required for recovery (for review, see Tyystjarvi, 2008). Photoinhibition of PSI is also discussed in Sonoike (1996).

1.3.2.1 The photoprotective roles of carotenoids

Light is absorbed by chlorophyll (Chl) and carotenoid molecules bound to LHC-proteins in the thylakoid membranes of chloroplasts, resulting in singlet state excitation of the pigment molecules. Excitation energy is then transferred to reaction centers to drive electron transport, which oxidizes H_2O, reduces $NADP^+$, and generates a pH that is necessary for ATP synthesis.

The photosynthetic apparatus must adapt to changes in light intensity. Directional movements of whole leaves and/or chloroplasts, allowing the plant to optimize light absorption are relatively slow processes. Instead of regulating light absorption and as a rapid response, plants can profit from the mechanisms for dissipating photons that have already been absorbed. Under normal conditions, most of the energy in singlet-excited chlorophyll (^{1}Chl*) is used at the RC to drive electron transport. In this case, Chl fluorescence quenching is correlated to charge separation (photochemical quenching, qP). However, when the rate of formation of ^{1}Chl* exceeds the overall rate of its energy conversion at the RC, intersystem crossing leads to an increased population of triplet Chl (^{3}Chl*) in LHCs, which is a long-lived state that is incapable of initiating photosynthetic electron transfer. ^{3}Chl* can activate molecular oxygen to its highly reactive singlet state ($^1O_2$). Singlet oxygen molecules, as well as the other forms of reactive oxygen species (ROS), are known to induce oxidative damage to pigments, proteins and lipids in the thylakoid membrane, thereby impairing overall photosynthetic efficiency (photoinhibition). ^{3}Chl* is efficiently quenched by energy transfer to carotenoids, which are closely associated with Chls in the photosynthetic apparatus. Excited carotenoid molecules dissipate energy in the form of heat. It has been estimated that between 4-25% of the photons absorbed by PSII can be dissipated via this triplet valve. $^1O_2$ can directly damage the proteins, pigments, and lipids and lead to complete destruction of the photosynthetic apparatus. Quenching of $^1O_2$ is also achieved by carotenoids (Niyogi, 2000).

Chl + $h\upsilon$ → Singlet excited Chl (^{1}Chl*) **State 1**

^{1}Chl* + $h\upsilon$ → Triplet excited Chl (^{3}Chl*) **State 2**

^{3}Chl* → Triplet carotenoids → carotenoids + heat

ROS production in thylakoids throughout the light phase of photosynthesis is summarized below (adapted from Foyer *et al.*, 1997):

O_2 + ^{3}Chl* → $^1O_2$ **Singlet state oxygen**

$O_2 + e^- \rightarrow O_2^-$ **Superoxide anion**

$2O_2^- + 2H + (\text{lumen}) \rightarrow 2H_2O$ (Superoxide dismutation)

$2H_2O \rightarrow O_2 + H_2O_2$ (stroma) **Hydrogen peroxide** (Superoxide protonation)

$H_2O_2 + Fe^{2+} \rightarrow Fe^{3+} + OH^- + OH\cdot$ **Hydroxyl radical**

$O_2^- + Fe^{3+} \rightarrow Fe^{2+} + O_2$

1.3.2.2 The xanthophyll cycle

The importance of the xanthophyll cycle (Yamamoto *et al.*, 1979) in high light conditions became clear more than a decade ago (Verhoeven *et al.*, 1996). Violaxanthin (V) is synthesized from zeaxanthin (Z) via antheraxanthin (A) under low light conditions by the stromal activity of zeaxanthin epoxidase. Under intense light, lumenal pH decreases and violaxanthin de-epoxidase converts V back to Z when a critical threshold has reached (Fig 1.5). A has a similar photoprotection function as Z, and can replace Z in its absence (Goss *et al.*, 1998). Accordingly, the level of de-epoxidation can be calculated as the amount of A and Z compared with the total number of xanthophylls (V+A+Z) (Muller *et al.*, 2001).

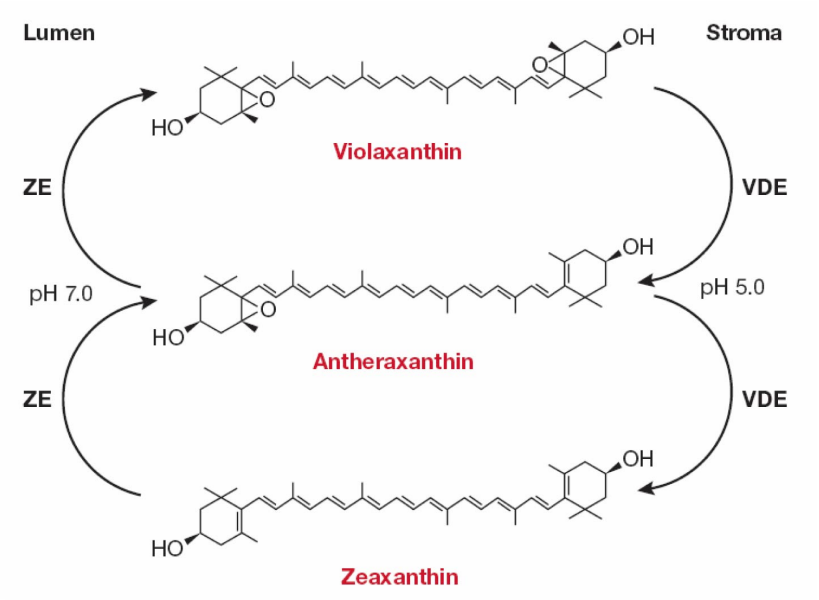

FIGURE 1.5 – **The xanthophyll cycle. VDE, violaxanthin de-epoxidase; ZE, zeaxanthin epoxidase.**

All carotenoids are able to dissipate excitation energy by rapid internal conversion, but it has been calculated that only those with ten or more conjugated carbon-carbon double bonds

have an excited singlet state (S1) at an energy level low enough to accept energy from ^{1}Chl*. However, direct determination of the *in vitro* energy levels reveals that Z (11 double bonds) and V (9 double bonds) have an S1 state that enables direct quenching of ^{1}Chl* through singlet-singlet energy transfer (Polivka *et al.*, 1999). The S1 state of Z has a particularly short lifetime (10 psec), allowing rapid thermal dissipation of excitation energy (Polivka *et al.*, 2002; Ma *et al.*, 2003). In addition, Z may protect the thylakoid membrane against photooxidation by directly quenching $^1O_2$* and other reactive oxygen species (Havaux and Niyogi, 1999).

Apart from Z's ability to directly quenching the chlorophyll excitation, it is also greatly involved in qE which is a part of nonphotochemical quenching (NPQ). The latter involves a role for Z in the conformational change in antenna proteins and also a role in PsbS-dependent qE which are discussed below (*cf.* § 1.3.2.3, review in Szabo *et al.*, 2005).

Overexpression of zeaxanthin epoxidase in tomato decreases the level of de-epoxidation and aggravates the photoinhibition of PSII under high light and chilling stress (Wang *et al.*, 2008).

1.3.2.3 Nonphotochemical quenching mechanism

Because Chl fluorescence is sensitive to a wide range of changes in overall photosynthesis, it is used to assess photosynthetic function and its subsequent downregulation under excess light conditions as a common physical observable trait. As shown in figure 1.6, processes that decrease the overall Chl fluorescence quantum yield (ΦChl) are generally divided into two categories, photochemical quenching (qP), which is exclusively associated with photochemical charge separation in the RC of PSII, and nonphotochemical quenching (NPQ, Krause and Weis, 1991; Muller *et al.*, 2001).

There are multiple components in NPQ: a rapidly reversible pH-dependent quenching (qE), the slowly relaxing components (qI) and state transition (qT) (Krause and Weis, 1991). qE is the main component of NPQ and also an important short-term photoprotective mechanism upon exposure to excess light (Muller *et al.*, 2001). It dissipates excess absorbed energy as heat, minimizing the damage caused by excitation energy to PSII. qI is associated with photoinhibition which is slowly reversible or even partially irreversible.

There is increasing evidence that qE proceeds via conformational change in the subunits of the PSII antenna, and that interaction between these subunits are an integral part of the process. PsbS is a small subunit of PSII (22 kDa), which is not required for PSII photochemistry but is essential for qE induction as a pH sensor (Li *et al.*, 2002). It has been proposed that protonation

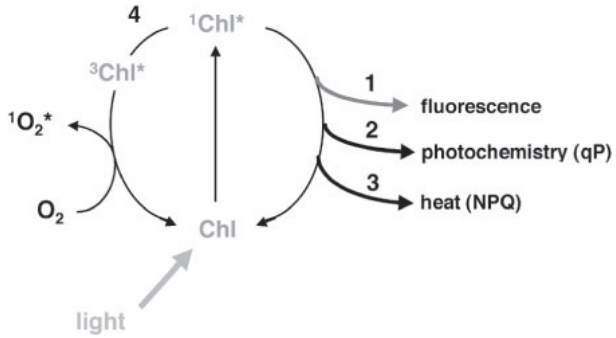

FIGURE 1.6 – **Possible fates of excited Chlorophyll (Chl). When Chl absorbs light it is excited from its ground state to its singlet excited state, ^{1}Chl*. There are several ways to relax back to the ground state: it can relax by light emission [fluorescence (1)], the excitation can be used to fuel photosynthetic reactions (2), or it can de-excite by dissipating heat (3).These latter two mechanisms reduce the amount of fluorescence (adapted from Muller *et al.*, 2001).**

of PsbS drives the concerted conformational change in LHCII and thus the formation of qE. Under excess light, a low thylakoid lumen pH leads to binding of H^+ to the carboxylates of two glutamate residues in PsbS, and zeaxanthin synthesis from violaxanthin is induced. Binding of zeaxanthin to sites in PsbS results in the qE state in which de-exitation of ^{1}Chl* occurs (review in Holt *et al.*, 2004; Kiss *et al.*, 2008). The xanthophyll cycle is essential for qE induction, but the *Arabidopsis* mutant *npq4* (*npq4* encodes PsbS), shows no alteration in any other PSII and LHCII proteins or in the xanthophyll cycle activity (Li *et al.*, 2000; Holt *et al.*, 2004; Szabo *et al.*, 2005).

Using the *Arabidopsis* double mutant *lut2/npq2* (*lut2* mutant deficient in lutein which does not contain any xanthophyll carotenoid except zeaxanthin crossed with NPQ mutant), it has been proposed that, in addition to the role of zeaxanthin in "direct quenching", it has also a role in "indirect quenching" regulating the organization of LHCII-PSII complexes. Zeaxanthin functions to decrease LHC antenna size and stability inducing LHCII monomerization. Therefore, the excess light energy is diminished suggesting a role for zeaxanthin in long-term photoadaptation (Havaux, 1998; Havaux *et al.*, 2004).

1.3.3 "Safety valves" and dissipation of excess electrons

Overreduction of electron-transport carriers and limited availability of acceptors, especially CO_2, can result in an excess of electrons in the photosynthetic electron transport chain, despite the efficient dissipation of excess photons in PSII. When the NADPH/ATP ratio is high

and ATP demand due to stress condition is high, there is a high electron pressure on PSI acceptors and PSI photoinhibition take places (Sonoike, 1996). This leads to activation of cyclic electron transfer (CET) around PSI. Plants may dissipate excess photons and electrons using "Safety valves" by alternative electron acceptors such as oxygen. Alternative electron acceptors may serve as sinks for excess electrons, thereby helping to prevent overreduction of electron carriers. Oxygen-dependent alternative electron sinks include detoxification mechanisms and O_2 photoreduction in the water-water cycle (WWC), chlororespiration, and photorespiration reactions. WWC (*cf.* § 1.4.1) and chlororespiration pathways are discussed later (*cf.* § 1.4.3).

The best characterized alternative sink for electrons is photorespiratory metabolism. Oxygenation of ribulose-1,5-bisphosphate by rubisco (ribulose-1,5-bisphosphate carboxylase/oxygenase) results in the formation of one molecule of 3-phosphoglycerate and one molecule of a toxic by-product, 2-phosphoglycolate, which can be metabolized only outside chloroplasts by photorespiratory events in peroxisomes and mitochondria.

Photorespiratory metabolism utilizes both NADPH and ATP in reactions occurring in chloroplasts and two other organelles (peroxisome and mitochondria) to recover fixed carbon that would otherwise be lost. Photorespiration is a seemingly wasteful reaction that adversely affects photosynthesis in C3 plants. However, it protects plants from high light intensity by playing a crucial role in dissipating excess photochemical energy and thus protecting chloroplasts from overreduction (for a review of photorespiration research, see Ogren, 2003).

1.4 Alternative electron transfer to the Z scheme

Besides linear electron flow from water to $NADP^+$ (*i.e.* the Z scheme) used for CO_2 assimilation and photorespiration, there are several electron transport pathways in photosynthesis of higher plants and algae. Additional electron pathways in chloroplasts, including the Mehler reaction, the cyclic electron flow around PSI, and the cyclic electron flow within PSII all been referred to as alternative electron flows.

1.4.1 Mehler reaction and ROS detoxifying pathways

The Mehler reaction represents the photoreduction of O_2 at PSI (Mehler, 1951). This photoreduction produces superoxide radicals (O_2^-), which are disproportionate to H_2O_2 and O_2 with the aid of superoxide dismutase (SOD). The H_2O_2 is rapidly detoxified to water by the ascorbate

peroxidase (APX) pathway (oxygen reduction and ROS detoxifying pathways are summarized in figure 1.7, adapted from Foyer and Noctor, 2000). Prompt scavenging of the ROS produced in thylakoids prior to its release from the generation site is indispensable to protect the target molecules in thylakoid and stroma.

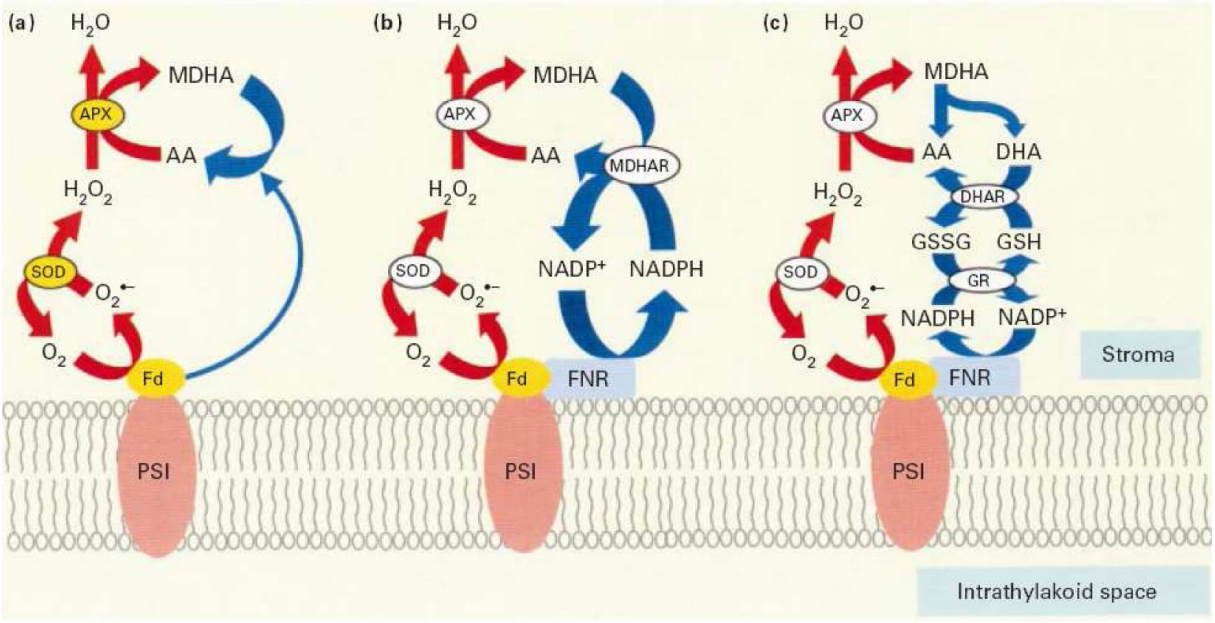

FIGURE 1.7 – **Oxygen reduction at PSI and processing of chloroplastic H_2O_2. The predominant path producing H_2O_2 from O_2 is denoted by red arrows. The initiating reaction of the reduction of O_2 to water involves the generation of superoxide (O_2^-) by Fd or other PSI acceptors. Membrane-associated and soluble SOD catalyze the conversion of superoxide to H_2O_2 (superoxide can also be reduced to H_2O_2 by PSI acceptors). H_2O_2 is reduced to water through the action of ascorbate peroxidase (APX) found in both thylakoid-bound and stromal forms. The blue arrows show three distinct paths of ascorbate (AA) regeneration. (a) The Mehler-peroxidase cycle, a reaction closely associated with the thylakoid membrane in which the primary product of ascorbate peroxidation, monodehydroascorbate (MDHA), is photochemically reduced to ascorbate by Fd. Colored ellipses indicate association with the thylakoid membrane. (b) Regeneration of ascorbate from MDHA by the NADPH-dependent enzyme MDHA reductase (MDHAR). (c) Regeneration of ascorbate via the ascorbate±glutathione cycle. Dehydroascorbate (DHA) is formed from MDHA by spontaneous dismutation, and is reduced by reduced glutathione (GSH), a reaction catalysed by DHA reductase (DHAR). Oxidized glutathione (GSSG) is reduced to GSH by glutathione reductase (GR), at the expense of NADPH. In (b) and (c), white ellipses denote a primarily soluble phase reaction. FNR, ferredoxin:$NADP^+$ oxidoreductase. (adapted from Foyer and Noctor, 2000).**

Since the electron flow from water in PSII to water in PSI occurs during this process, it has been termed the water-water cycle (WWC, Asada, 1999; Foyer and Noctor, 2000; Makino *et al.*, 2002). The WWC not only scavenges O_2^- and H_2O_2, but also functions to dissipate the energy of excess photons PSII, irrespective of O_2 concentration. It functions as an initiator of photosynthesis in dark-adapted leaves by generating pH across thylakoid membranes for

nonphotochemical quenching (NPQ) formation, supplying ATP for carbon assimilation without photooxidative damage. However, WWC does not act to maintain a high NPQ (Asada, 2000; Makino *et al.*, 2002). The importance of this pathway is variable depending on species. In C4 plants, a greater proportion of the observed O_2 uptake may be due to a Mehler reaction compared with C3 plants. In contrast to algae and higher plants, cyanobacteria appear to have a high capacity for Mehler O_2 uptake, which does not appear to be well coupled with a proton gradient and it is not limited by ATP consumption (Badger *et al.*, 2000).

Therefore, WWC functions as a relaxation system to suppress the photoproduction of O_2^- in PSII prior to its diffusion to stromal targets. As an alternative electron flux, it can down-regulate PSII quantum yield by the generation of a proton gradient across the thylakoid membrane. In dark-adapted leaves and prior to the photoactivation of the Calvin cycle, WWC is the major alternative pathway. In this respect, the WWC appears to be indispensable to initiate photosynthesis of dark-adapted leaves (Makino *et al.*, 2002). A similar increase in the electron flux through the WWC has been observed when the CO_2 assimilation is suppressed by CO_2-limiting conditions (reviewed by Asada, 2006).

1.4.2 Cyclic electron transport chain around PS I

The photosynthetic linear electron transport chain links the oxidation of water (O_2 evolution) to the reduction of $NADP^+$ and the production of ATP. Chloroplasts also carry out two major cyclic electron transports (CET) that involving PSI, which will be discussed below. PSI CET reduces the intersystem electron intermediates at the level of PQ using stromal electron carriers Fd and NADPH (Bukhov and Carpentier, 2004). Only ATP is produced via pH generation, without accumulating NADPH. Therefore, PSI CET is involved in regulating photosynthesis, by lumen acidification (Heber and Walker, 1992). In fact, the proton gradient is a key factor for inducing a rapid regulation of photosynthesis to light intensity variations, via the process of nonphotochemical quenching (NPQ, reviewed by Holt *et al.*, 2004).

In C3 plants, the contribution of CET in photosynthesis becomes significant under certain stress conditions such as low CO_2, high light and in the induction phase of photosynthesis during dark to light transition (Golding *et al.*, 2004; Joliot and Joliot, 2005; Miyake *et al.*, 2005). The physiological significance of PSI CET has been reviewed recently (Johnson, 2005; Joliot *et al.*, 2006; Rumeau *et al.*, 2007; Shikanai, 2007). PSI CET consists of two partially redundant

pathways, the NDH-dependent and the PGR5-dependent pathways, which are summarized in figure 1.8.

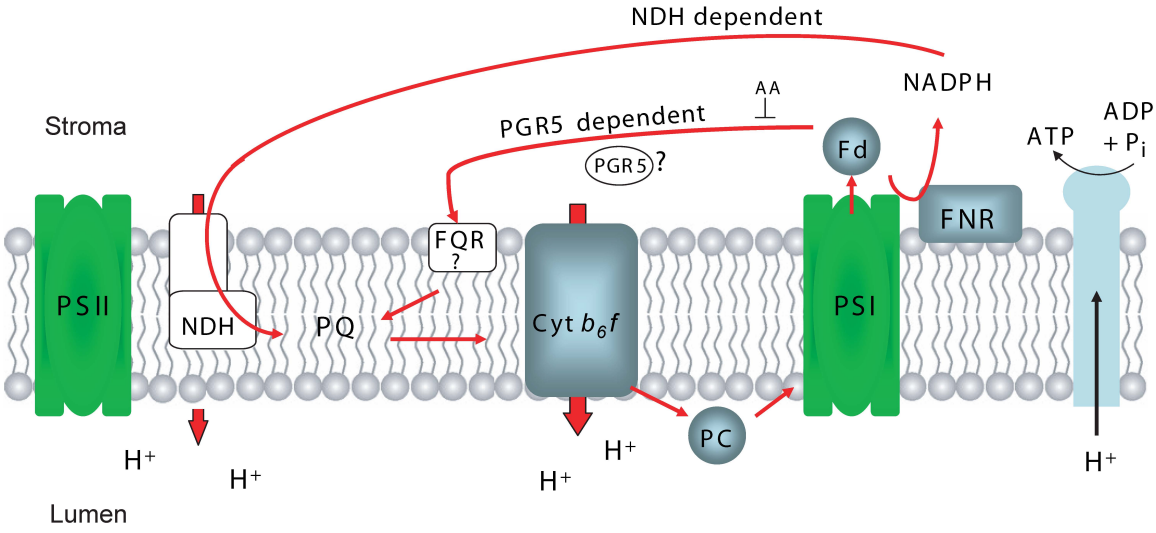

FIGURE 1.8 – **A schematic representation of photosystem I (PSI) cyclic electron transport (CET). In higher plants, PSI CET consists of two partially redundant pathways, the NDH-dependent and the PGR5-dependent pathway. The PGR5-dependent pathway is inhibited by antimycin A (AA). The route taken by electrons in the PGR5-dependent pathway is unknown. The exact localization of PGR5 is unclear. PC, plastocyanin and PTOX, plastid terminal oxidase.**

1.4.2.1 Arnon's cyclic electron transport pathway (PGR5-dependent PSI CET)

Ferredoxin (Fd) can act as an electron mediator for PSI CET (Arnon, 1965). Given that CET generates a pH, it was postulated that an enzyme must exist that could use Fd to reduce PQ. Electrons would then be fed into the Cyt b_6f complex, *i.e.* ferredoxin quinone oxidoreductase (FQR). Early observations indicated that this pathway was sensitive to the electron transport inhibitor antimycin. Antimycin is known to bind Q_i (stromal quinone binding pocket of the Cyt b_6f complex), leading to the suggestion that this site could be involved in electron flow. The observation that FNR binds tightly to the Cyt b_6f complex provides a possible Fd binding site on this complex (Zhang *et al.*, 2001). The most probable pathway of electron flow is considered to be from the acceptor side of PSI to PQ, via Fd, FNR and heme x in the Cyt b_6f complex. From there, electrons would follow the normal direction through Cyt f and PC to P700 (Johnson, 2005).

As PSI CET contributes to pH generation, and to NPQ induction, a mutant defective in PSI CET should be identifiable by its *npq* phenotype. The *Arabidopsis* mutant *proton gradi-*

ent regulation (*pgr5*) was identified based on its *npq* phenotype using chlorophyll fluorescence imaging (Shikanai *et al.*, 1999). In *pgr5*, the ratio of $P700^+$/P700 (oxidized/reduced PSI reaction center) is low at high light intensity compared to wild type. In *pgr5* leaves, the ratio can be stored in the presence of methylviologen, an artrifial electron acceptor from PSI. Furthermore, linear electron transfer was not affected in thylakoids isolated from *pgr5* leaves. These results indicate that *pgr5* is defective in alternative electron acceptance from PSI, most probably PSI CET (Munekage *et al.*, 2004). A defect in the PSI CET causes stromal overreduction, leading to PSI photoinhibition in *pgr5* even at room temperature (Endo *et al.*, 2005). In addition to qE induction, pH is a driving force for ATP synthesis. The *pgr5* mutant plants can grow as well as the wild type at low light intensity, suggesting the preferential function of PGR5 in photoprotection. However, the yield of PSII photochemistry is reduced at high light intensity in *pgr5*, a phenotype which cannot be explained uniquely by a defect in photoprotection (Munekage *et al.*, 2002). *PGR5* overexpression activates PSI CET. The PGR5 product does not exhibit any known features of electron transfer enzymes and it is possible that PGR5 is a regulator of photosynthetic electron transport and is indirectly required to operate PSI CET (Shikanai, 2007).

The FNR enzyme maybe involved in both linear and cyclic photosynthetic electron pathways (*cf.* § 1.2.3.1). The participation of FNR in nonphotochemical PQ reduction is probably via association with either FQR or the NDH complex, because FNR cannot reduce PQs directly. PSI-FNR complexes would mainly function in linear flow, since the presence of a firm complex (PSI-Fd-FNR) would result in efficient reduction of $NADP^+$. On the other hand, FNR-free PSI complexes may only reduce Fd, which could then diffuse into solution and feed electrons back into the cyclic pathway, possibly via FNR bound to Cyt b_6f (Breyton *et al.*, 2006).

1.4.2.2 NDH-dependent cyclic electron transport pathway

In addition to the above Fd dependent-antimycin sensitive pathway, evidence also exists for a pathway that does not directly involve Fd, which is insensitive to antimycin. This would involve the transfer of electrons from NADPH to PQ. The observation that a complex homologous to the mitochondrial NAD(P)H dehydrogenase (NDH; complex I) exists in the chloroplast provides a possible mediator for this pathway (Sazanov and Jackson, 1995). The *ndh* knockout lines displayed a minor but clear alteration in electron transport in chloroplasts. In wild-type tobacco, chlorophyll fluorescence levels transiently increase after turning off actinic light (*i.e.* postillu-

mination F_0 rise). This fluorescence change is attributed to PQ reduction and is impaired in the knockout tobacco defective in NDH activity. This result indicates that the chloroplast NDH complex is involved in electron transport from a stromal electron pool to PQ. There is some evidence that the NDH complex can mediate a cyclic electron flow *in vivo*, but concentrations of this enzyme are extremely low so it remains unclear whether this flux would ever be significant under physiological conditions (Ogawa, 1991; Sazanov *et al.*, 1998b; Joët *et al.*, 2002a). The NDH complex plays a crucial role in the chlororespiration pathway in the dark (Casano *et al.*, 2000; Joët *et al.*, 2001; Peltier and Cournac, 2002, *cf.* § 1.4.3).

The NDH complex is formed by eleven plastid-encoded gene products (*ndhA-K*) and three nucleus-encoded subunits (*ndhM, N* and *O*). Mutation studies of NDH complex have determined its physiological roles (Burrows *et al.*, 1998; Shikanai *et al.*, 1998; Rumeau *et al.*, 2005). Interestingly, it has been shown that *ndh* mutants displayed a reduced NPQ capacity. The major component of nonphotochemical quenching, qE, arises from the *trans*-thylakoid pH gradient. In the wild-type, oxidation of stromal reductant by the NDH complex, accompanied by proton pumping, generates a proton gradient necessary to form qE. Thus, the NDH complex-mediated electron transport may also be important for the down-regulation of PSII (Burrows *et al.*, 1998). NADH has been reported as a preferential substrate of the NDH complex (Sazanov *et al.*, 1998b; Rumeau *et al.*, 2005). The NDH-dependent PQ reduction also requires Fd in an *in vitro* assay system (Munekage *et al.*, 2004). The electron donor to the chloroplast NDH complex is still controversial, so the two pathways cannot be distinguished by their electron donor. Although the NDH complex is a mediator of electron flow to PQ, PGR5 may be indirectly involved in electron transport.

In NDH-deficient lines, no obvious phenotype is observed under optimal growth conditions. By studying the effect of antimycin A on a *ndhB* knockout mutant, the existence of two parallel cyclic pathways around PSI was proposed (Joët *et al.*, 2001). Simultaneous impairment of these pathways and also using a double mutant *crr2 pgr5* deficient in both NDH complex (*crr, chlororespiratory reduction*) and PGR5 leads to a severe inhibition of electron transport and photoautotrophic growth, even under optimal growth conditions. The remaining activity in *crr2* was totally inhibited by AA (Joët *et al.*, 2001; Munekage *et al.*, 2004).

Although FQR and NDH activities are individually dispensable for photosynthesis under optimal growth conditions, at least one component of CET is required for photosynthesis. The

importance of FQR and NDH in PQ reduction may vary from one species to another (Havaux *et al.*, 2005).

There is some evidence that NDH complex-dependent PSI CET possibly energizes C4 photosynthesis and is the preferential pathway (Takabayashi *et al.*, 2005). It is also possible that FdII (Bundle sheet cell type) effectively transfers electrons to the NDH complex via selective electron donation to a specific FNR (Okutani *et al.*, 2005).

1.4.3 Chlororespiration

In higher plants, oxygenic photosynthesis and respiration are the oxido-reduction bioenergetic mechanisms implicating electron transport in the membranes of specialized organelles, chloroplast and mitochondria respectively. In photosynthetic procaryotes including cyanobacteria, photosynthetic and respiratory oxido-reduction reactions are located in the same membranes and use the same electron carriers. By studying the effects of respiratory inhibitors on chlorophyll fluorescence induction curves in unicellular green algae, the existence of a respiratory chain in thylakoid membranes connected to the photosynthetic electron transport chain was proposed (Bennoun, 1982). This respiratory activity has been called chlororespiration, *i.e.* a respiratory electron transfer chain in thylakoid membranes.

According to the initial model of chlororespiration, a nonphotochemical reduction of PQ in the dark through a stromal pool of NAD(P)H is followed by a nonphotochemical oxidation by a putative chloroplastic oxidase using molecular oxygen as a final acceptor (for reviewing, see Peltier and Cournac, 2002; Rumeau *et al.*, 2007). The determination of electron transport carriers possibly involved in chlororespiration, such as the NAD(P)H-dehydrogenase (NDH) complex (encoded by both the plastid and nuclear genomes)(Burrows *et al.*, 1998; Casano *et al.*, 2000; Sazanov *et al.*, 1998b; Shikanai *et al.*, 1998), and a plastid terminal oxidase (PTOX, encoded by the nuclear genome) (Wu *et al.*, 1989; Carol *et al.*, 1999; Cournac *et al.*, 2000a), has provided molecular evidence for a chlororespiration pathway. There is no direct evidence that a pH gradient across thylakoid membranes and the electrogenicity corresponding to the chlororespiratory chain (Peltier and Cournac, 2002). A schematic representation of chlororespiration is presented in figure 1.9.

There are other candidates for nonphotochemical reduction of PQ including of a NDH2 complex, FQR (Peltier and Cournac, 2002), glycolate-quinone oxidoreductase (Goyal and Tolbert, 1996), and FNR (Bojko *et al.*, 2003; Breyton *et al.*, 2006).

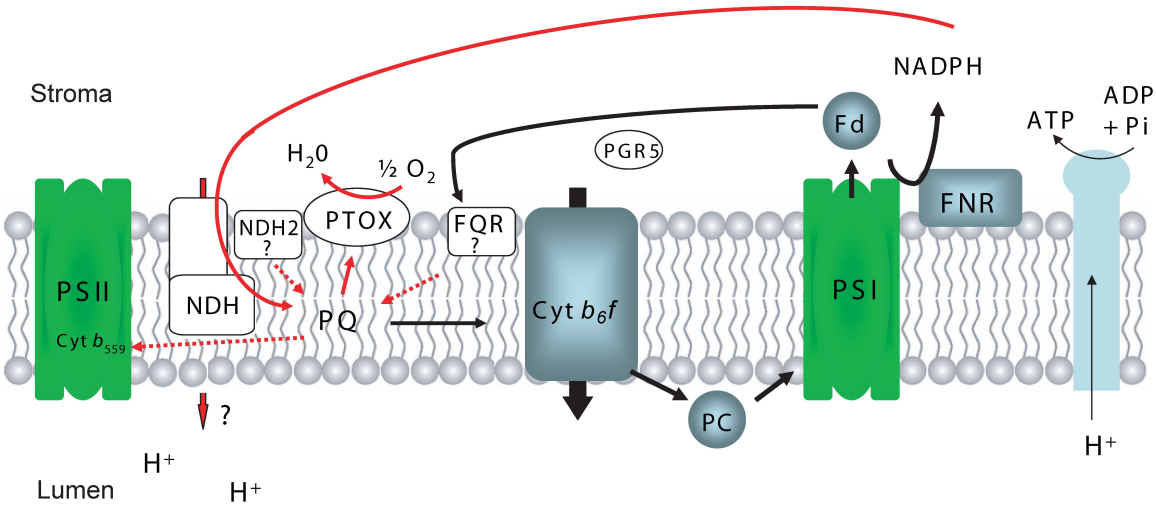

FIGURE 1.9 – **A schematic representation of chlororespiration. NADPH is oxidized by NDH complex, generating plastoquinol, which is then oxidized by PTOX to generate water. NDH2 complex, FQR as alternatives for NDH complex, and Cyt b_{559} as another candidate for plastoquinol oxidase are presented.**

In addition, there is some evidence for the participation of Cyt b_{559} in its low potential form in plastoquinol oxidation (Kruk and Strzalka, 2001), and a mutant deficient in Cyt b_{559} shows overreduction of the PQ pool in the dark (Bondarava *et al.*, 2003). A hydroquinone peroxidase was also proposed as a plastoquinol oxidase using H_2O_2 as a substrate (Casano *et al.*, 2000). Non-enzymatic PQ oxidation in thylakoid membranes may also occur. During this reaction, the generated superoxide is reduced by plastohydroquinone to produce hydrogen peroxide (Khorobrykh and Ivanov, 2002; Mubarakshina *et al.*, 2006).

The activity of nonphotochemical reduction of the PQs and expression of chlororespiratory enzymes are increased under certain stress conditions, such as heat, high light or water stress (Burrows *et al.*, 1998; Endo *et al.*, 1999; Bukhov and Carpentier, 2004; Streb *et al.*, 2005; Quiles, 2006). Chlororespiration is thought to be important to protect the photosynthetic apparatus from oxidative damage and may provide an H_2O_2 detoxification pathway within chloroplasts (Casano *et al.*, 2000, 2001; Rizhsky *et al.*, 2002). Therefore, chlororespiration appears to be implicated in protective or adaptive mechanisms of plants in response to a particular environmental stress. Chlororespiration and CET under stress conditions are reviewed by Rumeau *et al.* (2007).

The abundance of chlororespiratory components in non-photosynthetic plastids such as etioplasts or chromoplasts (Catala *et al.*, 1997; Fischer *et al.*, 1997; Josse *et al.*, 2000; Guera and Sabater, 2002; Morstadt *et al.*, 2002), suggests the presence of a "chromorespiratory" redox pathway in these organelles. But its putative role in the bioenergetics metabolism (either in ATP supply or in reoxidation of the NAD(P)H pools) needs further confirmatory work, because a lower amount of NDH complex is present in chromoplasts compared to green fruit chloroplasts (Guera and Sabater, 2002).

1.5 Plastid Terminal Oxidase (PTOX)

1.5.1 History of mutants

The plastid terminal oxidase (PTOX) has been recently identified following the isolation and characterization of *immutans* (*im*), an *Arabidopsis* pigmentation mutant impaired in the gene encoding PTOX (Carol *et al.*, 1999; Wu *et al.*, 1999b; Kuntz, 2004).

The *Arabidopsis* mutant, *immutans*, exhibits a variegated phenotype consisting of white sectors in normally green tissues and organs under low/medium light conditions. The mutant bleaches under high light condition (Fig. 1.10, see Carol and Kuntz, 2001), showing a poor or inadequate response to photo-oxidative stress. Whereas the white sectors contain defective plastids that lack colored pigments, the green sectors contain morphologically normal chloroplasts. It has been shown that the variable pattern of green and white sectoring in *im* leaves is caused by a nuclear recessive gene and that the gene has a normal Mendelian mode of transmission (Rédei, 1975; Josse *et al.*, 2000; Rodermel, 2001). The tomato *ghost* mutant is also impaired in the corresponding gene (Josse *et al.*, 2000). In bleached leaves, both mutants show a lower carotenoid content and accumulation of phytoene, which is a carotenoid biosynthesis precursor (*cf.* § 1.1.3.2).

In addition, *ghost* exhibits poorly colored flowers and fruits that do not redden but accumulate phytoene. Thus, the mutated gene has an essential role in carotenoid biosynthesis at early stage of chloroplast differentiation. PTOX plays an essential role in carotenoid biosynthesis at early stage of chloroplast differentiation. The mechanism of the variegated phenotypes has been discussed by Kuntz (2004). In brief, at the early stage of chloroplast differentiation in the mutant and under moderate light conditions, some leaf segments suffer from irreversible photo-oxidative bleaching, while others are able to avoid bleaching. According to "threshold model of

FIGURE 1.10 – **The *immutans* variegation mutant of *Arabidopsis*.**

photooxidation" (Wu *et al.*, 1999b), one or more activities are able to compensate for a lack of PTOX in some plastids and cells of the mutant, allowing the production of chloroplasts, green cells and green sectors. This compensatory activity could be another plastoquinol oxidase, or the other alternative pathways to PTOX (*cf.* § 1.4.3, see also Yu *et al.*, 2007). In general, the heterogeneity within leaves is a general feature in variegated mutants and is not fully understood (Sakamoto *et al.*, 2002).

There are significant anatomical and biochemical alterations in variegated *im* leaves. The green sectors are thicker than normal due to an increase in epidermal and mesophyll cell sizes and air space volume, while the white sectors have a normal thickness but the palisade cells fail to expand (Aluru *et al.*, 2001). The *im* green sectors also have enhanced rates of oxygen evolution, suggesting that they are able to compensate for the lack of photosynthesis in the white sectors as a way to maximize whole plant growth (Baerr *et al.*, 2005).

The cDNA from the mutated gene in *im* shows a weak, but significant, homology (45%) to polypeptides of the mitochondrial alternative oxidase (AOX) family and the name PTOX (plastid terminal oxidase) was proposed. In the various known *immutans* mutants, the PTOX gene is disrupted by a DNA inversion, a splice junction error, or a point mutation resulting in a stop codon (Carol *et al.*, 1999; Wu *et al.*, 1999a). Similarly, the *ghost* phenotype of tomato is due to a frameshift in the orthologous gene (Fig. 1.11, see Josse *et al.*, 2000). Phylogenic

sequence analysis of AOXs and PTOXs shows that they are grouped in separate families (Carol and Kuntz, 2001). The PTOX polypeptide could be immunodetected in plastid fractions as a polypeptide of approximately 37-41 kDa. This is larger than the theoretical molecular mass of the mature polypeptide (34.3 kDa). This difference may be due to the partially hydrophobic nature of PTOX (Josse *et al.*, 2000).

Wild type	**AAG**	**AAT**	**TTG**	**CCC**	**GCT**	**CCA**	**AAG**	**ATT**	**GCA**	**GTG**	**GAC**	**TAC**	**TAC**	**ACG**	**GCA**	**GGT**	**GA..**
	K	**N**	**L**	**P**	**A**	**P**	**K**	**I**	**A**	**V**	**D**	**Y**	**Y**	**T**	**G**	**G**	**D**
			258														
Ghost	**AAG**	**AAT**	**TTT**	**GCC**	**CGC**	**TCC**	**AAA**	**GAT**	**TGC**	**AGT**	**GGA**	**CTA**	**CTA**	**CAC**	**GGG**	**AGG**	**TGA..**
	K	**N**	*F*	*A*	*R*	*S*	*K*	*D*	*C*	*S*	*G*	*L*	*L*	*H*	*G*	*R*	*

FIGURE 1.11 – **Partial sequence of the PTOX cDNA showing a T insertion (underlined) in *gh* plants when compared to wild-type and deduced amino acid sequences. The amino acid sequence created by the mutation is shown in italics (adapted from Josse *et al.*, 2000).**

Mitochondrial AOXs belong to the diiron carboxylate class of proteins. AOXs are inner membrane proteins that function as terminal oxidases in the alternative pathway of mitochondrial respiration (alternative to cytochrome *c* oxidase pathways), by transferring electrons from ubiquinol to water using molecular oxygen as a terminal acceptor. The AOX pathway is KCN-resistant and, contrary to previous belief, is present in numerous animal phyla, as well as heterotrophic and marine phototrophic proteobacteria (McDonald and Vanlerberghe, 2006). It is thought to limit active oxygen species formation. When the energetic charges, reducing equivalents (*i.e.* NAD(P)H), and pyruvate are elevated, this pathway is activated to act as a security valve (Vanlerberghe and McIntosh, 1997; Maxwell *et al.*, 1999). Several copies of AOX genes are present in plants and their expression is variable in different organs (Vanlerberghe and McIntosh, 1997). This respiration pathway is important in ripening stages of flower and fruit development, in the presence of cytochrome respiratory inhibitors and also under particular stress conditions such as oxidative and cold stress, senescence, and pathogenic infections (Cruz Hernandez and Gomezlim, 1995; Vanlerberghe and McIntosh, 1997; Hiser *et al.*, 1996; Richter and Schweitzer, 1997; Simons *et al.*, 1999; Maxwell *et al.*, 2002). Under most of the above-mentioned conditions, ROS appears to be implicated. Recently, it has been suggested that AOX inhibition caused the overreduction of the photosynthetic electron transport chain and induced the cyclic electron flow around PSI even at low light. In fact, AOX is considered to be a major extra-chloroplastic sink of the reducing equivalents (Yoshida *et al.*, 2006).

PTOX genes are found in different plants and algae species and a cyanobacterium lacking thylakoids. It has been proposed that both AOX and PTOX originated in procaryotes from a common ancestral diiron carboxylate protein that diversified to AOX within ancient proteobacteria and to PTOX within ancient cyanobacteria. Each then entered the eukaryotic lineage separately; AOX by the endosymbiotic process that gave rise to mitochondria and PTOX by the endosymbiotic event that gave rise to chloroplasts (Finnegan *et al.*, 2003; Kuntz, 2004; McDonald and Vanlerberghe, 2006). The presence of a (plasto)quinol oxidase in thylakoids (such as a PTOX homolog or a Cyt *b*-type quinol oxidase in many cyanobacteria) appears to be a conserved characteristic in oxygenic photosynthesis (McDonald and Vanlerberghe, 2006).

1.5.2 PTOX as a plastoquinol-oxidase is a cofactor for carotenoid desaturation

Biochemical studies have shown that PDS activity in carotenoid desaturation requires several redox components, including PQ and molecular oxygen (Mayer *et al.*, 1990). In addition, plastoquinone-deficient mutants are disrupted in phytoene desaturation (Norris *et al.*, 1995). Therefore, the sequence similarity between PTOX and AOX suggests that PTOX is a component of the phytoene desaturation pathway and functions as a terminal oxidase by transferring electrons from the PQ pool to molecular oxygen (Fig. 1.12, for a review, see Carol and Kuntz, 2001). In agreement with this conception, recombinant PTOX protein has been shown to have plastoquinol oxidase activity *in vitro* (Josse *et al.*, 2000), and PTOX has been implicated in the transfer of electrons from PSII to molecular oxygen via the PQ pool in a PSI-deficient *Chlamydomonas* mutant (Cournac *et al.*, 2000b).

The requirement for PTOX activity, and more generally for a functional redox chain for carotenoid biosynthesis, is likely due to a need for membrane energization in order to drive the desaturation reactions. In fruit chromoplasts, the PTOX polypeptide was found mainly in the achlorophyllous membrane fraction (Josse *et al.*, 2000), which is known to contain carotenoid biosynthetic enzymes (Bouvier *et al.*, 1994). Gene expression studies in sweet pepper and tomato have shown that the PTOX genes are induced during fruit ripening, and their expression profiles are comparable with the profile of PDS and ZDS gene induction during fruit ripening (Josse *et al.*, 2000; Barr *et al.*, 2004).

It has been shown that in the absence of PTOX, the biogenesis of chloroplasts and of chromoplasts during the ripening process is impaired and that the pericarp tissue morphogenesis

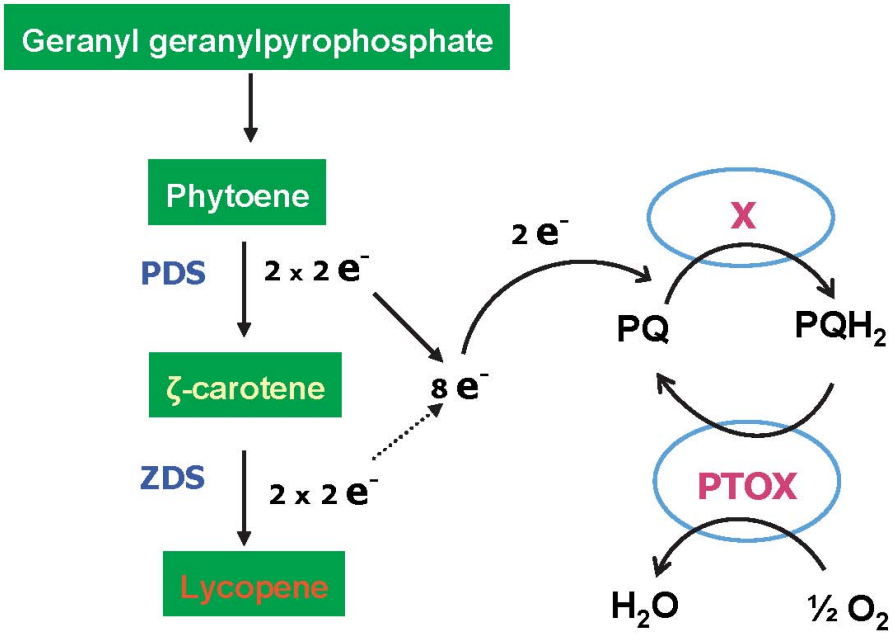

FIGURE 1.12 – **The electron transport mechanisms involving plastid terminal oxidases (PTOX). Phytoene desaturation and each subsequent desaturation step involving phytoene desaturase (PDS) and ζ carotene desaturase (ZDS) require the transfer of two electrons to oxidized quinones. The reduced plastoquinones are, in turn, reoxidized by PTOX using O_2 as a terminal acceptor. A component X (which might consist of PSII, NDH complex, FQR etc.) is postulated that can reduce quinones. Thus, an intermediate redox state of the quinone pool can be maintained and, under these conditions, electrons can be accepted from PDS and ZDS as well as donated to these enzymes.**

was affected. Most ripening-related genes are expressed normally during *gh* fruit development, but there is an important repression of mRNA accumulation from carotenoid biosynthetic genes, maybe due to retrograde (plastid-to-nucleus) signaling mediated by lycopene (Barr *et al.*, 2004). PTOX is thus necessary for a normal carotenoid biosynthetic flux and composition, and the *gh* mutation disrupts the normal regulation of total carotenoid content in tomato fruit (Barr *et al.*, 2004). The composition of carotenoid and the ripening process in tomato is regulated by the other genes such as *Cnr* (Fraser *et al.*, 2001).

In an *in vitro* PTOX activity assay following the heterologous production of PTOX in *E. coli*, NADH was used as a primary electron donor to *E. coli* membranes. A cyanide-resistant O_2 consumption was observed in the presence of PQ but not ubiquinone (Josse *et al.*, 2003). PTOX enzymatic activity is KCN resistant and sensitive to known inhibitors of the mitochondrial AOX, following the order n-octyl gallate(OG) > n-propyl gallate (nPG) > salicylhydroxamic acid (SHAM). Iron is a catalytic co-factor of PTOX (Josse *et al.*, 2003) and it is reasonable

to propose that PTOX has a diiron carboxylate center and a secondary structure similar to AOX (Berthold and Stenmark, 2003).

Based on X-ray crystallography studies of the members of non-heme diiron carboxylate protein class, a structural model of PTOX has been proposed, in which the ligation sphere of the diiron center is composed of six conserved histidine and glutamate residues (Fig. 1.13). The significance of these residues was examined by site-directed mutagenesis of PTOX *in vitro* and *in planta*. These experiments showed that the six iron-binding sites are very conservative for enzymatic activity. Moreover, exon 8 domain in the gene sequence is necessary for both PTOX activity and its stability (Fu *et al.*, 2005).

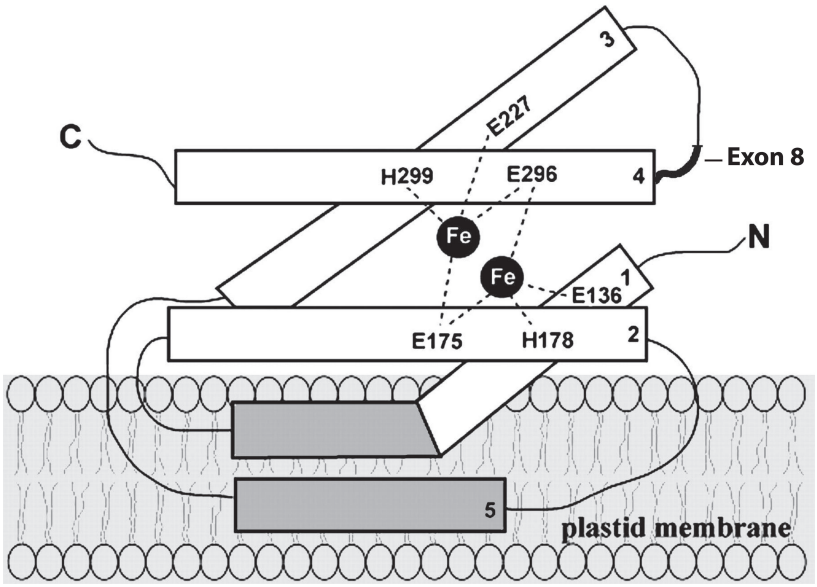

FIGURE 1.13 – **Structure of PTOX protein.**
PTOX is proposed to be an interfacial membrane protein with a diiron center composed of two EXXH motifs on helices 2 and 4 (oriented anti-parallel to each other), and two Glu residues on helices 1 and 3 (also oriented anti-parallel to each other). The exon 8 insertion is indicated by a bold line (adapted from Fu *et al.*, 2005).

1.5.3 PTOX involvement in chlororespiration

PTOX protein, like the NDH complex, is a minor component of the thylakoid membrane and has been localized to the stromal side of the thylakoid lamellae. PTOX behaves as an intrinsic membrane protein and is absent from the plastid envelope membranes. Interestingly, both the NDH complex and the PTOX protein accumulate in etiolated leaf tissue, which lacks the PSII complex (Lennon *et al.*, 2003). In addition, a plastoquinol-oxidizing activity showing nPG and

SHAM sensitivity could be monitored in *Chlamydomonas* PSI-less mutants (Cournac *et al.*, 2000b).

Based on these features and the detection of a thylakoid protein that cross-reacts with an antibody raised against PTOX, it was proposed that chlororespiratory O_2 uptake is due to a *Chlamydomonas* homolog of PTOX (Cournac *et al.*, 2000b). Moreover, the overexpression of *Arabidopsis* PTOX in tobacco and the inhibitory effect of nPG were used to show that PTOX facilitates the reoxidation of PQ either during the induction of photosynthesis or after a period of strong illumination (Joët *et al.*, 2002b). Consistent with the probable role of PTOX in both chlororespiratory and photosynthetic electron transfer chains, a tobacco mutant lacking PSII showed a 10-fold higher stoichiometry of PTOX and the NDH complex with respect to total protein or chlorophyll content (Baena-Gonzalez *et al.*, 2003).

A tobacco *rbcL* deletion mutant, which lacks rubisco, the key enzyme for photosynthetic carbon assimilation, was analyzed at the molecular level for plant acclimation to a sudden exposure to high irradiance. Flash-induced fluorescence relaxation and thermoluminescence measurements revealed slow electron transfer and decreased redox gap between Q_A and Q_B, whereas the donor side function of the PSII complex was unaffected. The results showed that the lack of terminal electron acceptors leads to a multitude of effects that help plants to acclimate to increased excitation pressure under certain growth conditions. This mutant has a low amount of photooxidisible P700 and an increased ratio of PSII to PSI. An elevated level of PTOX and the lack of "F_0 dark rise" in fluorescence measurements suggest a chlororespiratory-mediated electron flow to O_2 in thylakoids of this mutant (Allahverdiyeva *et al.*, 2005).

In contrast to *Chlamydomonas*, *Arabidopsis* PSI-deficient mutants have a low chlororespiratory capacity and these mutants are unable to avoid overreduction of the PQ pool in the light and are thus unable to avoid PSII photoinhibition (Melis, 1999; Haldrup *et al.*, 2003). In these experiments, PTOX levels were not measured, but it appears that PTOX activity could not compensate for the absence of PSI activity in this mutant. On the other hand, it has been shown that the high mountain plant *Ranunculus glacialis* contains remarkably high levels of PTOX and also strong alternative sinks to dissipate photosynthetic electrons compared to other plants (Streb *et al.*, 2005). However, PTOX overexpression did not increase PSII photoinhibition resistance either in tobacco (Joët *et al.*, 2002b) or in *Arabidopsis* plants (Rosso *et al.*, 2006).

However, there is evidence suggesting that PTOX may be involved in ROS protection under high light. In the *immutans* plants treated with cysteine, chloroplast differentiation was promoted and resulted in higher numbers of green sectors (Rédei, 1975). Cysteine is a precursor of glutathione, which together with ascorbate, plays a role in protecting against oxidative stress and regulates photosynthesis in response to high light conditions (reviewed by Rodermel, 2002). Moreover, in transgenic *Arabidopsis* lines lacking catalase and ascorbate peroxidase, the expression of PTOX is increased, indicating that PTOX may, in certain cases, compensate a deficiency in detoxifying enzymes (Rizhsky *et al.*, 2002).

As well as photooxidative stress, PTOX gene induction upon salt or abscissic acid treatments (Kong *et al.*, 2003), heat and high light stress (Quiles, 2006), and PTOX gene repression in darkness or upon DCMU treatment have been reported previously (Simkin *et al.*, 2003).

1.6 Objective of this study

Mutants lacking the plastid terminal oxidase (PTOX) have a variegated phenotype: whereas the green sectors have a normal chlorophyll and colored carotenoid content, the white sectors show an accumulation of the colorless carotenoid precursor phytoene (Wetzel *et al.*, 1994). Moreover, since carotenoid desaturation requires donation of electrons to PQs (Norris *et al.*, 1995) and since PTOX is a plastoquinol oxidase, the role of PTOX seems to be linked to the re-oxidation of PQs reduced during the desaturation during the conversion of phytoene into photoprotective carotenoids. In the absence of this oxidase, the overreduction of these PQs would lead to the inhibition of phytoene desaturation. This in turn would lead to phytoene accumulation, Chl photooxidation, and the appearance of white sectors (Carol *et al.*, 1999; Wu *et al.*, 1999b). This (probably oversimplified) view is complicated by the existence of green sectors on PTOX mutant leaves, which suggests that the desaturation reaction can, to some extent, occur without PTOX.

On other hand, since PTOX shows clear sequence similarity to the alternative oxidase (AOX) of the respiratory chain of plant mitochondria, both proteins are members of the non-heme diiron carboxylate protein family, and since they catalyze similar reactions, maybe PTOX, by analogy to AOX, provides an alternative electron sink in electron transport chains. AOX catalyses the so-called alternative pathway of mitochondrial electron transport, which is insensitive to cyanide in contrast to the general Cyt pathway. As a second pathway of electron flow, AOX

may serve to prevent the overreduction of electron transport components, which may occur in response to environmental stress (Maxwell *et al.*, 1999) and to inhibit the formation of damaging reactive oxygen species (Moore *et al.*, 2002). Thus, it has been proposed that PTOX may be functionally analogous to AOX and serve to keep the photosynthetic electron transport chain relatively oxidized.

Recent *in vitro* and *in vivo* evidence indicates that PTOX may be a plastid terminal oxidase involved in chlororespiration (Cournac *et al.*, 2000b; Josse *et al.*, 2000, 2003; Joët *et al.*, 2002b; Peltier and Cournac, 2002). During chlororespiration, one can hypothesize that NAD(P)H is reduced by the plastid membrane-bound NADPH dehydrogenase (NDH), generating plastoquinol, which is then oxidized by PTOX to re-generate plastoquinone. In addition, PTOX, like the NDH complex, is located in the stromal lamellae where cyclic electron transfer reactions around PSI occur (Joët *et al.*, 2002b; Lennon *et al.*, 2003). Chlororespiration may play a role in the acclimation of photosynthesis to changing environmental conditions. Increased chlororespiratory component levels under stress conditions suggest that chlororespiration can act as a safety valve for excess electrons to prevent the overreduction of the photosynthetic electron transport (Melis, 1999; Niyogi, 2000; Burrows *et al.*, 1998; Endo *et al.*, 1999; Bukhov and Carpentier, 2004; Quiles, 2006). There is some evidence to support the participation of PTOX in a chlororespiratory pathway. *Ranunculus glacialis*, as an alpine plant species acclimated to high light and low temperature, exhibits increased levels of PTOX, and a more oxidized electron transport chain as reflected by lower excitation pressure (Streb *et al.*, 2005). It also appears that, by mediating re-oxidation of intersystem electron carriers, PTOX can facilitate the function of cyclic electron transfers around PSI (Joët *et al.*, 2002b). In contrast, functional analyses of the *Arabidopsis im* PTOX knockout mutant and At-PTOX overexpressing lines did not support the hypothesis that PTOX regulates the redox state of the PQ pool during stress and acclimation (Rosso *et al.*, 2006). Consequently, it has been concluded that PTOX is an important mediator during chloroplast biogenesis and the assembly of the photosynthetic apparatus, but it has a minimal effect in keeping the PQ pool oxidized and mainting the flux of electrons between PSII and PSI in fully developed leaves. In addition, PTOX overexpression does not increase PSII photoinhibition resistance in tobacco or in *Arabidopsis* (Joët *et al.*, 2002b; Rosso *et al.*, 2006).

In summary, the involvement of PTOX in chlororespiration, and serving as a "safety valve" preventing overreduction of the electron transfer chain in excess light has been the subject of controversy during the last decade (Cournac *et al.*, 2000b; Joët *et al.*, 2002b; Baena-Gonzalez

et al., 2003; Streb *et al.*, 2005; Aluru *et al.*, 2006; Rosso *et al.*, 2006). The exact function(s) of PTOX in photosynthesis has not been thoroughly investigated, because the remarkable phenotype of PTOX-deficient mutants (*i.e.* showing a deficit in carotenoid content) confuses the conclusions. In fact, the causes of bleaching in PTOX-deficient plants are poorly understood: is bleaching due to a lack of carotenoids or to a redox imbalance or to both?

To address these questions, the potential roles of PTOX under high light conditions has been studied using the tomato *ghost* mutant (chapter 3.1) . This mutant was used to give a particular emphasis to the redox state of the photosynthetic electron transport chain (chapter 3.2). In addition, using At-PTOX-overexpressing transgenics tomato lines in comparison to wild-type tomato, it was examined whether a high level of PTOX influences carotenoid accumulation and protection against PSII photoinhibition (chapter 3.3).

Chapter 2

Materials and Methods

2.1 Plant Materials

The tomato (*Solanum lycopersicum* Mill) San Marzano wild-type line (accession no. LA0180) and the ghost (*gh*) monogenic mutant (accession no. LA0295) in the San Marzano background were obtained from the Tomato Genetic Resource Center (University of California, Davis). The tomato seedlings were first grown at low light intensity (10 μmol.m^{-2}.s^{-1} for 1 week and then at 20 μmol.m^{-2}.s^{-1} for 4 weeks). The plants were then grown at 22-24°C with a 16h photoperiod (white light, 60 μmol.m^{-2}.s^{-1}), to obtain adult plants with green leaves for *gh* (Fig. 2.1A). The *gh* seedlings directly germinated under 60 μmol.m^{-2}.s^{-1} were entirely bleached (Fig. 2.1B). Both white and variegated *gh* leaves were obtained by incubation of seedlings directly under 50-60 μmol.m^{-2}.s^{-1} (Fig. 2.1C).

Occasionally, variegated leaves formed even before transferring to 60 μmol.m^{-2} .s^{-1} and even 10-20 μmol.m^{-2}.s^{-1} for young *ghost* plants can sometimes be too strong, because the cotyledons can become pale green under this condition. If so, the apical meristem was removed to allow lateral buds to shoot. If these lateral buds were maintained under low light (by covering the buds with a hand towel), their new leaves become fully green. Then cuttings could be taken (Fig. 2.1D).

The plants adapted under 50-60 μmol.m^{-2}.s^{-1} for several weeks were used for fruit production (Fig. 2.1E). Plants were grown under growth chamber illumination conditions with the lateral and flower buds or fruits covered with a hand towel. Immature fruit from *gh* plants can be white (without shading) or green or green/white variegated (with shading by a hand towel). As ripening proceeds, they turn yellow and red-orange, respectively (*cf.* § Fig. 3-9). For pigment analysis, the fruit from wild type plants were harvested at four different stages of development: mature green (MG), breaker (BR), and red-ripe (10 days post-breaker, 10 DPB). *gh* fruits were harvested at the same stages of development: white or green, breaker[1] (BR), and yellow or orange (10 DPB), respectively (*cf.* § Fig. 3-9).

Tomato (dwarf MicroTom type, MT) plants and transgenic MT lines expressing the At-PTOX cDNA were grown at 22-24°C with a 16 h photoperiod (white light, 60 μmol.m^{-2}.s^{-1}). For pigment analysis, the fruits were harvested at a red stage of development (4 DPB).

[1] first sign of color changing and lycopene accumulation on the blossom end of the mature green fruit

To compare the WT and PTOX$^+$ lines, the influence of the high light intensity on the plants over a long time period was investigated. Four week-old plants grown in a growth chamber under 60 μmol.m^{-2}.s^{-1} at 24°C were exposed to high light intensity (700 μmol.m^{-2}.s^{-1}) at 24°C (measured at the level of the plants) for 3 weeks. Another set of plants remained in a growth chamber under low light intensity for the same time period as control plants (*cf.* chapter 3.3).

2.1.1 Application of different stresses and treatments

2.1.1.1 Photostress

- Cotyledons

For experiments with cotyledons, SM and *gh* seedlings were both grown in darkness for 4 days after seed imbibition to obtain white cotyledons and for 6 days to obtain pale yellow cotyledons. Seedlings were then transferred to either low light (20 μmol.m^{-2}.s^{-1}) or high light intensities (200 μmol.m^{-2}.s^{-1}).

- Green leaves and fruits

For light stress experiments, young (third or fourth pinnate leaf from top and fully elongated) leaves or mature green fruits were harvested 3-4h after the beginning of the photoperiod and incubated at 24°C or 15°C under 60 μmol.m^{-2}.s^{-1} (control) and 1,000 μmol.m^{-2}.s^{-1} (stress). For NADH dehydrogenase enzyme assay and its protein immuno-detection, 250 μmol.m^{-2}.s^{-1} at 24°C was used as a relative high light intensity.

2.1.1.2 Heat treatment

Discs from fully green leaves were placed on moist filter paper and exposed for 10 min to an elevated temperature (42°C) on a thermoelectric plate (Teche, Dri. Block DB 2A, U.K.), covered with aluminium foil (in darkness). Heat treated leaves were then transferred to 25°C and kept at this temperature on moist filter paper for 5 min in dark before fluorescence measurements (*cf.* § 2.3).

2.1.1.3 Inhibitors treatments prior to fluorescence measurement

The effects of various potential inhibitors on photosynthetic electron transfer chain were examined:

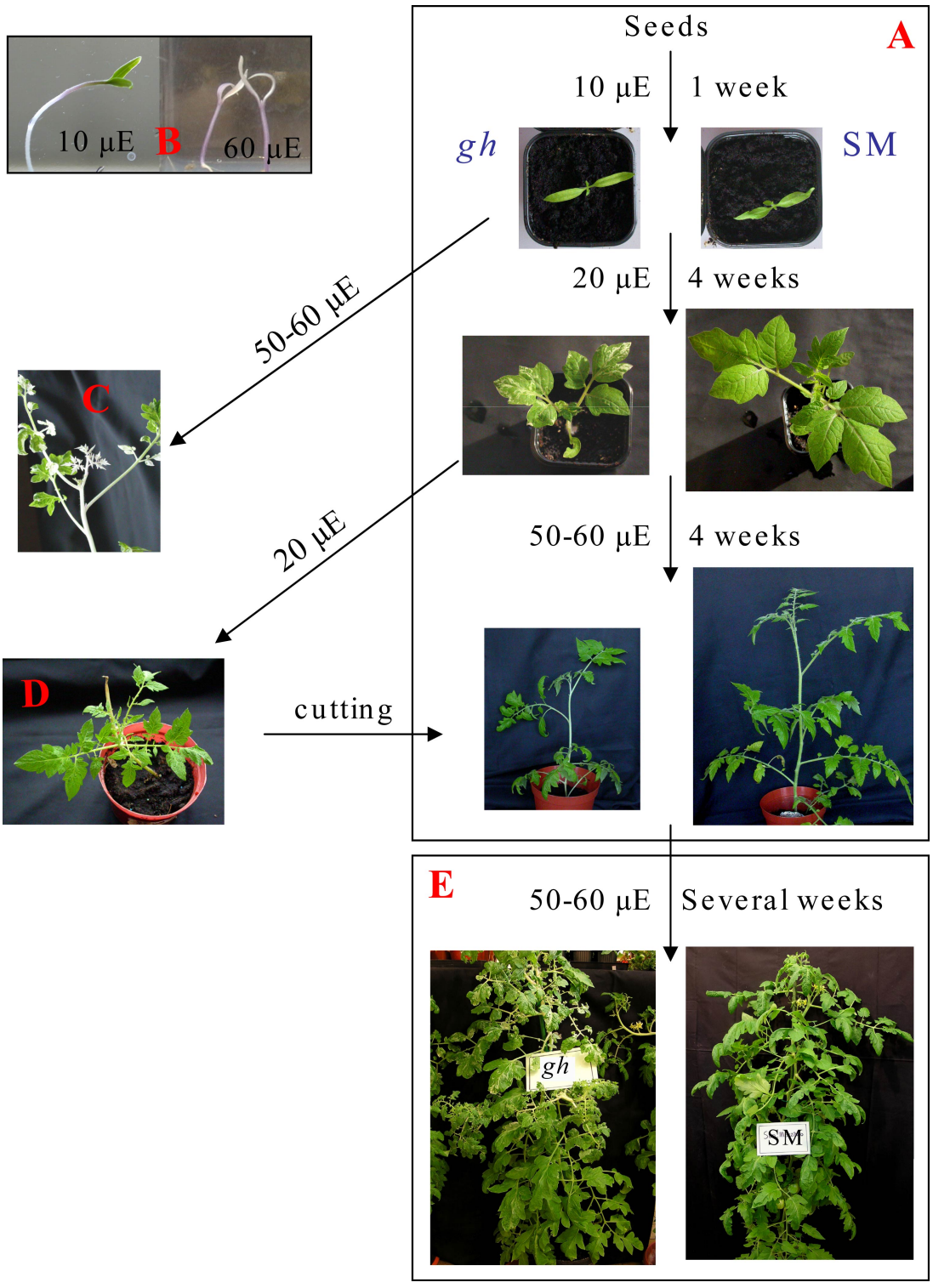

FIGURE 2.1 – **Growth conditions for SM and *ghost* (*gh*) plants to obtain *gh* adult plants with green leaves.**

The leaf discs were infiltrated with or without 50 μM dichlorophenyl dimethylurea (DCMU, 5 min in the dark) for estimating the reduced plastoquinone pool size (*cf.* § 2.3).

Prior to heat stress, we have used diphenyleneiodonium (DPI), a flavoenzyme inhibitor at 50 and 100 μM (in dimethyl sulfoxide, DMSO as a solvent, maximum 1%), and antimycin A (AA) as an inhibitor for PGR5-dependent pathway at 10 μM or 20 μM (in ethanol as a solvent, maximum 1%). Petioles of excised leaves were incubated overnight in the presence of these inhibitors under low light (20 μmol.m^{-2}.s^{-1}).

2.1.1.4 Effects of bleaching herbicides on fruit carotenoids

Bleaching herbicides provided by the Syngentha Company (listed in appendix A.1) were examined to determine their effects on carotenoid desaturation in fruits. The green and ripening fruit explants (pericarp) of *gh* and SM (aproximately 1×1 cm) were incubated with different concentrations of herbicides for given times in each experiment under low light (20 μmol.m^{-2}.s^{-1}, for details see chapter 3.1 and appendix A.3).

2.2 Bacterial system

2.2.1 PTOX overproduction

PTOX is encoded as a precursor proein containig an N terminal transit peptide for its targeting to the plastid. In order to overproduce the mature PTOX protein in *Escherichia coli*, a DNA fragment encoding the mature polypeptids, corresponding to aminoacids 57 to 351 of the precursor was generated by PCR using *Arabidopsis thaliana* (*im*) cDNA as template. Primers IMM2 and IMM3 (see appendix A.2) were used to amplify a 906 bp DNA fragment, adding respectively BamH I and Pst I restriction sites at the 5′ and 3′ ends of the PCR product. These restriction sites allowed the insertion of the DNA fragment into the PQE 31 plasmid (Qiagen, Valencia, CA). This vectot has ampicilline resistant gene and an expression cassette build of a T5 promotor/lac operator element for inducible expression of the recombinant protein and 6x Histidine coding sequence permitting protein affinity purification through Ni-NTA matrices (Qiagen). The mature PTOX coding region was inserted in frame with His tag to generate an N terminal tagged recombinanat protein. *E. coli* XL1-Blue strain (Stratagene) was the host for overexpressing *Arabidopsis* PTOX mature protein. The XL1-Blue strain is tetracycline resis-

tant. Transformation and cloning were performed as described previously (Josse, 2003). In parallel, a control strain with empty PQE 31 vector (without *im* cDNA) was also transformed.

2.2.1.1 Culture conditions

A preculture of the clones containing PTOX in Luria-Bertani broth (LB) medium including of ampicillin (100 μg.L^{-1}) and tetracycline (100 μg.L^{-1}) was performed at 37°C. Then the *E. coli* cells (strain XL1-Blue) were diluted (1/50) in the same medium and grown at 37°C with vigorous shaking until 0.3 OD_{600}. Isopropyl thio-β-D-galactoside (IPTG) was then added (final concentration 40 μM) to induce expression of the recombinant gene during 3h at 30°C. The control strain was grown in parallel. The bacterial pellet was used for both membrane preparation and for protein purification.

2.2.1.2 Bacterial membrane preparation

Bacterial pellet from exponential phase (*cf.* § 2.2.1.1) was resuspended in TMS buffer (200 mM Tris-HCl, pH 7.5, 10 mM $MgCl_2$, 750 mM sucrose) and then diluted in TS buffer (200 mM Tris-HCl, pH 7.5, 750 mM sucrose) to obtain a suspension of bacteria 0.2 g.ml^{-1}. After adding a mixture of anti-proteases [1 mM phenylmethylsulfonyl fluoride (PMSF), 1 μM pepstatin, 1 μM Leu-peptin], lysozyme (200 μg.ml^{-1}) and 25 mM EDTA, pH 8, an incubation was performed for 30 min at 30°C. After disrupting the cells using a French press and by elimination of the debris by centrifugation at 20,000g for 1 min, membranes were pelleted by centrifugation at 100,000g for 1h. The membranes were resuspended in 20 mM Tris-HCl pH 7.5, 10 mM $MgCl_2$, 400 mM sucrose and were used for oxygen consumption measurement (*cf.* § 2.12).

2.2.1.3 PTOX purification under denaturing conditions

Cells were disrupted in a lysis buffer (6 M Urea, 0.1% Triton X-100, 10 mM Tris-HCl, pH 7,5) containing 5 mM imidazole using a French press. The resulting crude extract was clarified by centrifugation at 20,000g for 1 min. The recombinant protein was fixed on affinity Ni-NTA resin (Qiagen) by shaking for 1h at 4°C and then purified. Buffer used for washing the resin was lysis buffer with 5, 10, 20, 30, and 50 mM imidazole successively. Protein elution was performed with 300 mM imidazole. The residual imidazole concentration in the stock suspension was reduced from 300 mM to aproximately 2.5 mM using an exclusion Sephadex G25 column. Purified protein was obtained at a yield of 2.5 mg.g^{-1} of induced culture pellet, aliquoted and

stored at -80°C for subsequent experiments. The amount of proteins was analyzed and the purity was checked by SDS/PAGE and only a single polypeptide band was detected.

2.2.2 Transgenic At-PTOX MicroTom tomato plants over-expressing At-PTOX

In this study, the transgenic At-PTOX MicroTom tomato plants containing the CaMV promoter and the *Arabidopsis thaliana* PTOX cDNA were used.

The construction of transgene was constructed by Joët *et al.* (2002b) as follows: The *Arabidopsis thaliana* PTOX cDNA (GenBank^{TM} accession number AJ004881) was used as a template for PCR amplification using the PTOX primers (see appendix A.2) and the amplified fragment introduced in a sense orientation into a plant binary vector (pKYLX71). Expression of At-PTOX was driven by a double sequence of the cauliflower mosaic virus ^{35}S-labeled constitutive promoter.

Plant transformation was performed by Josse (2003). Briefly, the recombinant plasmid was introduced by electroporation into *Agrobacterium tumefaciens* (strain C58), which was used for tobacco transformation employing the standard leaf disc transformation method (Josse, 2003).

2.2.3 Production of phytoene desaturase *in vitro* and effects of herbicides

The membrane-bound cyanobacter–plant-type phytoene desaturase (PDS) from *Synechococcus* was produced heterologously in *Escherichia coli* Top 10 cells (Invitrogen) using pPDSdeI35 plasmid Schneider *et al.* (1997). *E. coli* transformation was performed by heat shock. Transformants were routinely grown for 30h at 28°C in LB containing chloramphenicol (50 μg.ml^{-1}). After 5h induction with 0.25 mM IPTG at 28°C, herbicides were added (50 μM) for 25h. DMSO was used (0.2%) as a solvent control. The bacterial pellets were used for pigment analysis by HPLC (*cf.* § 2.8.2).

2.3 Chlorophyll fluorescence measurement

Chlorophyll *a* fluorescence was measured with a pulse modulated fluorometer (Walz, Effeltrich, Germany) at room temperature. Leaves and fruits were kept in the dark for 30 min prior to the

measurements. Variable fluorescence (F_v) was calculated as F_m-F_0, where F_0 is the minimum fluorescence (under a weak measuring beam) and F_m the maximum fluorescence (determined after an 800 ms saturating pulse of white light at 2,500 μmol.m^{-2}.s^{-1}). Prior to fluorescence measurements, photoinhibitory conditions were obtained by exposing plant samples to an irradiance of 1,000 μmol.m^{-2}.s^{-1} for 6h or 16h and at 15°C or 24°C.

For experiments using prolonged illumination, actinic white light (200 μmol.m^{-2} .s^{-1}) was used and saturating pulses were applied at 1 min intervals for 10 min to determine the maximum fluorescence (F_m), the steady-state fluorescence (F_s) and, after actinic light was switched off and a brief far-red pulse was applied, to measure the minimum fluorescence (F'_0). The coefficient qP was calculated as (F'_m-F_s)/(F'_m- F'_0) (Schreiber *et al.*, 1989), qN as 1-(F'_m- F'_0)/(F_m-F_0), NPQ as (F_m- F'_m)/F'_m and ΦPS-II as (F'_m-F_s)/ F'_m.

The reduced plastoquinone pool size was estimated as described previously (Weis, 1984). The leaf discs were infiltrated with or without 50 μM DCMU (5 min in the dark) and incubated for 30 min in the dark. The induction of variable chlorophyll fluorescence from the upper side of green leaf discs was examined at 25°C. The intensity of the actinic high light was 20 μmol.m^{-2}.s^{-1}.

Fast fluorescence induction kinetic curves (OJIP) were performed by Dr. Mathias Gilbert (Institute of Biology I, University of Leipzig, Germany), using a Handy-PEA fluorometer (Hansatech Ltd., King's Lynn, Norfolk, UK) as described by (Strasser *et al.*, 2004). Plant leaves were dark-adapted for 5 min, 30 min and 4h in a leaf clip prior to illumination with saturating light of 3,500 μmol.m^{-2}.s^{-1} from 3 red light-emitting diodes (LEDs, duration 1 sec).

2.4 Chlorophyll fluorescence measurement at low temperature (77k)

Chlorophyll fluorescence emission spectra of thylakoid membrane suspensions were recorded in liquid nitrogen (77K) as described by Bellafiore *et al.* (2005). Thylakoid membranes were prepared in a matrix consisting of ice and quartz particles in 20 mM Hepes-NaOH, 3 mM $MgCl_2$, pH 7.5 buffer, and the chlorophyll concentration of the membrane preparations was determined in 80% acetone. Chlorophyll fluorescence emission spectra were recorded with a Jasco FP-750 spectrofluorimeter using thylakoid preparations diluted to an equal chlorophyll concentration (5 μg.ml^{-1}). Excitation light was at 435 nm (10 nm slit width) and emission was

detected from 650 to 800 nm (5 nm slit width). Thylakoid membranes (400 μl) were frozen in liquid nitrogen. Chlorophyll fluorescence emission spectra exhibits one peak at 685 nm and one small shoulder at 695 nm, due to chlorophyll *a* associated with Chl-binding CP43 and CP47 proteins of core antenna of PSII, respectively and one at 735 nm from chlorophyll a molecules associated principally with PSI. All spectra were normalized at 685 nm.

For state transition analysis, after incubation for 30 min in dark, an intact leaf was illuminated for 15 min with 80 μmol m^{-2} s^{-1} blue light (PSII light) from high intensity light source LS2 (Hansatech Ltd., King's Lynn, U.K.) equipped with a Scott BG38 filter. Subsequently a far-red light (PSI light) provided by a LED source with a peak wavelength at 735 nm was switched on (Hansatech Ltd., King's Lynn, U.K.). After each state, Chlorophyll fluorescence emission spectra of thylakoid membrane suspensions were recorded in liquid nitrogen (77K) as described above. This experiment was performed in Department of Molecular Biology and Plant Biology, University of Geneva (Switzerland) by the kind assistance of Dr. Stephane Lobreaux.

2.5 Thermoluminescence measurements

Thermoluminescence measurements were performed on 6 mm leaf discs as described previously (Gilbert *et al.*, 2004). Briefly, leaf discs were pre-illuminated by 2 single turnover flashes at 20°C then dark-adapted for 5 min to establish a defined ratio of S_0/S_1 states in the water-splitting complex and a defined ratio of Q_B/Q_B^- at the acceptor side of PSII. Samples were then cooled to 2°C and illuminated with a single turnover flash to induce charge separation. Then the samples were heated from 2°C to 180°C at a rate of 20°C. min^{-1}. All thermoluminescence steps were performed under N_2 atmosphere to reduce auto-oxidation by O_2. A change in the intensity of the B-band ($S_2Q_B^-$) peaking at 25°C indicates damage of PSII. The amplitude of the 130°C thermoluminescence band (HTL2 band) was used as an index of lipid peroxidation. This experiment was performed in the Institute of Biology I, University of Leipzig (Germany) by a kind collaboration of Dr. Mathias Gilbert.

2.6 Lipid peroxidation measurement

Malondialdehyde (MDA) assays were performed as described by Hodges *et al.* (1999) and Sairam and Srivastava (2001). Aproximately 100 mg of fresh tissue were ground with inert

sand in 1 ml of chilled reagent containing 0.25% (w/v) thiobarbituric acid (TBA) in 10% (w/v) trichloroacetic acid (TCA), followed by centrifugation at 3,000 g for 10 min. After incubation at 95°C for 20 min, the extracts were cooled to room temperature and then centrifuged. TBA reactivity was determined in the supernatant by measuring the absorbance at 532 nm. Non-specific turbidy was determined at 600 nm. For fruit samples, the Hodges protocol was applied to further increase the accuracy of determining TBA-MDA levels by correcting for interfering compounds other than MDA which absorb at 532 nm. The correction was performed by subtracting the absorbance at 532 nm of a solution containing plant extract incubated without TBA from an identical solution containing TBA.

2.7 Isolation of chloroplasts

2.7.1 Intact chloroplasts for NDH enzyme assay

Intact chloroplasts from tomato leaves were isolated as described previously (Martin *et al.*, 1996; Sazanov *et al.*, 1998b) to exclude mitochondrial contamination. All steps were performed at 4°C or on ice, under very low light and within 2h from the start. Leaf segments were homogenized in a blender with six volumes of freshly prepared isotonic buffer (50 mM potassium phosphate buffer, 1 mM L-ascorbic acid, 1 mM EDTA, 330 mM sorbitol, pH 7.0). Intact chloroplasts were collected by low-speed centrifugation of the filtrate. The homogenate was filtered through eight layers of muslin and centrifuged at 200 g for 5 min. The supernatant was centrifuged at 2000 g for 10 min. The chloroplast pellet was washed with this buffer (10 ml per 1 g original leaves) to obtain a preparation of chloroplasts free from soluble or mitochondrial fractions. To obtain a high percentage (>80%) of intact chloroplasts, all steps from leaf segments to washed chloroplast pellet were performed at 0-5°C within 45 min. The chloroplast pellet was resuspended in this buffer without sorbitol at 0-4°C for osmotic shock. After gentle shaking for 6 min, centrifugation was for 15 min at 4,500g. The thylakoid pellet was resuspended to approximately 2 mg protein per ml in re-suspension buffer and used for solubilisation of thylakoid-bound NDH complex. An equal volume of the re-suspension buffer supplemented with 2% dedecyl maltoside (DM, a non-ionic detergent) was added to the thylakoid suspension in a drop wise manner (0.1 mg detergent per mg protein). Samples were briefly vortexed and kept for 5 min on ice. Non-solubilized material was removed by centrifugation at 20,000g for 20

min. The supernatant (aproximately 1 mg protein per ml) contained the NADH dehydrogenase solubilized from thylakoids.

Normally, no mitochondrial contamination is detected in the thylakoid preparation following this protocol (Sazanov *et al.*, 1998b). However, to check for any possible mitochondrial contamination, we used an antibody specific for plant mitochondrial protein, protein T as a probe, and no contamination was detected (data not shown).

The chloroplast pellets were used for protein analysis by SDS-PAGE (*cf.* § 2.10.3) and then immunological detection of proteins (*cf.* § 2.10.5).

2.7.2 Highly purified intact chloroplasts

An intact chloroplast fraction was obtained according to "*Methods in Molecular Biology*", vol. 82 (described by J. Martinez-Zapater and J. Salinas) with some modifications for fruits as discussed below. All steps were performed at 4°C or on ice, under very low light. Leaf or fruit segments were rinsed in deionised water prior to homogenisation in buffer (330 mM sorbitol, 2 mM EDTA, 1 mM $MgCl_2$, 250 mM Hepes-NaOH pH 6.8, 0.1% BSA) in a Waring Blender for 3×4 sec. The homogenate was filtered through muslin and cheese cloth then centrifuged at 3,000g for 10 min at 4°C. The chloroplast pellet was resuspended in resuspension buffer (RB, 330 mM sorbitol, 20 mM Hepes-NaOH, pH 7.6, 5 mM $MgCl_2$, 25 mM EDTA), and loaded on a discontinuous 40%-80% Percoll gradient (in RB buffer). After centrifugation at 3,500g at 4°C for 20 min, highly purified intact chloroplasts were obtained on the 40% Percoll cushion. The chloroplasts were then washed in RB buffer (Percoll-free) and centrifuged for 3 min at 5,000g.

The intact chloroplasts were subjected to osmotic shock in diluted RB buffer or in shock buffer (10 mM MOPS/NaOH, pH 7.8, 4 mM $MgCl_2$, 2.5 mM EDTA). Magnesium can be preserving the membranes. The thylakoid suspension was kept at 4°C until required for oxygen consumption (§ 2.12.2) electron chain activity (*cf.* § 2.13) measurements. To check for any possible mitochondrial contamination, we used an antibody specific for plant mitochondrial protein, protein T as a probe and no contamination was detected.

2.7.3 Isolation of thylakoid membranes

Thylakoid membranes from tomato leaves were isolated basically as described previously (Baena-Gonzalez *et al.*, 2003). Leaves were homogenized in ice-cold buffer containing 50 mM Hepes,

pH 7.5, 5 mM $MgCl_2$, 1 mM EDTA, 330 mM sorbitol, and 1% BSA. The homogenate was filtered through muslin and cheese cloth then centrifuged for 5 min at 6,000 g. The resulting pellet was washed with 10 mM Hepes, pH 7.5, 5 mM $MgCl_2$, and 5 mM sorbitol and re-centrifuged. The thylakoid membranes were then finally suspended in 10 mM Hepes, pH 7.5, 10 mM $MgCl_2$, 5 mM NaCl and 100 mM sorbitol. These solubilized thylakoid membranes were used for Blue native (BN) gel electrophoresis(*cf.* § 2.10.6).

2.7.4 Chlorophyll content determination

In all the above-mentioned experiments, after solubilization of the plastidial suspension in 80% acetone (v/v), chlorophyll content was estimated at 652 nm using the equation:

[Total chlorophyll] ($mg.ml^{-1}$) = ($A_{652} \times d$)/36

Where, d equals the dilution factor of the membrane suspension in acetone 80% (Bruinsma, 1961).

2.8 Pigment analysis

2.8.1 Pigment extraction

2.8.1.1 Leaf or fruit samples

Pigments were extracted from minced lyophilized samples (5 mg leaves or cotyledons, 10 mg fruit pericarp) using methanol (neutralized with 5 mM Tris-HCl, pH 7.5). In addition, one volume of 5 mM Tris-HCl, pH 7.5 was added to fruit methanolic extracts, then phase-partitioned with a volume of chloroform. The aqueous phase was re-extracted twice with chloroform and the pigments dried under N_2 from the pooled chloroform phases. The pigments were resuspended in a minimum volume of either dimethylformamide (DMF, for leaf) or ethyl acetate (for fruit).

2.8.1.2 Pigments extraction from bacterial pellets

The bacterial pellets (*cf.* § 2.2.3) were obtained after 5 min centrifugation at 3,000g. Pigments were extracted from lyophilized pellets using methanol. The methanolic extracts were dried under N_2 before resuspension in a minimum volume of ethyl acetate.

2.8.2 High-performance liquid chromatography analysis

The HPLC method used to analyze and quantify phytoene, carotenoids and chlorophylls has been detailed by Fraser *et al.* (2000). Briefly, separations were performed on a C_{30} reverse-phase column (250×4.6 mm) manufactured by YMC Co. Ltd., and purchased from Interchim (France). The mobile phases used were: methanol (A), methanol 80% in water (v/v) containing 0.2% ammonium acetate (B) and tert-methyl butyl ether (C). The gradient used was 95% A / 5% B isocratically for 12 min, a step to 80% A / 5% B / 15% C at 12 min, followed by a linear gradient to 30% A / 5% B / 65% C for 30 min. Identification of carotenoids was achieved by comparing retention times and spectral properties of authentic standards. Quantification was performed from standard curves.

2.9 Nucleic acids analysis

2.9.1 Nucleic acids extraction methods

2.9.1.1 Genomic DNA extraction

Isolation of DNA from plants was performed according to Doyle and Doyle (1987). Small amounts of plant material (fresh leaf tissue) were homogenized with 100 μl extraction buffer [CTAB (hexadecyltrimethyl-ammonium bromide 1%), 1 M NaCl, 50 mM EDTA, 200 mM Tris-HCl, pH 7.5, 0.02% β-mercaptoethanol, 0.2% sarcosyl] and then heated for 15 min at 65°C. Proteins were removed from samples by two phenol-chloroform (50:50) washing steps and DNA was precipitated with 2/3 assay volume of cooled iso-propanol. The DNA was pelleted by centrifugation for 20 min at 10,000g, washed with 70% then 100% ethanol, and dissolved in TE buffer or sterile water. The isolated DNA was used for both DNA amplification by Polymerase Chain Reaction (PCR) and Southern blot analysis.

2.9.1.2 Extraction of total RNA

Isolation of total RNA from tomato leaf was carried out as described previously (Simkin, 2002). Frozen and ground material was added to the extraction buffer (0.1 M Tris-HCl, pH 8.0, 10 mM EDTA, 0.1 M LiCl, 1% SDS), mixed with 1 volume water-saturated phenol preheated to 65°C then vortexed. The samples were centrifuged and the aqueous phase was recovered and re-extracted with 1 ml of chloroform. The aqueous phase was collected upon centrifugation and

precipitated overnight with 0.5 volumes 6 M LiCl. Following centrifugation, the pellet was washed with 70% ethanol then 100% ethanol, dried and resuspended in water and precipitated with 2 volumes absolute ethanol and 0.1 volume Na acetate.

2.9.2 RNA quantification

Concentration and purity of total plant RNA was determined by spectrophotometric analysis (Spectrometry Hitachi) at 260 nm. All RNA samples in each experiment were analyzed by agarose/MOPS/formaldehyde gel electrophoresis and rRNA bands were detected with ethidium bromide staining (Sambrook *et al.*, 1989).

2.9.3 RNA purification and DNAase treatment

RNA samples were treated with DNAase I in 25 μl buffer (20 mM Tris-HCl pH 7.0, 6 mM $MgCl_2$, 40U RNAase inhibitor [RNAase-out, GibcoBRL], 1U DNAase I) to remove DNA contamination, followed by re-purification by phenol/chloroform extraction.

2.9.4 Complementary DNA synthesis through Reverse Transcription (RT)

The reverse transcription (RT) technique enables synthesis of single strand cDNA from RNA matrices. RT was carried out using 500 ng of total RNA and oligo-dT as a primer. The reaction mixture included 1 mM dNTPs, 0.5 μM oligo-dT, and 20U RNAase inhibitor, 10 mM DTT, 1$\times$ RT buffer and 150U M-MLV reverse transcriptase. The reaction mixture was incubated for 60 min at 37°C then 15 min at 75°C.

2.9.5 DNA amplification by Polymerase Chain Reaction (PCR)

The PCR reaction contained 100-250 ng of each primer, 1$\times$ Taq polymerase buffer, 2.5 mM MnCl2, 0.20 mM dNTPs, 1.5U Taq polymerase (GibcoBRL) and 2 μl genomic DNA, or 2 μl RT reaction mixture, RNA (25 ng.μl^{-1}).

The primers used for reactions were IMM-2, 3 and PDS-1, 2 for identification of transgenic plants and TIM-3, 4, Elip, APX 2, and Act-I were used as a control for RT-PCR (sequences of the primers are listed in appendix A.2). After initial denaturation for 1.5 min at 95°C, the amplification reactions included 22 to 24 cycles (RT-PCR) and 30 cycles (genomic DNA) of 45

sec at 95°C for denaturation, 30 sec at 55°C for annealing and, 90 sec at 72°C for extention and 10 min at 72°C for final extention.

2.9.6 Sequencing

PCR products were purified using the Qiaquick kit (Qiagen) follwing the manufacturer's instruction. Purified PCR products were used as the template in 20 μl BigDye Terminator Cycle Seqencing Kit version 3.1 (Applied Biosystems). SeqScape 2.5 (Applied Biosystems) was used to reconcile chromatograms of complementary fragments and to aligne sequence across tomato MicroTom transgenic lines and *immutans* (EMBL accession number AJ004881).

2.9.7 Southern hybridization

This DNA-DNA hybridization technique is used for characterization of a PCR amplified cDNA fragment through or directly for genomic DNA analysis. The genomic DNA was restricted with the desired enzyme (in presence of the corresponding buffer) for 2-3h at 37°C and digestion was terminated by enzyme denaturization at 65°C for 15 min. For a Southern analysis, 5 μg of digested genomic DNA was electrophoretically separated in an agarose gel. DNA transfer from the gel to nitrocellulose membrane was performed by capillary blotting as described in Sambrook *et al.* (1989).

2.9.7.1 Radioactive probe labeling

- Radioactive labeling of PCR products

PCR products (100 ng DNA) were radio labeled by the random priming method with Klenow enzyme and ^{32}P-dCTP (according to Sambrook *et al.*, 1989). For this assay, the Random Primed DNA Labeling Beads Kit (Amersham Pharmacia BioTech.) was used according to the manufacturer's protocol.

- Radioactive labeling of oligodeoxynucleotides

The reaction mixture (45 μl) contained 0.5 mM oligodeoxynucleotides, 2.5 μl 10$\times$ PNK buffer, 5 μl [α-^{32}P]-CTP, 2U of *E. coli* DNA polymerase Klenow. The 5$'$ hydroxy group of synthetic oligonucleotides (primers) was radioactively labeled by a 30 min incubation at 37°C with DNA polymerase. Residual radioactive mononucleotides were removed by filtration through an exclusion Sephadex G50 column.

2.9.7.2 Hybridization procedure

The membrane was prehybridized for at least 2h at 65°C in the hybridization buffer (50 μl.ml$^-$1 Denhardt's solution [containing 1% Ficoll, 1% PVP and 1% BSA], 6× SSC, 0.5% SDS (w/v), 20 μg.ml^{-1} herring sperm DNA). Hybridization was performed by incubation of the membrane with the denatured radiolabeled probe in 25 ml of hybridization buffer overnight at 65°C. The membranes were successively washed by 2× SSC, 0.1% SDS and finally with 0.2× SSC to eliminate SDS. The membranes were autoradiographed (Kodak BioMax MR Film) and the exposition time was normally 16h at -80°C.

2.10 Protein analysis

2.10.1 Extraction of total proteins

Total proteins was extracted from frozen and ground material using the Hurkman and Tanaka method (Hurkman and Tanaka, 1986). The samples (300 mg) were extracted using the Tanaka buffer (700 mM sucrose, 500 mM Tris-HCl, pH 8, 5 mM EDTA, 10 mM NaCl, 2% β-mercaptoethanol (v/v), 2 mM PMSF). One volume of phenol was added for 20 min with vigorous shaking at room temperature. The phenolic phase was separated by 5 min centrifugation at 12,000g. The proteins in the phenolic phase were precipitated with (5:1) 100 mM ammonium acetate (in methanol) overnight. The proteins were washed with 100% acetone (v/v), and solubilized in deposit buffer (2.5% glycerol (v/v), 0.6% SDS (w/v), 15 mM Tris-HCl, pH 6.8, 37.5 mM NaCl). The protein pellet were stored at -20°C.

2.10.2 Determination of the protein concentration

A protein assay quantification kit (Dc, Bio-Rad), based on the Lowry method (Lowry *et al.*, 1951) was used. The protein concentration was determined using a standard curve with samples of known protein concentrations (BSA from 0.2 to 1.5 mg.ml^{-1}). Absorbance measurments were performed at 750nm.

2.10.3 Protein analysis by SDS-polyacrylamide electrophoresis (SDS-PAGE)

Protein samples were fractionated by SDS/polyacrylamide gel electrophoresis. The "separation" and "concentration" gels were prepared according to *Molecular Cloning* : *a Laboratory*

Manual (Sambrook *et al.*, 1989) (chapter 18.52). The protein pellet (*cf.* § 2.10.1) was solubilized in deposit buffer (2.5% glycerol (v/v), 0.6% SDS (w/v), 15 mM Tris-HCl, pH 6.8, 37.5 mM NaCl) and proteins were denatured in the presence of 5% β-mercaptoethanol (v/v) and 0.05% bromophenol blue (w/v) at 95°C for 3-5 min. To avoid protein dimer formation, denaturation of the thylakoid complex proteins including of NDH complex, was performed at 37°C for 30 min. The same protein amounts were loaded on the gel. The electrophoresis buffer was 25 mM Tris-HCl, pH 8.6, 200 mM glycine, 0.1% SDS. For PTOX protein, 13% acrylamide gels were used. The protein separation was performed at constant current (30 mA per mini-gel) for 1h10 to 1h30.

2.10.4 Staining of polyacrylamide gels with Coomassie Brilliant Blue

The gels were incubated in staining solution (25% isopropanol (v/v), 10% acetic acid (v/v), 0,15% (w/v) Coomassie blue R250 (Serva) for 1h with constant shaking. Destaining with Solution I [40% ethanol (v/v), 10% acetic acid (v/v)] for 30 min was followed by destaining with Solution II [10% ethanol (v/v), 7% acetic acid (v/v)] until protein bands were clearly visible.

2.10.5 Immunological detection of proteins on membranes

(Burnette, 1981)

2.10.5.1 Transfer of proteins onto nitrocellulose and PVDF membranes

The proteins separated by SDS-PAGE were transferred onto membranes using an electrophoretic liquid blotting system (Burnette, 1981). PVDF membranes were pre-soaked in 100% ethanol for 10 sec. 3 mm Whatman paper and membranes were soaked in transfer buffer (Tris-HCl 25 mM, pH 8.6, glycine 192 mM, 0.04% SDS (w/v), 20% ethanol (v/v)) for 5 min. A sandwich system was set up. The gel was placed on the cathode side and transfer membrane was placed on the anode side and this assembly was covered with transfer buffer in a buffer tank. The transfer was performed at constant current of 200 mA for 1h10 to 1h30.

2.10.5.2 Staining of blots with Ponceau S

To determine transfer quality, after blotting the membrane was incubated in Ponceau S (3-hydroxy-4-[2-sulfo-4- sulfophenylazo) phenylazo]-2,7-naphtalene disulfonic acid) solution (0.2%

(w/v) Ponceau S, 1.0% acetic acid) for few minutes at room temperature with agitation. The membrane was rinsed with water and the positions of the molecular marker bands were marked. The membrane was finally destained in water.

2.10.5.3 Western analysis using horseradish peroxidase-conjugated antibodies

After electrophoretic transfer of the proteins from a polyacrylamide gel the membrane was incubated in blocking buffer (1× TBS, 5% dry milk powder (w/v), 0.1% Tween 20 (v/v)) for 1h at room temperature. The antiserum was diluted to the desired concentration in blocking buffer was incubated with the membrane for 3h at room temperature or overnight at 4°C. Antibody was removed by washing the membrane three times for 10 min in washing buffer (1× TBS, 0.1% Tween 20 (v/v)). Immuno-detection was performed using the horseradish peroxidase-conjugate substrate kit (Bio-Rad). Anti-rabbit antibodies were diluted in blocking buffer and incubated with the membrane for 1h at room temperature. The membranes were then washed three times for 10 min in washing buffer and developed in a mixture of solution 1 and 2 (1:1) of "Enhanced Chemi-Luminescence" (ECL western blotting kit, Amersham) by incubation for 1 min. Exposuree to X-ray films was for the required time (Hyperfilm; Amersham Life Science, U.K.).

2.10.5.4 Antibodies

Anti-PTOX antibodies were produced in our laboratory (Josse *et al.*, 2000). The antibodies against the H subunit of the NDH complex were kindly provided by Dr. Dominique Rumeau (Laboratoire d'écophysiologie de la photosynthèse, CEA de Cadarache). The other antibodies were obtained from Agrisera AB (Vännäs, Sweden). Polyclonal goat anti-rabbit IgG peroxidase-conjugate antibody were obtained from Bio-Rad.

2.10.5.5 Densitometry analysis of the immunoblots

Densitometry analysis of the immunoblots was performed using the Image J software (Wayne Rasband, NIMH, Maryland, USA).

2.10.6 Blue Native Acrylamide gel Electrophoresis (BN/PAGE)

Freshly isolated thylakoid samples were electrophoretically fractioned in a BN acrylamide gel. BN/PAGE was carried out as described by Baena-Gonzalez *et al.* (2003). Washed thylakoids

were suspended in the re-suspension buffer (20% (w/v) glycerol and 25 mM BisTris-HCl, pH 7.0) at a concentration of 1.0 mg chlorophyll per ml. An equal volume of the re-suspension buffer supplemented with 2% DM was added to the thylakoid suspension in a drop wise manner. Samples were briefly vortexed and kept for 5 min on ice. Non-solubilized material was removed by centrifugation at 20,000g for 20 min. The supernatant was combined with 1:10 volume of 5% Serva blue G (100 mM BisTris-HCl, pH 7.0, 500 mM 6-amino-n-caproic acid, 30% glycerol) and applied to a 1.0-mm-thick 5-13% acrylamide gradient gel in a small vertical electrophoresis unit (Amersham Pharmacia Biotech, USA). Electrophoresis was performed at 4°C as follows: 75 V, 30 min, 100 V, 30 min, 125 V, 30 min, then 150 V, 30 min. At this point, when the dye had migrated half way on the gel, the cathode buffer was replaced by buffer without dye, and electrophoresis was continued as follows: 150 V, 30 min, 175 V, 30 min, then 200 V, 60 min.

2.11 NADH:FeCN oxidoreductase enzyme assay

The NADH:FeCN oxidoreductase activity specific of NDH complex was assayed at 30°C by measuring the reduction of FeCN at 420 nm (extinction coefficient: 1.03 $mM^{-1}.cm^{-1}$) and the oxidation of NADH at 340 nm (extinction coefficient: 6.22 $mM^{-1}.cm^{-1}$) in a Varian spectrophotometer (Carry 50 scan-UV visible with single cell Peltier accessory) as described by Casano and co-workers (1999). The reaction mixture, with a final volume of 1.0 ml, included 50 mM potassium phosphate, pH 7.5, 1 mM Na_2-EDTA, 0.2 mM NADH, 1 mM FeCN and 40 μg thylakoid protein preparation. The rate was determined from the linear absorbance decrease between 45 and 240 sec. Control values obtained without protein were subtracted.

2.12 Measurement of oxygen consumption

Measurement of oxygen consumption was performed using a Clark-type electrode (Hansatech, King's Lynn, U.K.). Calibration of the electrode was performed at 25°C. The zero point for O_2 synthesis was determined by calculation of the difference between measurements with oxygen-free water (1 ml H_2O + a few crystals of $Na_2S_2O_4$), and oxygen-saturated water (1 ml). Using the constant values of the oxygen content of air-saturated water, the μmol of O_2 produced could be calculated for 1 ml of solution and 1 cm of recorder printout.

2.12.1 Oxygen consumption in *E. coli* membranes

A typical assay for oxygen consumption in *E. coli* membranes overexpresssing *Arabidopsis* PTOX protein and *E. coli* control membranes (without PTOX) was performed as described by Josse *et al.* (2003). The respiration activity using 100 μg of membrane protein (*cf.* § 2.2.1.2) in the following buffer: 50 mM Tris-Maleate, pH 7.5, 10 mM KCl, 5 mM $MgCl_2$, 1 mM EDTA in the presence of 0.2 μM decyl-plastoquinone (dPQ) and 1 mM NADH, was measured. To block respiration, 2 mM KCN or 50 μM octyl gallat (OG) was used. In this set of experiments, the effects of different herbicides at 50 and 100 μM were examined prior to KCN or OG addition.

2.12.2 Dark oxygen uptake measurement in intact chloroplasts

Intact chloroplasts from sweet pepper or tomato fruits (§ 2.7.2) were subjected to a gentle osmotic shock and thylakoid suspensions were immediately used for dark oxygen uptake measurement (as described by Nievelstein *et al.*, 1995) with modifications as described below. For measurements, 1 ml of intact chloroplast suspension (equivalent to a chlorophyll concentration of 25 $\mu g.ml^{-1}$) in RB buffer (300 mM sorbitol, 20 mM Hepes-NaOH, 5 mM $MgCl_2$, 25 mM EDTA, pH 7.6) in the presence of 0.2 μM decyl-plastoquinone (dPQ) and 1 mM NADH or 1 mM NAD(P)H was used. To block respiration, 2 mM KCN or 50 μM octyl gallat (OG) was used.

The following treatments were applied to thylakoid membranes, prior to O_2 uptake measurements, in order to examine the effects of protein denaturation or plastid membrane disturbance: 1- the thylakoid suspensions were heated at 95°C for 30 sec. 2- A non-ionic detergent such as Triton X-100 [0.1% (v/v) in final volume] was added to samples, 3- The thylakoid suspension was incubated with subtilisin (20 $mg.ml^{-1}$) as a global protease for 5 min at 25°C (Subtilisin enzyme stock in buffer 100 mM Tris-HCl, pH 8, 100 mM $CaCl_2$), 4- The thylakoid suspension was sonicated at maximum intensity using an ultra-sound electrode (*i.e.* 60v for 3×30 sec)

2.13 Electron transport chain assay (Hill reaction)

The intact chloroplasts from tobacco leaves (*cf.* § 2.7.2) were subjected to osmotic shock and the thylakoid suspensions were used for a typical transport chain assay in photosynthetic membranes Simkin *et al.* (2007). 2,6-dichlorophenolindophenol (DCIP, 0.2 mM final concentration) was used as final electron acceptor during measurement of electron chain transport in thylakoid

suspensions (with 15 μg.ml^{-1} chlorophyll final concentration) in RB buffer (300 mM sorbitol, 20 mM Hepes-NaOH, pH 7.6 5 mM $MgCl_2$, 25 mM EDTA). Reduction of DCIP was followed at 600 nm using an UVIKON spectrophotometer under 90 klux illuminations. The average values of DCIP reduction over the illumination times in three independent experiments are presented.

Chapter 3

Results

3.1 The Dual Role of the Plastid Terminal Oxidase (PTOX) in Tomato

PTOX is a plastoquinone (PQ)-O_2 oxidoreductase (plastoquinol oxidase) whose absence gives rise to the *immutans* phenotype in *Arabidopsis thaliana* and to the *ghost* (*gh*) phenotype in tomato (Carol *et al.*, 1999; Wu *et al.*, 1999b; Josse *et al.*, 2000; Carol and Kuntz, 2001; Rodermel, 2001; Aluru *et al.*, 2006). These phenotypes are characterized by variegated leaves consisting of green and bleached sectors and, in addition, in tomato by a yellow-orangey ripe fruit. The latter is characterized by reduced carotenoid content (Barr *et al.*, 2004). In addition, bleached leaf sectors accumulate the carotenoid precursor phytoene, indicating that PTOX functions as a co-factor for the carotenoid dehydrogenases, namely phytoene desaturase (PDS) and most likely ζ-carotene desaturase (ZDS). These conclusions are consistent with the known involvement of a quinone as a co-factor for PDS (Mayer *et al.*, 1990; Norris *et al.*, 1995). PDS and ZDS sequentially catalyze the conversion of the colorless phytoene to lycopene (the main pigment in red tomato fruit), which in turn is converted to various photoprotective carotenoids. Thus, the phenotype observed in the absence of PTOX can be explained by a reduced ability to synthesize carotenoids leading to photobleaching of green tissues. However, based on *in situ* hybridization and reporter gene experiments, it has been shown that PTOX gene expression is not strictly connected with carotenoid accumulation as it can been detected in all tissues and organs throughout development (Aluru *et al.*, 2001).

The sequence homology of PTOX to mitochondrial alternative oxidase (AOX) and its function as a plastoquinol oxidase suggested that it might be involved in the reoxidation of plastoquinonol in chlororespiration (Carol *et al.*, 1999; Wu *et al.*, 1999a; Josse *et al.*, 2000; Carol and Kuntz, 2001). The first evidence for this role has come from experiments in PSI-deficient *Chlamydomonas* and in tobacco that overexpress *Arabidopsis* PTOX (Cournac *et al.*, 2002; Joët *et al.*, 2002a), which suggested that PTOX might interact with the photosynthetic electron transport system by decreasing the overreduction of the photosynthetic electron carriers. Interestingly, PTOX, like the NDH complex, was found to be present in the stromal lamellae where

cyclic electrons transfer reactions around PSI take place (Lennon *et al.*, 2003). This has led to the idea that PTOX plays a role in regulating the cyclic flow of electrons around PSI.

A further PTOX function is as a "safety valve" in photooxidative stress. PTOX protein levels increase under low light in double antisense tobacco plants lacking two hydrogen peroxide detoxifying enzymes, catalase and ascorbate peroxidase (Rizhsky *et al.*, 2002). PTOX is also induced under high light and high temperature conditions (Quiles, 2006). These studies suggest that PTOX may be involved in detoxifying excess electrons via chlororespiration. However, apart from implication of PTOX in carotenoids biosynthesis, a more direct role for PTOX in photosynthesis has not been throughly investigated due to the carotenoid-deficient phenotype of PTOX^{-} mutants making such studies very complex.

In the present chapter, various tomato organs including of the cotyledons, leaves and fruits were used under experimental conditions leading to photobleaching to examine whether the absence of PTOX is linked to an abnormal carotenoid content or to an abnormal photosynthetic electron transport. We used gradually increasing light intensities during the plant growth period in order to obtain fully green leaves and fruits in *ghost* plants. These fully green leaves and fruits are ideal for studying a potential role of PTOX in photosynthesis, because their homogenous pigments content will avoid the well-known photooxidative conditions imposed by a deficiency in photoprotective carotenoids. In contrast, the green sectors of variegated leaves and fruits are less suitable since these tissues contain a heterogeneous population of photosynthetically competent cells with photooxidized tissue displaying vastly different physiological properties than green tissue.

3.1.1 Effect of PTOX deficiency in cotyledons

SM and *gh* seedlings were grown in darkness for 4 days after seed imbibition to obtain white cotyledons (time point T_0). Seedlings were then transferred to either low light (20 μmol.m^{-2}.s^{-1}) or high light intensity (200 μmol.m^{-2}.s^{-1}) for 24h. As shown in figure 3.1A, after 24h high light illumination, the *gh* cotyledons became photo-bleached, and anthocyanins were clearly formed even under low light conditions. Pigment analysis was performed by high-performance liquid chromatography (HPLC). Figure 3.1B shows that at T_0 cotyledons from both SM and *gh* were almost devoid of chlorophylls, and the carotenoid (mainly lutein and violaxanthin) levels were low, but slightly higher in SM than in *gh*. Within the low light period, both cotyledon types

accumulated substantial amounts of chlorophylls *a* and *b* and carotenoids (including β-carotene and traces of other compounds). All pigment levels in *gh* were reduced to around half the amount found in SM.

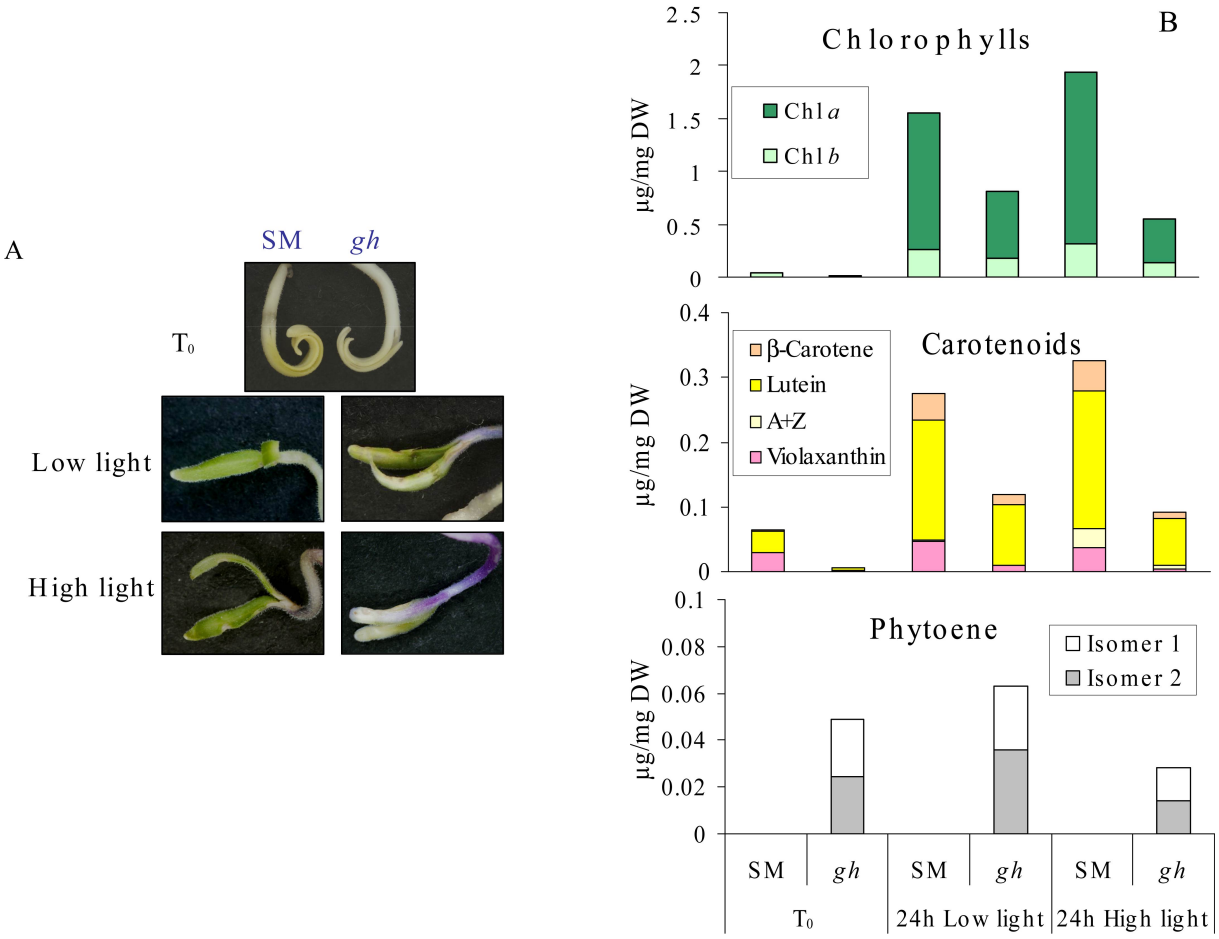

FIGURE 3.1 – **Effects of low and high light intensity on the dark-adapted San Marzano (SM) and *ghost* (*gh*) tomato seedlings. Photobleaching in *gh* cotyledons (A) and cotyledons pigment contents (B). Seedlings were grown in darkness for 4 days after seed imbibition to obtain white cotyledons (T_0 time point). Seedlings were then transferred to either low light (20 μmol.m^{-2}.s^{-1} PAR) or a high light intensity (200 μmol.m^{-2}.s^{-1} PAR). Samples were analyzed after 24h illumination. Eight cotyledons were pooled for a given measurement. Each measurement was repeated 3 times with a different pool of cotyledons. Standard errors of the mean values were all lower than 12% (not shown). Whether changes are statistically significant is discussed in text.**

Under high light conditions (Fig. 3.1B), a slightly higher level (not statistically significant) of pigments was observed in SM (including the xanthophyll cycle pigments antheraxanthin and zeaxanthin, A+Z) when compared to low light, while this increase was not observed in *gh* (the chlorophyll content is even reduced in *gh* under high light compared to low light).

The carotenoid precursor phytoene was not detected in SM under any condition but was present (as 2 isomers) in *gh* at T_0 (Fig. 3.1B). A rise in phytoene level was observed in *gh* under

low light but was not statistically significant. The accumulation of phytoene is most likely the result of 2 parameters: (i) the activity of the whole biosynthetic pathway, (ii) the limiting rate of PDS activity in the absence of PTOX. However, phytoene levels in *gh* were lower under high light than under low light (statistically significant, P<0.01), despite the fact that the carotenoid biosynthetic pathway seems active under high light (as deduced from the high levels of colored carotenoid in SM). Since lower levels of colored carotenoids and chlorophylls are also found in *gh* under high light *vs*. low light, the simplest explanation for these observations is an increased photodestruction of all these compounds.

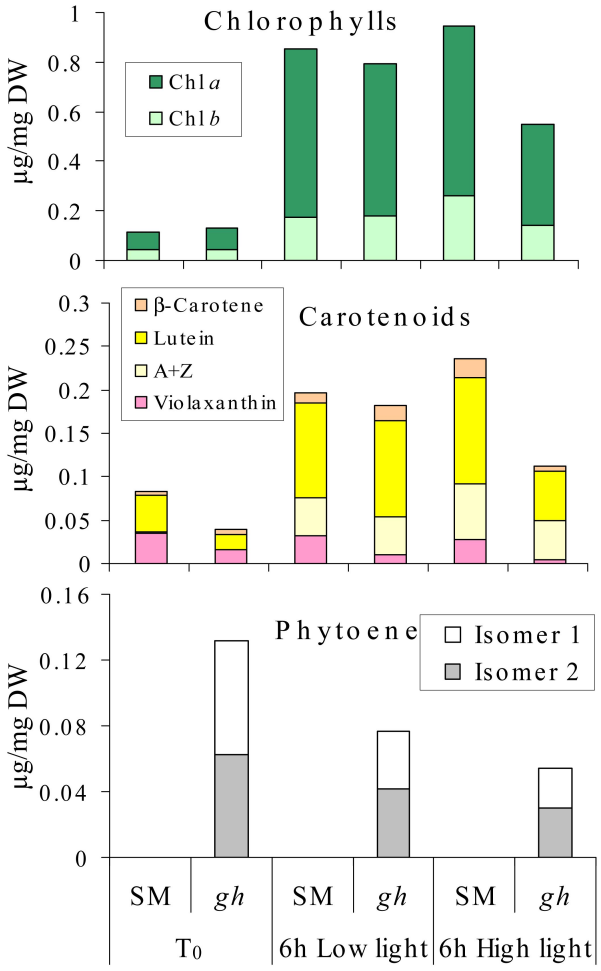

FIGURE 3.2 – **Pigment contents of cotyledons from SM and *gh* tomato lines. Seedlings were grown in darkness for 6 days after seed imbibition to obtain pale yellow cotyledons (T_0 time point). Seedlings were then transferred to either low light (20 μmol.m^{-2}.s^{-1} PAR) or a high light intensity (200 μmol.m^{-2}.s^{-1} PAR). Samples were analyzed after 6h illumination. Eight cotyledons were pooled for a given measurement. Each measurement was repeated 3 times with a different pool of cotyledons. Standard errors of the mean values were all lower than 12% (not shown). Whether changes are statistically significant is discussed in text.**

Seedlings grown for a longer period (6 days) in darkness (time point T_0 in Fig. 3.2) showed a faint yellow color. Significantly higher carotenoid levels were present in SM than in *gh*. The same low or high light conditions were then applied during 6h. Low light led to an increase in chlorophyll and carotenoid levels, with no significant difference between SM and *gh*. Compared to low light, high light triggered again a slight increase (not statistically significant) in pigment levels in SM. In *gh*, significantly lower pigment levels were observed under high light compared to SM. In addition, its phytoene levels under high light were lower than at T_0 (statistically significant, $P<0.01$) which can be explained in part by photodestruction. The fact that lower levels of phytoene were also observed in *gh* under low light at 6h than at T_0 (statistically significant, $P<0.05$) is more surprising and may suggest that carotenoid biosynthesis is less active (since the carotenoid content was almost normal; see Fig. 3.2).

Taken together, these data suggest that PTOX deficiency leads to photobleaching in cotyledons exposed to high light primarily as a consequence of a reduced ability to synthesize colored carotenoids in the mutant, which is fully consistent with the known role of PTOX as a PDS cofactor.

3.1.2 Effect of PTOX deficiency in leaf

3.1.2.1 Pigment content under low and moderate light conditions

When grown under standard growth chamber conditions, SM and *gh* plants produce green and variegated leaves, respectively. The color aspect of *gh* leaves is decided at a very early leaf developmental stage. As shown in figure 3.3A, depending on light intensity at an early seedling developmental stage (see Materials and Methods) *gh* leaves which are mainly green, variegated, or mainly white could be obtained (sample numbers 2, 3, and 4, respectively in Fig. 3.3A). Initially, we allowed the plants to germinate and grow at low light intensity (10 μmol.m^{-2}.s^{-1} for 1 week and then 20 μmol.m^{-2}.s^{-1} for 4 weeks) and subsequently they were placed at 60 μmol.m^{-2}.s^{-1} to obtain adult plants with green leaves for *gh*. Both white and variegated *gh* leaves were obtained by incubation of seedlings directly at 60 μmol.m^{-2}.s^{-1}.

Pigment analysis of SM leaves and fully green, mainly variegated or mainly white *gh* leaves (sample numbers 1, 2, 3, and 4, respectively in Fig. 3.3) were performed by HPLC. The results presented in figure 3.3 illustrate that mainly white leaves (of adult size) showed a clear reduction in carotenoids (neoxanthin, violaxanthin, lutein and β-carotene, Fig. 3.3B) and chlorophylls *a*

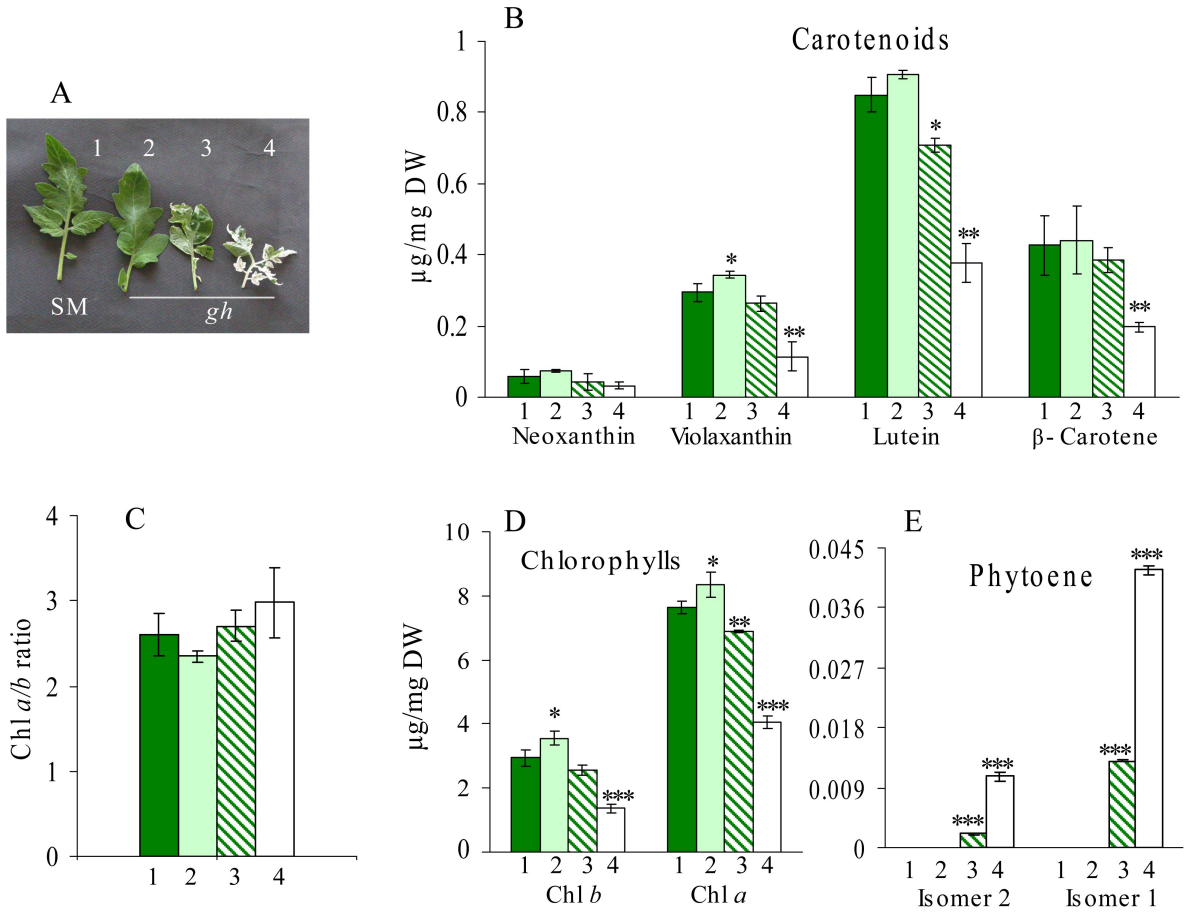

FIGURE 3.3 – **Effect of PTOX deficiency in tomato leaf. A) SM leaves (1) and various types of *gh* leaves produced under different light intensities at an early seedling developmental stage: green *gh* (2), variegated (3) and mainly white (4). For details, see Materials and Methods. Carotenoid (B), Chl *a/b* ratio (C), chlorophylls (D) and phytoen isomers (E) contents from SM and different types of *gh* leaves as shown in (A). The numbers refer to the leaf type in (A). Statistically significant differences are indicated compared to SM leaves: * P< 0.05, ** P< 0.01, *** P< 0.001**

and *b* (Fig. 3.3D) when compared to green leaves, while, as expected, this reduction was not as pronounced in variegated leaves (Fig. 3.3B,D). There is no significant differences in Chl *a/b* ratio between SM and *gh* green leaves, but this ratio is slightly increased in *gh* variegated and white leaves (Fig. 3.3C). A slight (but significant) trend for higher chlorophyll content was observed in fully green leaves from *gh vs*. SM, accompanied by a slight increase in carotenoid content (although it does not appear to be statistically significant for all carotenoids). Such an increase was also reported in green sectors of variegated leaves from the *immutans* mutant (Baerr *et al.*, 2005), and is accompanied by an increase in the rate of carbon assimilation (Aluru *et al.*, 2007). These observations were interpreted as the necessity for green sectors to compensate for the limited photosynthetic and metabolic activities of adjacent white sectors. The latter

data cannot be compared directly with ours which were obtained with entirely green tomato leaves. In the *gh* mutant, phytoene was detected in white but not in green leaves (Fig. 3.3C). This latter observation suggests that, despite the absence of PTOX, PDS activity is not limiting carotenoid biosynthesis in green leaves from *gh*. Using the high resolution of a C_{30} HPLC column, we detected two major isomers of phytoene and a third minor isomer (Fig. 3.4).

We have shown that in cotyledons of dark-grown *gh* seedlings, the lower capacity to desaturate carotenoids is primarily responsible for the phenotype when these seedlings are transferred to light. These tissues have reduced colored carotenoid levels and accumulate their precursor phytoene. Considering the well-known photoprotective role of carotenoids, this pigment deficiency will lead to bleaching in tissues where assembly of the photosynthetic apparatus is initiated upon transfer to light. Although not studied here, it can be speculated that such a pigment deficit is also (at least partially) responsible for the variegated leaf phenotype which is initiated at an early chloroplast developmental stage (when optimal carotenoid biosynthesis is likely to be important). Consistent with this view, bleached sectors in variegated leaves contain phytoene. However, an additional role for PTOX in photosynthetic electron transport (see below) during the build-up of the photosynthetic apparatus cannot be excluded.

3.1.2.2 Pigment content under high light stress

Detached SM and fully *gh* green leaves (with no visible deficit in pigments, as shown in Fig. 3.3, sample 2) were exposed to high light (1,000 μmol.m^{-2}.s^{-1}) for long incubation periods. Leaves from both SM and *gh* showed early bleaching symptoms in some sectors after 20-24h. This trend appears earlier and is stronger in *gh* (insert in Fig. 3.4) and extends to larger leaf sectors with longer incubation time.

Pigments were extracted separately from green and bleached sectors. As expected, these leaves showed accumulation of the xanthophyll cycle pigments A and Z (see Table 3.1) and bleached sectors contained reduced chlorophyll and carotenoid content. This reduction was more pronounced in *gh* than in SM.

However, an unexpected observation was that phytoene was not detected in any tissues, in contrast to that observed in cotyledons (Figs. 3.1 and 3.2) or mainly white or variegated leaves (Fig. 3.3B). Figure 3.4 compares typical HPLC elution profiles from a bleached sector

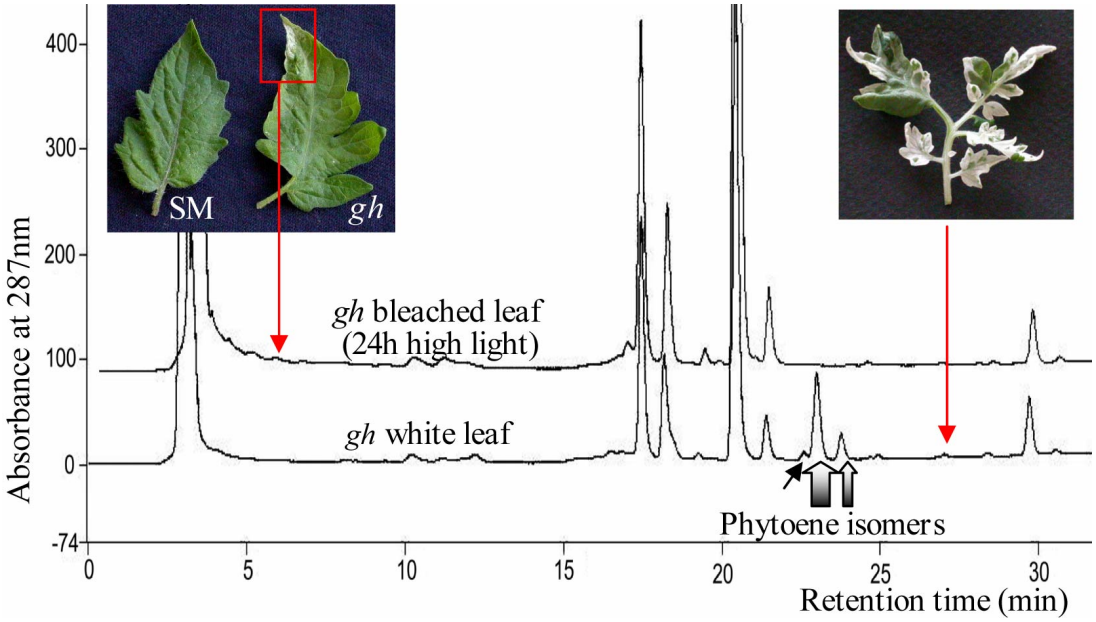

FIGURE 3.4 – **Effect of high light stress on the fully green leaves. Early bleaching symptoms in adult green leaves of SM and *gh* subjected to prolonged incubation under high light conditions (1,000 μmol.m^{-2}.s^{-1}), and HPLC elution profiles (absorbance at 287 nm) of pigments extracted from sectors showing bleaching after 24h under light conditions (upper trace) and from mainly white *gh* leaves (lower trace). The thick arrows point to the two major phytoene isomers which are quantified in (B); the thin arrow points to a minor phytoene isomer.**

after 24h high light and from a mainly white leaf whose aspect is determined early during leaf development (as shown in figure 3.3B).

In order to shed more light on changes occurring in chloroplasts under these experimental conditions, a series of experiments were performed at earlier time points (before bleaching was evident). First, pigment analyses (Table 3.1 and 3.2) were performed using plants grown under low light (60 μmol.m^{-2}.s^{-1}) conditions (T_0) and then green leaves were detached and incubated either under low light (60 μmol.m^{-2}.s^{-1}) or high light (1,000 μmol.m^{-2}.s^{-1}) for 6h (T6h) or 16h (T16h), respectively. At T6h under low light, only slight changes in pigment content were observed with respect to T_0 in both SM and *gh* leaves, with the exception of an increase in the levels of the xanthophyll A and Z for both SM and *gh*. This increase was unexpected since this light intensity is identical to that experienced by the plants prior to these experiments and is most likely due to the leaf detachment. At T6h under high light conditions, higher A+Z levels were observed, as expected, and interestingly with a greater increase in SM *vs*. *gh*. The only other significant change in pigment content observed at T6h under high light was a decrease in violaxanthin, the precursor of A and Z during activation of the xanthophyll cycle. Compared

TABLE 3.1 – **Pigment content of SM and *gh* green leaves. Plants were grown under low light (60 μmol.m^{-2}.s^{-1}). At T_0, leaves were detached and incubated 6h under either low light (60 μmol.m^{-2}.s^{-1}) or high light (1,000 μmol.m^{-2}.s^{-1}).**

	T_0		6h			
			Low Light		High Light	
	SM	*gh*	SM	*gh*	SM	*gh*
Neoxanthin	0.13 (0.02)	0.13 (0.02)	0.12 (0.02)	0.17 (0.03)	0.09 (0.01)	0.14 (0.02)
Violaxanthin	0.53 (0.03)	0.66 (0.13)	0.56 (0.05)	0.61 (0.06)	0.35 (0.03)***	0.55 (0.02)
Z+A	n.d.	n.d.	0.17 (0.01)	0.16 (0.02)	0.39 (0.08)**	0.24 (0.03)**
Lutein	1.60 (0.10)	1.94 (0.17)	1.91 (0.10)	2.21 (0.17)	1.72 (0.22)	2.07 (0.11)
β-Carotene	0.74 (0.04)	0.86 (0.05)	0.72 (0.03)	0.93 (0.08)	0.68 (0.04)	0.85 (0.03)
Total Carotenoids	2.90 (0.23)	3.61 (0.35)	3.49 (0.17)	4.09 (0.29)	3.23 (0.34)	3.85 (0.13)
(Z+A)/(Z+A+V)	0	0	23.58 (2.49)	21.14 (0.80)	53.16 (3.61)***	30.03 (1.71)***
Chl *b*	6.52 (0.71)	7.55 (0.30)	6.94 (0.44)	8.51 (0.72)	6.65 (0.74)	8.14 (0.50)
Chl *a*	13.86 (0.70)	14.67 (0.11)	13.76 (0.73)	15.86 (1.71)	12.84 (0.82)	15.47 (0.77)

A: antheraxanthin, Z: zeaxanthin, V: violaxanthin, Chl: chlorophyll, n.d.: not detected.
Values (given as μg/mg dry weight) are the mean of 4 measurements.
S.D. is given in brackets. Statistically significant differences under high light compared to low light are indicated: ** P<0.01, *** P<0.001.

to T6h, at T16h under high light conditions, the most notable change was an increase in A+Z levels in *gh*, which equaled the levels in SM (Table 3.2). No phytoene was detected in any sample.

TABLE 3.2 – **Pigment content of SM and *gh* green leaves. Plants were grown under low light (60 μmol.m^{-2}.s^{-1}). At T_0, leaves were detached and incubated 16h under either low light (60 μmol.m^{-2}.s^{-1}) or high light (1,000 μmol.m^{-2}.s^{-1}).**

	16h			
	Low Light		High Light	
	SM	*gh*	SM	*gh*
Neoxanthin	0.11 (0.01)	0.11 (0.00)	0.08 (0.02)	0.09 (0.01)
Violaxanthin	0.52 (0.06)	0.54 (0.03)	0.34 (0.05)*	0.38 (0.06)*
Z+A	0.15 (0.01)	0.17 (0.02)	0.40 (0.01)**	0.46 (0.13)*
Lutein	1.38 (0.06)	1.90 (0.15)	1.57 (0.14)	1.93 (0.28)
β-Carotene	0.69 (0.04)	0.93 (0.03)	0.69 (0.06)	0.74 (0.10)
Total Carotenoids	2.86 (0.04)	3.65 (0.28)	3.09 (0.28)	3.61 (0.58)
(Z+A)/(Z+A+V)	22.93 (0.8)	23.69 (1.6)	54.06 (3.5)***	53.88 (3.29)***
Chl *b*	5.68 (1.60)	6.97 (0.10)	5.39 (0.71)	6.34 (0.79)
Chl *a*	12.97 (0.96)	14.84 (0.48)	10.91 (1.17)	12.46 (1.53)

S.D. is given in brackets. Statistically significant differences under high light compared to low light are indicated: ** P<0.01, *** P<0.001 (See legend of Tab. 3.1).

3.1.2.3 Gene expression under high light stress

Proteins were extracted from leaves at T_0 and over a time course up to T16h, under either low or high light. As expected, immunodetection did not reveal any signal for PTOX in *gh* (data not shown), but a 37 kDa band was visible in SM (Fig. 3.5A). High light conditions led to a gradual rise in PTOX level in SM (which is particularly evident at T16h). Under low light, only a slight increase with time is apparent (most likely due to leaf detachment). It should be mentioned that a slight decrease in PTOX level was consistently observed at T3h under high light (when compared to T_0) but not under low light. The PsaD polypeptide level was not found to change during this time course and can therefore be considered as an internal control to ensure equal gel loading. Coomassie Brilliant Blue stained PAGE shows equal loading of the samples (Fig. 3.5B). Figure 3.5C shows the densitometric scanning of the PTOX band from figure 3.5A after normalization using the PsaD band as a standard.

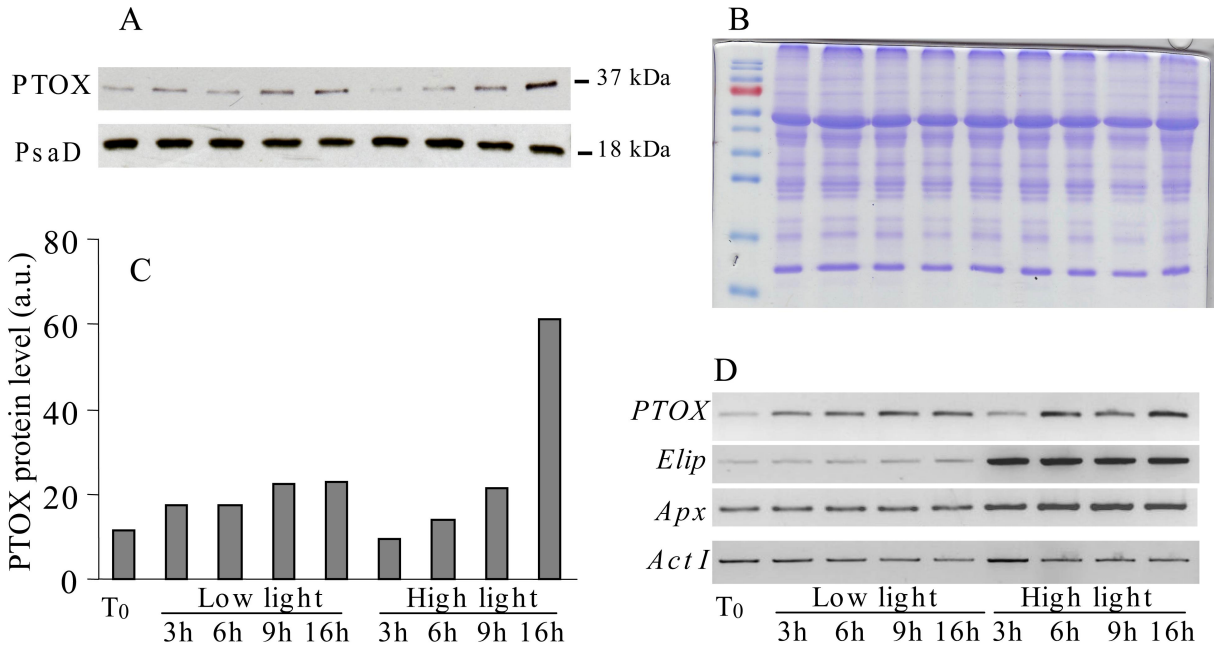

FIGURE 3.5 – **PTOX protein and mRNA levels in SM leaves during photostress. Plants were grown under low light (60 μmol.m^{-2}.s^{-1}) and, at T$_0$, leaves were incubated during a 16-hour time course under low light (60 μmol.m^{-2}.s^{-1}) or high (1,000 μmol.m^{-2}.s^{-1}) light. A- Leaf proteins samples were separated by gel electrophoresis and immunodetected as described in Materials and Methods. B- Coomassie blue stained PAGE (40 μg protein per lane) shows equal loading of the samples. C- Densitometric scanning values of the PTOX band in (A) after normalization using the PsaD values as a standard. D- *PTOX*, *ELIP* and *APX* transcript levels during the same times under LL or HL, determined by semiquantitative RT-PCR as described in Materials and Methods. *Actin* 1 RNA was analyzed as a constitutive control standard.**

Reverse transcriptase (RT)-PCR monitoring of RNA levels (Fig. 3.5D) revealed that these changes in PTOX protein levels are accompanied by changes in PTOX mRNA level, although not in a strictly parallel manner. One can, however, note that the transient decrease in PTOX protein level at T3h under high light is accompanied by a delayed rise in PTOX mRNA level. These data show that under our experimental conditions there is a progressive induction of the PTOX gene. In contrast, there is a rapid induction of the expression of an Early Light Induced Protein (*ELIP*) gene under high light but not under low light, and, to a lesser extent, an ascorbate peroxidase (*APX*) gene. It has been reported that *ELIP* and *APX*, light stress-responsive genes, are immediately induced in mature green plants exposed to light stress or during acclimation of plants to increased light intensities (Kimura *et al.*, 2003; Heddad *et al.*, 2006). To exclude differences in the efficiency of the RT and PCR reactions from sample to sample, *Actin 1* was used as a constitutive control gene in tomato.

3.1.2.4 Photoinhibition and damage to photosystem II and oxidative stress in SM and *gh* leaves

- Photochemical efficiency of PSII

The maximum quantum yield of PSII was estimated from the F_v/F_m ratio. Chlorophyll fluorescence has been used as a noninvasive probe of photochemical events taking place in intact leaves under high light and the other abiotic stresses. F_v and F_v/F_m ratio have been suggested as quantitative measures of the photochemical efficiency of PSII complex and the photon yield of oxygen evolution under different environmental stresses (Krause and Weis, 1991).

At T6h, under high light (Fig. 3.6A), the F_v/F_m ratio was found to decrease, as expected under these photoinhibitory conditions, in both SM and *gh* leaves (but more in *gh*). The same observation was made when the temperature was shifted to 15°C instead of 24°C: again *gh* leaves showed a lower F_v/F_m ratio than SM leaves under high light (Fig. 3.6A). At T16h, the further decrease in F_v/F_m was also greater in *gh* than in SM leaves (Fig. 3.6B).

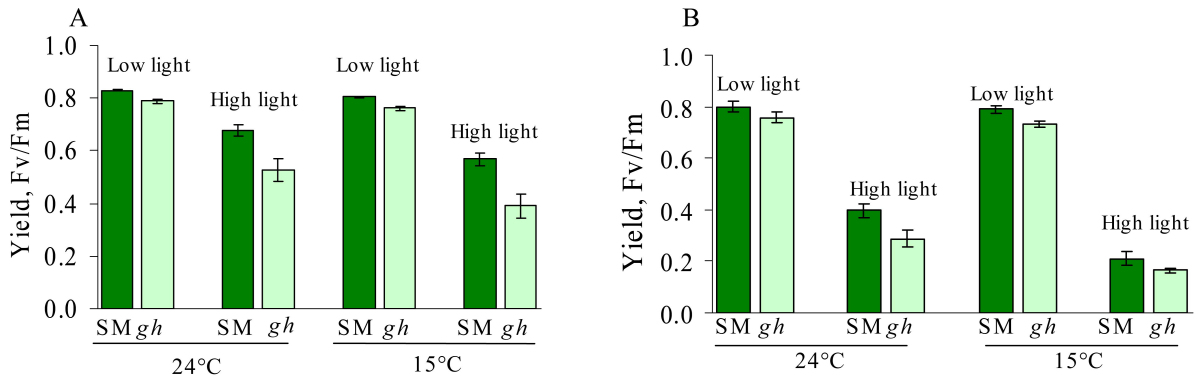

FIGURE 3.6 – **Photoinhibition of SM and *gh* leaves. The maximal quantum yield of photosystem-II is expressed as the F_v/F_m ratio. SM and *gh* leaves were incubated at 24°C or 15°C for 6h (A) or 16h (B) under either low light (60 μmol.m^{-2}.s^{-1}) or high light (1,000 μmol.m^{-2}.s^{-1}) and then kept for 30 min in the dark before chlorophyll fluorescence measurement. Mean values of 6 measurements (*i.e.* 6 different leaves) are shown.**

- Lipid peroxidation

We have also estimated lipid peroxidation in stressed leaves. It is known that a variety of abiotic stresses, including high irradiance, cause molecular damage through the formation of

reactive oxygene species (ROS) and these free radical mediators might be involved in the peroxidative degradation of polyunsaturated fatty acyl residues of the thylakoid lipids. Measurement of malondialdehyde (MDA) level as a secondary end product of the oxidation of polyunsaturated fatty acids is routinely used as an index of lipid peroxidation under stress conditions (Hodges *et al.*, 1999; Sairam and Srivastava, 2001). This measurement was performed over a 6h time course after transfer of leaves to high light. The results (Fig. 3.7) suggest an increase in lipid peroxidation in both *gh* and SM but greater in *gh*.

- Thermoluminescence measurements

Thermoluminescence (TL) is a technique consisting of a rapid cooling followed by the progressive warming of a preilluminated sample in order to monitor the successive emission bands of different types of charge pairs in photosystem II, which are resolved better than the corresponding decay phases recorded at constant temperature. TL in the $0\pm60^{\circ}$C temperature range, not only provides informations on the state of photosystem II in leaf tissue and its possible alterations, but also gives a broader insight into the energetic state inside the chloroplast by probing. First, there is the light-induced or dark-stable thylakoid proton gradient via the protonation of the Mn oxygen-evolving complex, then the induction of cyclic/chlororespiratory electron flow towards the plastoquinone pool, and finally the [NADPH+ATP] assimilatory potential. By a different mechanism, heating to above 60°C without preillumination reveals chemiluminescence high temperature TL (HTL) bands due to the radiative thermolysis of peroxides (*e.g.* lipid peroxides level), which are indicators of oxidative stress in leaves. Despite the fact that the mechanisms of high-temperature TL emission (HTL) is completely different from photosynthetic TL, recording through a single temperature scan from 0°C to 160°C on the same leaf disc both the photosynthesis TL bands and the oxidative stress HTL bands has proven to be of practical interest in environmental physiology (Vavilin and Ducruet, 1998; Vavilin *et al.*, 1998; Ducruet, 2003).

Thermoluminescence measurements were performed on attached green leaves directly after 6h high light stress and after an additional 24h recovery period under low light conditions. As controls, leaves maintained for 6h under low light were used. TL glow curves (Ducruet, 2003) show a B-band peaking at 25°C and a high temperature band peaking at 130-140°C (HTL2). As shown in figure 3.8A, the B-band is shifted after light stress to a position corresponding to a lower temperature accompanied by a 43% decrease in light stressed SM leaves, indicating pho-

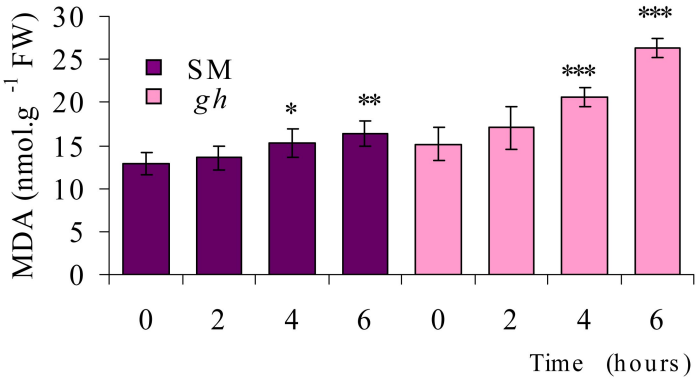

FIGURE 3.7 – **Lipid peroxidation in SM and *gh* leaves. Detached leaves were exposed to high light stress (1,000 μmol.m^{-2}.s^{-1}) for 6h. Lipid peroxidation was estimated using the MDA method. Data are mean values of a minimum of five experiments. Statistically significant differences are indicated compared to T_0: * P< 0.05, ** P< 0.01 and *** P< 0.001.**

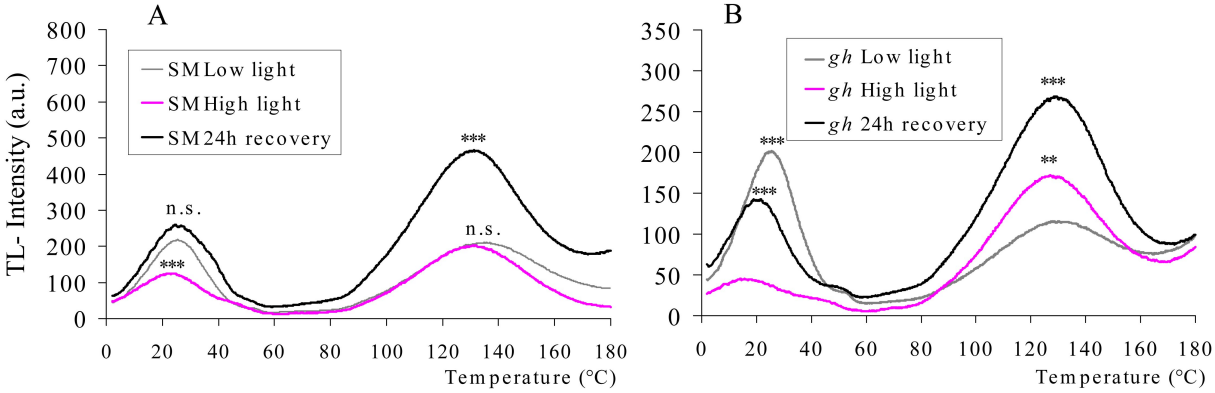

FIGURE 3.8 – **Thermoluminescence measurements to monitor the damage to photosystem II and oxidative stress in SM and *gh* leaves. TL glow curves in SM (left panel) and *gh* (right panel) leaf discs from control leaves (low light) or leaves treated for 6h under high light (1,000 μmol.m^{-2}.s^{-1}) or leaves treated under the same high light conditions but allowed to recover for 24h under the light conditions used for the control leaves. The samples were then treated as described in Materials and Methods, cooled to 2°C and flash-illuminated to induced charge separation. The samples were then heated to induce charge recombination of photosystem II radical pairs (2-60°C); the B-band represents the thermoinduced light emission from the recombination of Q_B^{2-} radical pairs after one light flash and chemiluminescent reactions (70-180°C) representing the chemical stress status (HTL2 band). n.s. : not significant ; ** P< 0.01 and *** P< 0.001, significant compared to control.**

toinhibition and damage to PSII. After 24h recovery, the B-band resumes its initial amplitude and peak position. In light stressed *gh* leaves, a decrease of 78% is observed for the B-band, also accompanied by a shift to lower temperature, but after 24h recovery the B-band returned to only 70% compared to control leaves and the peak shift was still visible (Fig. 3.8B).

No increase in the HTL2 band was visible after 6h for light stressed SM leaves (Fig. 3.8A). In contrast, the HTL2 band was 150% higher in light stressed *gh* leaves compared to control leaves (significant at $P<0.01$). After 24h recovery, a further increase was observed in *gh* but an increase was also observed in SM at that time point compared to 6h light stress. The observed delayed oxidative damage (occurring post-stress; HTL2 band) may appear surprising, but the continuation of lipid peroxidation (MDA levels) after stress-relief has also been observed under low temperature photoinhibition (Hegedus *et al.*, 2004) and drought stress (Olsson *et al.*, 1996). What is clear from our observations on this post-stress phenomenon (Fig. 3.8A,B) is that it affects both the *gh* and control lines and therefore seems independent of PTOX.

Therefore, it appears that the absence of PTOX renders the tomato leaf photosynthetic apparatus more sensitive to extreme conditions (in this case, excessive light). This increased sensitivity is observed in the absence of any detectable accumulation of phytoene or decrease in carotenoid content.

3.1.3 Effect of PTOX deficiency in tomato fruit

3.1.3.1 Pigment content in green and ripe fruit

In the *gh* line, young tomato fruits bleach under standard greenhouse conditions or show a variegated green/white color under shaded conditions (Barr *et al.*, 2004). Using controled growth chamber conditions, we produced white fruit (termed "*gh* white" in the subsequent experiments) as well as fully green fruit (termed "*gh* green") for *gh* (Fig. 3.9). The latter were obtained by keeping fruit under low light. In order to avoid plant etiolation under these conditions, only the fruits were kept under low light, which was achieved by wrapping the fruit in a cloth as soon as they started to develop. During ripening, *gh* white fruit become yellow, while *gh* green fruit become orangey. Under both light conditions, SM fruit are green before ripening and become fully red during ripening.

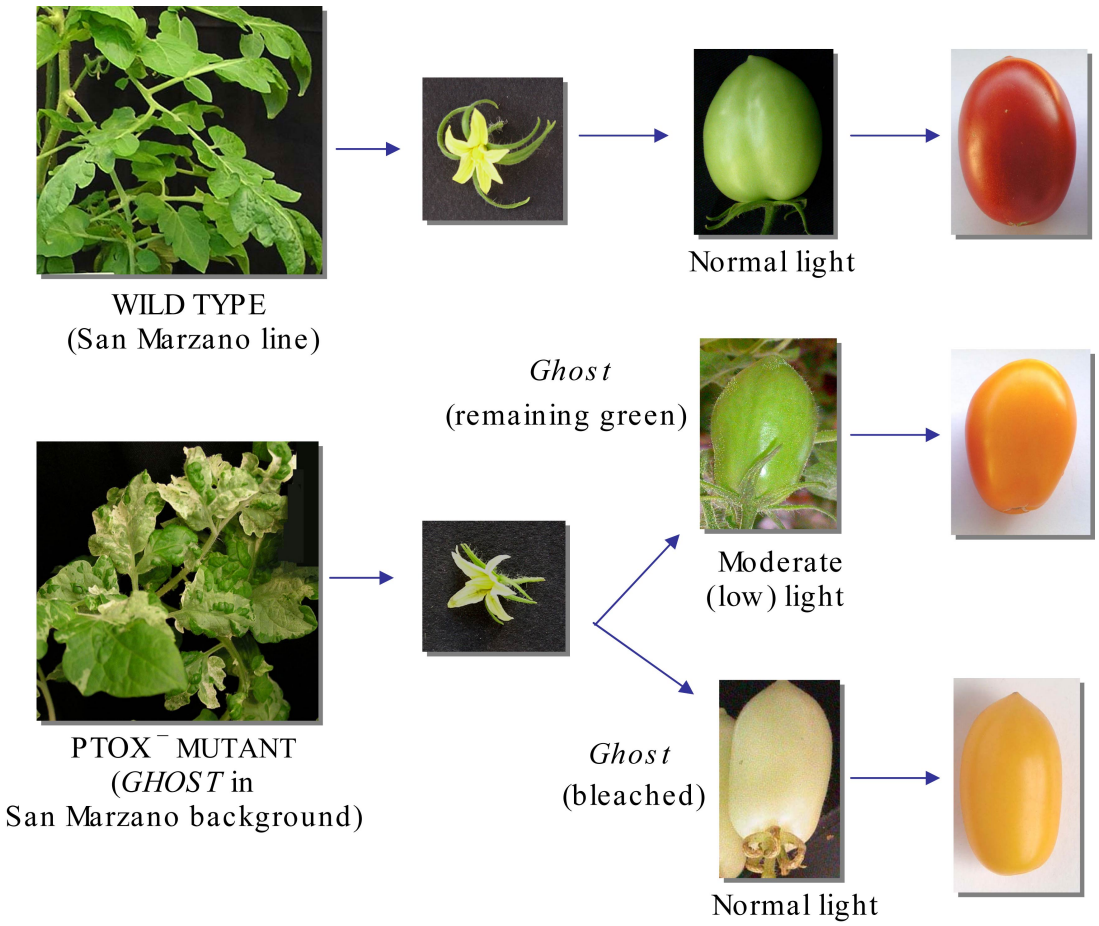

FIGURE 3.9 – **San Marzano and mutant *gh* plants under normal and low light growth conditions. Depending on light intensities at an early seedling developmental stage (see Materials and Methods), *gh* leaves which are mainly green, mainly white or variegated could be obtained. Immature fruit from *gh* plants may be white and green (or green/white variegated), but as ripening proceeds they turn yellow and red-orange under normal light and low light, respectively.**

As shown in figure 3.10A,B, SM and *gh* green fruits at the mature green stage (adult size) show only non-significant variation in pigment content. As expected, these pigment levels are severely reduced in *gh* white fruit. While phytoene is present in *gh* white fruit, only trace amounts of this pigment are found in *gh* green fruit (Fig. 3.10C).

During ripening, phytoene is present in all fruit types, including SM, but is present at the highest level in fruit ripened from the *gh* white type (Fig. 3.10D). The level of the newly accumulating pigments (all-trans lycopene and low amounts of its cis-isomers) is dramatically affected in fruit ripened from the *gh* white fruit type, and is reduced to around 17% of the SM level in fruit ripened from the *gh* green fruit type (Fig. 3.10E). The latter observation contrasts with the normal carotenoid amount of *gh* fruit at the green stage (Fig. 3.10A,B). It should be

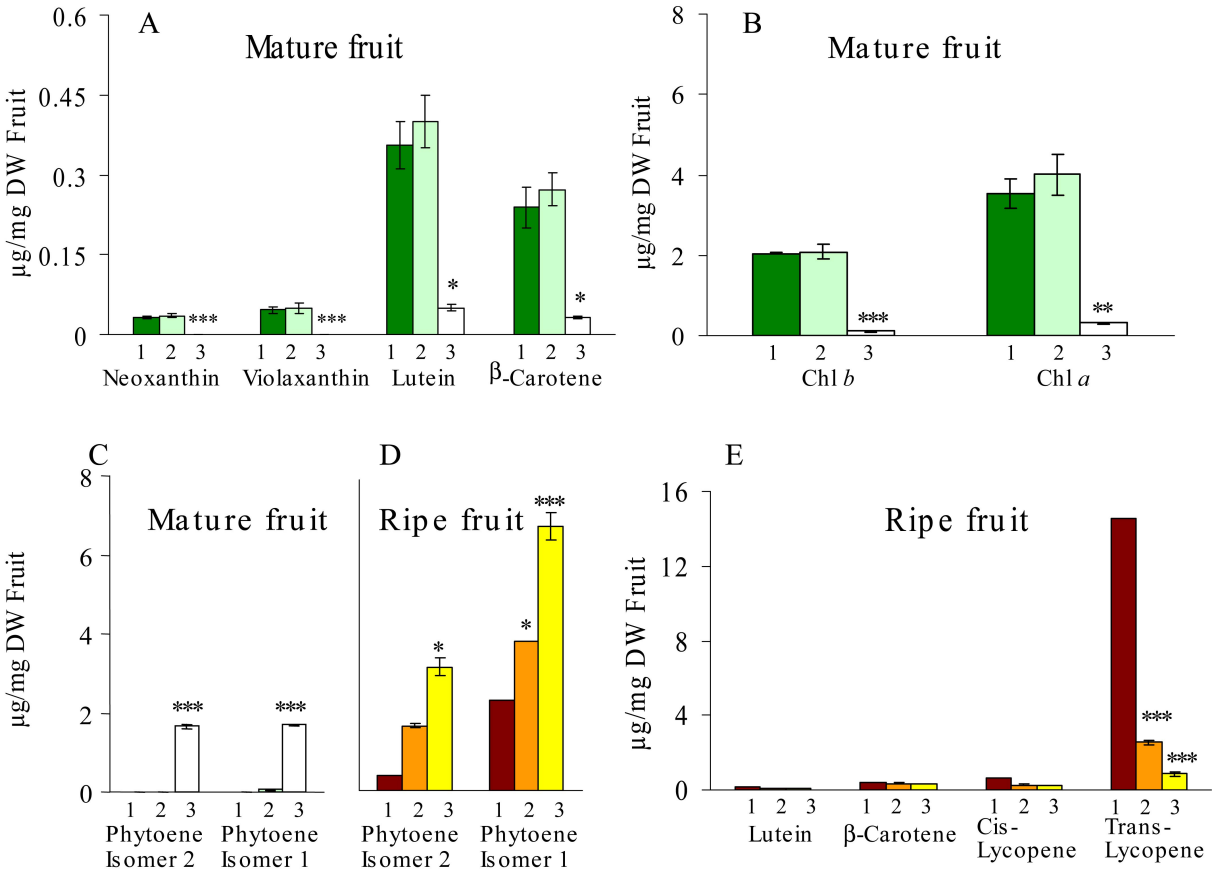

FIGURE 3.10 – **Pigment contents of mature and ripe SM and *gh* fruits. The colored carotenoid (panel A), chlorophylls (B) and phytoene (C) content were analyzed in mature (adult size) fruit. The phytoene (C) and colored carotenoid (D) content was analyzed in ripe fruit (10 days after the breaker stage). Samples were taken from SM green and red fruits (histogram areas indicated by 1), *gh* green and their derived orangy fruits (2) and *gh* bleached and their derived yellow fruits (3). Statistically significant differences are indicated compared to SM fruits: * P< 0.05, ** P< 0.01, *** P< 0.001.**

mentioned that our results are disagree with those reported by Barr *et al.* (2004) who claimed that the amount of total carotenoid (including phytoene) is higher in *gh* ripe fruit compared to SM (due to elevated phytoene levels). In contrast, under our experimental conditions, the total carotenoid amount (including phytoene) in orange and yellow *gh* fruit is only 50 and 60%, respectively, of the amount in red ripe SM fruits.

Figure 3.10E shows that the increased ratio of yellow or orange carotenoids (β-carotene and lutein) to red carotenoid (lycopene) in ripe *gh* fruits compared to ripe SM fruit is in line with the visible yellow or orange color of ripe *gh* fruit. However, other yellow pigments, such as the flavonoid chalconaringenin (Hunt and Baker, 1980) are likely to participate in this yellow color, especially in the cuticle.

It should be mentioned that the data in figure 3.10A-C do not exclude the possibility that the carotenoid biosynthetic pathway is inactive at the mature green stage (which would not allow any conclusion to be drawn regarding the importance of PTOX as a cofactor for the desaturation reactions at this stage). Such a possibility is, however, excluded in ripe fruit since the data in figure 3.10D,F show accumulation of a new pigment (lycopene) and the precursor phytoene. To demonstrate that this pathway is also active in mature green fruit, explants from mature green fruit were incubated in the presence of carotenoid biosynthetic pathway inhibitors (the bleaching herbicides listed in appendix A.1; for details see appendix A.3). Fruit pericarp explants (1×1 cm) were incubated upside down after 60 μl of various inhibitors (from 250 μM stock solutions in DMSO) were layered on them. The carotenoid content was then measured after 24h under low light.

The HPLC elution profiles (absorbance at 287 nm) in figure 3.11 show that treatment with both PDS inhibitors norflurazon and KPP-297 lead to phytoene accumulation in SM green fruit indicating that the carotenoid pathway was indeed active in these tissues. It should be noted that the quinone synthesis (HPPD) inhibitor did not lead to phytoene accumulation. It is possible that the decrease in quinone content, due to this inhibitor, was not sufficient to inhibitor carotenoid desaturation. An experimental herbicide (provided by Syngenta and called D) was also used and it was found that it efficiently blocks phytoene desaturation. These observations suggest that tomato fruit explants can be used as production lines for carotenoids and are amenable for examining the inhibitor influence of various compounds. Appendix A.1 lists the compounds used in parallel to the studies in this manuscript but which are not included.

The same results were obtained using explants from *gh* mature green fruit (Fig. 3.12) confirming that the carotenoid pathway was active in this PTOX deficient mutant. The absence of phytoene accumulation in the presence of DMSO alone confirms that PTOX is not required for carotenoid desaturation at this developmental stage. It can also be concluded from these experiments that the herbicide D is not an inhibitor of PTOX but rather of PDS. It showed also be noted that the HPPD inhibitor led to phytoene accumulation in this case (unlike in SM), suggesting that in *gh* a critically low quinone content was reached. Why this was not the case in SM is however unclear and was not examined further.

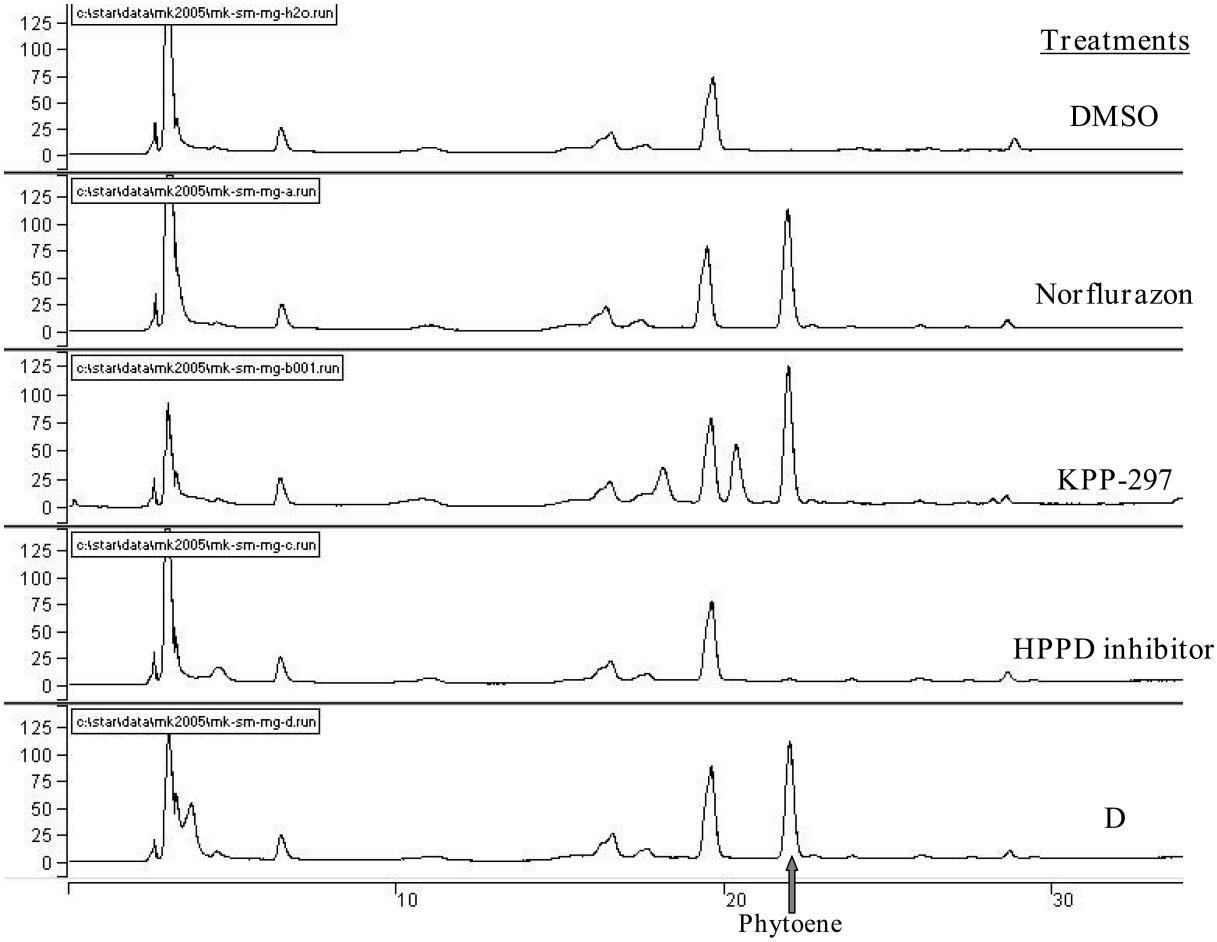

FIGURE 3.11 – **The effect of carotenoid biosynthetic pathway inhibitors on phytoene accumulation in SM mature green fruit. HPLC chromatograms are recorded at 287 nm.**

3.1.3.2 Photochemical efficiency of PSII and lipid peroxidation in green fruits under high light stress

Explants from mature green fruit were incubated under 1,000 μmol.m^{-2}.s^{-1} for up to 48h at 24°C. Bleaching symptoms were observed after *ca.* 24h in both SM and *gh* explants but were greater in *gh* (Fig. 3.13A). Analysis of their carotenoid content at various time points (6h, 18h, 30h and 42h) did not reveal any phytoene (not shown), indicating that the absence of PTOX does not limit carotenoid biosynthesis in these *gh* explants.

Estimation of the maximum quantum yield of PSII after 6h incubation (Fig. 3.13B) shows that *gh* fruits are more sensitive to photoinhibition than SM fruit under this high light condition at 24°C. At 15°C, both fruit types are fully photoinhibited under these light conditions. The lipid peroxidation was estimated using the MDA method during 8h after transfer of fruit explants

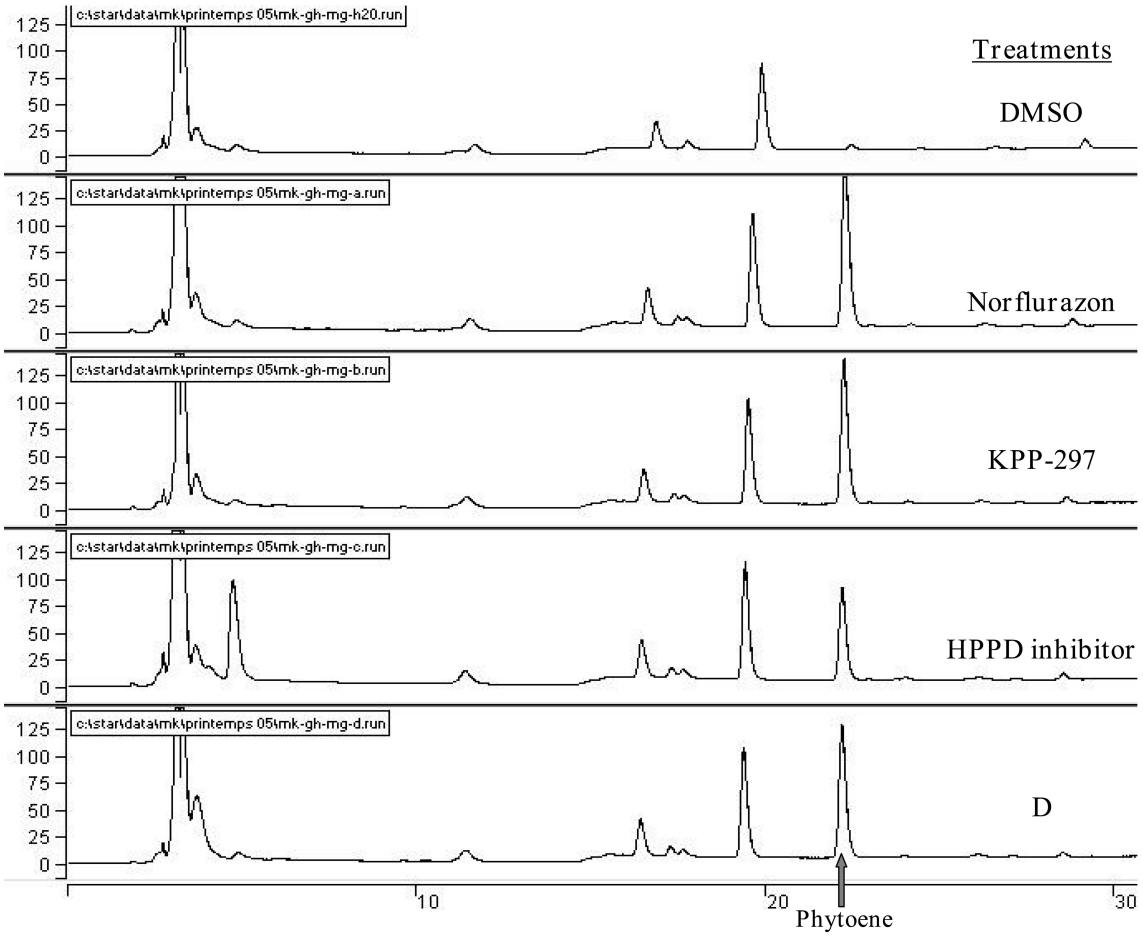

FIGURE 3.12 – **The effect of carotenoid biosynthetic pathway inhibitors on phytoene accumulation in *gh* mature green fruit. HPLC chromatograms are recorded at 287 nm.**

to high light. This estimation was performed using a modified method in order to remove interfering compounds such as carbohydrates (Hodges *et al.*, 1999), which is recommended for tomato fruits. The data in figure 3.13C show an increase in lipid peroxidation in both *gh* and SM. The MDA level in fruit is not as high as leaves; maybe there is a dilution effect in fruit samples, thus no difference between *gh* and SM could be detected by this method.

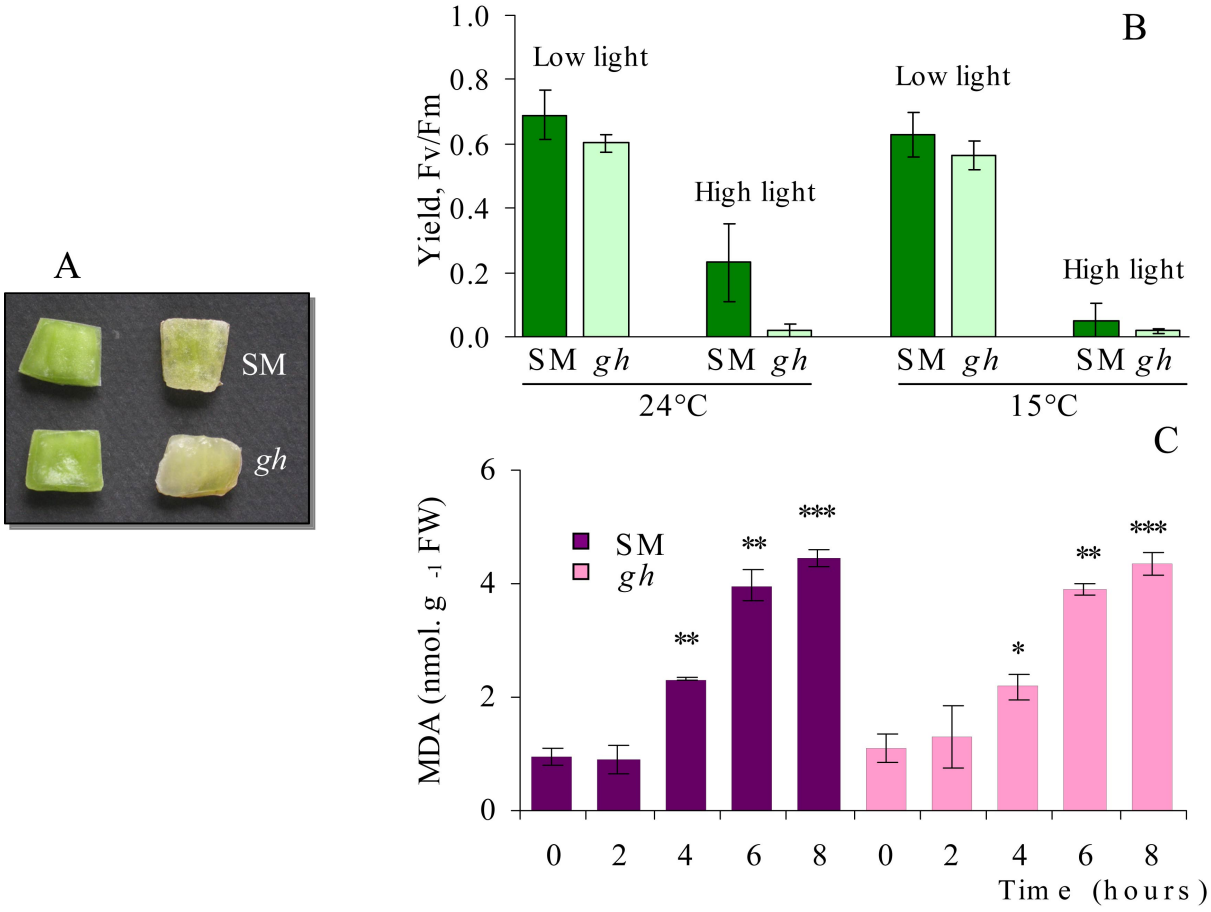

FIGURE 3.13 – **Photobleaching and oxidative stress in SM and *gh* green fruits explants. A- Bleaching symptoms in SM and *gh* green fruits due to prolonged incubation under high light conditions (1,000 μmol.m^{-2}.s^{-1}), as compared before stress. B- The maximal quantum yield of photosystem II is expressed as the F_v/F_m ratio. Fruit pericarp of SM and *gh* were incubated at 24°C or 15°C for 6h under either low light (60 μmol.m^{-2}.s^{-1}) or high light (1,000 μmol.m^{-2}.s^{-1}) and then kept 30 min in the dark before chlorophyll fluorescence measurement. Mean values are shown (n = 3). C- Lipid peroxidation in SM and *gh* fruits. Fruit pericarp were exposed to high light stress (1,000 μmol.m^{-2}.s^{-1}) for 8 h. Lipid peroxidation was estimated using the MDA method. Data are mean values of a minimum of three experiments. Statistically significant differences are indicated compared to T_0: * P< 0.05, ** P< 0.01 and *** P< 0.001.**

3.1.4 Discussion

3.1.4.1 Fully greened tissues can desaturate carotenoids without PTOX

When the normal chloroplast biogenesis was not impaired (*i.e.* when excessive light was avoided at an early stage), no phytoene nor a deficit in carotenoid content was observed in green adult *gh* leaves, even after a prolonged incubation (24h) under excessive light ultimately leading to bleaching. This is highly surprising since the carotenoid biosynthetic pathway is likely to be

very active under such conditions to compensate for carotenoid turnover and photodestruction (Simkin *et al.*, 2003). This contrasts with the accumulation of phytoene in adult tomato leaves when PDS is inhibited by the bleaching herbicide norflurazon (Simkin *et al.*, 2003). Thus, the absence of phytoene in leaves bleached under strong light is not due to its photodegradation, but rather to the fact that the carotenoid biosynthetic pathway is not limited by the lack of PTOX. In other words, PTOX is dispensable as a carotenoid desaturase co-factor in tissues with a fully functional photosynthetic apparatus. Since optimal carotenoid desaturation is obtained in the range of the midpoint potential of the plastoquinone/plastoquinol redox couple (Nievelstein *et al.*, 1995), this redox control may be obtained for PQs in the vicinity of the desaturases by a mechanism provided by photosynthetic membranes. Chemical reoxidation of plastoquinol may also participate (Khorobrykh and Ivanov, 2002).

3.1.4.2 *gh* leaves are affected in photosynthetic electron transport under high light stress

Since the experimental conditions leading to photobleaching in adult tomato leaves were not linked to a deficit in carotenoid content, a direct contribution of PTOX to photosynthesis was examined. Since such prolonged (24h) high light exposure and photobleaching are not normal phenomenon in nature (but were applied to ensure that extreme condition were created), earlier time points (6h and 16h) compatible with a normal photoperiod were used for these experiments.

Our results are fully consistent in suggesting that PTOX plays a special role in the protection of the fully assembled photosynthetic apparatus under high light stress. These results indicate higher PSII photoinhibition in *gh vs*. SM leaves after 6h and 16h light stress (Fig. 3.7), as well as higher damage level of PSII in *gh* than in SM and only partial recovery in *gh* (thermoluminescence B-band; Fig. 3.8B). High temperature thermoluminescence measurements (HTL2 band) also point to a reduced potential preventing oxidative damage in *gh vs*. SM leaves after 6h light stress. Estimation of lipid peroxidation by MDA level measurements (Fig. 3.8A) is consistent with the latter observations.

3.1.4.3 The changes in PTOX function during tomato fruit development

As in leaves, bleaching of young *gh* fruits is determined at an early developmental stage. The presence of phytoene in white *gh* fruit suggests it is linked (at least partially) to a deficit in

carotenoid biosynthesis. In contrast, the sensitivity to high light conditions of mature *gh* fruits that were maintained green could not be linked to a deficit in carotenoid biosynthesis. We found *gh* green fruits to be more susceptible to photoinhibition than SM control fruits, confirming to our observation in adult green *gh* leaves.

In ripening *gh* fruits derived from green fruits, the lycopene synthesizing capacity of fruit is reduced compared to wild type, but is not zero, which may suggest that, in the absence of PTOX, another co-factor of the carotenoid desaturase replaces PTOX. The identity of this co-factor (Carol and Kuntz, 2001) and whether it is identical to that operating in green or etiolated (dark-grown cotyledons) tissue remains to be determined. Alternatively, chemical reoxidation of plastoquinol may be sufficient for the low level of phytoene desaturation in *gh* ripening fruit as well as in dark-grown cotyledons.

Bleaching at the green stage in *gh* fruit influences the capacity to synthesize carotenoids during fruit ripening: the amount of lycopene present in ripe fruit derived from white *gh* fruit is decreased 3-fold compared to ripe fruit derived from green *gh* fruit (Fig. 3.9E). Since carotenoid biosynthesis is catalyzed by membrane bound enzymes, and since bleached *gh* fruit are affected in their plastid ultrastructure (Barr *et al.*, 2004), it seems reasonable to consider that irreversible damage to membranes in bleached tissues will affect this biosynthetic pathway. Since fruit ripening is characterized by the disassembly of photosynthetic membranes to re-synthesize new (achlorophyllous) ones, membrane disintegration at an early stage will affect this biosynthetic pathway during ripening. It is also likely that photobleaching will have additional pleiotropic effects that will affect the carotenoid biosynthetic pathway.

3.1.4.4 Role of PTOX in photosynthesis: safety valve or regulatory adjustment?

Correlative evidence for PTOX as a *bona fide* safety valve (*i.e.* allowing the transfer of excess electrons to O_2) is provided for higher plants essentially by gene expression/protein accumulation data (Rizhsky *et al.*, 2002; Baena-Gonzalez *et al.*, 2003; Quiles, 2006). However, PTOX remains a minor constituent of photosynthetic membranes (Lennon *et al.*, 2003) with the notable exception of alpine plants such as *Geum montanum* and *Ranunculus glacialis* (Streb *et al.*, 2005), which may have selected natural gene over-expressers as an additional protection mechanism. We could show here that PTOX protein levels do increase unambiguously (in wild type control plants) under strong light conditions but only after a long period (especially after 16h;

Fig. 3.6). In contrast, after 6h illumination no increase in PTOX level was observed, although we could demonstrate a clear involvement of PTOX in photoprotection at that time point. However, a rapid induction of PTOX protein in *Arabidopsis immutans* after 5h exposition under high light condition it has been reported (Rizhsky *et al.*, 2002). This would be explained by the different materials or methods employed, *e.g.* the quality of applied light, or maybe a difference between species. Nevertheless, it seems difficult to propose a role for PTOX merely as a safety valve allowing massive photosynthetic electron flow towards O_2.

Acclimation of plants to an environment and its constantly changing conditions implies a highly sophisticated regulation network probably involving chlororespiration (Rumeau *et al.*, 2007). Quiles (2006) has shown that an *in vitro* chlororespiratory activity (NADH dehydrogenase and a PTOX-like activity) is stimulated when thylakoids were isolated from heat and high light treated oat plants. PTOX activity, rather than directly compensating for an over-reduced PQ status, could be considered as a fine-tuning device. Together with the NDH complex(es) and the ferredoxin/PGR5-dependent PQ reductase, PTOX might provide photosynthetic regulatory mechanisms (Rumeau *et al.*, 2007; Shikanai, 2007). A regulatory function for PTOX is suggested by some of our present data. After 6h of photostress (but not after 16h when PTOX protein levels are at their highest in SM), lower levels of de-epoxidated xanthophyll cycle pigments (A+Z; Table 3.1) were observed in *gh vs*. SM. The more reduced state of Q_A during this time might also render PSII more sensitive to photobleaching since photoinhibition or photodamage to PSII strongly depends on the redox state of PSII and membrane energization (Ogren, 1991).

A regulatory role for PTOX is also suggested by the slightly higher pigment content of green leaves in *gh vs*. SM (Fig. 3.4B,C). However, this slight increase in both chlorophyll and carotenoid content is unlikely to be the causal link between the lack of PTOX and the various effects on photosynthetic electron transport described here. For instance, in *gh* the delay in full activation of the xanthophyll cycle during long incubation under severe light conditions (Table 3.1) must result from more complex regulatory mechanisms. In addition, a rise in chlorophyll content was observed in quite similar proportions when wild type and *immutans Arabidopsis* were compared (Rosso *et al.*, 2006), whereas these authors did not report effects on the photosynthetic electron chain for this species. This apparent discrepancy between tomato and *Arabidopsis* is also, in our opinion, more in favor of a regulatory role for PTOX: in a multi-component regulatory network, it is conceivable that the relative importance of a given

component differs from species to species. This is even more plausible since, within one single species (tomato; our present data), the relative importance of the dual role of PTOX (related to carotenoid biosynthesis and to photosynthesis) differs from organ to organ and also within a given organ (leaf, fruit) from one developmental stage to another.

3.1.5 Conclusion

In this chapter, we have demonstrated that at an early chloroplast biogenesis stage, PTOX is a dominant cofactor for carotenoid saturation. In contrast, when entirely green adult leaves or fruits from *ghost* were submitted to photobleaching high light conditions, no evidence for a deficiency in carotenoid biosynthesis was obtained. However, our results provide consistent evidence showing that in the absence of PTOX, the photosynthetic apparatus of tomato leaves and fruits is more sensitive to light. In contrast, ripening fruit are primarily dependent on PTOX and on plastid integrity for carotenoid desaturation.

In summary, our data show that PTOX activity is necessary during chloroplast and chromoplast biogenesis and also for efficient carotenoid desaturation in certain organs at some developmental stages. However, the existence of a PTOX-independent pathway for plastoquinol reoxidation in association with phytoene desaturase would have to exist to explain the normal carotenoid content at other developmental stages. In addition, we show that PTOX is implicated in the regulation of photosynthetic electron transport in green tissues.

3.2 The Regulatory Adjustment Roles of PTOX in Photosynthesis

PTOX is involved in carotenoid biosynthesis (as a cofactor in phytoene desaturation, see Introduction) and also influences the protection of the photosystems under stress conditions by a mechanism that is independent of the carotenoid content (*cf.* § 3.1).

Since PTOX shares sequence homology with the mitochondrial alternative oxidase (Berthold and Stenmark, 2003), it has been shown to be a plastoquinol oxidase (Josse *et al.*, 2003) and, in common with the NDH complex, it behaves as an intrinsic membrane protein in the thylakoid lamellae (Lennon *et al.*, 2003), then PTOX possesses all the characteristics expected of a terminal oxidase involved in chlororespiration (Peltier and Cournac, 2002; Kuntz, 2004). Such a role for PTOX is not incompatible with a role in carotenoid desaturation since this latter process is dependent on a redox pathway (Morstadt *et al.*, 2002).

Evidence was obtained that seems to confirm a chlororespiratory role for PTOX in algae (Cournac *et al.*, 2000b, 2002) and in tobacco over-expressing a PTOX gene (Joët *et al.*, 2002b). It was proposed that PTOX, by modulating the redox state of intersystem electron carriers, may participate in the regulation of cyclic electron flow around PSI. Furthermore, data indicate an induction of the PTOX gene and/or an accumulation of the protein under stress conditions in tobacco lacking both ascorbate peroxidase and catalase (Rizhsky *et al.*, 2002) or deficient in PSII (Baena-Gonzalez *et al.*, 2003). Strikingly, the high mountain plant *Ranunculus glacialis*, which has been shown to contain alternative sinks to dissipate photosynthetic electrons, was also found to contain high levels of PTOX (Streb *et al.*, 2005). PTOX has been proposed to serve as a "safety valve", preventing overreduction of the electron transfer chain in excess light (Aluru *et al.*, 2006). In contrast, using *Arabidopsis* lines either deficient in or over-expressing PTOX, Rosso *et al.* (2006) concluded that this enzyme does not act as a stress-induced safety valve involved in the protection of the photosynthetic apparatus. These authors claim that high PTOX levels may simply be correlative and not indicative of an energy dissipating role for this enzyme.

Hence, a possible function of PTOX in a chlororespiratory activity has not been clearly established. Furthermore, since the potential electron consumption by chlororespiration is currently thought to be very low (Ort and Baker, 2002) and since the PTOX content is low in many plant species (Streb *et al.*, 2005), this enzyme's influence on photosynthetic electron flow remains to be clarified. In the present chapter, the potential influence of PTOX on the redox status of the PQ pool and on adjustment in photosynthesis was examined by comparing the tomato PTOX deficient *ghost* (*gh*) mutant to the wild type San Marzano (SM) line.

3.2.1 Thylakoid protein composition

The defects in photosynthesis displayed by the *gh* mutant (as shown in chapter 3.1) can be mediated by a reduced level or malfunction of protein complexes in the electron transport chain. To examine this possibility, we analyzed mutant (green and variegated leaves) and wild-type thylakoid membranes by blue native polyacrylamide gel electrophoresis (BN/PAGE). BN gels using *gh* and SM extracts containing equal amounts of chlorophyll and also protein blot analysis (3 μg Chl per lane) revealed that the amounts of major protein subunits of PSII, PSI, and their antenna, as well as the Cyt b_6f complex, and the ATP synthase remained almost unchanged in the absence of PTOX (Fig. 3.14A,B).

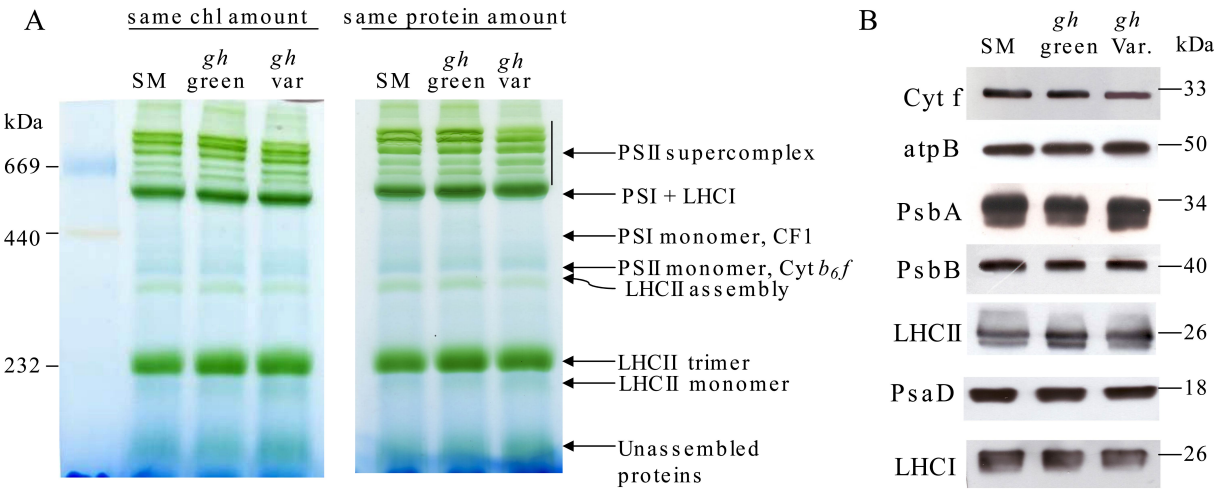

FIGURE 3.14 – **Thylakoid protein composition in SM and mutant *gh* green and variegated leaves. A- Blue native gel (BN/PAGE) analysis of thylakoid membrane complexes. Thylakoid membranes were solubilized with 1% DM and separated on a 5-13.5% gel (8 μg of chlorophyll or 50 μg of proteins per lane). Protein identification was based on Fu *et al.* (2007). B- Thylakoid polypepdtides immunoblots with thylakoid extracts (3 μg chlorophyll per lane)**

In variegated leaves of the mutant, however, levels of unassembled proteins were increased, which is not surprising because abnormal and unstructured chloroplasts are present in the white regions of leaves.

Our results showed that the increased sensitivity of the photosynthetic apparatus to extreme conditions in *gh* (in the absence of any detectable accumulation of phytoene or decrease in carotenoid content, chapter 3.1), were not caused by major rearrangements in protein complexes of the electron transport chain.

3.2.2 Fluorescence of PSII and PSI at low temperature (77k)

Methodologies based on 77K fluorescence emission spectra can distinguish between the characteristic emission bands belonging to PSII (F_{II}, chlorophyll *a* associated with Chl-binding CP43 and CP47 proteins of core antenna of PSII at 685 and 695 nm, respectively) and to PSI (F_I at 735 nm, from chlorophyll *a* molecules associated principally with PSI), and hence allow the study of specific Chl/protein complexes (Krause and Weis, 1991). These techniques were applied to compare thylakoids from SM and *gh* leaves.

As shown in figure 3.15A, after acclimation of plants for 48h at 10 μmol.m^{-2}.s^{-1}, the emission spectra of *gh* and SM thylakoids revealed no differences in the positions or relative heights of the PSII or PSI emission peaks, and F_I/F_{II} ratios in SM and *gh* were almost identical. But incubation of plants at 50 μmol.m^{-2}.s^{-1} for 2h, results in a clearly larger increase in the F_I/F_{II} ratio for SM than *gh*, indicating that these 2 leaf types differ in the way PSII and/or PSI adapt to the changing light conditions (Fig. 3.15B).

The light harvesting complex (LHC) II can tune energy conversion by both photosystems to the light quality (wavelength) by a short term mechanism called state transition. According to the state transition model (reviewed in Allen, 1995, 2003), overexcitation of PSII relative to PSI reduces the plastoquinone pool and activates a kinase that phosphorylates the peripheral LHC associated with PSII. Subsequent detachment of phospho-LHC from PSII decreases the effective size of the PSII antenna, and the phospho-LHC may then transfer excitation energy to PSI. State transition may be a balancing mechanism rather than a true photoprotective mechanism (Niyogi, 1999).

Figures 3.15 C,D show emission spectra from leaves incubated either under far-red (PSI light) or blue light (PSII light) to establish state 1 or state 2, respectively. After state transition, F_I/F_{II} ratios from both SM and *gh* leaves are increased, which shows that *gh* has ability for

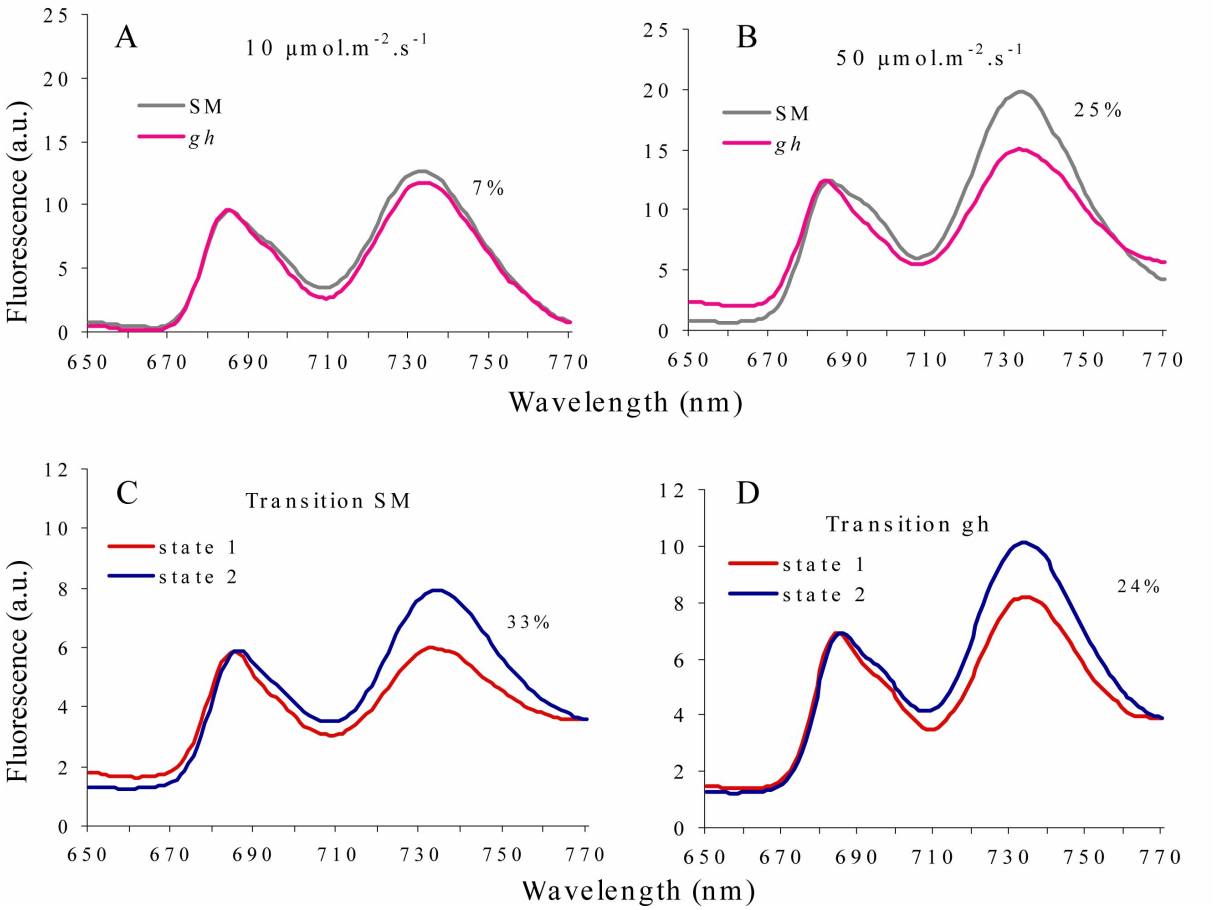

FIGURE 3.15 – **Chlorophyll fluorescence emission spectra of SM and mutant *gh* at low temperature (77K). The A and B panels correspond to thylakoids of plants grown at 10 μmol.m^{-2}.s^{-1} and adapted for 2h at 50 μmol.m^{-2}.s^{-1} light intensity, respectively, SM (grey lines) and mutant *gh* (pink lines). C, D, emission spectra from SM and *gh* thylakoids from leaves incubated either in PSI light (red lines) and in PSII light (blue lines) to establish a state 1 or state 2, respectively.**

state transition. However, while a 33% increase in F_I was observed in SM, it was only 24% in *gh*. This again indicates that adaptation of leaves to changing light condition is different in *gh* *vs*. SM. It should also be noted that the F_I/F_{II} ratio in state 1 was higher in *gh* than in SM: it seems that in *gh* the system is already in the pre-state 2, possibly because, even in the far-red acclimated leaves, reoxidation of the PQ pool by PSI is incomplete in *gh* (the level of reduced PQ remains higher).

3.2.3 Flurescence Induction Kinetics

3.2.3.1 Determination of the size of the PQ pool

The reduced plastoquinone pool size in SM and *gh* leaves was estimated by the induction of variable chlorophyll fluorescence from the upper side of green leaf discs at 25°C. The leaf discs were infiltrated with or without 50 μM DCMU. When the electron transfer from PSII to the PQ pool is blocked by DCMU, the increase from F_0 to the maximum level of fluorescence reflects the maximal reduction level of the primary acceptor Q_A. DCMU blocks electron transfer from Q_A^- to PQ, probably by binding to the Q_B site in the D1 protein. Therefore, in the presence of DCMU the fluorescence rise from F_0 to F_m is more rapid than in the absence of the inhibitor. As shown in figure 3.16, there is no difference between SM and *gh* leaves when incubated with DCMU.

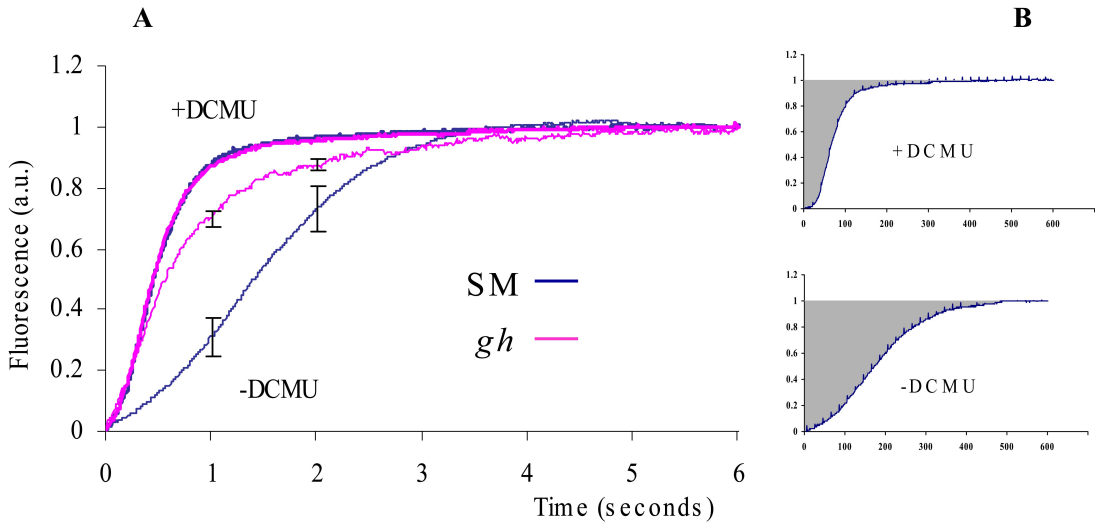

FIGURE 3.16 – **Induction curves of variable fluorescence emitted from SM and *gh* leaves and measured in the absence and in the presence of DCMU (A). The leaf discs were infiltrated in the dark for 5 min with 50 μM DCMU [in 2.5% ethanol-water (v/v)] or the same solvent without DCMU and incubated for 30 min at room temperature in the dark. A. The stable fluorescence value in the presence of DCMU was set at 1 and F_0 was set at 0. The intensity of the actinic light was 20 μmol.m^{-2}.s^{-1}. B. The complementary area (above the curve) was calculated as a relative measure of the oxidized plastoquinone pool.**

In the absence of DCMU, the reduction level of Q_A is influenced by the redox state of the PQ pool. As shown in figure 3.16A, the level of fluorescence presents more rapid in *gh* than in SM leaves, and clearly shows that the initial photochemical rise is increased in *gh*. This suggests a more reduced acceptor side of PSII (significant at 1 and 2 sec after actinic light) indicating a

more reduced PQ pool in *gh* under these experimental conditions (leaves were pre-incubated 30 min in darkness before fluorescence measurements).

The complementary area (CA; *i.e.* the integrated fluorescence deficit) above the curve represents a relative measure of the oxidized plastoquinone pool (whereas fluorescence yield is non-linearly related to the redox state of the acceptor side). When calculated from figure 3.16B, a smaller CA (and therefore a less oxidized PQ pool) was found for *gh* than for SM (0.98 and 1.48 in *gh* and SM, respectively; difference significant at P<0.001).

3.2.3.2 Fast chlorophyll *a* fluorescence induction (FI) kinetics

Chlorophyll *a* fluorescence induction (FI) has been widely used to probe the activity and integrity of the photosynthetic apparatus. Indeed, this method is highly sensitive to any change in electron transfer reactions on both donor and acceptor side of photosystem II (Strasser *et al.*, 2004; Schreiber, 2004). When dark-adapted oxygenic photosynthetic cells are illuminated, chlorophyll *a* fluorescence shows complex induction kinetics in the first miliseconds. The fast fluorescence kinetics is characterized by the different chlorophyll fluorescence induction steps, which are termed the OJIP transients (Strasser *et al.*, 1995, 2004). Each letter denotes a distinct inflection in the induction curve. As shown in figure 3.17 A, the O-level at 0.01 ms represents a fluorescence value close to F_0 and is influenced by the relative size of core antenna and peripheral antenna of the PSII reaction center. The fluorescence rise from O- to J-level (2 ms) indicates the reduction of Q_A, and corresponds most closely to the peak concentrations of Q_A Q_B^- and Q_A^- Q_B^-. The fluorescence rise from J- to I-level (30 ms) indicates the reduction of QB and partially of the PQ pool, and corresponds most closely to the first shoulder of the concentration change of Q_A^- Q_B^{2-}. The rise from I- to P-level (200-300 ms) corresponds to the full reduction of the PQ pool (at P-level), and corresponds most closely to the peak concentrations of Q_A^- Q_B^{2-} and PQH_2. The fluorescence emission at point P is influenced by both the rate constant of PQ oxidation and the PQ pool size. Fluorescence at P reflects a balance between light incident at the PSII side and the rate of utilization of the chemical (potential) energy and the rate of heat dissipation (Zhu *et al.*, 2005).

We performed fast fluorescence kinetics after 5 min, 30 min or 4h of dark adaptation and were recorded during a light pulse of 1 sec. Figure 3.17B shows that the O-level (0.01 ms; reflecting F_0) is increased significantly in the *gh* mutant *vs*. SM, after 5 or 30 min dark adapta-

tion, but not after a longer dark adaptation of 4h. In addition, for all dark adaptation times, the fluorescence at 2 ms (J-level) increases greatly during the light pulse in *gh* compared to SM. An increased J-level is an excellent indicator of a more reduced PQ pool and a more pronounced Q_A^- accumulation under light excitation (Haldimann and Strasser, 1999). Whereas the J-level decreases continuously with increasing dark adaptation time in SM, it increases in *gh* between 5 to 30 min dark adaptation and strongly decreases again after 4h. Similarly, the I-level is also increased significantly after 5 and 30 min dark adaptation in *gh vs.* SM. Strikingly, after 4h dark adaptation the P-level in *gh* remains at a similar level compared to that after 5 and 30 min, whereas a significant increase is observed in SM (Fig. 3.17B). These observations are discussed below.

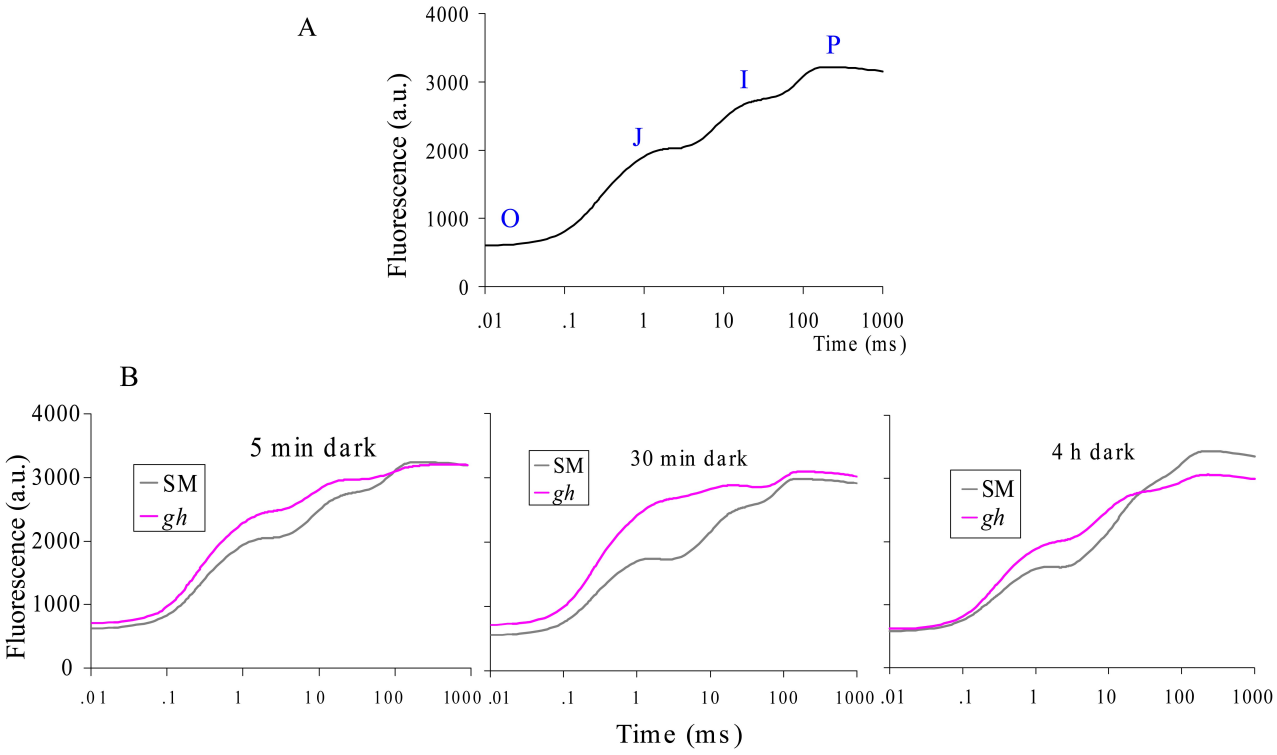

FIGURE 3.17 – **Fast fluorescence kinetics (OJIP).**
A- The O-level at 0.01 ms represents a fluorescence value close to F_0. The fluorescence rise from the O- to J-level (2 ms) indicates the reduction of Q_A. The fluorescence rise from J- to I-level (30 ms) indicates the reduction of Q_B and partially of the plastoquinone pool. The rise from I- to P-level (200-300 ms) indicates the electron flow through PSI (plastoquinone pool fully reduced at P-level). B- Fast fluorescence kinetics (OJIP) for fully green leaves from *gh* and SM plants, flash illuminated after different times of dark adaptation.

3.2.3.3 Long-term chlorophyll *a* fluorescence induction kinetics

In another set of experiments, induction kinetics of chlorophyll fluorescence were performed over a longer time range, 30 min incubation of leaves in the dark followed by exposure to actinic light (200 μmol.m^{-2}.s^{-1}) for 10 min (Fig. 3.18). In this time window, typical Kautsky kinetics describes the drop of fluorescence from the F_m level (P-level) to the steady state level (F_s) and is characterized by the complex superposition of processes including the light induced activation of PSI, of carbon assimilation (Calvin cycle), of alternative electron transfer (*e.g.* Mehler reaction) and the build-up of pH-dependent non-photochemical quenching. Consistent results were obtained showing that the effective quantum yield of PSII (ΦPSII) is lower in *gh vs.* SM and that the relative reduction state of Q_A (estimated as 1-qP) is higher in *gh vs.* SM. 1-qP also reflects the overall reduction state of the electron transport chain and therefore of the quinone pool. When this parameter was expressed as 1-qL (Kramer *et al.*, 2004), the same result was obtained (not shown). In contrast, the non-photochemical quenching parameter qN was not found to differ significantly between both leaf types.

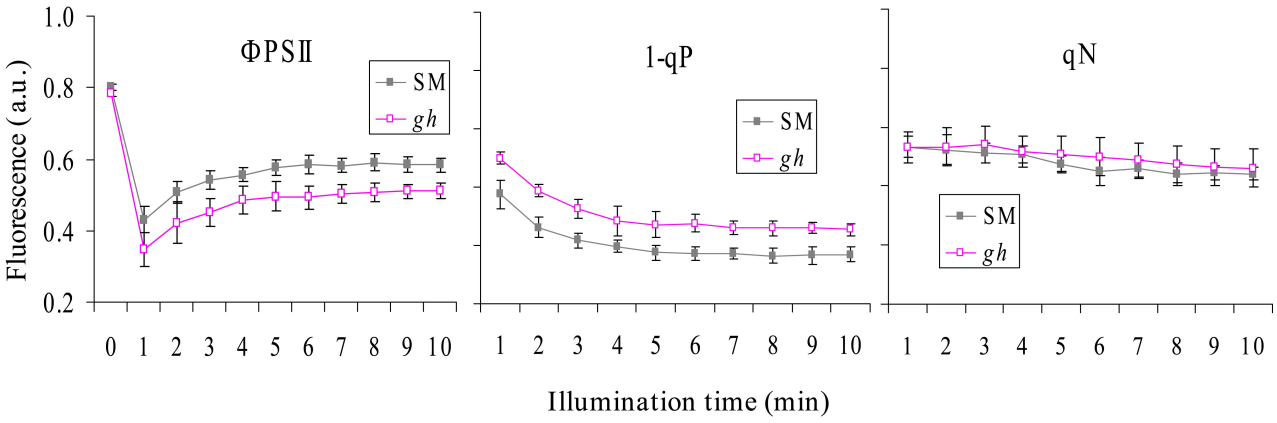

FIGURE 3.18 – **Induction kinetics for the chlorophyll fluorescence parameters ΦPSII, 1-qP and qN. SM and green *gh* leaves were dark-adapted for 30 min then illuminated with actinic light of 200 μmol.m^{-2}.s^{-1} for 10 min. Mean values (n=6) were used.**

The long-term induction kinetics of chlorophyll fluorescence was also performed after 4h dark incubation or after 1h low light incubation followed by exposure to actinic light (200 μmol.m^{-2}.s^{-1}) for 10 min. Again, lower ΦPSII and higher 1-qP values were found for *gh vs.* SM leaves (Figs. 3.19A and B), as found for a 30 min dark incubation period before exposure to actinic light (Fig. 3.18). In addition, qN values were similar in both leaf types after either 4h dark adaptation or 1h low light incubation. It can be noted that, after 4h dark adaptation, these

qN values remained low during the first min of illumination and increased gradually during several min. Compared to the rather constant qN values in the case of 30 min dark-adaptation and 1h low-light adaptation, after such a long dark-adaptation, it seems that a lower pH gradient can be established during the initial phase of actinic light exposure, but this occurs in both SM and *gh* leaves.

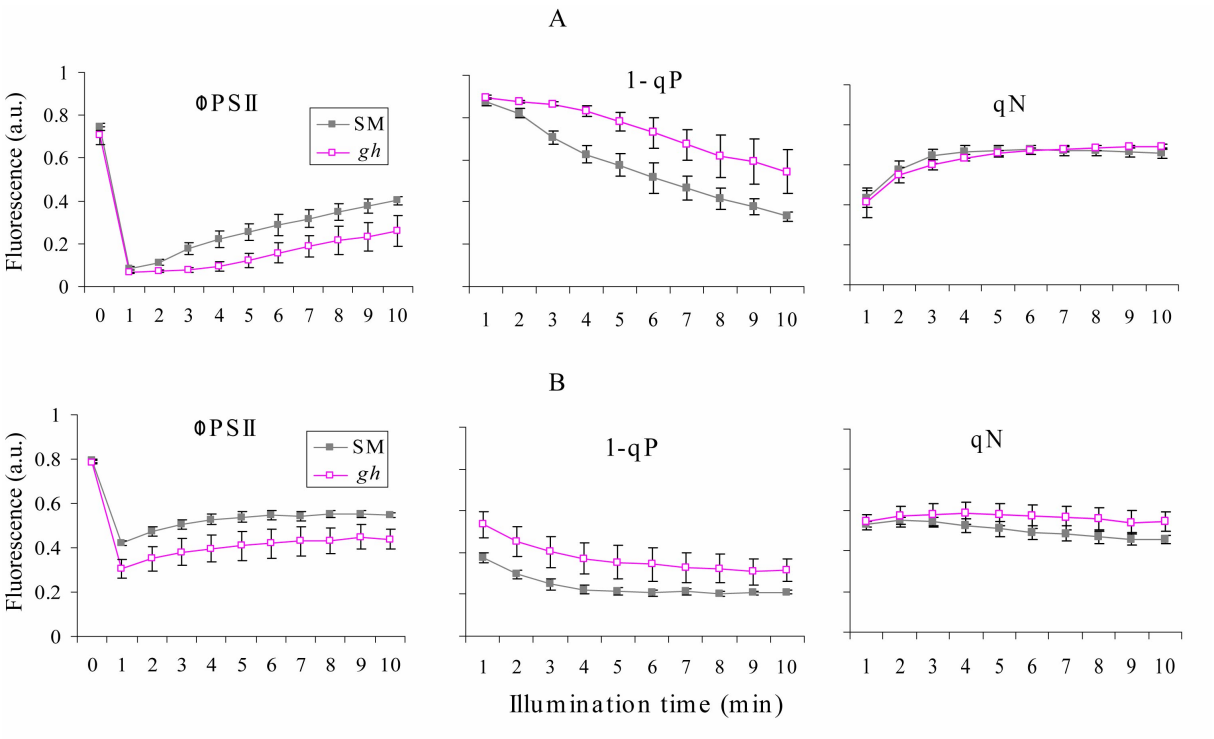

FIGURE 3.19 – **Induction kinetics for the chlorophyll fluorescence parameters ΦPSII, 1-qP and qN after 4h dark and 1h low light-adaptation. SM and green *gh* leaves were 4h dark-adapted (panel A) or 1h low light-adapted (panel B), then illuminated with actinic light of 200 μmol.m^{-2}.s^{-1} for 10 min. Mean values (n=4) were used.**

3.2.4 PTOX influence on pre- and postillumination fluorescence (F_0)

3.2.4.1 Pre- and postillumination F_0 measurements under standard conditions

When leaves are harvested from their growth chamber conditions and incubated in darkness for 30 min, it is expected that (in WT leaves) Q_A is fully oxidized, in redox equilibrium with the PQ pool. In this re-oxidized state of the photosynthetic apparatus, exposure to measuring light (non-actinic) typically yields a low chlorophyll fluorescence level (termed F_0). At the onset

of measuring light, this initial fluorescence originates from antenna chlorophyll *a* fluorescence (reviewed by Krause and Weis, 1991, see also Chapter 3.1). After exposure to strong actinic light for a few min, a return to measuring light reduces chlorophyll fluorescence to low levels which are usually characterized by a transient postillumination increase in chlorophyll fluorescence (often referred to as the "F_0 rise") (see Joët *et al.*, 2002b). This transient postillumination increase in fluorescence is considered to arise from the reduction of PQ by NAD(P)H or other reducing substances accumulating in the light (Burrows *et al.*, 1998; Shikanai *et al.*, 1998). The postillumination chlorophyll fluorescence increase is normally absent in NDH-less mutants.

Experiments were performed in parallel using SM and *gh* leaves to evaluate both pre- and post-actinic illumination F_0 levels. Strikingly, steady-state chlorophyll fluorescence (F_s) under actinic illumination remains at a higher level in *gh* than in SM leaves (Fig. 3.20A; a small but highly reproducible difference). After return to measuring light, we expected that the PQ state would be more reduced in *gh* than SM, in the absence of PTOX. To our surprise, under our experimental conditions, there was no notable difference in the transient rise in F_0 fluorescence between SM and *gh* (Fig. 3.20A).

In contrast, as shown in figure 3.20A, the typical rise in pre-illumination F_0 is not identical in SM and *gh* leaves. In SM, F_0 reaches a steady-state level, while in *gh* this level is slightly higher and diminishes gradually (Fig. 3.20A). This difference is shown on a larger scale in figure 3.20B. This phenomenon indicates that a portion of Q_A^- is not re-oxidized in *gh* during the 30 min dark period before measuring light is applied. This F_0 increase in *gh* leaves was reproducible and was never observed in SM.

3.2.4.2 Influence of light conditions prior to F_0 measurements

In these experiments, detached leaves from SM and *gh* plants grown in a growth chamber (50-60 μmol.m^{-2}.s^{-1}) were photostressed under 200 μmol.m^{-2}.s^{-1} during 30 min. This photostress was followed by a dark period of 5 min, 30 min or 4h. The initial F_0 fluorescence (termed apparent F_0 in Fig. 3.21A) increased (with respect to the non-photostressed leaves from section 3.2.4.1) in both genotypes after 5 or 30 min recovery from photostress, but the extent of this increase was higher in *gh*. Moreover, the initial apparent F_0 decrease slightly with time to reach a steady state level in *gh*, but not in SM which reache a steady state F_0 level immediately. Dark

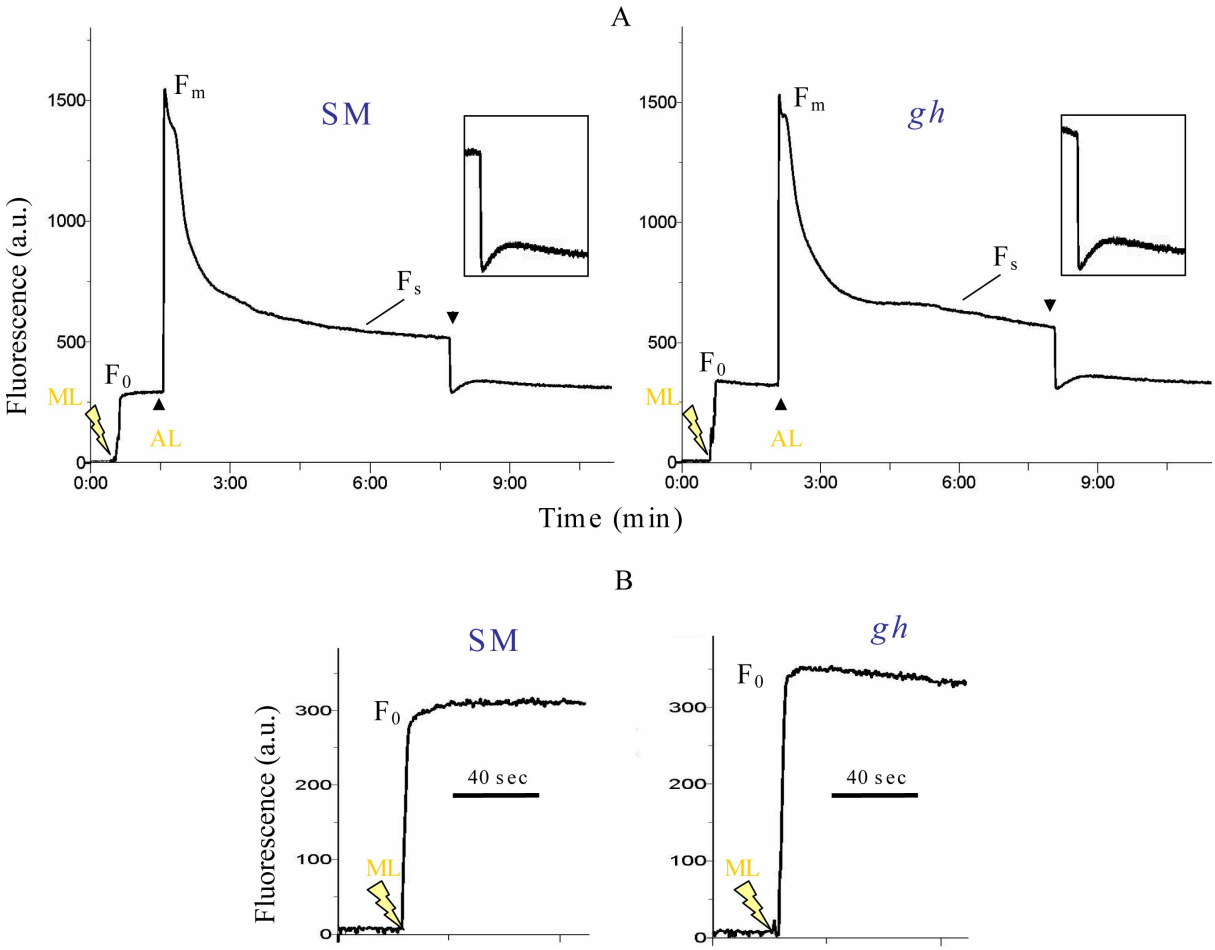

FIGURE 3.20 – **Pre and postillumination fluorescence measurements (F_0 rise) following a dark to light and then light to dark transition in SM and *gh* detached green leaves. A- Light was switched off when indicated after a 10 min period of actinic illumination (200 μmol.m^{-2}.s^{-1}). B- The initial fluorescence level, F_0 with measuring light (ML) in SM and gh after 30 min dark-adaptation. ML, measuring light; AL, actinic light; F_0, initial fluorescence value; F_m, maximum fluorescence value; F_s, steady state fluorescence value.**

incubation for 4h after photostress led to the disappearance of this increased F_0 (F_0 values being identical in both SM and *gh* leaves).

Far-red illumination could only partially quench this increased F_0 fluorescence in SM leaves after 5 min poststress dark incubation, but with longer dark incubation this effect was not evident (Fig. 3.21A). In contrast, in *gh* leaves, a strong far-red quenching effect was observed for 5 and 30 min dark incubation after stress. Since far-red light promotes PSI-induced oxidation of the photosynthetic electron transport chain, the above observation indicates that the F_0 increase in *gh vs.* SM leaves is primarily due to a larger PQ pool reduction in *gh* lasting for at least 30 min.

Figure 3.21B shows that after 30 min incubation of leaves at 200 μmol.m^{-2}.s^{-1} and subsequent dark incubation for 5 min or even 30 min, the transient postillumination chlorophyll fluorescence increase (F_0 rise) remained unchanged in both genotypes. In both cases, the F_0 rise completely disappeared after 4h dark incubation.

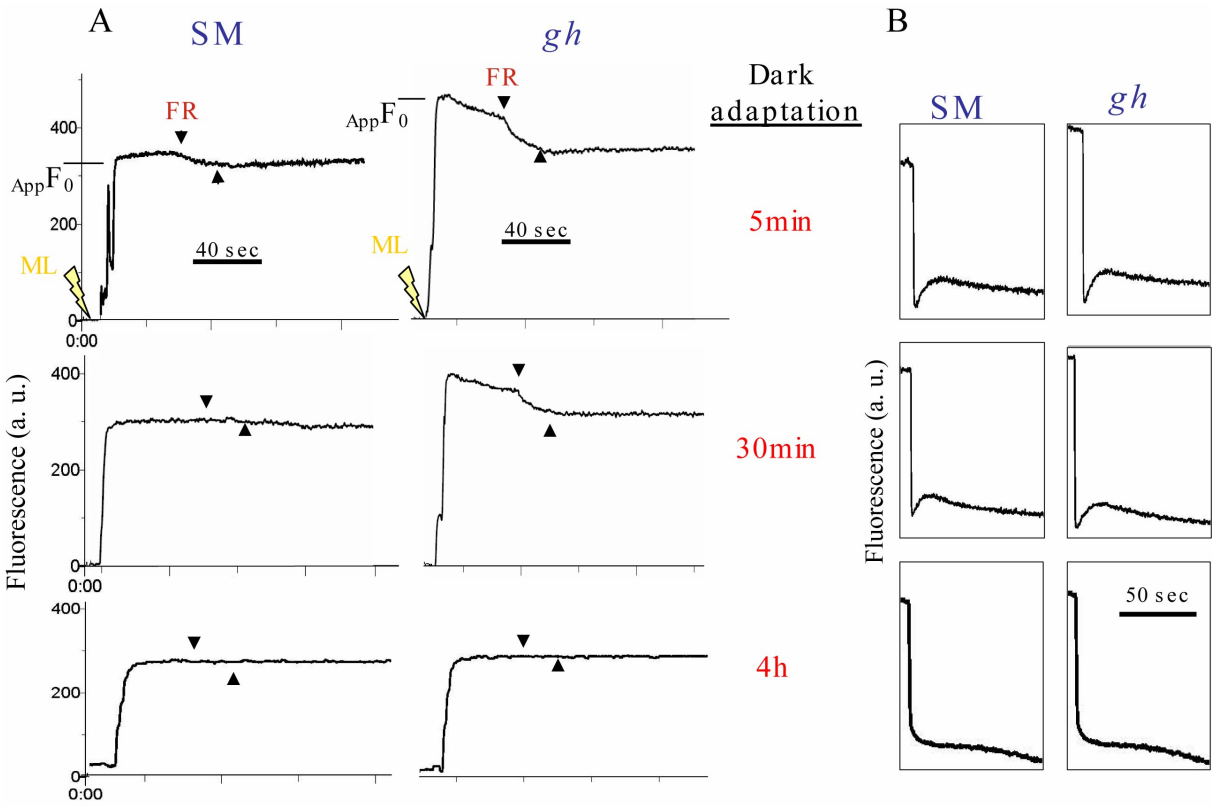

FIGURE 3.21 – **Pre and postillumination fluorescence- measurements following 30 min incubation under 200 μmol.m^{-2}.s^{-1} light intensity in SM and *gh* detached green leaves. A- Quenching of apparent initial fluorescence by far-red light and 5 min, 30 min and 4h dark-adaptation times. B- F_0 rise after different dark-adaption times (for details see legend of Fig. 3.20A). $_{App}F_0$, apparent initial fluorescence value; FR, far-red light (15 sec).**

3.2.4.3 Influence of heat shock prior to F_0 measurements

Heat is a common stress for plants and is often associated with strong illumination. Among the various machineries of photosynthesis, the PSII complex is rapidly inactivated either in its oxygen-evolving complex or by a significant impact on the structure and function of the photochemical reaction center (Enami *et al.*, 1994; Yamane *et al.*, 1998; Allakhverdiev *et al.*, 2007). Moderate heat can also cause a functional separation of LHC from the PSII. Heat is known to have an opposite effect on photosynthetic electron transport, namely stimulation of

PSI which is related to enhanced reduction of the PQ pool by either ferredoxin or NADPH (Havaux, 1996; Bukhov *et al.*, 1999). Whether PTOX plays a role during this stress is therefore a possibility to be investigated, especially since it is known that heat stress leads to F_0 increase. The latter phenomenon can be linked to release of LHCII from PSII, to partial inactivation of PSII or to dark reduction of Q_A by a back flow from the PQ pool or alternative electron donors (Sazanov *et al.*, 1998a; Yamane *et al.*, 2000; Toth *et al.*, 2007). In addition, inhibition of CO_2 assimilation induced by heat could also lead to overreduction of the electron transport chain and a remarkable increase in NDH activity (Wang *et al.*, 2006).

It has been reported that heat stress induces some events in PSII which are rapidly reversible within min after cooling the samples to normal temperatures. This is the case for the release of the 33 kDa manganese-binding protein of the PSII complex (Yamane *et al.*, 1998), as well as the reversible conformational changes in the D1 and D2 proteins of PSII reaction centers (Wen *et al.*, 2005).

Since these events are likely to occur in both SM and *gh* leaves, and may hide PTOX-related events, we applied a 5 min recovery at 25°C after heat stress for our experiments. Leaves from light-grown plants (at 60 μmol.m^{-2}.s^{-1}) were detached and exposed for 10 min at 42°C in darkness and then incubated for 5 min at 25°C in darkness and cooled to room temperature. A number of changes in the fluorescence induction profile can be seen (Fig. 3.22). The initial F_0 level (with measuring light) was increased after heat stress in SM compared with control non-heat-stressed SM leaves. F_0 level was increased considerably in heat-stressed *gh vs.* SM leaves (about 200% in *gh* and only 118% in SM), a phenomenon which is further investigated below. The rise in F_0 in both SM and *gh* indicates that the heat treatment triggered changes, most likely in PSII and PSII antenna, as expected. Accordingly, it should be mentioned that heat stress noticeably lowered F_m after actinic illumination in both genotypes.

After actinic light is turned off, the postillumination F_0 rise is enhanced greatly in *gh*, with only a marginal increase in SM (Figs. 3.22C,D), in heat-stressed leaves as compared to non-heat-stressed control leaves (Figs. 3.22A,B). It has been shown that, when samples were re-cooled to 25°C after the high temperature treatment, the rate of the postillumination fluorescence increase became low, suggesting that reduction of PQ pool, via NDH or another component of the cyclic electron flow, after being activated by heat is inactivated after cooling (Yamane *et al.*, 2000). But the present data demonstrates that even after 5 min recovery, *gh* leaves could not re-equilibrate the electron flow from the reductants to PQ.

A potential explanation for the stronger heat-induced pre-illumination F_0 increase in *gh* *vs*. SM leaves could be an enhanced reduction state of the PQ pool leading to closure of PSII centers by back electron flow (Havaux, 1996; Yamane *et al.*, 2000). Figure 3.23 shows that far-red light could partially quench the increased fluorescence in *gh* (Fig. 3.23B), but had no effect in SM leaves (Fig. 3.23A). This experiment was repeated more than 6 times and showed that this particular component of F_0 corresponds to approximately 35% of the total increase in F_0 in *gh* compared with control.

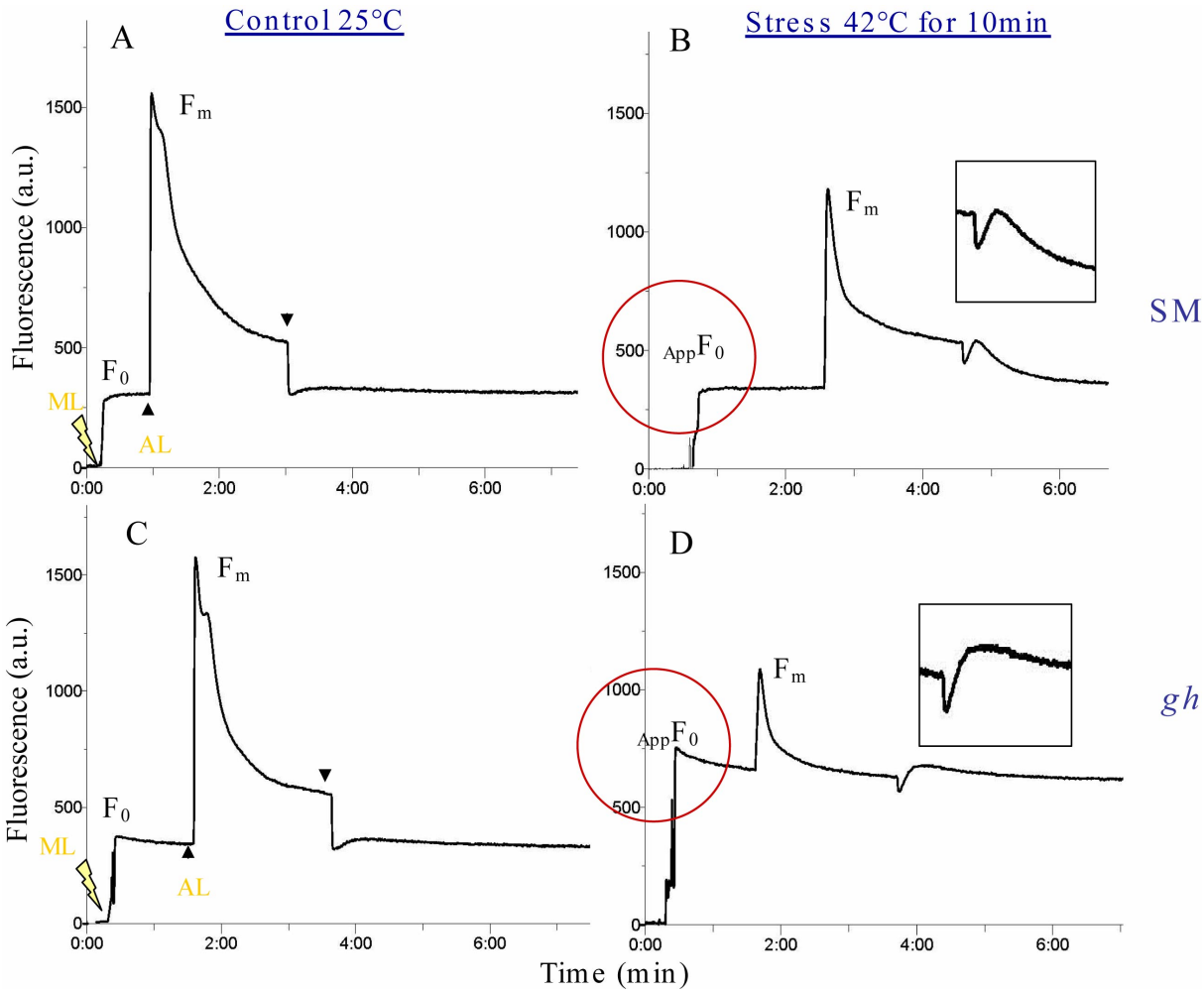

FIGURE 3.22 – **Fluorescence induction analysis after heat stress. Dark-adapted leaves of SM (A, B) and *gh* (C, D) after heat stress (10 min at 42°C then 5 min 25°C) and control (15 min at 25°C). ML, measuring light; AL, actinic light; $_{App}F_0$, apparent initial fluorescence value; F_m, maximum fluorescence value.**

Figure 3.24 shows that when 22°C-grown *gh* leaves were exposed to elevated temperature, the first symptoms of PSII alteration could be detected at around 38°C and dramatic inactivation of PSII started at around 40°C where initial F_0 is increased and F_m is clearly decreased. The

rate of postillumination fluorescence increase and also the quenching effect of far-red light on the pre-illumination F_0 level are high at temperatures above 40°C (Fig. 3.24C,D), which is consistent with the fact that PSI and PSII-to-PSI electron transport is more tolerant to heat stress. The rate of postillumination F_0 rise became low at 44°C and above, although the initial F_0 increase remained very high (data not shown).

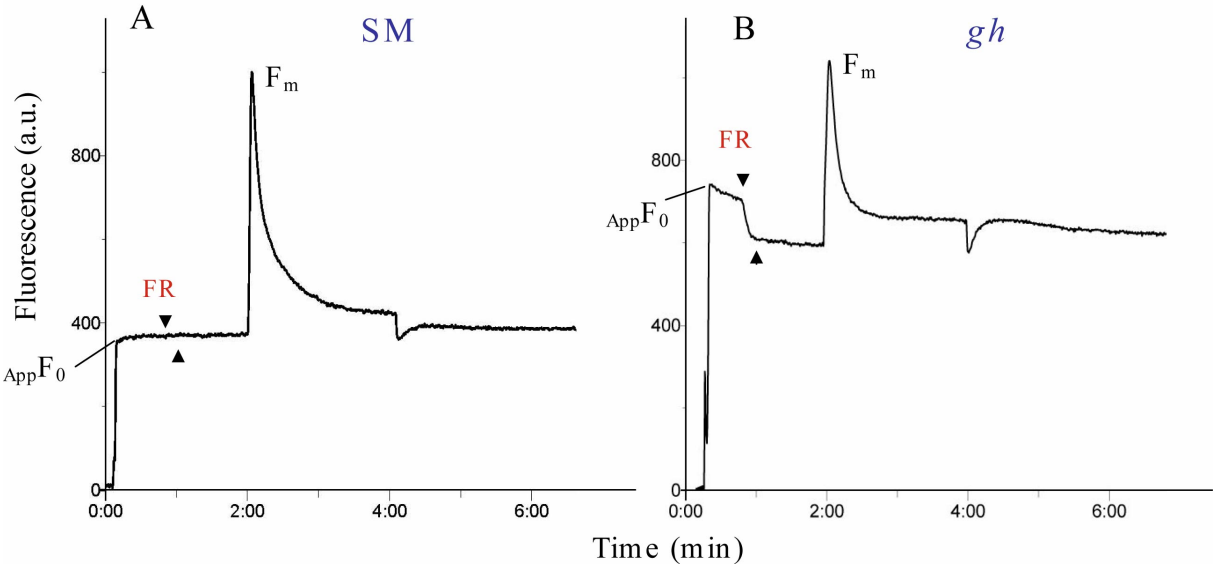

FIGURE 3.23 – **Quenching of apparent initial fluorescence by far-red light in the dark-adapted leaves of SM (A) and *gh* (B) after heat stress (10 min at 42°C then 5 min 25°C) in *gh* but not SM. ML, measuring light; AL, actinic light; $_{App}F_0$, apparent initial fluorescence value; F_m, maximum fluorescence value; FR, far-red light (15 sec).**

We also examined the effects of 4h dark incubation prior to heat stress., This dark adaptation could significantly lower the increased "apparent" F_0 values in *gh* (Fig. 3.25) and abolish the quenching effect far-red light exposition had in leaves not adapted to darkness (not shown). In addition, in the case of 4h dark-adaptation, the increase in postillumination fluorescence (F_0 rise) triggered by heat was lowered in both genotypes. Interestingly, during actinic illumination, fluorescence quenching (to reach F_s) was not identical in *gh vs.* SM leaves: the respective contribution of photochemical and non-photochemical quenching was different (the photochemical quenching being roughly proportional to the fluorescence spikes corresponding to saturating flashes in Fig. 3.25) especially during the first min. The different profiles of the qN and NPQ parameters (in heat stressed leaves, after long dark adaptation) in *gh vs.* SM suggest that a stronger pH gradient is established in *gh* immediately after actinic illumination (Fig. 3.25E). These differences are linked to heat stress since they are not observed at 25°C (Fig. 3.25E).

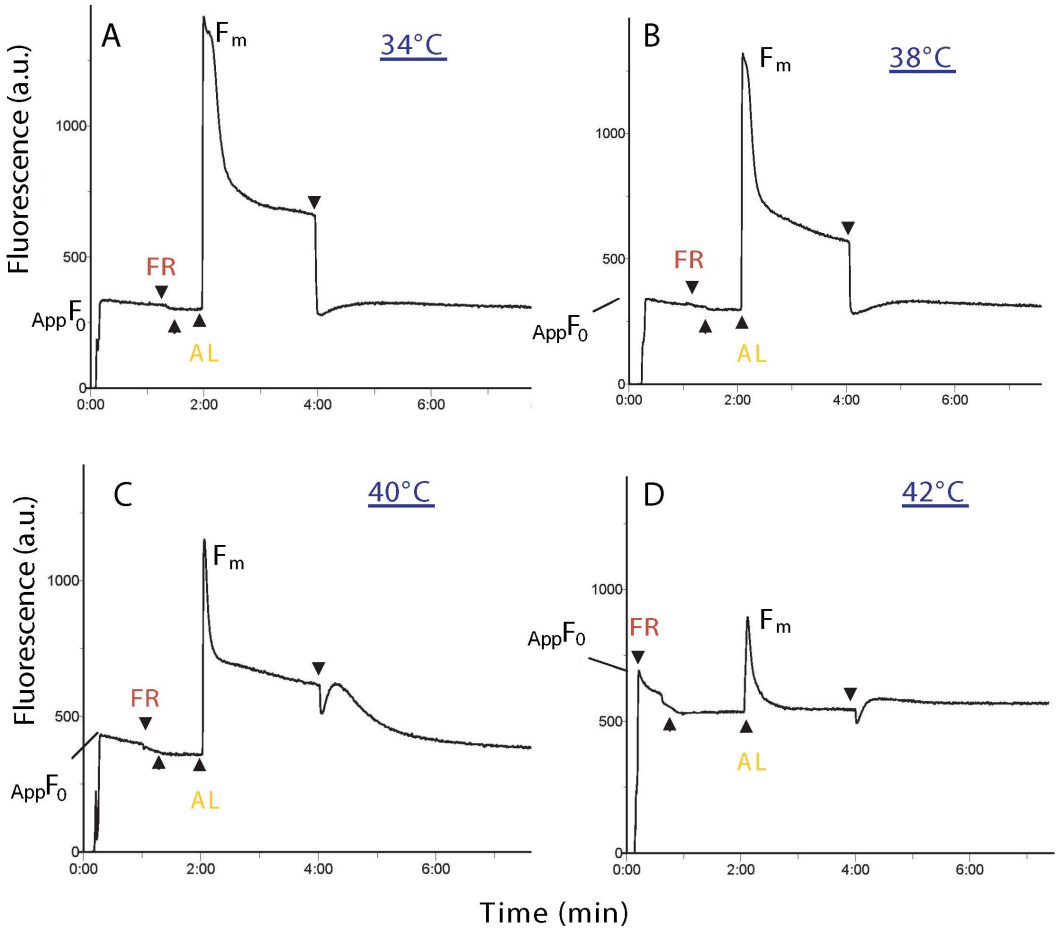

FIGURE 3.24 – **Fluorescence induction analysis of dark-adapted *gh* leaves after heat stress (10 min) at different temperatures. 34°C (A), 38°C (B), 40°C (C) and 42°C (D). ML, measuring light; AL, actinic light; $_{App}F_0$, apparent initial fluorescence value; F_m, maximum fluorescence value; FR, far-red light (15 sec).**

We also examined the effects of various potential inhibitors on this F_0 increase. Diphenyleneiodonium (DPI), a flavoenzyme inhibitor, was chosen since data indicate it can inhibit the heat-induced Q_A^- reduction component of F_0 increase (Yamane *et al.*, 2000). However, in our experiments, DPI (50 μM, 100 μM) had no effect (data not shown). Higher concentrations could not be examined because the solvent DMSO tended to induce leaf necrosis.

The reduction of PQ may be related to cyclic electron transport around PSI via ferrodoxin (Munekage *et al.*, 2004; Shikanai, 2007). Since this PGR5-dependent pathway is sensitive to antimycin A, we also used this inhibitor prior to heat stress. Petioles of excised leaves were incubated overnight in the presence of this inhibitor under low light (20 μmole.m^{-2}.s^{-1}). At

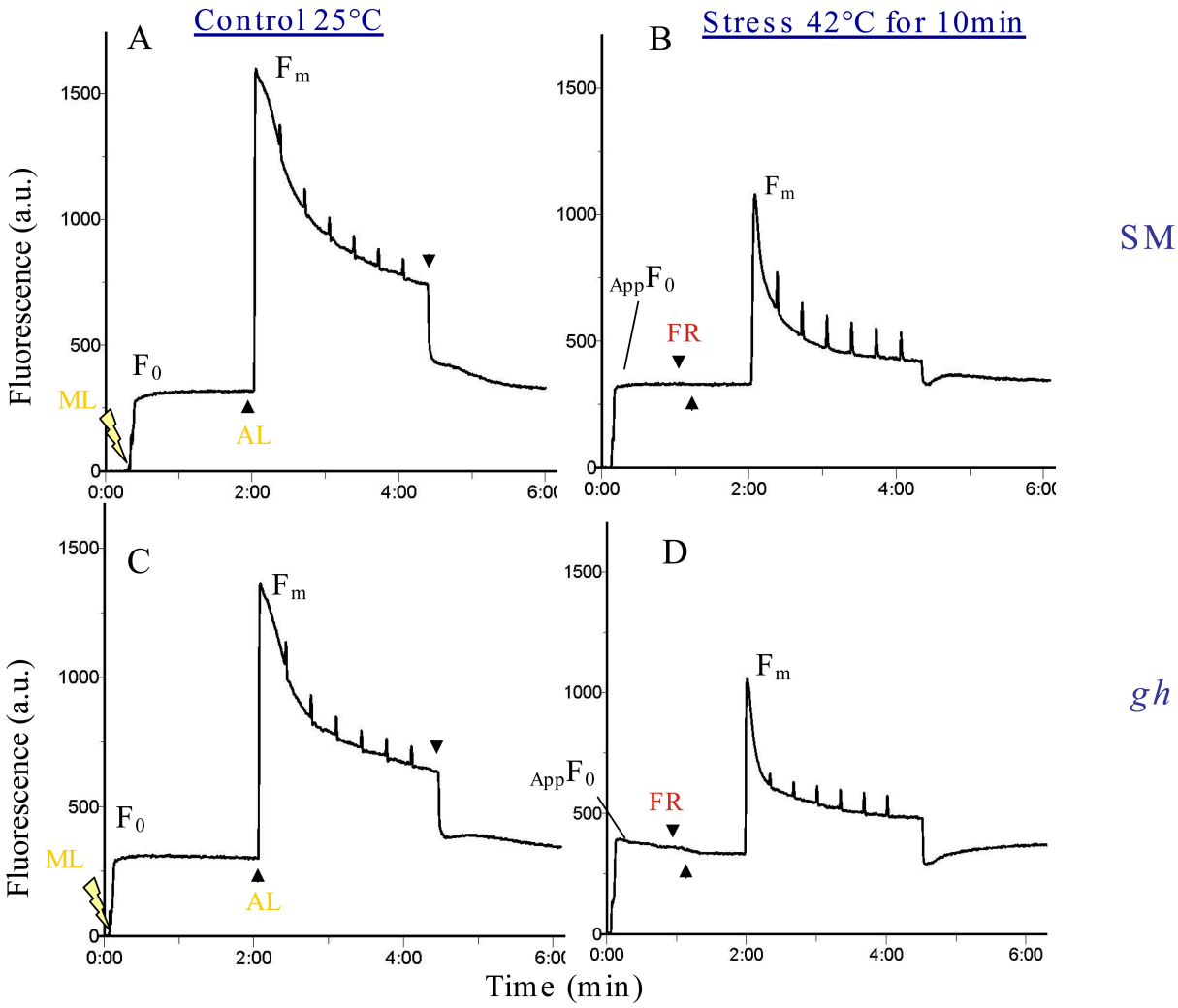

FIGURE 3.25 – **Effects of 4 h dark adaptation prior to heat stress on the fluorescence induction analysis. SM (A, B) and *gh* (C, D) leaves in heat stress (10 min at 42°C then 5 min 25°C) and control (15 min at 25°C). ML, measuring light; AL, actinic light; $_{App}F_0$, apparent initial fluorescence value; F_m, maximum fluorescence value; FR, far-red light (15 sec).**

10μM or 20μM, Antimycin A did not influence the pre-illumination F_0 increase, but preliminary results showed an important decrease in postillumination F_0 increase (Fig. 3.26).

3.2.5 Effects of photo-oxidative stress on NADH dehydrogenase complex (NDH) activity and protein expression

When leaves are subjected to high light intensity or another photo-oxidative stress (*e.g.* paraquat or H_2O_2), the level and activity of the NDH complex have been shown to increase (Casano *et al.*, 2001; Lascano *et al.*, 2003; Martin *et al.*, 2004). Photo-oxidative stress also induces

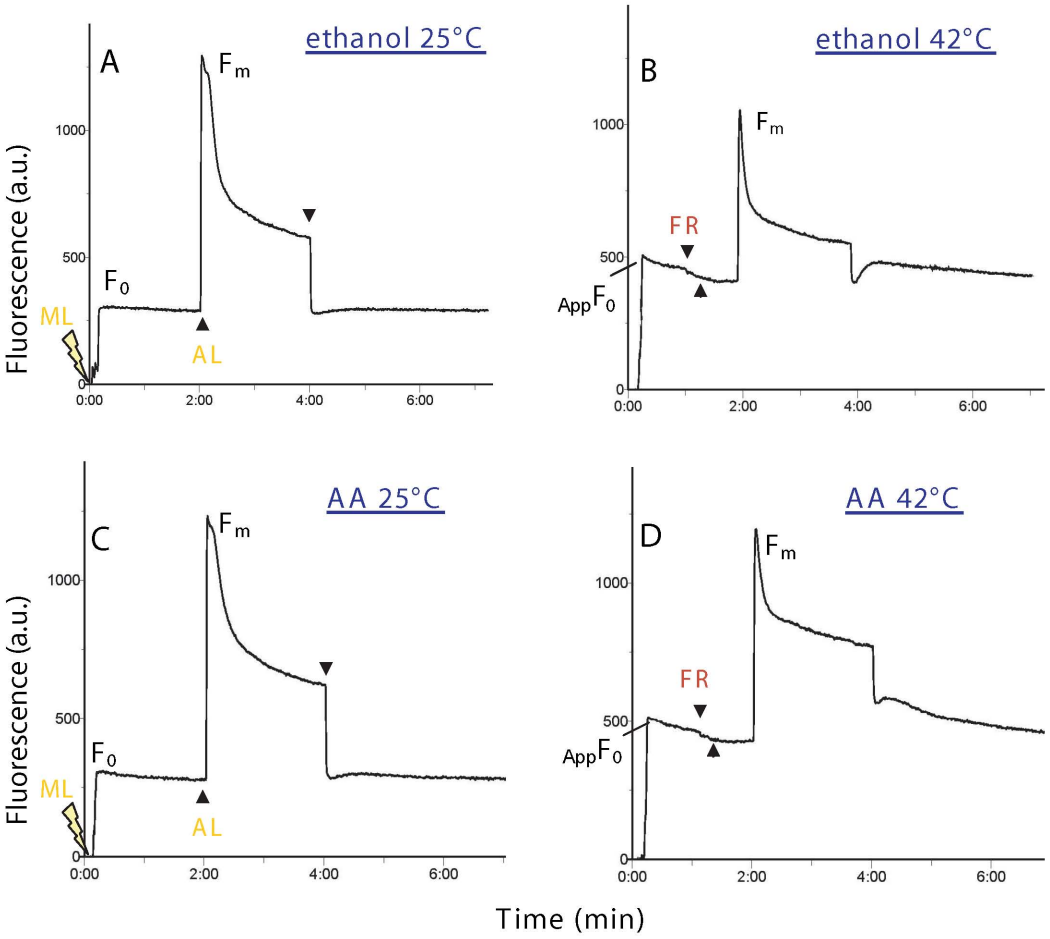

FIGURE 3.26 – **Effect of antimycin A-incubation prior to heat stress on fluorescence induction analysis. Prior to heat stress, the petioles of excised *gh* leaves were incubated in 0.9% ethanol as a control solvent (A, B) and 20 μM antimycin A (C, D) leaves under low light overnight. AL, actinic light; $_{App}F_0$, apparent initial fluorescence value; F_m, maximum fluorescence value; FR, far-red light.**

other enzymes such as those scavenging reactive oxygen species or preventing their formation. But, under very strong photo-oxidative stress, these protective enzymes could be more rapidly destroyed than induced (Casano *et al.*, 1999) leading to photo-oxidative damage. Therefore, to compare the level and activity of the NDH complex between wild type SM and the PTOX-deficient *gh* mutant, while avoiding photo-oxidative damage to the complex, light stress of 5-6 fold higher intensity compared with growth light was used.

Fully green leaves of 60 day-old SM and *gh* plants grown under low light intensity (LL, 50 μmol.m^{-2}.s^{-1}, see Materials and Methods) were detached and either kept under low light (growth light intensity, LL) or transferred to high light intensity (HL, 250 μmol.m^{-2}.s^{-1}) for 3h,

6h and 20h. Figure 3.27 A shows the changes in PTOX and NDH protein levels (detected with antibodies against PTOX, NDH-H, using PsaD as a standard control). The protein profiles after SDS-PAGE and then red Ponceau coloration showed approximately the same protein levels in each sample and lane. While immunodetection and did not reveal any signal for PTOX in *gh* as expected, a PTOX band of 37 kDa was visible in SM. Detachment and incubation under LL and HL increased both PTOX and NDH-H protein level in SM leaves which was more pronounced under HL than LL. However, the increase in PTOX and NDH-H levels was not concomitant. The greater increase was observed after 20h HL for PTOX, wheras the NDH protein is accumulated after 3h under both LL and HL. In *gh* leaves, there is no increase in NDH-H level under stress (HL). Thus, there seems to be some cross-talks between NDH levels but the latter appear to be also influenced by other factors: this is the case for example for the increase in NDH-H protein level in the first hours after leaf. We have confirmed these results in 3 independent experiments.

Figure 3.27B shows PTOX and NDH protein levels and in parallel NADH dehydrogenase complex activity in SM and *gh* leaves, after incubation for 20h under LL and HL intensity. When SM leaves were cut and incubated under HL, NDH activity increased significantly ($P<0.001$) compared with T_0 at 20h under LL, which is consistent with the changes observed in NDH-H protein levels. Interestingly, no increase in NDH activity was observed in *gh* leaves in any sample, which is also consistent with the constant NDH-H protein levels in these samples. Thus, it seems that the PTOX level exerts some influence on the NDH complex levels which in turn influence NDH activity *in vitro*.

3.2.6 Discussion

3.2.6.1 The photosynthesis imperfections in *gh* green leaves are due to a more reduced PQ pool

Adult *gh* leaves have the same relative chlorophyll and carotenoid composition as wild type leaves and do not show any detectable accumulation of phytoene (*cf.* § 3.1). Analysis of thylakoid protein composition revealed that the increased sensitivity of the photosynthetic apparatus to extreme conditions in *gh* were not caused by major rearrangements in protein complexes in the electron transport chain.

When light intensity was moderately increased, fluorescence measurements at low temperature (77K; Fig. 3.15) revealed a clear difference in the F_I/F_{II} ratio between *gh* and SM. This

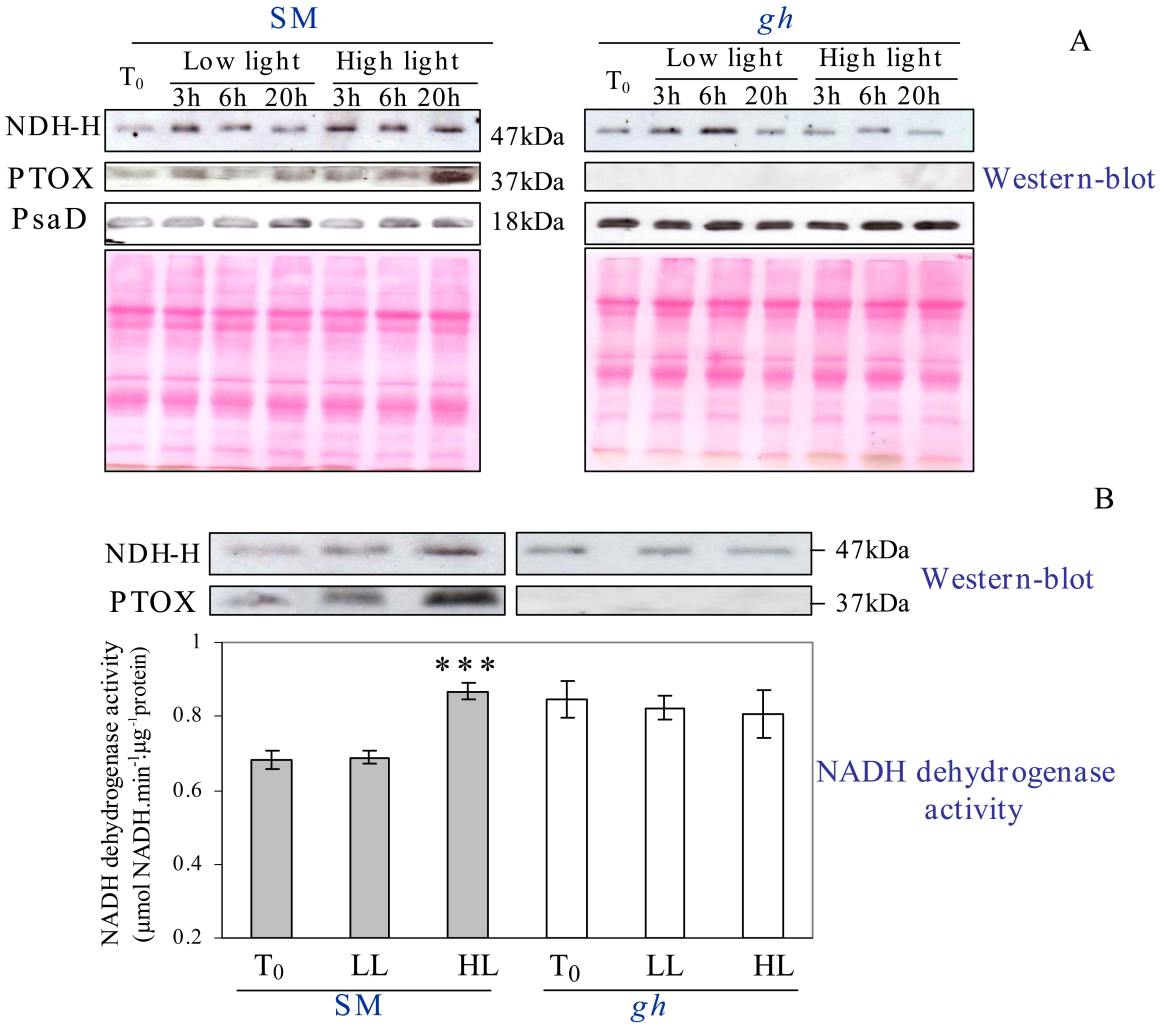

FIGURE 3.27 – **NADH dehydrogenase complex activity and PTOX and NDH protein levels under high light intensity in SM and *gh* leaves. A- PTOX and NDH protein level changes (detected with respective antibodies and PsaD as a control) in SM and *gh* detached leaves after incubation during 3h, 6h and 20h under low light intensity (50 μmol.m^{-2}.s^{-1}, LL) and relative high light (250 μmol.m^{-2}.s^{-1}, HL). Red Ponceau stained PAGE (40 μg protein per lane) shows equal loading of the samples. B- NADH dehydrogenase complex activity (with thylakoid membranes solubilized with 1% DM) and PTOX and NDH protein levels in SM and *gh* leaves after incubation for 20h under LL and HL. Mean values for enzyme activity from minimum 4 measurements (*i.e.* 4 different leaves). Statistically significant differences are indicated compared to T_0: *** P< 0.001.**

ratio normally changes as a consequence of acclimation of the photosynthetic machinery to the prevailing growth irradiance (Baena-Gonzalez *et al.*, 2001). Thus, it appears that *gh* leaves could not rapidly acclimate to this change in light condition. Moreover, the 77K fluorescence emission spectra of far-red light-adapted leaves (PSI excitation light; state 1) after illumination with blue light (PSII excitation light; state 2) show that state transition does occur in *gh* leaves suggesting that its photosynthetic apparatus in state 1 is already in a pre-state 2, most likely as a

consequence of more reduced state of the PQ pool. According to the state transition mechanism, when plants or algae are illuminated by light that is absorbed preferentially by PSII (blue light), the PQ pool becomes reduced and the binding of reduced PQ to the Q_o site of Cyt b_6f complex leads to the activation of the LHCII kinases resulting in the movement of phosphorylated mobile LHC antenna from PSII to PSI. In contrast, under PSI absorbed light (far-red), the PQ pool becomes oxidized. This leads to the inactivation of the LHCII kinase, the dephosphorylation of the LHCII associated with PSI via some phosphatase and the return of LHCII to PSII. This state is called state 1 (Allen, 2003; Bellafiore *et al.*, 2005; Rochaix, 2007).

PTOX functions as a plastoquinol oxidase *in vitro* (Josse *et al.*, 2000, 2003). Consistent *in vivo* data were obtained here suggesting that PTOX indeed affects the redox status of PQ in leaves. This is especially evident from the results of OJIP fast kinetics (Fig. 3.17) and from the more rapid rise in fluorescence kinetics in *gh* leaves during a transition from dark to low light (Fig. 3.16). Under 10 min actinic illumination, induction kinetics of chlorophyll fluorescence (Fig. 3.17) shows higher 1-qP values (lower photochemical quenching) in *gh* consistent with the reduced operational quantum yield of PSII. This is indicative of a more reduced status of PSII acceptors (Q_A) in *gh* leaves compared to control SM leaves, indicating that the PQ pool is more reduced. Unlike 1-qP values, the qN parameter was not significantly different in *gh* and control SM leaves, indicating that the extent of nonphotochemical quenching reached similar levels. This implies that a similar photosynthetic gradient is established in *gh* and SM under these experimental conditions. The higher reduction state of the electron transport chain under steady state illumination in *gh vs.* SM leaves suggests that the lack of PTOX leads to less efficient utilization of photosynthetic or alternative electron sinks (Ort and Baker, 2002).

Furthermore, the more greatly reduced electron transport chain in *gh* leaves during dark to light transitions are applied (Fig. 3.16 and 3.17) indicates a lack of fine-tuning for the optimal allocation of electrons to photosynthetic and non-photosynthetic sinks. This is important in the first min of illumination (Fig. 3.18 and 3.19) before light-activation of the Calvin cycle, when the development of pH-dependent nonphotochemical and photochemical quenching is critical. The more reduced state of Q_A during this period might also render PSII more sensitive to photobleaching since photoinhibition or photodamage to PSII is highly dependent on the redox state of PSII and membrane energization (Ogren, 1991).

A regulatory role for PTOX is also suggested by the slightly higher pigment content of green leaves in *gh vs.* SM (Fig. 3.3B and D in chapter 3.1). However, this slight increase in

both chlorophyll and carotenoid content is unlikely to be the causal link between the lack of PTOX and the various effects on photosynthetic electron transport described here. For instance, in *gh* the influence of dark adaptation time on fast fluorescence kinetics (Fig. 3.17) or the delay before full activation of the xanthophyll cycle during long incubation under severe light conditions (*cf.* § Table 3.1) must result from more complex regulatory mechanisms.

3.2.6.2 In the dark, the first quinone acceptor (Q_A) of PSII and the intersystem electron carriers are overreduced in *gh* green leaves

The present work has shown for the first time an elevated initial fluorescence (F_0) under standard (non-stressed) conditions for a PTOX knock-out mutant; indicating that part of Q_A^- is not re-oxidized, even after a period of dark incubation. This particular phenotype became more important after a short light stress. Interestingly, both a long dark incubation (quenching complete after 4h) and a rapid far-red light exposition could quench this increased F_0 fluorescence. Therefore, in the absence of PTOX, PSII electron acceptors are susceptible to be more reduced under changing light conditions.

Since the NDH complex may possibly use NADH produced by starch degradation to reduce the PQ pool in the dark (Sazanov *et al.*, 1998a), the long delay (4h in our experiments) before the light-induced increase in F_0 disappears (Fig. 3.21) could be linked to starch consumption in the dark (Geiger *et al.*, 1995; Sazanov *et al.*, 1998a).

In agreement with our results, a high level of F_0 fluorescence was previously reported in a cytochrome b_{559} mutant (Bondarava *et al.*, 2003). It has been suggested that cytochrome b_{559} may also function as a plastoquinol oxidase associated with PSII in order to keep the acceptor side of PSII oxidized in the dark (Kruk and Strzalka, 2001). Moreover, in transplastomic tobacco plants overexpressing Fd, apparent F_0 fluorescence was also higher than in the wild type, which was suppressed to wild-type level upon illumination with far-red light, implying an enhanced nonphotochemical reduction of PQs (*i.e.* the transfer of electrons by FQR from the chloroplast stroma to PQ was increased) in these transplastomic plants (Yamamoto *et al.*, 2006). In general, the inactivation or the damage of PSII may cause an increase of F_0 (Xu and Wu, 1996).

Surprisingly, the postillumination F_0 fluorescence increase was not enhanced in the PTOX knock-out mutant under our experimental conditions implying changing light conditions. In contrast, in transgenic tobacco plants over-expressing At-PTOX, this transient dark reduction of

photosynthetic electron carriers is decreased substantially, indicating that electrons are diverted to O_2 via PTOX (Joët *et al.*, 2002b), and PTOX potentially prevents overreduction of PQs in the light.

An elevated initial fluorescence (F_0) in *gh* compared with SM and in the other hand, no difference in the level of postillumination F_0 fluorescence increase lead to a conclusion that PTOX contributes to the transfer of photosynthetic electrons to O_2, possibly from a sub-pool of PQ, which may exchange electrons with the general (photosynthetic or NDH corresponding) PQ pool later.

3.2.6.3 *gh* exhibits drastically enhanced heat-induced reduction of the intersystem photosynthetic electron transport chain

Here, we have investigated the role of PTOX during a heat shock stress. We were interested in this stress since it is known that heat stress also leads to F_0 increase and induces reduction of the PQ pool. Normally, the photosynthetic membranes are known to be very sensitive to high temperature, and PSII appears more sensible to heat stress than PSI and PSII-to-PSI electron transport (Havaux, 1996). The results presented in figure 3.25 are consistent with this. It has been frequently reported that when photosynthetic organisms are exposed to heat stress, F_0 level increases (Schreiber and Berry, 1977; Havaux, 1996; Yamane *et al.*, 2000). Causes of this F_0 increase have been suggested to be release of LHCII from the PSII complex and inactivation of PSII-photochemical reaction (Schreiber and Armond, 1978), inhibition of electron flow from Q_A to Q_B (Ducruet and Lemoine, 1985; Bukhov *et al.*, 1990), or reduction of Q_A through PQ in the dark (Sazanov *et al.*, 1998a; Yamane *et al.*, 2000). The reduction of PQ is thought to be related to cyclic electron flow around PSI (Munekage *et al.*, 2004) and/or chlororespiration-like electron transport from the stroma (Burrows *et al.*, 1998; Bukhov and Carpentier, 2004). A flavoenzyme, acting as an electron carrier (Yamane *et al.*, 2000), and also the NDH complex may function to reduce PQ in the dark at high temperature (Sazanov *et al.*, 1998a; Yamane *et al.*, 2000). By deleting *ndhC* or *ndhK* genes, Sazanov and co-workers showed that, in tobacco leaves, dark reduction of Q_A after high-temperature stress was inhibited, but re-reduction of $P700^+$ after far-red illumination was unaffected. In these mutants, the fluorescence level (F_0) after heat stress is lower, and quenching by far-red light was not observed. The authors concluded that the heat-induced reduction of the intersystem electron transport chain can be mediated by NDH-independent pathways in the light (*i.e.* postillumination F_0 increase), but in

the dark the dominant pathway for reduction of the PQ pool is catalyzed by the NDH (Sazanov *et al.*, 1998a).

Enhancement of the postillumination increase in chlorophyll fluorescence as a consequence of stimulation of the NDH-dependent cyclic pathway under photo-oxidative stress and also oxidative conditions caused by heat stress has been reported previously (Martin *et al.*, 2004; Wang *et al.*, 2006). To prevent overreduction of stromal components, excess electrons must be efficiently consumed. Chlorespiration seems a good candidate for balancing the redox state of transporters, to provide and remove electrons by NDH complex and PTOX, respectively.

The observed substantial increase in pre-illumination F_0 fluorescence after a heat stress and in the absence of PTOX consists of two phases. One phase can be quenched partially by far-red light or prolonged pre-incubation in darkness and, therefore, reflects an enhanced reduction state of the PQ pool in *gh* leading to more electron backflow towards PSII. Two other mechanisms can explain the second phase (insensitive to far-red exposure): (1) release of LHCII from PSII core, (2) inhibition of charge separation at PSII reaction center (Schreiber and Berry, 1977; Havaux, 1996; Yamane *et al.*, 2000). Since the ratio of their contribution to the observed F_0 increase is variable depending on species, it is difficult to predict which is the primarily mechanism involved here. The importance of phase 2 of F_0 increase in *gh* may suggest a potential PTOX role in the membrane stability of thylakoids. It has been found previously that normalization of the *im* phenotype occurs when the *immutans* mutant is grown on media containing kinetin, whereas the cytokinins are necessary for plastid biogenesis and the greening process (reviewed in Rédei, 1975; Rodermel, 2002). It is worthwhile to examiner the membrane stability in PTOX knock-out mutants in the further experiments.

We also observed an enhancement of the postillumination increase in F_0 fluorescence as a result of PQ overreduction in *gh* mutant (Fig. 3.22 and Fig. 3.23). This heat-induced reduction of the intersystem electron transport chain can be mediated by NDH-dependent or NDH-independents pathways (Sazanov *et al.*, 1998a). Together, the pre- and postillumination F_0 rise, and also the effect of dark-adaptation prior to heat stress (Fig. 3.25) show that the heat stress induced an increase the electron transport rate from stromal reductants, which in the absence of PTOX in the *gh* mutant leads to overreduction of the intersystem electron transport chain.

After a long dark adaptation and a subsequent heat stress, the different profiles of the nonphotochemical quenching parameters in *gh vs.* SM leaves suggest the establishment of a stronger pH gradient in thylakoid in *gh* immediately after actinic illumination. These differ-

ences are not observed at 25°C indicating a general regulatory role of PTOX for the cyclic flow around PSI (which contributes to the formation of the proton gradient), under stress conditions (Rumeau *et al.*, 2007; Shikanai, 2007).

3.2.6.4 NDH complex may be down-regulated in *gh* under high light stress condition

Examination of effects of a relatively high light stress on *gh* and SM detached leaves points to a certain cross-talk between the levels of PTOX and NDH complex. In SM, NDH-H protein levels and NDH activity increased considerably under HL stress compared with T_0 and LL, but no increase of NDH activity was observed in *gh* leaves in any sample, which is also consistent with the constant NDH-H protein levels in these samples. This suggests that the absence of PTOX influences the whole chlorespiration process under photo-oxidative stress conditions. It has been reported previously that chlororespiration could participate in the scavenging of reactive oxygen species and also in redox poising of the intersystem chain transporters in order to optimize electron transport to PSI under variable environmental conditions (Casano *et al.*, 2000). The levels of NDH polypeptides and NADH dehydrogenase activity of the NDH complex (NADH-DH) were also found to increase under relatively high light (Martin *et al.*, 1996; Casano *et al.*, 1999, 2000, 2001). Several studies have also indicated that the NDH complex mediates the oxidation of NADH to reduce plastoquinone (Burrows *et al.*, 1998; Feild *et al.*, 1998) and that PTOX or a thylakoid PQ peroxidase in conjunction with a superoxide dismutase could mediate the reduction of oxygen as a final electron acceptor of any probable chlororespiratory route (Casano *et al.*, 2000; Peltier and Cournac, 2002).

Nevertheless, due to the low abundance of the NDH complex (Burrows *et al.*, 1998) and PTOX protein (Streb *et al.*, 2005) in certain species, it appears that the electron transfer rate of chlororespiration is too low to explanation the bioenergetically significant ATP production (Joliot and Joliot, 2005) and also to be a security valve. In addition, the overexpression of PTOX by itself could not enhance plant resistance against photoinhibition (Joët *et al.*, 2002b; Rosso *et al.*, 2006).

3.2.7 Conclusion

In this chapter, we have demonstrated that there is no major difference in the amount of protein complex in the photosynthetic apparatus between SM and *gh* green leaves. Furthermore, the photosynthesis imperfections in *gh* green leaves (as shown in chapter 3.1, without any detectable

phytoene accumulation or carotenoid decline) are a result of a higher reduction state of the electron transport chain under steady state illumination in *gh vs.* SM leaves.

Our conclusion is that PTOX has a regulatory role in the distribution of electrons to different linear and alternative electron pathways which is in agreement with previous reports (Joët *et al.*, 2002b; Peltier and Cournac, 2002). The presence of PTOX is particularly important during dark to light and low light to high light transitions.

3.3 Analysis of PTOX Over-expression in Tomato

The leaf phenotype of the *ghost* (*gh*) variegation mutant of tomato is similar to that of *im*, and *im* and *gh* define genes for orthologous proteins (Bae *et al.*, 1999; Josse *et al.*, 2000; Rodermel, 2001). To gain further insight into the function of PTOX in carotenoid biosynthesis, tomato plants constitutively expressing At-PTOX were used in this chapter.

Transgenic tomato plants (dwarf MicroTom type, MT) expressing the At-PTOX cDNA sequence under the control of the doubled constitutive 35S promoter of the cauliflower mosaic virus (Fig. 3.28A) were generated by *Agrobacterium*-mediated transformation (transformation carried out by Josse, 2003). Transgenic kanamycin-resistant lines were self-pollinated. In this study, the T2 generation was used for further experiments. We have used the tomato cultivar Micro-Tom, because it has been proposed as a convenient model system for its small size, rapid growth, and easy transformation (Meissner *et al.*, 1997).

3.3.1 Verification of transgenic plants

We checked the presence of the T-DNA in genomic DNA of various T2 plants using PCR. Specific primers were used to amplify At-PTOX DNA, and also *pds* (phytoene desaturase gene) as a control. As shown in figure 3.28B, four independent transgenic plants contained the transgene (L2, L3, L4, and L5). The T1 seeds were germinated and the homogeny of the T2 generation was examined by PCR (Fig 3.28C), and L2 was found to be a homozygote line.

In order to perform Southern genomic analysis, tomato (MT) DNA was digested with the restriction endonucleases BamH I, Hind III and Xho I, and hybridized with the radiolabeled tomato full-length cDNA probe. The results in figure 3.28D confirmed the presence of T-DNA in 4 transgenic lines (L2, L3, L4, L5 but not in L1) and revealed one locus of insertion of T-DNA in the genome for L2 and L4, and 2 loci in L3 and L5. L3 and L5 may be identical.

An antibody raised against PTOX was used to characterize At-PTOX expression in the Micro Tom transgenic lines by western-blot analysis (Fig. 3.28E). Unfortunately, only one transformed line, L2, produced a large amount of a 41 kDa protein corresponding to *Arabidopsis* PTOX in total fruit proteins, and can be considered as a PTOX over expressing line ($PTOX^{+}$)[1].

[1] another PTOX over-expressing line was obtained by (Josse, 2003) but this line could not be propagated.

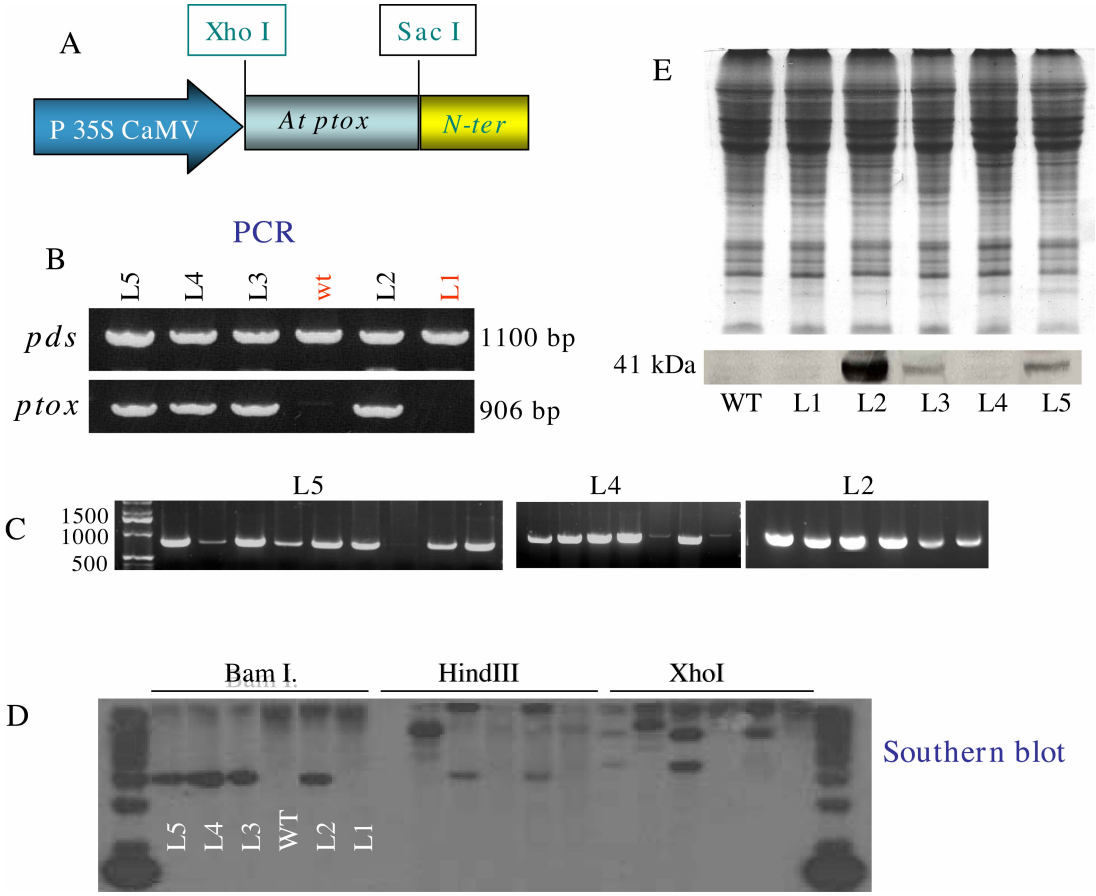

FIGURE 3.28 – **Verification of transgenic tomato plants (MT) expressing the At-PTOX cDNA sequence. A. The construction of cDNA under the control of the doubled constitutive 35S promoter of the cauliflower mosaic virus. The presence of the T-DNA in genomic DNA of various T2 plants (B) and also homogeny of their generation (C) were verified using specific primers to amplify At-PTOX DNA, and also *pds* (phytoene desaturase gene) as a control. D. Southern-blot analysis of transgenic tomato plants using the indicated restriction endonucleases and hybridized with the radiolabeled tomato full-length cDNA probe. E. Extracted proteins from mature green fruits were separated by gel electrophoresis and immunodetected as described in Materials and Methods. Coomassie blue stained PAGE (30 μg protein per lane) shows equal loading of the samples.**

A weak band was detected in total protein extract of L3 and L5 lines, and no band was observed in the WT, although a faint band was identified in WT insoluble protein fractions (Josse, 2003). The protein separation was performed using a denaturing gel electrophoresis system (SDS-PAGE) and revealed by Coomassie Brilliant Blue staining, which shows similar protein loading per lane (Fig. 3.28).

The first objective of this work was to examine the effect of PTOX over-expression in tissues containing chromoplasts, especially on carotenoid content. Increasing carotenoid content in fruit is of biotechnological interest. It should be mentioned here that a *ca.* 2-fold rise in carotenoid content was achieved by over-producing another protein studied in our laboratory,

namely the structural protein fibrillin (Simkin *et al.*, 2007). On the other hand, using the same construct of transgene no effect on carotenoid content in tobacco leaves was observed despite the format the over-expressed At-PTOX was obviously functional in tobacco chloroplasts (Joët *et al.*, 2002b). They demonstrated that At-PTOX over-expression facilitates the oxidation of reduced PQs via O_2 as a terminal acceptor in tobacco leaves (Joët *et al.*, 2002b). Therefore, the second objective of the present work was to examine the influence of PTOX over-expression on photosynthetic electron transport in tomato leaves. Since this represent a comparative work with the data from tobacco, having only one tomato PTOX$^+$ line available discourage us for performing this work.

3.3.2 PTOX Over-expression effect on carotenoid contents

3.3.2.1 Phenotype

Under growth chamber conditions, at 60 μmol.m^{-2}.s^{-1}, the WT MT and the L2 PTOX$^+$ line showed the same growth rate, and the flowering period and the fruit ripening stages were similar in two genotypes. The PTOX$^+$ line developed dark green young leaves compared with WT plant, but this difference disappeared in the adult leaves. This suggests that PTOX over-expression can accelerate chloroplast development, but we cannot exclude that this is due to a transgene effect unrelated to PTOX.

3.3.2.2 Carotenoid content in young and mature leaves

Since PTOX is an important cofactor for carotenoid biosynthesis in tomato, the carotenoid content of transgenic plants was analyzed. The pigment analysis using opened and newly developed leaves and adult leaves (third leaf from the top), were performed by the HPLC method. The results are presented in figure 3.29. Although, there was a significant increase in the level of all pigments in PTOX$^+$ (L2) compared with WT in newly developed leaves, no difference was observed in adult leaves.

3.3.2.3 Carotenoid content in ripe fruits

Carotenoid content was also measured precisely in total pericarp extracts prepared from 4 days post-breaker (4 DPB, red) fruit. Three major carotenoids in ripening fruit are compared in figure 3.30. There was no difference in β-carotene and lutein levels between WT MT, PTOX$^+$ (L2)

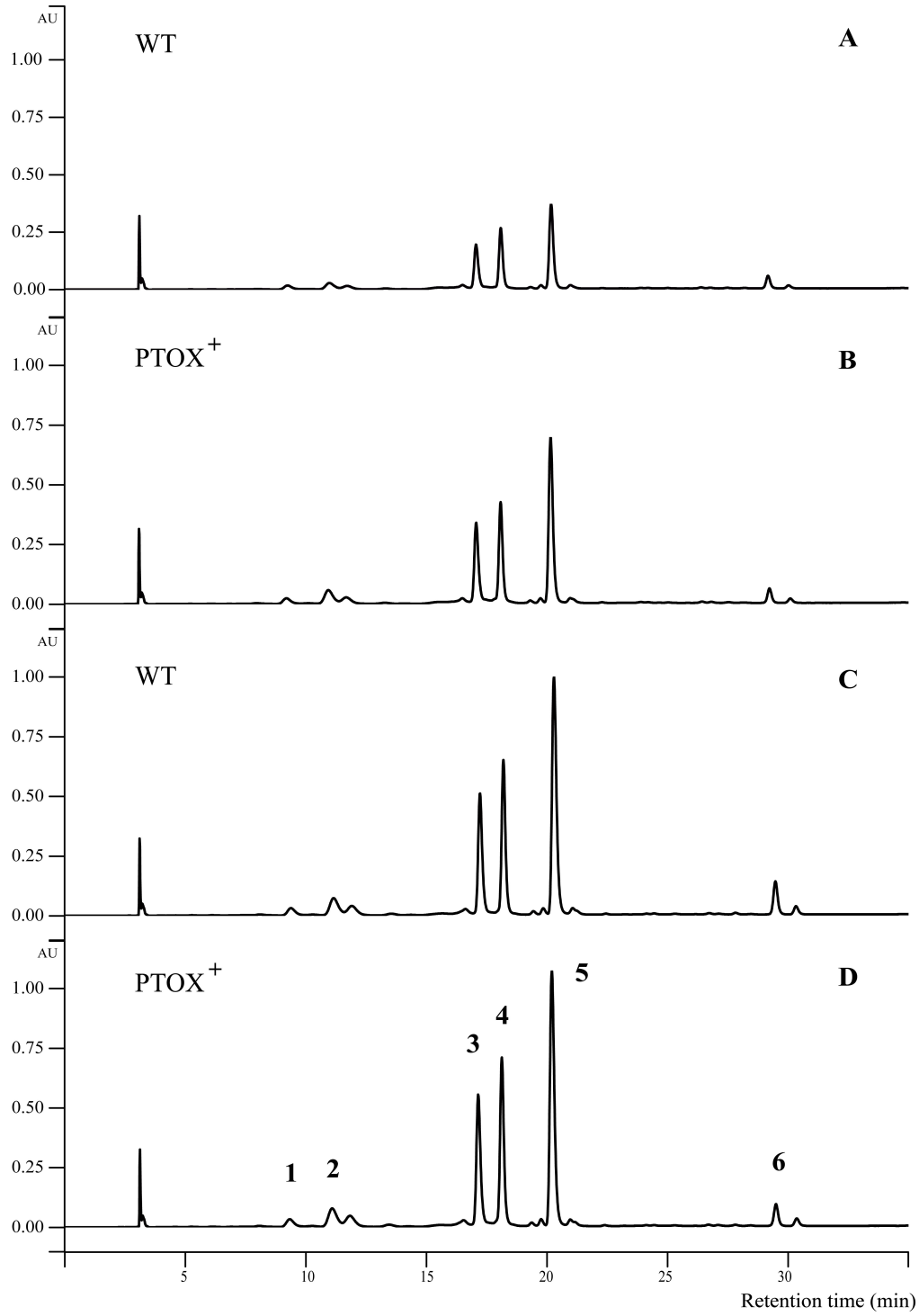

FIGURE 3.29 – **Pigment contents in leaves from PTOX$^+$ (L2) plant comparing with wild-type (MT). HPLC chromatograms for the 6-week old plants at young (A, B) and developed (C,D) stage (for details see text), recorded at 450 nm. Chromatogram components are numbered: 1- neoxanthin, 2- violaxanthin, 3- Chl *b*, 4- lutein, 5- Chl *a*, and 6- β-carotene.**

and a lower PTOX expressing line (L4). Slightly lower levels of lycopene (especially of the trans-isomer) were found, but these differences do not appear meaningful since they correspond to variations usually observed in such measurements. It can be concluded that over-expression of At-PTOX in MT tomato did not influence the carotenoid content at this fruit stage (4 DPB).

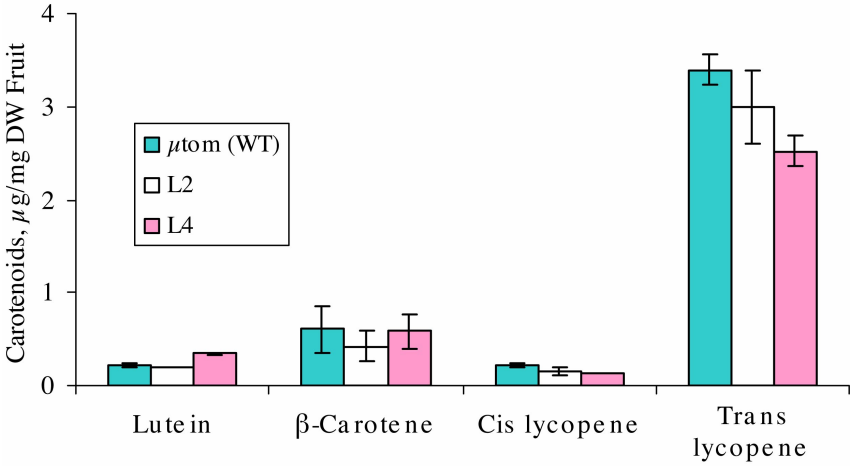

FIGURE 3.30 – **Carotenoid contents of ripe fruits (4 days post breaker) from L4 and PTOX$^+$ (L2) plant compared with wild-type (MT).**

3.3.3 PTOX over-expression effect on photosynthesis

3.3.3.1 Photoinhibition

The effect of high light stress on the photochemical efficiency of PSII in WT (MT) and PTOX$^+$ (L2) was studied by various experiments series. First, detached leaves were exposed to high light (700, 1,000 and 1,500 μmol.m^{-2}.s^{-1}) over a time course up to 6h, and subsequently incubated at low light intensity (50 μmol.m^{-2}.s^{-1}) for 1h recovery (PSII repair). The data in figure 3.31A show that there was no difference between WT and PTOX$^+$ maximum quantum yield of PSII (F_v/F_m) of under different high light intensities. In fact, the expression of At-PTOX did not result in increased resistance of the transgenic line to photoinhibition, nor did it influence recovery from photoinhibition.

To investigate any potential difference between the WT and PTOX$^+$ lines in response to long-term photostress, the influence of high light intensity on the plants over 3 weeks was studied. One set of four week old plants grown in a growth chamber under 60 μmol.m^{-2}.s^{-1} at 24°C were exposed to high light intensity (700 μmol.m^{-2}.s^{-1}) at 24°C (measured at the level

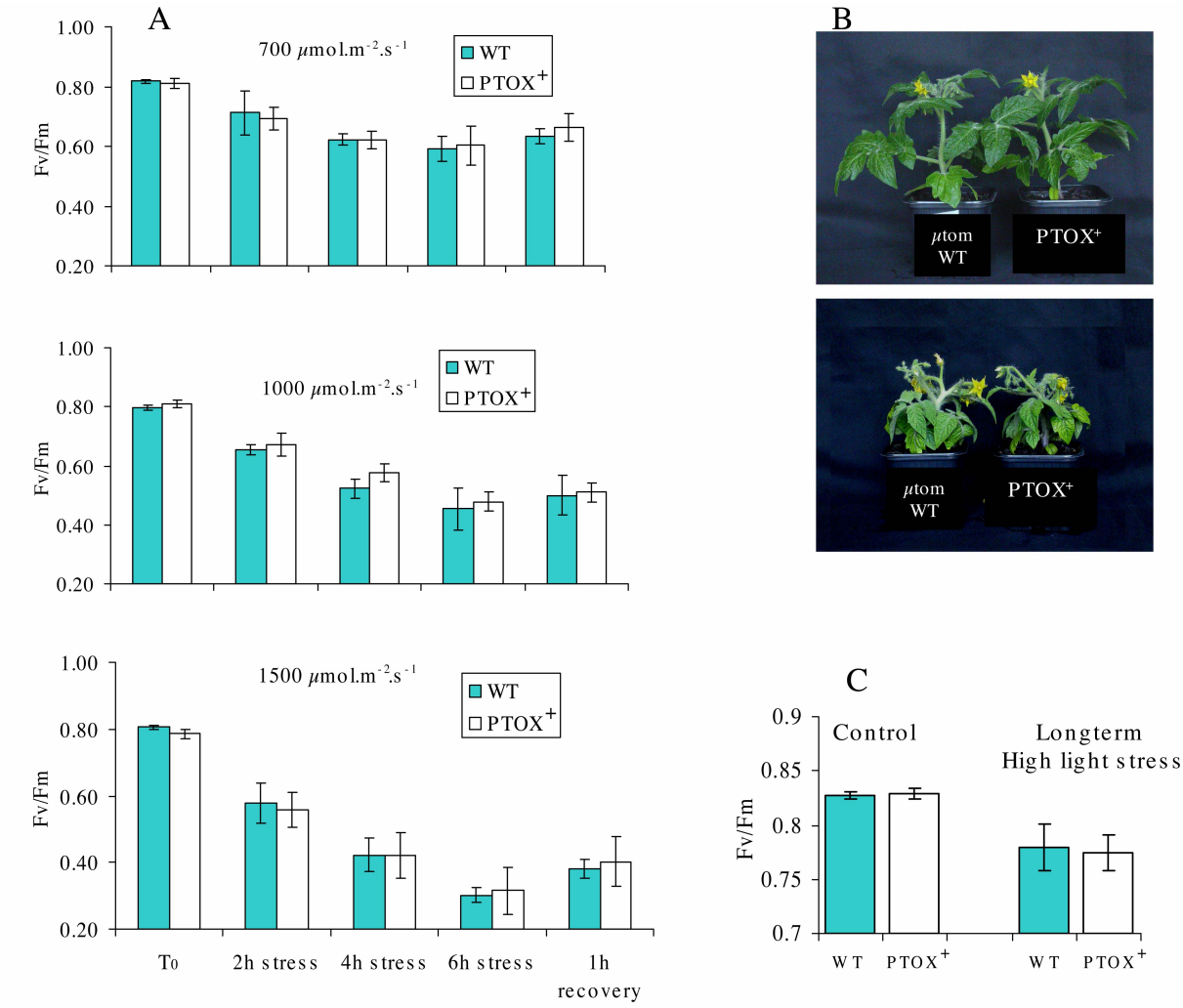

FIGURE 3.31 – **The effect of high light stress on the photochemical efficiency of PSII in WT (MT) and PTOX$^+$ (L2). A. Detached leaves were incubated at 24°C for 6h under high light (700, 1,000 and 1,500 μmol.m^{-2}.s^{-1}) and subsequently incubated at low light intensity (50 μmol.m^{-2}.s^{-1}) for 1 hour recovery. B. Four week-old plants grown in a growth chamber under 60 μmol.m^{-2}.s^{-1} at 24°C were exposed to high light intensity (700 μmol.m^{-2}.s^{-1}) at 24°C for 3 weeks (lower panel), and control plants remained in growth chamber (upper panel). C. Detached leaves of control and stressed plants (for 3 weeks) were used for measuring of the F_v/F_m ratio at midday.**

of the plants) for 3 weeks, and another set of plants remained in a growth chamber under low light intensity as control plants. The growth parameters in WT and PTOX$^+$ plants at T_0 (before stress) were identical. At this stage, they had two true developed leaf pairs. Every 3 days, leaf number, stem height and flowering date were recorded. Figure 3.31B shows that there was no obvious difference in these parameters between WT and PTOX$^+$ plants under control and stress conditions. In addition, quantitative data (not shown) did not reveal any significant difference.

To estimate the electron flux through PSII and the photosynthetic activity of the plants, the F_v/F_m ratio was measured at midday in the detached leaves from control and stressed plants after 3 weeks. In agreement to the trsults presented in figure 3.31C, no significant difference in F_v/F_m ratio between WT and PTOX$^+$ was observed, indicating unaltered photosynthetic activity of the PTOX$^+$ tomato plant (Fig. 3.31C).

3.3.3.2 Chlorophyll *a* fluorescence induction kinetics

To determine whether the over-produced At-PTOX has an effect during steady state illumination, Kautsky fluorescence kinetics were measured following a dark to light transition. We used WT and PTOX$^+$ adult leaves from plants grown under our usual growth conditions. After 30 min dark incubation, we illuminated the leaves with 200 μmol.m^{-2}.s^{-1} light intensity for 10 min. During this time course, saturating light pulses and subsequent short far-red light exposition were applied to determine F'_m and F'_0. Photochemical (qP) and nonphotochemical (qN, NPQ) quenching parameters were calculated. The results presented in figure 3.32 show that the effective quantum yield of PSII (ΦPSII) was similar in WT and PTOX$^+$ line. No clear difference in F_s level between WT and PTOX$^+$ line was detected, and the qP values were almost identical in the two leaf types. In contrast, after a few min, F'_m was decreased less in the PTOX$^+$ line than WT, and consequently both qN and NPQ values were lowered compared with WT (Fig 3.32).

3.3.3.3 Postillumination F_0 fluorescence increase

When intact leaves were illuminated for a few min and the light turned off, a transient increase in F_0 level occurs (see chapter 3.2), reflecting the reduction of photosynthetic electron carriers from reductants accumulated during the light period. Contrary to expectations, both the WT and PTOX$^+$ lines exhibited similar transient rise in F_0 fluorescence.

3.3.4 PTOX over-expression in a different tomato genetic background

The phenotpe of tomato cultivar Micro-Tom is the result of point mutations in the genes *Dwarf* (*D*, encoding an enzyme of the brassinosteroid biosynthesis pathway), *Self-Pruning* (*SP*, which controls the determinate/indeterminate phenotype) and *Internode length reduction* (*Ilr*) (references in Serrani *et al.*, 2007). Since the mutations responsible for its dwarf phenotype are recessive (Meissner *et al.*, 1997) and since these mutations can be complemented by a single

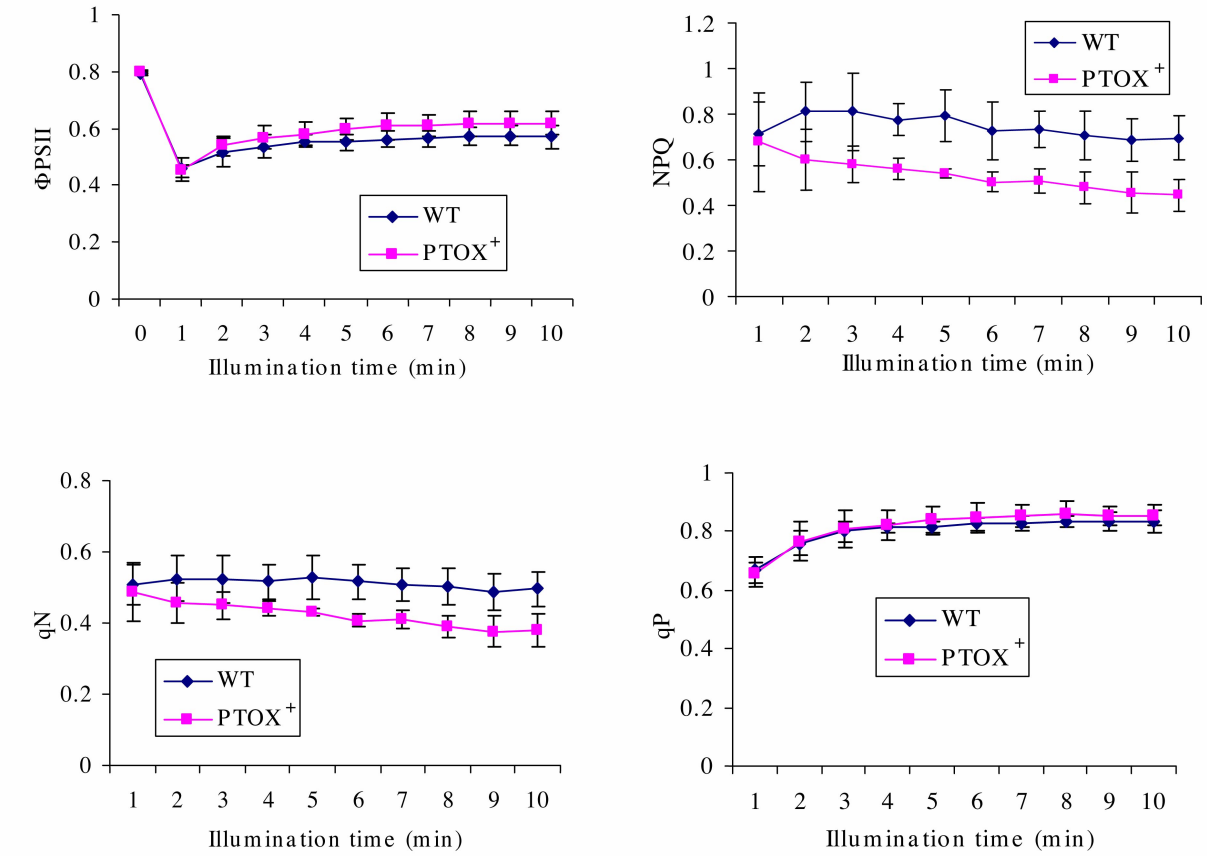

FIGURE 3.32 – **Induction kinetics for the chlorophyll fluorescence parameters ΦPSII, 1-qP, qN and NPQ. The leaves of PTOX$^+$ (L2) and WT (MT) were dark-adapted for 30 min then illuminated with an actinic light of 200 μmol.m^{-2}.s^{-1} for 10 min. Mean values (n=4) were used.**

cross with a WT line, the L2 (PTOX$^+$) line was crossed with WT San Marzano (SM). The hybrid was called hL2. As a control plant, WT MicroTom (MT) was also crossed with WT SM and the hybrid was called hC (control). Figure 3.33A and B display plant and fruit size, respectively, of L2, hL2 and SM plants.

Proteins were extracted from leaves of *gh*, SM, MT (WT), L2, hC (SM×MT), and hL2 (SM×L2). Coomassie Brilliant Blue stained PAGE shows equal loading of the samples for PTOX immunodetection (Fig. 3.33C). These experiments did not reveal any signal for PTOX in *gh* and MT, but a 37-kDa band was visible in SM and hC. L2 and hL2 showed large amounts of a 41-kDa band. Using a higher resolution gel, the two bands can be clearly distinguished (Fig. 3.33D). Thus, it appears that the transgene product (the cDNA originates from *Arabidopsis*) has a larger molecular weight than the one encoded by the native tomato gene. It is also clear that

the SM line contains higher PTOX levels than MT, the levels in hC being in between these levels.

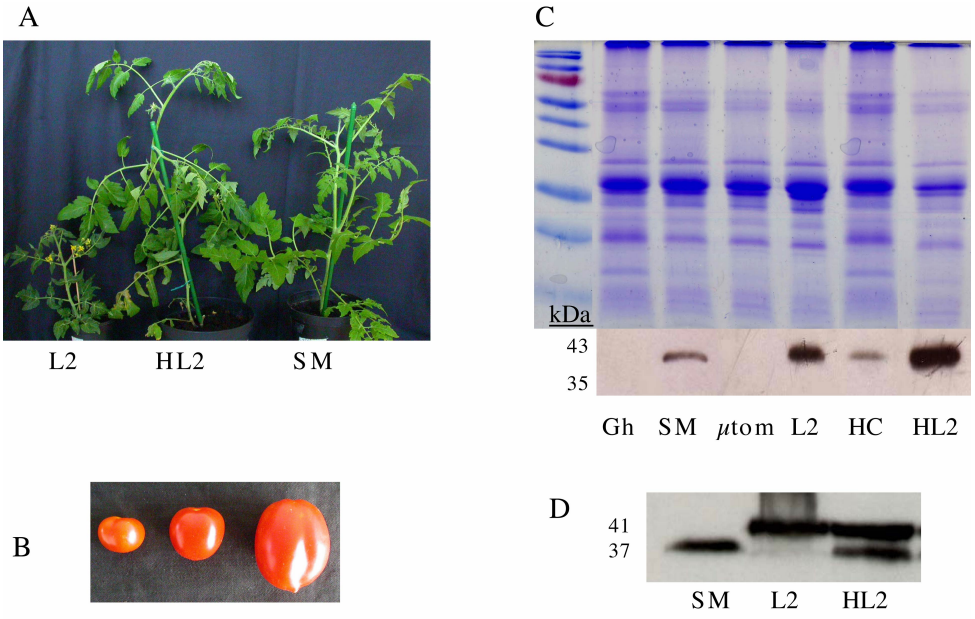

FIGURE 3.33 – **PTOX over-expression in a different tomato genetic background (SM). Plant (A) and fruit size (B) of L2, hL2 (SM×L2) and SM plants. C- Extracted proteins from mature green fruits were separated by gel electrophoresis and immunodetected. Coomassie blue stained PAGE (30 μg protein per lane) shows equal loading of the samples. D. Using a higher resolution gel, two bands of PTOX protein (37 and 41-kDa) were visible in hL2.**

Similar to the data obtained for MT and L2, the hybrids hC and hL2 showed no differences in maximum quantum yield under high stress conditions (data not shown), neither did they show any difference in the extent of the transient rise in F_0 fluorescence when actinic light is switched off (Fig 3.34). However, data in this section clearly show that the genetic background of the tomato line strongly influences PTOX protein levels.

3.3.5 Discussion

Transgenic tomato plants (dwarf MicroTom type, MT) expressing the *Arabidopsis thaliana* PTOX cDNA under the control of the CaMV promoter were used in this study. After checking the presence of the T-DNA in tomato transgenic lines, a line producing a high amount of the PTOX protein was selected. Only this sole $PTOX^+$ line has similar growth parameters to WT plants; however, its young leaves have a darker green color as compared to WT.

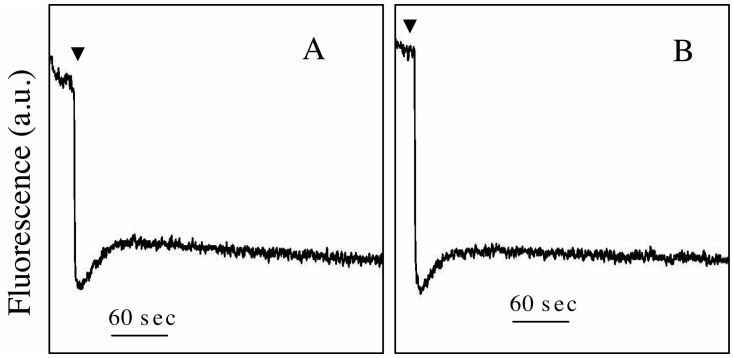

FIGURE 3.34 – **Postillumination fluorescence measurements (F_0 rise) following a light to dark transition in detached leaves of hybrids hC (A) and hL2 (B). After a 10 min period of actinic illumination (200 μmol.m^{-2}.s^{-1}), light was switched off.**

The over-expression of At-PTOX in MT tomato did not influence carotenoid content in adult leaves nor in fruit at the 4 DPB ripening stage. Over expression of At-PTOX in tomato did not result in increased resistance of transgenic lines to photoinhibition and this result is consistent with PTOX overexpression in tobacco and *A. thaliana* (Joët *et al.*, 2002b; Rosso *et al.*, 2006).

In the tobacco PTOX$^+$ transgenic lines, the postillumination F_0 fluorescence increase is absent (Joët *et al.*, 2002b), but over-expression in tomato (the present data) and in *Arabidopsis thaliana* (Rosso *et al.*, 2006) did not give the same results. This could be explained by wide difference in PQ-reducing activity among plant species (Yamane *et al.*, 2000).

After a few min illumination, nonphotochemical quenching (qN and NPQ) values were lowered in the tomato PTOX$^+$ line, indicating that a lower pH gradient compared with the WT. However the photochemical yield of PSII and the photochemical quenching value remained equal to those of the WT plant. A lower pH gradient in the tomato PTOX$^+$ line is in agreement with the results obtained in the tobacco PTOX$^+$ transgenic lines, and could indicate that cyclic electron reactions around PSI are down-regulated in PTOX$^+$. Overexpression of PTOX could modulate the redox state of intersystem electron carriers, and the establishment of cyclic electron transfer reactions may be disturbed (Joët *et al.*, 2002b).

Taken together, the influence of an over-accumulation of the At-PTOX in tomato seems minimal. One can not rule out the possibility that the enzyme produced was inactive. However, this is unlikely since the same cDNA construct was used for tobacco PTOX$^+$ transgenic lines (Joët *et al.*, 2002b). A mutation in the coding region of this enzyme during the transformation process can be excluded (the aligned sequences of coding region in tomato MicroTom trans-

genic lines and *immutans* were identical, data not shown). Although some minor effects are observed in the PTOX$^+$ line, as mentioned above, but these points could not be fully carified since only a single tomato PTOX$^+$ line was available for study.

3.3.6 Conclusion

As discussed in chapter 3.1, it becomes clear that differences exist between different plant species regarding the importance of PTOX, especially its influence on the regulatory mechanisms of photosynthesis. Therefore, it was necessary to re-examine potential effects of PTOX over-production in another species than tobacco or *Arabidopsis*. Tomato seemed a good choice, bearing in mind the fact that the relative importance of the dual role of PTOX (related to carotenoid biosynthesis and to photosynthesis) differs from organ to organ and also within a given organ (leaf, fruit) from one developmental stage to another. Unfortunately, little information could be obtained from PTOX over-expressing lines, in contrast with the fruitful study of knock-out mutants, as shown in chapters 3.1 and 3.2.

Chapter 4

Concluding Remarks

In higher plants, oxygenic photosynthesis and respiration are the oxido-reduction bioenergetics mechanisms; they have in common the involvement of an ATP synthase complex and a number of electron transport intermediates (quinones, cytochromes, *etc.*) allowing the establishment of a proton gradient that will be used by the ATP synthase. In addition, alternative (non-energenic) pathways in plant cells for both respiratory and photosynthetic electron transport chains: they comprise the alternative oxidase (AOX) in mitochondria and the plastid terminal oxidase (PTOX) in chloroplasts. These quinol oxidases appear to be a conserved characteristic in oxygenic photosynthetic organisms. AOX and PTOX proteins share sequence homology, indicating they originated in procaryotes from a common ancestral form and then diversified and entered the eucaryotic lineage separately in mitochondria and chloroplast, respectively, via endosymbiotic events. The early transition from an anaerobic to aerobic environment could have been the driving force for the evolution of such an oxidase, the ancestor of AOX and PTOX. Since these alternative pathways are non-energy conserving, they may act to diminish the rate of electron transport pressure in the membranes and thus allow plants to acclimate to changing environmental conditions.

Assuming such an ancient (in terms of Evolution) protective role of PTOX, as a component of the photosynthetic electron transport chain, could imply that its function in carotenoid biosynthesis, as a cofactor for phytoene desaturation, was acquired later in Evolution. This seems consistent with the observation that this latter function is essentially important at some developmental stage such as plastid de-etiolation or chromoplast differentiation (which can be viewed as more recent evolutionary developments). Furthermore, PTOX-independent pathways in association with phytoene desaturase have been demonstrated in regular (fully differentiated) chloroplasts, consistent with the above-mentioned evolutionary considerations.

The main objective of this work was to characterize the dual role of PTOX. Tomato was chosen as a model system. It allowed the demonstration of an indispensable and direct role of PTOX in photosynthesis, namely its influence on the redox status of the PQ pool between PSII and PSI. Such a role could not be demonstrated to date using *Arabidopsis* (Rosso *et al.*, 2006). In this study, we have demonstrated that under low light tomato plants lacking PTOX (*gh*) can produce green leaves and fruits containing a similar carotenoid content as WT (SM), without phytoene accumulation, but with a reduced potential to prevent oxidative damage, as well as a higher PSII sensitivity to photoinhibition and damage. In other words, the absence of

PTOX renders the tomato leaf photosynthetic apparatus more sensitive to light. We have shown that the above-mentioned photosynthesis defects in *gh* green leaves are a consequence of non-photochemical overreduction of PQs in the dark, and a higher reduction state of the electron transport chain under steady state illumination in *gh vs.* SM leaves.

In addition, using tomato as a model system allowed investigation of other developmental stages namely etiolated cotyledons/early chloroplast biogenesis and ripening fruit/chromoplast differentiation, which are more difficult or impossible to study in *Arabidopsis*.

Figure 4.1 summarizes the current view of the dual role of PTOX in both a developmental and evolutionary perspective.

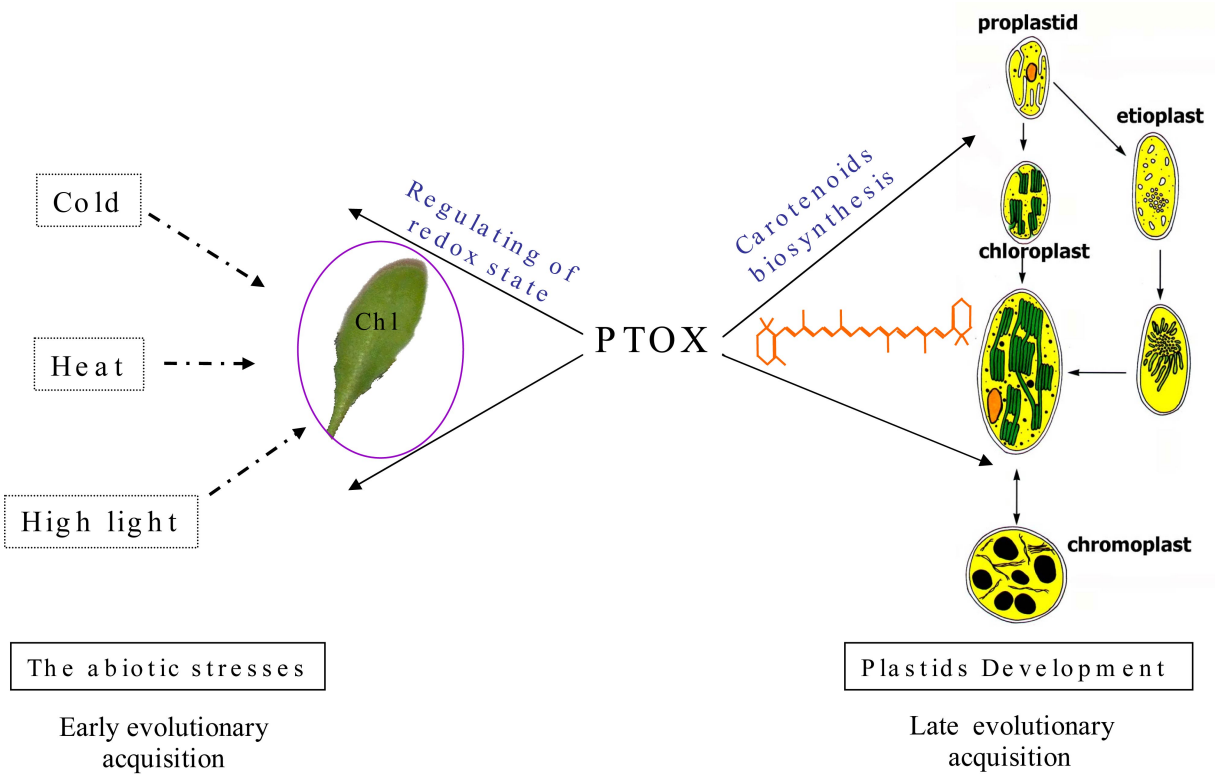

FIGURE 4.1 – **Dual roles of PTOX**

Although our original strategy was to use both a tomato PTOX knock-out mutant and an At-PTOX over-expressing tomato line, it turned out that most of the data were provided in our study by the knock-out mutant. This may be explained either by the regulatory nature of PTOX function and/or by an inappropriate location of PTOX in case of its overproduction. During the course of this work an attempt was made to find specific and potent inhibitors of PTOX. Such inhibitors would allow local inactivation of PTOX and in a timely controled manner. However,

as shown in appendix A.3, no such inhibitor could be identified. The known inhibitor of PTOX *in vitro*, namely octyl-gallate, proved poorly efficient *in vivo* and all examined bleaching herbicides that inhibit carotenoid desaturation seem to act on phytoene desaturase rather that on PTOX. Identification of inhibitors that inhibit the alternative cofactor of carotenoid desaturation (Carol and Kuntz, 2001) would require further experiments.

Our results suggest a regulatory role for PTOX in the cyclic flow around PSI, primarily under stress conditions, rather than as a major electron sink. But being a plastoquinol oxidase, PTOX must somehow contribute to the transfer of photosynthetic electrons to O_2, possibly from a sub-pool of PQ. This remains to be clarified via direct PSI measurements and in particular whether such a sub-pool is more closely associated to cyclic electron transfer around PSI rather than to linear electron flow from PSII to PSI.

In agreement with the implication of PTOX in reducing the electron pressure on PSI acceptors by recycling electrons to the PQ via chlororespiration, we observed a down-regulation of NDH complex in a PTOX-deficit mutant under photo-oxidative stress conditions. However, a possible function of PTOX in a chromorespiratory activity in non-green plastids remains to be examined, especially in association with a NDH complex.

Our conclusion that PTOX has a regulatory role in the distribution of electrons to different linear and alternative electron pathways, and that the presence of PTOX as a minor component in the photosynthetic apparatus is particularly important during dark to light and low light to high light transitions, needs to be substantiated by further investigations in other model plants, such as alpine plants. In certain alpine plants (Streb *et al.*, 2005), PTOX may act as a safety valve allowing considerable photosynthetic electron flows towards O_2.

Chapter 5

Version abrégée en français

5.1 Introduction

Les mutants déficients en oxydase terminale plastidiale (PTOX) présentent un phénotype panaché défini par des secteurs verts qui ont une teneur en chlorophylle et en caroténoïdes normale et des secteurs blancs qui montrent une accumulation de phytoène, le précurseur non coloré des caroténoïdes (Wetzel *et al.*, 1994). Par ailleurs, puisque la désaturation du phytoène, pour former des caroténoïdes photoprotecteurs, exige la donation d'électrons à des plastoquinone (PQ)s (Norris *et al.*, 1995) et puisque PTOX est une plastoquinol oxydase, le rôle de PTOX semble être lié à la réoxydation des PQs réduits pendant la désaturation du phytoene. En absence de cette oxydase, la sur-réduction des PQs mènerait à l'inhibition de la désaturation du phytoene. Ce déficit en caroténoïdes photoprotecteurs entraîne la photo-oxydation de la chlorophylle, et par voie de conséquence la formation des secteurs blancs (Carol *et al.*, 1999; Wu *et al.*, 1999a). Cette vue (trop simplifiée probablement) peut être compliquée par l'existence de secteurs verts sur des feuilles de mutant déficient en PTOX, ce qui suggère que, même en absence de PTOX, le processus de désaturation puisse se produire sous certaines conditions.

Puisque PTOX montre une homologie de séquence importante avec l'oxydase alternative (AOX) de la chaîne respiratoire des mitochondries, et comme les deux protéines sont des membres de la famille de protéine non-hème carboxylate à deux fer, et puisqu'elles catalysent des réactions semblables, on peut supposer que PTOX, par analogie à AOX, fournit un puits alternatif d'électrons dans des chaînes de transfert d'électrons. AOX catalyse la voie dite alternative du transfert d'électrons mitochondrial, qui n'est pas sensible au cyanure contrairement à la voie générale des cytochromes. Dans cette voie alternative de transfert d'électron, AOX peut empêcher la sur-réduction des médiateurs du transport d'électrons, ce qui peut se produire en réponse au stress environnemental (Maxwell *et al.*, 1999), et empêcher la formation d'espèces activées de l'oxygène (Moore *et al.*, 2002). Ainsi, PTOX peut fonctionnellement être analogue à AOX et servir à maintenir relativement oxydée la chaîne de transport photosynthétique d'électrons.

Les données récentes, *in vitro* et *in vivo*, indiquent que PTOX peut être une oxydase terminale plastidiale impliquée dans le chlororespiration (Josse *et al.*, 2000; Cournac *et al.*, 2000b; Josse *et al.*, 2003; Joët *et al.*, 2002a; Peltier and Cournac, 2002). La chlororespiration con-

siste en la réduction de plastoquinone par la NAD(P)H déshydrogénase plastidiale (complexe NDH) en utilisant le NAD(P)H, produisant ainsi du plastoquinol, qui pourrait être re-oxydé par PTOX pour régénérer la plastoquinone. PTOX, comme le complexe de NDH, est situé dans les lamelles stromatiques où les réactions cycliques de transfert d'électrons autour de PSI se produisent (Joët *et al.*, 2002a; Lennon *et al.*, 2003). La chlororespiration pourrait jouer un rôle dans l'acclimatation de la photosynthèse aux conditions environnementales variables. En conditions de stress, le niveau élevé des enzymes impliquées dans la chlororespiration suggère que celle-ci peut agir en tant que "valve de sécurité" pour que les électrons excédentaires ne surréduisent pas la chaîne de transfert d'électrons photosynthétique (Melis, 1999; Niyogi, 2000; Endo *et al.*, 1999; Bukhov and Carpentier, 2004; Quiles, 2006). Il existe une indication pour envisager la participation de PTOX dans une voie chlororespiratoire chez une plante supérieure : *Ranunculus glacialis*, une espèce alpine adaptée à la lumière forte et à la basse température, possède un niveau élevé de PTOX, et une chaîne de transfert d'électrons relativement oxydée en condition de stress, ce qui est reflété par une pression d'excitation inférieure (Streb *et al.*, 2005). Il s'avère également que PTOX peut faciliter la fonction de transfert cyclique d'électrons autour de PSI par la réoxidation des transporteurs d'électrons intersystèmes (Joët *et al.*, 2002a). En revanche, les analyses fonctionnelles du mutant d'*Arabidopsis im* (déficient en PTOX) et de lignées surexpresseurs de PTOX n'ont pas confirmé l'hypothèse que PTOX règlerait l'état redox du pool de PQ pendant l'acclimatation au stress (Rosso *et al.*, 2006). En conséquence, il a été conclu que PTOX est un médiateur redox important pendant la biogenèse des chloroplastes et de l'ensemble de l'appareil photosynthétique, mais qu'elle a un effet minimal sur l'oxydation du pool de PQ et sur le flux des électrons entre PSII et PSI dans les feuilles adultes. La surexpression de PTOX n'augmente pas à la résistance à la photoinhibition de PSII ni chez le tabac ni chez *Arabidopsis* (Joët *et al.*, 2002a; Rosso *et al.*, 2006).

En résumé, la participation de PTOX dans chlororespiration et sa fonction comme "valve de sécurité" empêchant la sur-réduction de la chaîne de transfert d'électrons sous forte lumière a été sujette à controverse pendant la dernière décennie (Cournac *et al.*, 2000b; Joët *et al.*, 2002a; Baena-Gonzalez *et al.*, 2003; Streb *et al.*, 2005; Aluru *et al.*, 2006; Rosso *et al.*, 2006). La fonction exacte de PTOX dans la photosynthèse n'avait pas été suffisamment étudiée, parce que le phénotype remarquable des mutants déficients en PTOX (présentant un déficit en caroténoïdes) rend difficile les conclusions. En fait, les causes du blanchiment des plantes déficientes en

PTOX ne sont pas bien comprises : le blanchiment est-il dû à un manque de caroténoïdes ou à un déséquilibre redox, ou aux deux ?

Pour répondre à ces questions: les rôles potentiels de PTOX sous conditions de stress lumineux ont été étudiés en utilisant le mutant *ghost* de tomate (chapitre 3.1). Nous avons étudié particulièrement l'état redox de la chaîne de transport photosynthétique d'électrons chez des plantes *ghost* (chapitre 3.2). Nous avons aussi examiné des plantes transgéniques surexprimant PTOX, en les comparant à des plantes contrôles (tomates MicroTom), pour examiner l'influence d'un niveau élevé de PTOX sur l'accumulation des caroténoïdes et la protection contre la photoinhibition du PSII (chapitre 3.3).

5.2 Le double rôle de l'oxydase terminale plastidiale (PTOX) chez la tomate (chapitre 3.1)

Dans ce chapitre, nous avons démontré que lorsque la biogenèse normale des chloroplastes est altérée, notamment chez des cotylédons étiolés exposés à la lumière forte, PTOX est un cofacteur dominant pour la désaturation des caroténoïdes et son absence mène au photoblanchiment dans le mutant *ghost*, principalement en raison d'une capacité réduite de synthèse des caroténoïdes. En revanche, quand des feuilles adultes et entièrement vertes de *ghost* sont produites et soumises à des conditions de stress lumineux provocant un photoblanchiment, aucune évidence d'insuffisance dans la biosynthèse de caroténoïdes et ni d'accumulation de phytoène a été obtenue. Nos résultats sont entièrement cohérents en suggérant que PTOX joue un rôle spécifique dans la protection de l'appareil photosynthétique sous stress lumineux. Après un stress lumineux de 6h et 16h, par rapport au contrôle de la lignée San Marzano (SM) nos résultats indiquent une photoinhibition plus importante de PSII dans les feuilles *ghost*, ainsi qu'un niveau plus élevé de dommages au PSII et un rétablissement partiel chez *ghost* (bande B de thermoluminescence). Après un stress lumineux de 6h, les mesures de thermoluminescence à hautes températures (bande HTL2) indiquent également un potentiel réduit pour empêcher des dommages oxydants dans les feuilles de *ghost* par rapport à SM. L'évaluation de la peroxydation des lipides par des mesures de niveau de MDA est conforme à ces dernières observations.

Comme dans feuilles, le blanchiment des jeunes fruits de *ghost* est déterminé à une étape développementale précoce. La présence de phytoène dans le fruit blanc de *ghost* suggère que ce blanchiment est lié (au moins partiellement) à un déficit dans la biosynthèse des caroténoïdes.

Cependant, des fruits verts adultes de *ghost* peuvent être obtenus puis soumis à un photoblanchiment sous conditions de stress lumineux. Dans ce cas également, aucun déficit en caroténoïdes n'est observé. Nous avons constaté que les fruits verts de *ghost* sont plus sensibles à la photoinhibition que les fruits de SM, confirmant notre observation dans les feuilles adultes et vertes de *ghost*.

Dans les fruits mûrs de *ghost* issus des fruits verts, le contenu en lycopène est réduit par rapport au contrôle SM, mais n'est pas nul, ce qui permet de suggérer que, en l'absence de PTOX, un autre cofacteur de la désaturation des caroténoïdes peut partiellement remplacer PTOX. Néanmoins, les fruits mûrs sont principalement dépendants de PTOX pour la désaturation des caroténoïdes. L'intégrité plastidiale joue également un rôle car les fruits mûrs issus de fruits *ghost* photoblanchis au stade immature contiennent moins de caroténoïdes.

En résumé, nos données prouvent que l'activité de PTOX est nécessaire pendant la biogenèse des chloroplastes et des chromoplastes, et également pour la désaturation efficace des caroténoïdes dans certains organes et à certaines étapes développementales. Cependant, l'existence d'une voie indépendante de PTOX pour la réoxydation du plastoquinol en association avec la désaturation du phytoène doit exister pour expliquer le contenu normal en caroténoïdes à d'autres étapes développementales. Nous prouvons également que PTOX est impliquée dans la régulation du transport d'électrons photosynthétiques dans les tissus verts.

5.3 Les rôles régulateurs d'ajustement de PTOX dans la photosynthèse (chapitre 3.2)

Dans ce chapitre, l'analyse des protéines thylacoïdiennes a indiqué que la sensibilité de l'appareil photosynthétique aux conditions extrêmes chez *ghost* n'est pas due à un réarrangement des complexes protéiques dans la chaîne de transfert d'électrons. Par contre, les mesures de fluorescence 77k ont indiqué que les feuilles de SM et de *ghost* diffèrent dans le rapport de la fluorescence de PSII et de PSI (F_I/F_{II}) lors de conditions lumineuses variables. De plus, la réoxydation du pool de PQ par PSI dans les feuilles de *ghost* adaptées à la lumière rouge lointain était incomplète. A température ambiante, la cinétique d'induction de fluorescence de la chlorophylle a a montré un pool plus réduit de PQ et un niveau de QA^- plus prononcé chez *ghost*.

Nous avons conclu que les imperfections photosynthétiques dans les feuilles verts de *ghost* en condition de forte lumière (comme nous l'avons montré au chapitre 3.1, sans aucun déficit

discernable en caroténoïdes et sans accumulation de phytoène) sont dues à un état plus réduit de la chaîne de transfert d'électrons à la lumière dans les feuilles de *ghost vs.* SM. Ces résultats suggèrent une utilisation inefficace de puits d'électrons photosynthétiques ou alternatifs chez les plantes déficientes en PTOX.

Nos résultats ont également montré une fluorescence initiale (F_0) apparente plus élevée chez *ghost* que chez SM, différence qui disparaît après une adaptation prolongée à l'obscurité ou lors d'une exposition à la lumière rouge lointain, ce qui indique une réduction non-photochimique augmentée de PQs à l'obscurité après une phase lumineuse. Lors d'un stress de chaleur, la fluorescence F_0 de la chlorophylle normalement augmente et traduit une réduction de PQ plus élevée. Nous avons étudié le rôle de PTOX pendant un choc thermique : les feuilles *ghost* montrent une nette augmentation dans le taux de réduction de la chaîne de transfert d'électrons photosynthétique provoquée par la chaleur. Chez *ghost*, il y a deux composants dans cette augmentation de F_0. L'un peut être éliminé par la lumière rouge lointain (indiquant un état élevé de réduction du pool de PQ). Le deuxième est peu sensible au rouge lointain et peut correspondre à la dissociation de LHC du PSII ou à l'inactivation partiellement réversible de PSII. Après une longue adaptation à l'obscurité, le choc thermique conduit chez *ghost* à une plus grande acidification du lumen des thylacoïdes dans la phase initiale de réillumination, ce qui suggère pour PTOX un rôle de régulation générale du flux cyclique autour de PSI, en particulier dans des conditions de stress.

Nous avons également montré un certain lien entre niveaux de PTOX et du complexe NDH, mais qui n'est pas absolu. Cela conduit chez le mutant *ghost*, sous un stress de forte lumière, à l'absence de l'augmentation de l'activité NDH observée chez les plantes contrôles.

Notre conclusion de ce chapitre est que PTOX joue un rôle régulateur dans la distribution des électrons entre différentes voies linéaires et alternatives d'électrons, ce qui est en accord avec des rapports précédents (Joët *et al.*, 2002a; Peltier and Cournac, 2002). La présence de PTOX est particulièrement importante dans la transition de l'obscurité à la lumière, et de la faible lumière à la forte lumière.

5.4 Analyse des plantes surexprimant de PTOX chez la tomate (chapitre 3.3)

Des plantes de tomate transgéniques (type nain : MicroTom) exprimant l'ADNc de PTOX d'Arabidopsis thaliana (At-PTOX) sous le contrôle d'un promoteur fort de CaMV ont été examinées dans cette étude. Après vérification de la présence du transgène dans les lignées transgéniques, une lignée présentant une accumulation forte de PTOX a été choisie. Cette unique lignée PTOX$^+$ montre des paramètres de croissance similaires aux plantes contrôles ; mais ses jeunes feuilles ont une couleur verte plus foncée.

La surproduction de At-PTOX chez la tomate n'a pas influencé la teneur de caroténoïdes dans des feuilles adultes ni dans les fruits au stade 4 jours de mûrissement. Les plantes exprimant At-PTOX ne présentent pas une résistance accrue à la photoinhibition et ce résultat est conforme aux observations en cas de surproduction de PTOX chez le tabac et *A. thaliana* (Joët *et al.*, 2002a; Rosso *et al.*, 2006).

Chez les lignées transgéniques PTOX$^+$ de tabac, l'augmentation transitoire de la fluorescence F_0 après une transition de la lumière à l'obscurité est absente (Joët *et al.*, 2002a), mais les mêmes résultats n'ont pas été observés chez les plantes PTOX$^+$ de tomate (les données actuelles) et *Arabidopsis thaliana* (Rosso *et al.*, 2006). Des différences dans l'activité de la réduction du pool des PQ pourraient exister entre espèces (Yamane *et al.*, 2000).

La cinétique d'induction de la fluorescence de la chlorophylle lors d'un passage obscurité/lumière indique l'établissement d'un gradient de pH inférieur chez la lignée PTOX$^+$ par rapport au contrôle. Cela semble confirmer que des réactions cycliques d'électrons autour du PSI sont régulées par PTOX.

Cependant, en général, l'influence d'une surproduction de At-PTOX chez la tomate semble minimale. La possibilité d'une synthèse de protéine non active ou d'une mutation dans la région codant de cette enzyme pendant le processus de transformation ne peuvent être exclues. C'est cependant peu probable puisqu'on observe quelques effets mineurs, comme mentionné ci-dessus.

5.5 Conclusions générales

Chez les plantes supérieures, la photosynthèse oxygénique et la respiration sont les mécanismes bioénergétique d'oxydo-réduction ; ils ont en commun la participation d'un complexe d'ATP synthase et d'un certain nombre d'intermédiaires de transport d'électrons (quinones, cytochromes, *etc.*) permettant l'établissement d'un gradient de protons qui sera utilisé par ATP synthase. Les voies alternatives (non énergétiques) des chaînes de transfert d'électrons respiratoire et photosynthétique comportent l'oxydase alternative (AOX) dans des mitochondries et l'oxydase terminale plastidiale (PTOX) dans les chloroplastes. Ces quinol oxydases semblent être une caractéristique conservée chez les organismes photosynthétiques oxygéniques. Les protéines d'AOX et de PTOX partagent une homologie de séquence, indiquant qu'elles dérivent d'une forme procaryotique ancestrale commune, non diversifiée, et qui a rejoint la lignée eucaryote séparément dans les mitochondries et les chloroplastes, respectivement, par l'intermédiaire événements endosymbiotiques. La transition d'un environnement anaérobie à aérobie pourrait avoir été la force d'entraînement pour l'évolution d'une telle oxydase, ancêtre d'AOX et de PTOX. Puisque ces voies alternatives sont non énergétiques, elles peuvent agir sur la diminution de taux de pression de transfert d'électrons dans les membranes et permettre aux plantes de s'acclimater dans des conditions environnementales variables.

Assumer un rôle protecteur si ancien (en terme d'évolution) de PTOX, comme composant de la chaîne de transport photosynthétique d'électrons, pourrait impliquer que sa fonction dans la biosynthèse des caroténoïdes, comme cofacteur pour la désaturation de phytoène, a été acquise plus tard dans l'évolution. Cela semble conforme à l'observation que cette dernière fonction est essentiellement importante à certaines étapes développementales telles que la dé-etiolation du plaste ou la différentiation de chromoplastes. Ces étapes peuvent être regardées en tant que développements évolutionnaires plus récents. De plus, des voies indépendantes de PTOX associées à la phytoene désaturase existent dans les chloroplasts différenciés, ce qui semble compatible avec les aspects d'évolution mentionnés ci-dessus.

L'objectif principal de ce travail était de caractériser les deux rôles de PTOX. La tomate a été choisie comme système modèle. Ces résultats ont permis la démonstration d'un rôle nécessaire et direct de PTOX dans la photosynthèse, à savoir son influence sur l'état redox du pool de PQ entre PSII et PSI. Jusqu'à maintenant un tel rôle n'a pas pu être démontré chez l'*Arabidopsis* (Rosso *et al.*, 2006). Dans cette étude, nous avons démontré qu'en faible lumière, *ghost* peut produire des feuilles adultes et des fruits verts, qui contiennent la même quantité des

caroténoïdes que ceux de la tomate non-déficiente en PTOX (SM) et qui n'accumulent pas de phytoène. Ces tissus verts de *ghost* sont moins capables d'éviter des dommages oxydatifs et sont plus sensibles à la photoinhibition et aux dommages de PSII. D'autre part, l'absence de PTOX rend l'appareil photosynthétique de feuille de tomate plus sensible à la lumière. Nous avons prouvé que cette sensibilité de la photosynthèse mentionnée ci-dessus chez *ghost* vient d'un niveau élevé de sur-réduction non-photochimique des PQs à l'obscurité et d'un état réduit plus important de la chaîne de transfert d'électrons photosynthétiques à la lumière. L'utilisation de la tomate comme système modèle a permis d'étudier le rôle de PTOX à d'autres étapes développementales notamment dans les cotylédons étiolés (biogenèse des chloroplastes) et dans les fruits mûrs (différentiation des chromoplastes), des stades qu'il est impossible ou plus difficile d'étudier chez *Arabidopsis*.

Bien que notre stratégie originale ait été d'examiner un mutant de tomate PTOX- et des plantes tomates surexprimant PTOX, il s'est avéré que la majeure partie des données a été fournie dans notre étude par le mutant. Cela peut être expliqué soit par une régulation de l'activité de PTOX et/ou par la localisation inadéquate de PTOX en cas de surproduction. Une tentative a également été faite de trouver des inhibiteurs spécifiques et efficaces pour PTOX. De tels inhibiteurs permettraient l'inactivation locale de PTOX et d'une façon dirigée et opportune. Cependant, comme montré dans l'annexe A.3, aucun inhibiteur n'a pas pu être identifié. L'inhibiteur connu de PTOX *in vitro*, l'octyl-gallate, est moins efficace *in vivo* et tous les herbicides de blanchiment examinés, qui empêchent la désaturation des caroténoïdes, semblent agir sur la désaturase plutôt que sur PTOX l'identification d'inhibiteurs agissant sur le cofacteur alternatif de la désaturation des caroténoïdes (Carol and Kuntz, 2001) exigerait d'autres expériences.

En conclusion, PTOX possède un rôle régulateur dans la distribution des électrons vers différentes voies linéaires et alternatives d'électrons. Bien que composant mineur de l'appareil photosynthétique, PTOX est particulièrement important dans la transition de l'obscurité à la lumière et ainsi que de la faible lumière à la forte lumière. D'autres investigations dans les autres plantes modèles seraient intéressantes, telles que les plantes alpines où PTOX pourrait agir en tant que " valve de sécurité " permettant un flux considérable d'électron photosynthétique vers O_2 (Streb *et al.*, 2005).

Bibliography

Albertsson, P.-A. (2001). A quantitative model of the domain structure of the photosynthetic membrane. *Trends in Plant Science* **6**, 349.

Albrecht, M., Klein, A., Hugueney, P., Sandmann, G. and Kuntz, M. (1995). Molecular-cloning and functional expression in *E. coli* of a novel plant enzyme mediating ζ-carotene desaturation. *Febs Letters* **372**, 199–202.

Aldridge, C., Maple, J. and Moller, S. G. (2005). The molecular biology of plastid division in higher plants. *Journal of Experimental Botany* **56**, 1061–1077.

Allahverdiyeva, Y., Mamedov, F., Maenpaa, P., Vass, I. and Aro, E. M. (2005). Modulation of photosynthetic electron transport in the absence of terminal electron acceptors: Characterization of the *rbcL* deletion mutant of tobacco. *Biochimica et Biophysica Acta-Bioenergetics* **1709**, 69–83.

Allakhverdiev, S. I., Los, D. A., Mohanty, P., Nishiyama, Y. and Murata, N. (2007). Glycinebetaine alleviates the inhibitory effect of moderate heat stress on the repair of photosystem II during photoinhibition. *Biochimica et Biophysica Acta* **1767**, 1363–71.

Allen, J. F. (1995). Thylakoid protein-phosphorylation, state-1-state-2 transitions, and photosystem stoichiometry adjustment - redox control at multiple levels of gene-expression. *Physiologia Plantarum* **93**, 196–205.

Allen, J. F. (2003). State transitions - a question of balance. *Science* **299**, 1530–1532.

Allen, J. F. and Forsberg, J. (2001). Molecular recognition in thylakoid structure and function. *Trends in Plant Science* **6**, 317–326.

Aluru, M. R., Bae, H., Wu, D. Y. and Rodermel, S. R. (2001). The *Arabidopsis immutans* mutation affects plastid differentiation and the morphogenesis of white and green sectors in variegated plants. *Plant Physiology* **127**, 67–77.

Aluru, M. R., Stessman, D. J., Spalding, M. H. and Rodermel, S. R. (2007). Alterations in photosynthesis in *Arabidopsis* lacking *immutans*, a chloroplast terminal oxidase. *Photosynthesis Research* **91**, 11–23.

Aluru, M. R., Yu, F., Fu, A. and Rodermel, S. (2006). *Arabidopsis* variegation mutants: new insights into chloroplast biogenesis. *Journal of Experimental botany* **57**, 1871–81.

Arnon, D. I. (1965). Ferredoxin and photosynthesis. *Science* **149**, 1460–&.

Asada, K. (1999). The water-water cycle in chloroplasts: Scavenging of active oxygens and dissipation of excess photons. *Annual Review of Plant Physiology and Plant Molecular Biology* **50**, 601–639.

Asada, K. (2000). The water-water cycle as alternative photon and electron sinks. *Philosophical Transactions of The Royal Society of London Series B-Biological Sciences* **355**, 1419–1430.

Asada, K. (2006). Production and scavenging of reactive oxygen species in chloroplasts and their functions. *Plant Physiology* **141**, 391–396.

Bach, T. J., Boronat, A., Campos, N., Ferrer, A. and Vollack, K. U. (1999). Mevalonate biosynthesis in plants. *Critical Reviews in Biochemistry and Molecular Biology* **34**, 107–122.

Badger, M. R., von Caemmerer, S., Ruuska, S. and Nakano, H. (2000). Electron flow to oxygen in higher plants and algae: Rates and control of direct photoreduction (Mehler reaction) and rubisco oxygenase. *Philosophical Transactions of the Royal Society of London B Biological Sciences* **355**, 1433–1446.

Bae, H., Rodermel, S. R., Behringer, F. and Wetzel, C. (1999). Tomato *Ghost* and *Arabidopsis immutans* are homologous variegation loci that function in phytoene desaturation and chloroplast development. *Plant Biology (Rockville)* **1999**, 140.

Baena-Gonzalez, E., Allahverdiyeva, Y., Svab, Z., Maliga, P., Josse, E. M., Kuntz, M., Maenpaa, P. and Aro, E. M. (2003). Deletion of the tobacco plastid *psbA* gene triggers an upregulation of the thylakoid-associated NAD(P)H dehydrogenase complex and the plastid terminal oxidase (PTOX). *The Plant Journal* **35**, 704–16.

Baena-Gonzalez, E., Gray, J. C., Tyystjarvi, E., Aro, E. M. and Maenpaa, P. (2001). Abnormal regulation of photosynthetic electron transport in a chloroplast *ycf*9 inactivation mutant. *Journal of Biological Chemistry* **276**, 20795–20802.

Baerr, J. N., Thomas, J. D., Taylor, B. G., Rodermel, S. R. and Gray, G. R. (2005). Differential photosynthetic compensatory mechanisms exist in the *immutans* mutant of *Arabidopsis thaliana*. *Physiologia Plantarum* **124**, 390–402.

Baker, N. R. and Rosenqvist, E. (2004). Applications of chlorophyll fluorescence can improve crop production strategies: an examination of future possibilities. *Journal of Experimental Botany* **55**, 1607–1621.

Barr, J., White, W. S., Chen, L., Bae, H. and Rodermel, S. (2004). The *Ghost* terminal oxidase regulates developmental programming in tomato fruit. *Plant, Cell and Environment* **27**, 840–852.

Bartley, G. E., Viitanen, P. V., Bacot, K. O. and Scolnik, P. A. (1992). A tomato gene expressed during fruit ripening encodes an enzyme of the carotenoid biosynthesis pathway. *Journal of Biological Chemistry* **267**, 5036–5039.

Bellafiore, S., Bameche, F., Peltier, G. and Rochaix, J. D. (2005). State transitions and light adaptation require chloroplast thylakoid protein kinase STN7. *Nature* **433**, 892–895.

Bennoun, P. (1982). Evidence for a respiratory-chain in the chloroplast. *Proceedings of The National Academy of Sciences of The United States of America-Biological Sciences* **79**, 4352–4356.

Berthold, D. A. and Stenmark, P. (2003). Membrane-bound diiron carboxylate proteins. *Annual Review of Plant Biology* **54**, 497–517.

Bojko, M., Kruk, J. and Wieckowski, S. (2003). Plastoquinones are effectively reduced by ferredoxin: $NADP^+$ oxidoreductase in the presence of sodium cholate micelles significance for cyclic electron transport and chlororespiration. *Phytochemistry* **64**, 1055–1060.

Bondarava, N., De Pascalis, L., Al-Babili, S., Goussias, C., Golecki, J. R., Beyer, P., Bock, R. and Krieger-Liszkay, A. (2003). Evidence that cytochrome b_{559} mediates the oxidation of reduced plastoquinone in the dark. *Journal of Biological Chemistry* **278**, 13554–13560.

Bouvier, F., D'Harlingue, A., Backhaus, R. A., Kumagai, M. H. and Camara, B. (2000). Identification of neoxanthin synthase as a carotenoid cyclase paralog. *European Journal of Biochemistry* **267**, 6346–6352.

Bouvier, F., dHarlingue, A., Hugueney, P., Marin, E., MarionPoll, A. and Camara, B. (1996). Xanthophyll biosynthesis - cloning, expression, functional reconstitution, and regulation of β-cyclohexenyl carotenoid epoxidase from pepper (*Capsicum annuum*). *Journal of Biological Chemistry* **271**, 28861–28867.

Bouvier, F., Hugueney, P., Dharlingue, A., Kuntz, M. and Camara, B. (1994). Xanthophyll biosynthesis in chromoplasts - isolation and molecular-cloning of an enzyme catalyzing the conversion of 5,6-epoxycarotenoid into ketocarotenoid. *Plant Journal* **6**, 45–54.

Bramley, P., Teulieres, C., Blain, I., Bird, C. and Schuch, W. (1992). Biochemical-characterization of transgenic tomato plants in which carotenoid synthesis has been inhibited through the expression of antisense RNA to Ptom5. *Plant Journal* **2**, 343–349.

Breyton, C., Nandha, B., Johnson, G. N., Joliot, P. and Finazzi, G. (2006). Redox modulation of cyclic electron flow around photosystem I in C3 plants. *Biochemistry* **45**, 13465–13475.

Bruinsma, J. (1961). A comment on the spectrophotometric determination of chlorophyll. *Biochimica et Biophysica Acta* **52**, 576–578.

Buchanan, B. B., Gruissem, W. and Jones, R. L. (2000). *Biochemistry and Molecular Biology of Plant*. American Society of Plant physiologist.

Bukhov, N. and Carpentier, R. (2004). Alternative photosystem I-driven electron transport routes: mechanisms and functions. *Photosynthesis Research* **82**, 17–33.

Bukhov, N. G., Sabat, S. C. and Mohanty, P. (1990). Analysis of chlorophyll-*a* fluorescence changes in weak light in heat-treated *Amaranthus* chloroplasts. *Photosynthesis Research* **23**, 81–87.

Bukhov, N. G., Wiese, C., Neimanis, S. and Heber, U. (1999). Heat sensitivity of chloroplasts and leaves: Leakage of protons from thylakoids and reversible activation of cyclic electron transport. *Photosynthesis Research* **59**, 81–93.

Burnette, W. (1981). "Western blotting": electrophoretic transfer of proteins from sodium dodecyl sulfate-polyacrylamide gels to unmodified nitrocellulose and radiographic detection with antibody and radioiodinated protein A. *Anal Biochem* **112**, 195–203.

Burrows, P. A., Sazanov, L. A., Svab, Z., Maliga, P. and Nixon, P. J. (1998). Identification of a functional respiratory complex in chloroplasts through analysis of tobacco mutants containing disrupted plastid *ndh* genes. *Embo Journal* **17**, 868–876.

Camara, B., Hugueney, P., Bouvier, F., Kuntz, M. and Moneger, R. (1995). Biochemistry and molecular biology of chromoplast development. *International Review of Cytology* **163**, 175–247.

Cape, J. L., Bowman, M. K. and Kramer, D. M. (2006). Understanding the cytochrome *bc* complexes by what they don't do. the Q-cycle at 30. *Trends in Plant Science* **11**, 46–55.

Carol, P. and Kuntz, M. (2001). A plastid terminal oxidase comes to light: implications for carotenoid biosynthesis and chlororespiration. *Trends in Plant Science* **6**, 31–36.

Carol, P., Stevenson, D., Bisanz, C., Breitenbach, J., Sandmann, G., Mache, R., Coupland, G. and Kuntz, M. (1999). Mutations in the *Arabidopsis* gene *immutans* cause a variegated phenotype by inactivating a chloroplast terminal oxidase associated with phytoene desaturation. *The Plant cell* **11**, 57–68.

Casano, L. M., Martin, M. and Sabater, B. (2001). Hydrogen peroxide mediates the induction of chloroplastic NDH complex under photooxidative stress in barley. *Plant Physiology* **125**, 1450–1458.

Casano, L. M., Martin, M., Zapata, J. M. and Sabater, B. (1999). Leaf age- and paraquat concentration-dependent effects on the levels of enzymes protecting against photooxidative stress. *Plant Science* **149**, 13–22.

Casano, L. M., Zapata, J. M., Martin, M. and Sabater, B. (2000). Chlororespiration and poising of cyclic electron transport - plastoquinone as electron transporter between thylakoid NADH dehydrogenase and peroxidase. *Journal of Biological Chemistry* **275**, 942–948.

Catala, R., Sabater, B. and Guera, A. (1997). Expression of the plastid *ndhF* gene product in photosynthetic and non-photosynthetic tissues of developing barley seedlings. *Plant and Cell Physiology* **38**, 1382–1388.

Cavalier-Smith, T. (2000). Membrane heredity and early chloroplast evolution. *Trends in Plant Science* **5**, 174–182.

Cheniclet, C. and Carde, J. P. (1988). Differentiation of leucoplasts - comparative transition of proplastids to chloroplasts or leucoplasts in trichomes of *Stachys lanata* leaves. *Protoplasma* **143**, 74–83.

Chitnis, P. R. (1996). Photosystem I. *Plant Physiology* **111**, 661–669.

Choquet, Y. and Vallon, O. (2000). Synthesis, assembly and degradation of thylakoid membrane proteins. *Biochimie* **82**, 615.

Cline, K. and Henry, R. (1996). Import and routing of nucleus-encoded chloroplast proteins. *Annual Review of Cell and Developmental Biology* **12**, 1–26.

Cournac, L., Josse, E. M., Joët, T., Rumeau, D., Redding, K., Kuntz, M. and Peltier, G. (2000a). Flexibility in photosynthetic electron transport: a newly identified chloroplast oxidase involved in chlororespiration. *Philosophical Transactions of the Royal Society B: Biological Sciences* **355**, 1447–1454.

Cournac, L., Latouche, G., Cerovic, Z., Redding, K., Ravenel, J. and Peltier, G. (2002). *In vivo* interactions between photosynthesis, mitorespiration, and chlororespiration in *Chlamydomonas reinhardtii*. *Plant Physiology* **129**, 1921–1928.

Cournac, L., Redding, K., Ravenel, J., Rumeau, D., Josse, E. M., Kuntz, M. and Peltier, G. (2000b). Electron flow between photosystem II and oxygen in chloroplasts of photosystem I-deficient algae is mediated by a quinol oxidase involved in chlororespiration. *Journal of Biological Chemistry* **275**, 17256–17262.

Cramer, W. A., Soriano, G. M., Ponomarev, M., Huang, D., Zhang, H., Martinez, S. E. and Smith, J. L. (1996). Some new structural aspects and old controversies concerning the cytochrome b_6f complex of oxygenic photosynthesis. *Annual Review of Plant Physiology and Plant Molecular Biology* **47**, 477–508.

Cruz Hernandez, A. and Gomezlim, M. A. (1995). Alternative oxidase from mango (*Mangifera indica*, L.) is differentially regulated during fruit ripening. *Planta* **197**, 569–576.

Cunningham, F. X. and Gantt, E. (1998). Genes and enzymes of carotenoid biosynthesis in plants. *Annual Review of Plant Physiology and Plant Molecular Biology* **49**, 557–583.

Cunningham, F. X., Pogson, B., Sun, Z. R., McDonald, K. A., DellaPenna, D. and Gantt, E. (1996). Functional analysis of the β and epsilon lycopene cyclase enzymes of *Arabidopsis* reveals a mechanism for control of cyclic carotenoid formation. *Plant Cell* **8**, 1613–1626.

Debus, R. J., Barry, B. A., Sithole, I., Babcock, G. T. and McIntosh, L. (1988). Directed mutagenesis indicates that the donor to $P680^+$ in photosystem-II is Tyrosine-161 of the D1 polypeptide. *Biochemistry* **27**, 9071–9074.

Depege, N., Bellafiore, S. and Rochaix, J. D. (2003). Rote of chloroplast protein kinase Stt7 in LHCII phosphorylation and state transition in chlamydomonas. *Science* **299**, 1572–1575.

Deschamps, P., Colleoni, C., Nakamura, Y., Suzuki, E., Putaux, J.-L., Buleon, A., Haebel, S., Ritte, G., Steup, M., Falcon, L. I., Moreira, D., Loffelhardt, W., Raj, J. N., Plancke, C., d'Hulst, C., Dauvillee, D. and Ball, S. (2008). Metabolic symbiosis and the birth of the plant kingdom. *Molecular Biology and Evolution* **25**, 536–548.

Doyle, J. and Doyle, J. (1987). A rapid DNA isolation procedure for small quantities of fresh leaf tissue. *Phytochemical Bulltein* **1**, 11–15.

Ducruet, J. M. (2003). Chlorophyll thermoluminescence of leaf discs: simple instruments and progress in signal interpretation open the way to new ecophysiological indicators. *Journal of Experimental Botany* **54**, 2419–30.

Ducruet, J. M. and Lemoine, Y. (1985). Increased heat sensitivity of the photosynthetic apparatus in triazine resistant biotypes from different plant-species. *Plant and Cell Physiology* **26**, 419–429.

Eastmond, P. J. and Rawsthorne, S. (2000). Coordinate changes in carbon partitioning and plastidial metabolism during the development of oilseed rape embryo. *Plant Physiology* **122**, 767–774.

Eckhardt, U., Grimm, B. and Hortensteiner, S. (2004). Recent advances in chlorophyll biosynthesis and breakdown in higher plants. *Plant Molecular Biology* **56**, 1–14.

EFSA FEEDAP Panel (2005). Opinion of the scientific panel on additives and products or substances used in animal feed on the request from the european commission on the safety of use of colouring agents in animal nutrition part i general principles and astaxanthin. *European Food Safety Authority Journal* **291**, 1–40.

Enami, I., Kitamura, M., Tomo, T., Isokawa, Y., Ohta, H. and Katoh, S. (1994). Is the primary cause of thermal inactivation of oxygen evolution in spinach PSII membranes release of the extrinsic 33 kDa protein or of Mn. *Biochimica et Biophysica Acta-Bioenergetics* **1186**, 52–58.

Endo, T., Kawase, D. and Sato, F. (2005). Stromal over-reduction by high-light stress as measured by decreases in P700 oxidation by far-red light and its physiological relevance. *Plant and Cell Physiology* **46**, 775–781.

Endo, T., Shikanai, T., Takabayashi, A., Asada, K. and Sato, F. (1999). The role of chloroplastic NAD(P)H dehydrogenase in photoprotection. *Febs Letters* **457**, 5–8.

Feild, T. S., Nedbal, L. and Ort, D. R. (1998). Nonphotochemical reduction of the plastoquinone pool in sunflower leaves originates from chlororespiration. *Plant Physiology* **116**, 1209–1218.

Finazzi, G., Rappaport, F., Furia, A., Fleischmann, M., Rochaix, J. D., Zito, F. and Forti, G. (2002). Involvement of state transitions in the switch between linear and cyclic electron flow in *Chlamydomonas reinhardtii*. *Embo Reports* **3**, 280–285.

Finley, J. W. (2005). Proposed criteria for assessing the efficacy of cancer reduction by plant foods enriched in carotenoids, glucosinolates, polyphenols and selenocompounds. *Annals of Botany* **95**, 1075–1096.

Finnegan, P. M., Umbach, A. L. and Wilce, J. A. (2003). Prokaryotic origins for the mitochondrial alternative oxidase and plastid terminal oxidase nuclear genes. *Febs Letters* **555**, 425–430.

Fischer, M., Funk, E. and Steinmuller, K. (1997). The expression of subunits of the mitochondrial complex I-homologous NAD(P)H-plastoquinone-oxidoreductase during plastid development. *Zeitschrift Fur Naturforschung C-A Journal of Biosciences* **52**, 481–486.

Foyer, C. H., LopezDelgado, H., Dat, J. F. and Scott, I. M. (1997). Hydrogen peroxide- and glutathione-associated mechanisms of acclimatory stress tolerance and signalling. *Physiologia Plantarum* **100**, 241–254.

Foyer, C. H. and Noctor, G. (2000). Oxygen processing in photosynthesis: regulation and signalling. *New Phytologist* **146**, 359–388.

Foyer, C. H. and Noctor, G. (2003). Redox sensing and signalling associated with reactive oxygen in chloroplasts, peroxisomes and mitochondria. *Physiologia Plantarum* **119**, 355–364.

Frank, H. A. and Cogdell, R. J. (1996). Carotenoids in photosynthesis. *Photochemistry and Photobiology* **63**, 257–264.

Fraser, P. D., Bramley, P. and Seymour, G. B. (2001). Effect of the *Cnr* mutation on carotenoid formation during tomato fruit ripening. *Phytochemistry* **58**, 75–79.

Fraser, P. D. and Bramley, P. M. (2004). The biosynthesis and nutritional uses of carotenoids. *Progress in Lipid Research* **43**, 228–265.

Fraser, P. D., Pinto, M. E., Holloway, D. E. and Bramley, P. M. (2000). Technical advance: application of high-performance liquid chromatography with photodiode array detection to the metabolic profiling of plant isoprenoids. *The Plant Journal* **24**, 551–8.

Fu, A., He, Z. Y., Cho, H. S., Lima, A., Buchanan, B. B. and Luan, S. (2007). A chloroplast cyclophilin and maintenance of functions in the assembly photosystem II in *Arabidopsis thaliana*. *Proceedings of The National Academy of Sciences of The United States of America* **104**, 15947–15952.

Fu, A., Park, S. and Rodermel, S. (2005). Sequences required for the activity of PTOX (*immutans*), a plastid terminal oxidase: *in vitro* and *in planta* mutagenesis of iron-binding sites and a conserved sequence that corresponds to Exon 8. *The Journal of Biological Chemistry* **280**, 42489–42496.

Fukuyama, K. (2004). Structure and function of plant-type ferredoxins. *Photosynthesis Research* **81**, 289–301.

Gal, A., Zer, H. and Ohad, I. (1997). Redox-controlled thylakoid protein phosphorylation. news and views. *Physiologia Plantarum* **100**, 869–885.

Geiger, D. R., Shieh, W. J. and Yu, X. M. (1995). Photosynthetic carbon metabolism and translocation in wild-type and starch-deficient mutant *Nicotiana sylvestris* L. *Plant Physiology* **107**, 507–514.

Gilbert, M., Wagner, H., Weingart, I., Skotnica, J., Nieber, K., Tauer, G., Bergmann, F., Fischer, H. and Wilhelm, C. (2004). A new type of thermoluminometer: a highly sensitive tool in applied photosynthesis research and plant stress physiology. *Journal of Plant Physiology* **161**, 641– 651.

Golding, A. J., Finazzi, G. and Johnson, G. N. (2004). Reduction of the thylakoid electron transport chain by stromal reductants-evidence for activation of cyclic electron transport upon dark adaptation or under drought. *Planta* **220**, 356–363.

Goss, R., Bohme, K. and Wilhelm, C. (1998). The xanthophyll cycle of *Mantoniella squamata* converts violaxanthin into antheraxanthin but not to zeaxanthin: consequences for the mechanism of enhanced non-photochemical energy dissipation. *Planta* **205**, 613–621.

Goyal, A. and Tolbert, N. E. (1996). Association of glycolate oxidation with photosynthetic electron transport in plant and algal chloroplasts. *Proceedings of The National Academy of Sciences of The United States of America* **93**, 3319–3324.

Gray, M. W. (1992). The endosymbiont hypothesis revisited. *International Review of Cytology-A Survey of Cell Biology* **141**, 233–357.

Grzyb, J., Gagos, M., Gruszecki, W. I., Bojko, M. and Strzalka, K. (2008). Interaction of ferredoxin: $NADP^+$ oxidoreductase with model membranes. *Biochimica et Biophysica Acta-Biomembranes* **1778**, 133–142.

Guera, A. and Sabater, B. (2002). Changes in the protein and activity levels of the plastid NADH-plastoquinone-oxidoreductase complex during fruit development. *Plant Physiology and Biochemistry* **40**, 423–429.

Gutierrez-Nava, M. D. L., Gillmor, C. S., Jimenez, L. F., Guevara-Garcia, A. and Leon, P. (2004). Chloroplast biogenesis genes act cell and noncell autonomously in early chloroplast development. *Plant Physiology* **135**, 471–482.

Haldimann, P. and Strasser, R. J. (1999). Effects of anaerobiosis as probed by the polyphasic chlorophyll *a* fluorescence rise kinetic in pea (*Pisum sativum* L.). *Photosynthesis Research* **62**, 67–83.

Haldrup, A., Lunde, C. and Scheller, H. V. (2003). *Arabidopsis thaliana* plants lacking the PSI-D subunit of photosystem I suffer severe photoinhibition, have unstable photosystem I complexes, and altered redox homeostasis in the chloroplast stroma. *Journal of Biological Chemistry* **278**, 33276–33283.

Hamel, P., Olive, J., Pierre, Y., Wollman, F. A. and de Vitry, C. (2000). A new subunit of cytochrome b_6f complex undergoes reversible phosphorylation upon state transition. *Journal of Biological Chemistry* **275**, 17072–17079.

Hansson, A., Amann, K., Zygadlo, A., Meurer, J., Scheller, H. V. and Jensen, P. E. (2007). Knock-out of the chloroplast-encoded PSI-J subunit of photosystem I in *Nicotiana tabacum* - PSI-J is required for efficient electron transfer and stable accumulation of photosystem I. *Febs Journal* **274**, 1734–1746.

Havaux, M. (1996). Short-term responses of photosystem I to heat stress - induction of a PS II-independent electron transport through PS I fed by stromal components. *Photosynthesis Research* **47**, 85–97.

Havaux, M. (1998). Carotenoids as membrane stabilizers in chloroplasts. *Trends in Plant Science* **3**, 147.

Havaux, M., Dall'Osto, L., Cuine, S., Giuliano, G. and Bassi, R. (2004). The effect of zeaxanthin as the only xanthophyll on the structure and function of the photosynthetic apparatus in *Arabidopsis thaliana*. *Journal of Biological Chemistry* **279**, 13878–13888.

Havaux, M. and Niyogi, K. K. (1999). The violaxanthin cycle protects plants from photooxidative damage by more than one mechanism. *The Proceedings of the National Academy of Sciences of the United Stades of America* **96**, 8762–8767.

Havaux, M., Rumeau, D. and Ducruet, J. M. (2005). Probing the FQR and NDH activities involved in cyclic electron transport around photosystem I by the "afterglow" luminescence. *Biochimica et Biophysica Acta-Bioenergetics* **1709**, 203–213.

Heber, U. and Walker, D. (1992). Concerning a dual function of coupled cyclic electron-transport in leaves. *Plant Physiology* **100**, 1621–1626.

Heddad, M., Noren, H., Reiser, V., Dunaeva, M., Andersson, B. and Adamska, I. (2006). Differential expression and localization of early light-induced proteins in *Arabidopsis*. *Plant Physiology* **142**, 75–87.

Hegedus, A., Erdei, S., Janda, T., Toth, E., Horvath, G. and Dudits, D. (2004). Transgenic tobacco plants overproducing alfalfa aldose/aldehyde reductase show higher tolerance to low temperature and cadmium stress. *Plant Science* **166**, 1329–1333.

Hill, R. and Bendall, F. (1960). Function of the 2 cytochrome components in chloroplasts - working hyothesis. *Nature* **186**, 136–137.

Hiser, C., Kapranov, P. and McIntosh, L. (1996). Genetic modification of respiratory capacity in potato. *Plant Physiology* **110**, 277–286.

Hodges, D. M., DeLong, J. M., Forney, C. F. and Prange, R. K. (1999). Improving the thiobarbituric acid-reactive-substances assay for estimating lipid peroxidation in plant tissues containing anthocyanin and other interfering compounds. *Planta* **207**, 604–611.

Holt, N. E., Fleming, G. R. and Niyogi, K. K. (2004). Toward an understanding of the mechanism of nonphotochemical quenching in green plants. *Biochemistry* **43**, 8281–8289.

Hunt, G. M. and Baker, E. A. (1980). Phenolic constituents of tomato fruit cuticles. *Phytochemistry* **19**, 1415–1419.

Hurkman, W. J. and Tanaka, C. K. (1986). Solubilization of plant membrane proteins for analysis by two-dimensional gel electrophoresis. *Plant Physiology* **81**, 802–806.

Jansson, S. (1999). A guide to the *Lhc* genes and their relatives in *Arabidopsis*. *Trends in Plant Science* **4**, 236–240.

Jensen, P. E., Gilpin, M., Knoetzel, J. and Scheller, H. V. (2000). The PSI-K subunit of photosystem I is involved in the interaction between light-harvesting complex I and the photosystem I reaction center core. *Journal of Biological Chemistry* **275**, 24701–24708.

Jensen, P. E., Haldrup, A., Zhang, S. P. and Scheller, H. V. (2004). The PSI-O subunit of plant photosystem I is involved in balancing the excitation pressure between the two photosystems. *Journal of Biological Chemistry* **279**, 24212–24217.

Johnson, G. N. (2005). Cyclic electron transport in C-3 plants: fact or artefact? *Journal of Experimental Botany* **56**, 407–416.

Joliot, P. and Joliot, A. (2005). Quantification of cyclic and linear flows in plants. *Proceedings of The National Academy of Sciences of The United States of America* **102**, 4913–4918.

Joliot, P., Joliot, A. and Johnson, G. (2006). Cyclic electron transfer around photosystem I. *Advances in Photosynthesis and Respiration:THE LIGHT-DRIVEN PLASTOCYANIN: FERREDOXIN OXIDOREDUCTASE* , 639–656.

Jordan, P., Fromme, P., Witt, H. T., Klukas, O., Saenger, W. and Krauss, N. (2001). Three-dimensional structure of cyanobacterial photosystem I at 2.5 angstrom resolution. *Nature* **411**, 909–917.

Josse, E. M. (2003). *Caracterisation d'une oxydase terminale plastidiale impliquée dans la biosynthesis des carotenoïdes et dans la reponse au stress*. Ph.D. thesis, Laboratoire Plastes et Différenciation Cellulaire; Université Joseph Fourier; Grenoble.

Josse, E. M., Alcaraz, J. P., Laboure, A. M. and Kuntz, M. (2003). *In vitro* characterization of a plastid terminal oxidase (PTOX). *European Journal of Biochemistry* **270**, 3787–94.

Josse, E. M., Simkin, A. J., Gaffe, J., Laboure, A. M., Kuntz, M. and Carol, P. (2000). A plastid terminal oxidase associated with carotenoid desaturation during chromoplast differentiation. *Plant Physiology* **123**, 1427–1436.

Joët, T., Cournac, L., Horvath, E. M., Medgyesy, P. and Peltier, G. (2001). Increased sensitivity of photosynthesis to antimycin A induced by inactivation of the chloroplast *ndhB* gene. evidence for a participation of the NADH-dehydrogenase complex to cyclic electron flow around photosystem I. *Plant Physiology* **125**, 1919–1929.

Joët, T., Cournac, L., Peltier, G. and Havaux, M. (2002a). Cyclic electron flow around photosystem I in C(3) plants. *In vivo* control by the redox state of chloroplasts and involvement of the NADH-dehydrogenase complex. *Plant Physiology* **128**, 760–769.

Joët, T., Genty, B., Josse, E. M., Kuntz, M., Cournac, L. and Peltier, G. (2002b). Involvement of a plastid terminal oxidase in plastoquinone oxidation as evidenced by expression of the *Arabidopsis thaliana* enzyme in tobacco. *Journal of Biological Chemistry* **277**, 31623–30.

Kaminskaya, O., Renger, G. and Shuvalov, V. A. (2003). Effect of dehydration on light-induced reactions in photosystem II: Photoreactions of cytochrome b_{559}. *Biochemistry* **42**, 8119–8132.

Kaminskaya, O., Shuvalov, V. A. and Renger, G. (2007). Evidence for a novel quinone-binding site in the photosystem II (PS II) complex that regulates the redox potential of cytochrome b_{559}. *Biochemistry* **46**, 1091–1105.

Kessler, F., Schnell, D. and Blobel, G. (1999). Identification of proteins associated with plastoglobules isolated from pea (*Pisum sativum* L.) chloroplasts. *Planta* **208**, 107–113.

Khorobrykh, S. A. and Ivanov, B. N. (2002). Oxygen reduction in a plastoquinone pool of isolated pea thylakoids. *Photosynthesis Research* **71**, 209–219.

Kimura, M., Manabe, K., Abe, T., Yoshida, S., Matsui, M. and Yamamoto, Y. Y. (2003). Analysis of hydrogen peroxide-independent expression of the high-light-inducible *ELIP*2 gene with the aid of the *ELIP*2 promoter-luciferase fusions. *Photochemistry and Photobiology* **77**, 668–674.

Kirchhoff, H., Haase, W., Haferkamp, S., Schott, T., Borinski, M., Kubitscheck, U. and Rogner, M. (2007). Structural and functional self-organization of photosystem II in grana thylakoids. *Biochimica et Biophysica Acta-Bioenergetics* **1767**, 1180–1188.

Kiss, A. Z., Ruban, A. V. and Horton, P. (2008). The PsbS protein controls the organization of the photosystem II antenna in higher plant thylakoid membranes. *Journal of Biological Chemistry* **283**, 3972–3978.

Kleffmann, T., Hirsch-Hoffmann, M., Gruissem, W. and Baginsky, S. (2006). plprot: A comprehensive proteome database for different plastid types. *Plant and Cell Physiology* **47**, 432–436.

Kong, J., Gong, J. M., Zhang, Z. G., Zhang, J. S. and Chen, S. Y. (2003). A new AOX homologous gene *OsIM1* from rice (*Oryza sativa* L.) with an alternative splicing mechanism under salt stress. *Theoretical and Applied Genetics* **107**, 326–331.

Kramer, D., Johnson, G., Kiirats, O. and Edwards, G. (2004). New fluorescence parameters for the determination of Q_A redox state and excitation energy fluxes. *Photosynthesis Research* **79**, 209–218.

Krause, G. H. and Weis, E. (1991). Chlorophyll Fluorescence and Photosynthesis - The Basics. *Annual Review of Plant Physiology and Plant Molecular Biology* **42**, 313–349.

Kruk, J. and Strzalka, K. (2001). Redox changes of cytochrome b_{559} in the presence of plastoquinones. *Journal of Biological Chemistry* **276**, 86–91.

Kuntz, M. (2004). Plastid terminal oxidase and its biological significance. *Planta* **218**, 896–899.

Kuntz, M., Romer, S., Suire, C., Hugueney, P., Weil, J. H., Schantz, R. and Camara, B. (1992). Identification of a cDNA for the plastid-located geranylgeranyl pyrophosphate synthase from *Capsicum annuum*: correlative increase in enzyme activity and transcript level during fruit ripening. *The Plant Journal* **2**, 25–34. ISSN 0960-7412.

Lascano, H. R., Casano, L. M., Martin, M. and Sabater, B. (2003). The activity of the chloroplastic Ndh complex is regulated by phosphorylation of the NDH-F subunit. *Plant Physiology* **132**, 256–262.

Lennon, A. M., Prommeenate, P. and Nixon, P. J. (2003). Location, expression and orientation of the putative chlororespiratory enzymes, Ndh and *immutans*, in higher-plant plastids. *Planta* **218**, 254–260.

Li, X. P., Bjorkman, O., Shih, C., Grossman, A. R., Rosenquist, M., Jansson, S. and Niyogi, K. K. (2000). A pigment-binding protein essential for regulation of photosynthetic light harvesting. *Nature* **403**, 391–395.

Li, X. P., Muller-Moule, P., Gilmore, A. M. and Niyogi, K. K. (2002). PsbS-dependent enhancement of feedback de-excitation protects photosystem II from photoinhibition. *Proceedings of The National Academy of Sciences of The United States Of America* **99**, 15222–15227.

Lintala, M., Allahverdiyeva, Y., Kidron, H., Piippo, M., Battchikova, N., Suorsa, M., Rintamaki, E., Salminen, T. A., Aro, E. M. and Mulo, P. (2007). Structural and functional characterization of ferredoxin-$NADP^+$-oxidoreductase using knock-out mutants of *Arabidopsis*. *Plant Journal* **49**, 1041–1052.

Lowry, O., Rosebrough, N., Farr, A. and Randall, R. (1951). Protein measurement with the Folin-phenol reagent. *Journal of Biological Chemistry* **193**, 265–275.

Ma, Y. Z., Holt, N. E., Li, X. P., Niyogi, K. K. and Fleming, G. R. (2003). Evidence for direct carotenoid involvement in the regulation of photosynthetic light harvesting. *Proceedings of The National Academy of Sciences of The United States of America* **100**, 4377–4382.

Makino, A., Miyake, C. and Yokota, A. (2002). Physiological functions of the Water-Water Cycle (Mehler reaction) and the cyclic electron flow around PSI in rice leaves. *Plant and Cell physiology* **43**, 1017–1026.

Marin, E., Nussaume, L., Quesada, A., Gonneau, M., Sotta, B., Hugueney, P., Frey, A. and MarionPoll, A. (1996). Molecular identification of zeaxanthin epoxidase of *Nicotiana plumbaginifolia*, a gene involved in abscisic acid biosynthesis and corresponding to the ABA locus of *Arabidopsis thaliana*. *Embo Journal* **15**, 2331–2342.

Martin, M., Casano, L. M. and Sabater, B. (1996). Identification of the product of *ndha* gene as a thylakoid protein synthesized in response to photooxidative treatment. *Plant and Cell Physiology* **37**, 293–298.

Martin, M., Casano, L. M., Zapata, J. M., Guera, A., del Campo, E. M., Schmitz-Linneweber, C., Maier, R. M. and Sabater, B. (2004). Role of thylakoid Ndh complex and peroxidase in the protection against photo-oxidative stress: fluorescence and enzyme activities in wild-type and ndhF-deficient tobacco. *Physiologia Plantarum* **122**, 443–452.

Martin, W. and Herrmann, R. G. (1998). Gene transfer from organelles to the nucleus: How much, what happens, and why? *Plant Physiology* **118**, 9–17.

Martin, W., Rujan, T., Richly, E., Hansen, A., Cornelsen, S., Lins, T., Leister, D., Stoebe, B., Hasegawa, M. and Penny, D. (2002). Evolutionary analysis of *Arabidopsis*, cyanobacterial, and chloroplast genomes reveals plastid phylogeny and thousands of cyanobacterial genes in the nucleus. *Proceedings of The National Academy of Sciences of The United States of America* **99**, 12246–12251.

Maxwell, D. P., Nickels, R. and McIntosh, L. (2002). Evidence of mitochondrial involvement in the transduction of signals required for the induction of genes associated with pathogen attack and senescence. *Plant Journal* **29**, 269–279.

Maxwell, D. P., Wang, Y. and McIntosh, L. (1999). The alternative oxidase lowers mitochondrial reactive oxygen production in plant cells. *Proceedings of The National Academy of Sciences of The United States of America* **96**, 8271–8276.

Mayer, M. P., Beyer, P. and Kleinig, H. (1990). Quinone compounds are able to replace molecular oxygen as terminal electron acceptor in phytoene desaturation in chromoplasts of *Narcissus pseudonarcissus* L. *European Journal of Biochemistry* **191**, 359–363.

McDonald, A. E. and Vanlerberghe, G. C. (2006). Origins, evolutionary history, and taxonomic distribution of alternative oxidase and plastoquinol terminal oxidase. *Comparative Biochemistry and Physiology D-Genomics & Proteomics* **1**, 357–364.

Mehler, A. H. (1951). Studies on reactions of illuminated chloroplasts .1. mechanism of the reduction of oxygen and other Hill reagents. *Archives of Biochemistry and Biophysics* **33**, 65–77.

Meissner, R., Jacobson, Y., Melamed, S., Levyatuv, S., Ashri, G. S. A. and Levy, Y. E. A. (1997). A new model system for tomato genetics. *Plant Journal* **12**, 1465–1472.

Melis, A. (1999). Photosystem II damage and repair cycle in chloroplasts: what modulates the rate of photodamage *in vivo*? *Trends in Plant Science* **4**, 130–135.

Menz, R. I., Walker, J. E. and Leslie, A. G. W. (2001). Structure of bovine mitochondrial Fl-ATPase with nucleotide bound to all three catalytic sites: Implications for the mechanism of rotary catalysis. *Cell* **106**, 331–341.

Mitchell, P. (1975). Protonmotive Q-cycle - general formulation. *Febs Letters* **59**, 137–139.

Miyake, C., Horiguchi, S., Makino, A., Shinzaki, Y., Yamamoto, H. and Tomizawa, K. (2005). Effects of light intensity on cyclic electron flow around PSI and its relationship to non-photochemical quenching of Chl fluorescence in tobacco leaves. *Plant and Cell Physiology* **46**, 1819–1830.

Moore, A. L., Albury, M. S., Crichton, P. G. and Affourtit, C. (2002). Function of the alternative oxidase: is it still a scavenger? *Trends in Plant Science* **7**, 478–481.

Morita, M. T. and Tasaka, M. (2004). Gravity sensing and signaling. *Current Opinion in Plant Biology* **7**, 712–718.

Morstadt, L., Graber, P., De Pascalis, L., Kleinig, H., Speth, V. and Beyer, P. (2002). Chemiosmotic ATP synthesis in photosynthetically inactive chromoplasts from *Narcissus pseudonarcissus* L. linked to a redox pathway potentially also involved in carotene desaturation. *Planta* **215**, 134–140.

Mubarakshina, M., Khorobrykh, S. and Ivanov, B. (2006). Oxygen reduction in chloroplast thylakoids results in production of hydrogen peroxide inside the membrane. *Biochimica et Biophysica Acta* **1757**, 1496–1503.

Muller, P., Li, X. P. and Niyogi, K. K. (2001). Non-photochemical quenching. A response to excess light energy. *Plant Physiology* **125**, 1558–1566.

Mullineaux, P., Ball, L., Escobar, C., Karpinska, B., Creissen, G. and Karpinski, S. (2000). Are diverse signalling pathways integrated in the regulation of *Arabidopsis* antioxidant defence gene expression in response to excess excitation energy? *Philosophical Transactions Of The Royal Society Of London Series B-Biological Sciences* **355**, 1531–1540.

Munekage, Y., Hashimoto, M., Miyake, C., Tomizawa, K., Endo, T., Tasaka, M. and Shikanai, T. (2004). Cyclic electron flow around photosystem I is essential for photosynthesis. *Nature* **429**, 579–582.

Munekage, Y., Hojo, M., Meurer, J., Endo, T., Tasaka, M. and Shikanai, T. (2002). PGR5 is involved in cyclic electron flow around photosystem I and is essential for photoprotection in *Arabidopsis*. *Cell* **110**, 361–371.

Nievelstein, V., Vandekerchove, J., Tadros, M. H., Lintig, J. V., Nitschke, W. and Beyer, P. (1995). Carotene desaturation is linked to a respiratory redox pathway in *Narcissus pseudonarcissus* chromoplast membranes. involvement of a 23-kDa oxygen-evolving-complex-like protein. *European Journal of Biochemistry* **233**, 864–72.

Niyogi, K. K. (1999). Photoprotection revisited: Genetic and molecular approaches. *Annual Review of Plant Physiology and Plant Molecular Biology* **50**, 333–359.

Niyogi, K. K. (2000). Safety valves for photosynthesis. *Current Opinion in Plant Biology* **3**, 455.

Norris, S. R., Barrette, T. R. and DellaPenna, D. (1995). Genetic dissection of carotenoid synthesis in *Arabidopsis* defines plastoquinone as an essential component of phytoene desaturation. *Plant Cell* **7**, 2139–2149.

Ogawa, T. (1991). A gene homologous to the subunit-2 gene of NADH dehydrogenase is essential to inorganic carbon transport of synechocystis Pcc6803. *Proceedings of The National Academy of Sciences of The United States of America* **88**, 4275–4279.

Ogren, E. (1991). Prediction of photoinhibition of photosynthesis from measurements of fluorescence quenching components. *Planta* **184**, 538–544.

Ogren, W. L. (2003). Affixing the O to Rubisco: discovering the source of photorespiratory glycolate and its regulation. *Photosynthesis Research* **76**, 53–63.

Okutani, S., Hanke, G. T., Satomi, Y., Takao, T., Kurisu, G., Suzuki, A. and Hase, T. (2005). Three maize leaf ferredoxin: NADPH oxidoreductases vary in subchloroplast location, expression, and interaction with ferredoxin. *Plant Physiology* **139**, 1451–1459.

Olsson, M., Nilsson, K., Liljenberg, C. and Hendry, G. A. F. (1996). Drought stress in seedlings: Lipid metabolism and lipid peroxidation during recovery from drought in *Lotus corniculatus* and *Cerastium fontanum*. *Physiologia Plantarum* **96**, 577–584.

Ort, D. R. and Baker, N. R. (2002). A photoprotective role for O_2 as an alternative electron sink in photosynthesis? *Current Opinion in Plant Biology* **5**, 193–198.

Peltier, G. and Cournac, L. (2002). Chlororespiration. *Annual Review of Plant Biology* **53**, 523–550.

Peltier, J. B., Emanuelsson, O., Kalume, D. E., Ytterberg, J., Friso, G., Rudella, A., Liberles, D. A., Soderberg, L., Roepstorff, P., von Heijne, G. and van Wijk, K. J. (2002). Central functions of the lumenal and peripheral thylakoid proteome of *Arabidopsis* determined by experimentation and genome-wide prediction. *Plant Cell* **14**, 211–236.

Polivka, T., Herek, J. L., Zigmantas, D., Akerlund, H. E. and Sundstrom, V. (1999). Direct observation of the (forbidden) S-1 state in carotenoids. *Proceedings of The National Academy of Sciences of The United States of America* **96**, 4914–4917.

Polivka, T., Zigmantas, D., Sundstrom, V., Formaggio, E., Cinque, G. and Bassi, R. (2002). Carotenoid S-1 state in a recombinant light-harvesting complex of photosystem II. *Biochemistry* **41**, 439–450.

Quiles, M. J. (2006). Stimulation of chlororespiration by heat and high light intensity in oat plants. *Plant Cell and Environment* **29**, 1463–70.

Rédei, G. P. (1975). *Arabidopsis* as a genetic tool. *Annual Review of Genetics* **9**, 111–127.

Reinbothe, C., Lebedev, N. and Reinbothe, S. (1999). A protochlorophyllide light-harvesting complex involved in de-etiolation of higher plants. *Nature* **397**, 80–84.

Renger, G. and Kuhn, P. (2007). Reaction pattern and mechanism of light induced oxidative water splitting in photosynthesis. *Biochimica et Biophysica Acta-Bioenergetics* **1767**, 458–471.

Reyes-Prieto, A., Weber, A. P. M. and Bhattacharya, D. (2007). The origin and establishment of the plastid in algae and plants. *Annual Review of Genetics* **41**, 147–168.

Richter, C. and Schweitzer, M. (1997). *Oxidative stress in mitochondria. In CSHL Press, ed, Oxidative stress and the molecular biology of antioxydant defenses*. Rissler JF, Millar.

Rizhsky, L., Hallak-Herr, E., Van Breusegem, F., Rachmilevitch, S., Barr, J. E., Rodermel, S., Inze, D. and Mittler, R. (2002). Double antisense plants lacking ascorbate peroxidase and catalase are less sensitive to oxidative stress than single antisense plants lacking ascorbate peroxidase or catalase. *Plant Journal* **32**, 329–342.

Rochaix, J. D. (2007). Role of thylakoid protein kinases in photosynthetic acclimation. *Febs Letters* **581**, 2768–2775.

Rodermel, S. (2001). Pathways of plastid-to-nucleus signaling. *Trends in Plant Science* **6**, 471–8.

Rodermel, S. (2002). *The Arabidopsis Book*, chapter *Arabidopsis* variegation mutants. American Society of Plant Biologists, Rockville, MD, pages 1–28.

Rodriguez, R. E., Lodeyro, A., Poli, H. O., Zurbriggen, M., Peisker, M., Palatnik, J. F., Tognetti, V. B., Tschiersch, H., Hajirezaei, M. R., Valle, E. M. and Carrillo, N. (2007). Transgenic tobacco plants overexpressing chloroplastic ferredoxin-NADP(H) reductase display normal rates of photosynthesis and increased tolerance to oxidative stress. *Plant Physiology* **143**, 639–649.

Rodriguez-Concepcion, M. and Boronat, A. (2002). Elucidation of the methylerythritol phosphate pathway for isoprenoid biosynthesis in bacteria and plastids. a metabolic milestone achieved through genomics. *Plant Physiology* **130**, 1079–1089.

Rohmer, M., Seemann, M., Horbach, S., BringerMeyer, S. and Sahm, H. (1996). Glyceraldehyde 3-phosphate and pyruvate as precursors of isoprenic units in an alternative non-mevalonate pathway for terpenoid biosynthesis. *Journal of The American Chemical Society* **118**, 2564–2566.

Romer, S., Hugueney, P., Bouvier, F., Camara, B. and Kuntz, M. (1993). Expression of the genes encoding the early carotenoid biosynthetic enzymes in *Capsicum annuum*. *Biochemical and Biophysical Research Communications* **196**, 1414–1421.

Ronen, G., Cohen, M., Zamir, D. and Hirschberg, J. (1999). Regulation of carotenoid biosynthesis during tomato fruit development: Expression of the gene for lycopene epsilon-cyclase is down-regulated during ripening and is elevated in the mutant delta. *Plant Journal* **17**, 341–351.

Rosso, D., Ivanov, A. G., Fu, A., Geisler-Lee, J., Hendrickson, L., Geisler, M., Stewart, G., Krol, M., Hurry, V., Rodermel, S. R., Maxwell, D. P. and Huner, N. P. (2006). *immutans* does not act as a stress-induced safety valve in the protection of the photosynthetic apparatus of *Arabidopsis* during steady-state photosynthesis. *Plant Physiology* **142**, 574–85.

Rumeau, D., Becuwe-Linka, N., Beyly, A., Louwagie, M., Garin, J. and Peltier, G. (2005). New subunits NDH-M, -N, and -O, encoded by nuclear genes, are essential for plastid NDH complex functioning in higher plants. *Plant Cell* **17**, 219–232.

Rumeau, D., Peltier, G. and Cournac, L. (2007). Chlororespiration and cyclic electron flow around PSI during photosynthesis and plant stress response. *Plant Cell and Environment* **30**, 1041–1051.

Sairam, R. K. and Srivastava, G. C. (2001). Water stress tolerance of wheat (*Triticum aestivum* L.): Variations in hydrogen peroxide accumulation and antioxidant activity in tolerant and susceptible genotypes. *Journal of Agronomy and Crop Science* **186**, 63–70.

Sakamoto, W., Tamura, T., Hanba-Tomita, Y. and Murata, M. (2002). The *var1* locus of *Arabidopsis* encodes a chloroplastic *FtsH* and is responsible for leaf variegation in the mutant alleles. *Genes To Cells* **7**, 769–780.

Sambrook, J., Fritsch, E. and Maniatis, T. (1989). *Molecular cloning: A laboratory manual*.

Sandmann, G. (1994). Carotenoid biosynthesis in microorganisms and plants. *European Journal Of Biochemistry* **223**, 7–24.

Sazanov, L. A., Burrows, P. A. and Nixon, P. J. (1998a). The chloroplast NDH complex mediates the dark reduction of the plastoquinone pool in response to heat stress in tobacco leaves. *FEBS letters* **429**, 115–118.

Sazanov, L. A., Burrows, P. A. and Nixon, P. J. (1998b). The plastid ndh genes code for an NADH-specific dehydrogenase: isolation of a complex I analogue from pea thylakoid membranes. *Proceedings of The National Academy of Sciences of The United States of America* **95**, 1319–24.

Sazanov, L. A. and Jackson, J. B. (1995). Cyclic-reactions catalyzed by detergent-dispersed and reconstituted transhydrogenase from beef-heart mitochondria - implications for the mechanism of proton translocation. *Biochimica et Biophysica Acta-Bioenergetics* **1231**, 304–312.

Schmitz-Linneweber, C., Maier, R., Alcaraz, J., Cottet, A., Herrmann, R. and Mache, R. (2001). The plastid chromosome of spinach (*Spinacia oleracea*: complete nucleotide sequence and gene organization. *Plant Molelecular Biology* **45**, 307–315.

Schneider, C., Boger, P. and Sandmann, G. (1997). Phytoene desaturase: Heterologous expression in an active state, purification, and biochemical properties. *Protein Expression and Purification* **10**, 175–179.

Schreiber, U. (2004). Pulse-amplitude-modulation (PAM) fluorometry and saturation pulse method: An overview. *Chlorophyll A Fluoerescence: Signature of Photosynthesis* **19**, 279–319.

Schreiber, U. and Armond, P. A. (1978). Heat-induced changes of chlorophyll fluorescence in isolated-chloroplasts and related heat-damage at pigment level. *Biochimica et Biophysica Acta* **502**, 138–151.

Schreiber, U. and Berry, J. A. (1977). Heat-induced changes of chlorophyll fluorescence in intact leaves correlated with damage of photosynthetic apparatus. *Planta* **136**, 233–238.

Schreiber, U., Muller, J. F., Haugg, A. and Gademann, R. (2002). New type of dual-channel PAM chlorophyll fluorometer for highly sensitive water toxicity biotests. *Photosynthesis Research* **74**, 317–330.

Schreiber, U., Neubauer, C. and Klughammer, C. (1989). Devices and methods for room-temperature fluorescence analysis. *Philosophical Transactions of the Royal Society of London Series B-Biological Sciences* **323**, 241–251.

Serrani, J., Fos, M., Atarés, A. and Garcia-Martinez, J. (2007). Effect of gibberllin and auxin on parthenocarpic fruit growth induction in the cv micro-tom of tomato. *Journal of Plant Growth Regulation* **26**, 211–221.

Shikanai, T. (2007). Cyclic electron transport around photosystem I: genetic approaches. *Annual Review of Plant Biology* **58**, 199–217.

Shikanai, T., Endo, T., Hashimoto, T., Yamada, Y., Asada, K. and Yokota, A. (1998). Directed disruption of the tobacco *ndhB* gene impairs cyclic electron flow around photosystem I. *Proceedings of The National Academy of Sciences of The United States of America* **95**, 9705–9709.

Shikanai, T., Munekage, Y., Shimizu, K., Endo, T. and Hashimoto, T. (1999). Identification and characterization of *Arabidopsis* mutants with reduced quenching of chlorophyll fluorescence. *Plant and Cell Physiology* **40**, 1134–1142.

Simkin, A. J. (2002). *Etude de l'expression des gènes de la biosynthèse des caroténoïdes et de la surexpression hétérologue d'une protéine de structure chez la tomate*. Ph.D. thesis, Laboratoire Plastes et Différenciation Cellulaire; Université Joseph Fourier; Grenoble.

Simkin, A. J., Gaffe, J., Alcaraz, J. P., Carde, J. P., Bramley, P. M., Fraser, P. D. and Kuntz, M. (2007). Fibrillin influence on plastid ultrastructure and pigment content in tomato fruit. *Phytochemistry* **68**, 1545–1556.

Simkin, A. J., Laboure, A. M., Kuntz, M. and Sandmann, G. (2003). Comparison of carotenoid content, gene expression and enzyme levels in tomato (*Lycopersicon esculentum*) leaves. *Verlag der Zeitschrift für Naturforschung* **58**, 371–380.

Simons, B. H., Millenaar, F. F., Mulder, L., Van Loon, L. C. and Lambers, H. (1999). Enhanced expression and activation of the alternative oxidase during infection of *Arabidopsis* with *Pseudomonas syringae* pv tomato. *Plant Physiology* **120**, 529–538.

Snyders, S. and Kohorn, B. D. (2001). Disruption of thylakoid-associated kinase 1 leads to alteration of light harvesting in *Arabidopsis*. *Journal of Biological Chemistry* **276**, 32169–32176.

Sonoike, K. (1996). Photoinhihition of photosystem I: Its physiological significance in the chilling sensitivity of plants. *Plant and Cell Physiology* **37**, 239–247.

Strasser, R. J., Srivastava, A. and Govindjee (1995). Polyphasic chlorophyll-*a* fluorescence transient in plants and cyanobacteria. *Photochemistry and Photobiology* **61**, 32–42.

Strasser, R. J., Tsimilli-Michael, M. and Srivastava, A. (2004). Analysis of the chlorophyll *a* fluorescence transient. *Chlorophyll a Fluoerescence: Signature of Photosynthesis* **19**, 321–362.

Streb, P., Josse, E. M., Gallouet, E., Baptist, F., Kuntz, M. and Cornic, G. (2005). Evidence for alternative electron sinks to photosynthetic carbon assimilation in the high mountain plant speciesranunculus glacialis. *Plant Cell and Environment* **28**, 1123–1135. ISSN 0140-7791.

Su, J. H. and Shen, Y. K. (2005). Influence of state-2 transition on the proton motive force across the thylakoid membrane in spinach chloroplasts. *Photosynthesis Research* **85**, 235–245.

Szabo, I., Bergantino, E. and Giacometti, G. M. (2005). Light and oxygenic photosynthesis: energy dissipation as a protection mechanism against photo-oxidation. *Embo Reports* **6**, 629–634.

Takabayashi, A., Kishine, M., Asada, K., Endo, T. and Sato, F. (2005). Differential use of two cyclic electron flows around photosystem I for driving CO_2-concentration mechanism in C-4 photosynthesis. *Proceedings of The National Academy of Sciences of The United States of America* **102**, 16898–16903.

Thomson, W. W. and Whatley, J. M. (1980). Development of Non-green plastids. *Annual Review of Plant Physiology and Plant Molecular Biology* **31**, 375–394.

Toth, S. Z., Schansker, G. and Strasser, R. J. (2007). A non-invasive assay of the plastoquinone pool redox state based on the OJIP-transient. *Photosynthesis Research* **93**, 193–203.

Tyystjarvi, E. (2008). Photoinhibition of photosystem II and photodamage of the oxygen evolving manganese cluster. *Coordination Chemistry Reviews* **252**, 361–376.

Vanlerberghe, G. C. and McIntosh, L. (1997). Alternative oxidase: From gene to function. *Annual Review of Plant Physiology and Plant Molecular Biology* **48**, 703–734.

Vasil'ev, S., Orth, P., Zouni, A., Owens, T. G. and Bruce, D. (2001). Excited-state dynamics in photosystem II: Insights from the X-ray crystal structure. *Proceedings of The National Academy of Sciences of The United States of America* **98**, 8602–8607.

Vavilin, D. V. and Ducruet, J. M. (1998). The origin of 115-130 degrees C thermoluminescence bands in chlorophyll-containing material. *Photochemistry and Photobiology* **68**, 191–198.

Vavilin, D. V., Ducruet, J. M., Matorin, D. N., Venediktov, P. S. and Rubin, A. B. (1998). Membrane lipid peroxidation, cell viability and photosystem II activity in the green alga *Chlorella pyrenoidosa* subjected to various stress conditions. *Journal of Photochemistry and Photobiology B-Biology* **42**, 233–239.

Verhoeven, A. S., Adams, W. W. and DemmigAdams, B. (1996). Close relationship between the state of the xanthophyll cycle pigments and photosystem II efficiency during recovery from winter stress. *Physiologia Plantarum* **96**, 567–576.

Vink, M., Zer, H., Alumot, N., Gaathon, A., Niyogi, K., Herrmann, R. G., Andersson, B. and Ohad, I. (2004). Light-modulated exposure of the light-harvesting complex II (LHCII) to protein kinase(s) and state transition in *Chlamydomonas reinhardtii* xanthophyll mutants. *Biochemistry* **43**, 7824–7833.

Vothknecht, U. C. and Westhoff, P. (2001). Biogenesis and origin of thylakoid membranes. *Biochimica et Biophysica Acta-Molecular Cell Research* **1541**, 91–101.

Wang, N., Fang, W., Han, H., Sui, N., Li, B. and Meng, Q. W. (2008). Overexpression of zeaxanthin epoxidase gene enhances the sensitivity of tomato PSII photoinhibition to high light and chilling stress. *Physiologia Plantarum* **132**, 384–396.

Wang, P., Duan, W., Takabayashi, A., Endo, T., Shikanai, T., Ye, J. Y. and Mi, H. (2006). Chloroplastic NAD(P)H dehydrogenase in tobacco leaves functions in alleviation of oxidative damage caused by temperature stress. *Plant Physiology* **141**, 465–74.

Weis, E. (1984). Short-term acclimation of spinach to high-temperatures - effect on chlorophyll fluorescence at 293 and 77 Kelvin in intact leaves. *Plant Physiology* **74**, 402–407.

Wen, X. G., Gong, H. M. and Lu, C. M. (2005). Heat stress induces a reversible inhibition of electron transport at the acceptor side of photosystem II in a cyanobacterium *Spirulina platensis*. *Plant Science* **168**, 1471–1476.

Wetzel, C. M., Jiang, C. Z., Meehan, L. J., Voytas, D. F. and Rodermel, S. R. (1994). Nuclear-organelle interactions: the *immutans* variegation mutant of *Arabidopsis* is plastid autonomous and impaired in carotenoid biosynthesis. *Plant Journal* **6**, 161–75.

Wu, D., Wetzel, C., Rodermel, S. R., Wright, D. A. and Voytas, D. F. (1999a). Carotenoid biosynthesis: Positional cloning and expression of the *immutans* variegation locus of *Arabidopsis thaliana*. *Plant Biology (Rockville)* **1999**, 138.

Wu, D. Y., Wright, D. A., Wetzel, C., Voytas, D. F. and Rodermel, S. (1999b). The *immutans* variegation locus of *Arabidopsis* defines a mitochondrial alternative oxidase homolog that functions during early chloroplast biogenesis. *The Plant Cell* **11**, 43–55.

Wu, M., Nie, Z. Q. and Yang, J. (1989). The 18-kD protein that binds to the chloroplast DNA replicative origin is an iron-sulfur protein related to a subunit of NADH dehydrogenase. *The Plant Cell* **1**, 551–557.

Xu, D. Q. and Wu, S. (1996). Three phases of dark-recovery course from photoinhibition resolved by the chlorophyll fluorescence analysis in soybean leaves under field conditions. *Photosynthetica* **32**, 417–423.

Yamamoto, H., Kato, H., Shinzaki, Y., Horiguchi, S., Shikanai, T., Hase, T., Endo, T., Nishioka, M., Makino, A., Tomizawa, K. and Miyake, C. (2006). Ferredoxin limits cyclic electron flow around PSI (CEF-PSI) in higher plants-stimulation of CEF-PSI enhances non-photochemical quenching of Chl fluorescence in transplastomic tobacco. *Plant and Cell Physiology* **47**, 1355–1371.

Yamamoto, T., Michihiro, T., Yamakishi, S., Kato, F. and Koyama, Y. (1979). A study on plasmid participating in synthesis of light induced carotenoid. *Japanese Journal of Bacteriology* **34**, 146.

Yamane, Y., Kashino, Y., Koike, H. and Satoh, K. (1998). Effects of high temperatures on the photosynthetic systems in spinach: Oxygen-evolving activities, fluorescence characteristics and the denaturation process. *Photosynthesis Research* **57**, 51–59.

Yamane, Y., Shikanai, T., Kashino, Y., Koike, H. and Satoh, K. (2000). Reduction of Q_A in the dark: Another cause of fluorescence F_0 increases by high temperatures in higher plants. *Photosynthesis Research* **63**, 23–34.

Yoshida, K., Terashima, I. and Noguchi, K. (2006). Distinct roles of the cytochrome pathway and alternative oxidase in leaf photosynthesis. *Plant and Cell Physiology* **47**, 22–31.

Yu, F., Fu, A. G., Aluru, M., Park, S., Xu, Y., Liu, H. Y., Liu, X. Y., Foudree, A., Nambogga, M. and Rodermel, S. (2007). Variegation mutants and mechanisms of chloroplast biogenesis. *Plant Cell and Environment* **30**, 350–365.

Zhang, H. M., Whitelegge, J. P. and Cramer, W. A. (2001). Ferredoxin : $NADP^+$ oxidoreductase is a subunit of the chloroplast cytochrome b_6f complex. *Journal of Biological Chemistry* **276**, 38159–38165.

Zhang, S. P. and Scheller, H. V. (2004). Light-harvesting complex II binds to several small subunits of photosystem I. *Journal of Biological Chemistry* **279**, 3180–3187.

Zhu, X. G., Govindjee, Baker, N. R., deSturler, E., Ort, D. R. and Long, S. P. (2005). Chlorophyll *a* fluorescence induction kinetics in leaves predicted from a model describing each discrete step of excitation energy and electron transfer associated with photosystem II. *Planta* **223**, 114–133.

Zito, F., Finazzi, G., Delosme, R., Nitschke, W., Picot, D. and Wollman, F. A. (1999). The Q_o site of cytochrome b_6f complexes controls the activation of the LHCII kinase. *Embo Journal* **18**, 2961–2969.

Appendix A

A.1 Herbicide List

TABLE A.1 – List of bleaching herbicides from Syngentha

Code	Name	Mode of action	Chemical Formula
A	norflurazon	PDS-inhibitor	$C_{12}O_1N_3F_3ClH_9$
B	KPP-297	PDS-inhibitor	$C_{15}O_3N_3F_4H_{14}$
C	CSAA468316	HPPD-inhibitor[a]	$C_{19}O_6SH_2$
D	CSAA468316	PDS-inhibitor (?)	$C_{16}O_2N_3ClFH_{11}$
E	CSCC223272	PROTOX-inhibitor[b]	$C_{13}ON_4F_3ClH_{11}$
F	CSCC214945	PDS-inhibitor	$C_{18}O_2N_2Cl_2H_{11}$
G	diflufenican	PDS-inhibitor	$C_{18}O_2N_2F_5H_{11}$
H	CSAA632149	PDS-inhibitor	$C_{20}O_2N_4H_{28}$
I	dichlormate	ZDS-inhibitor	$C_9O_2NCl_5H_9$

a. The p-hydroxyphenylpyruvate dioxygenase (HPPD)-inhibiting herbicides block the formation of homogentisic acid, the aromatic precursor of plastoquinone and vitamin E.
b. Protoporphyrinogen Oxidase (Protox)-inhibiting herbicides block chlorophyll biosynthesis.

A.2 Primer list

TABLE A.2 – Primer list

Oligo Name	Sequence (5′ to 3′ end)	Utilization
Act-1 (5′)	TGGCATCATACTTTCTACAATG	RT-PCR
Act-1 (3′)	CTAATATCCACGTCACATTTCAT	RT-PCR
Apx-2 (5′)	CGGGAGGACCTGATGTTC	RT-PCR
Apx-2 (3′)	ACAATTCCAGCAAGCTTTTC	RT-PCR
Elip (5′)	CCTAGCTGTTACTTGCCACGC	RT-PCR
Elip (3′)	CCAGATCTCAGCATCAGCAGTC	RT-PCR
TIM-3 (5′)	GTATTCATGAACATTAGAGATGACG	RT-PCR
TIM-4 (3′)	GTATATACAAGTATAGTTTGTCCGC	RT-PCR
IMM-2 (5′)	CGGATCCGCAACGATTTTGCAAGACG	cDNA *im* of At
IMM-3 (3′)	GCGCTGCAGTTAACTTGTAATGGATTTCTTGAG	cDNA *im* of At
PDS-1 (5′)	TTTGCGCCTGCAGAAGAGTGG	Identification
PDS-2 (3′)	ATGCTATACTTCAACAAGTCATCCTTTT	Identification
PTOX (5′)	CCGCTCGAGCCTGACGGAGATGGCGGCGATTTCAGG	cDNA construction
PTOX (3′)	CCCGAGCTCTTATTAACTTGTAATGGATTTCTTGAGGC	cDNA construction

A.3 Experiments involving chemical inhibitors

This annex presents the outcome of some experiments performed in parallel to those using the available PTOX knock-out mutant from tomato (*ghost*) and the PTOX over-expressing line. Specific and potent inhibitors of PTOX would allow local inactivation of PTOX and in a timely controlled manner. In addition, herbicides potentially inhibiting the alternative (PTOX-independent) cofactor of carotenoid desaturation (Carol and Kuntz, 2001, see chapter 3.1) would be valuable tools since mutants impaired in such an alternative cofactor are not available. Also, it is not formally known whether inhibitors of PDS would also inhibit PTOX or another cofactor.

A.3.1 Octyl-gallate (OG) as an *in vivo* inhibitor of PTOX

Tomato fruit explants at 2 days post-breaker stage were used as in chapter 3.1. n-octyl-gallate (OG) is an esterified gallic acid derivative with a long-chain acyl group and was reported as a strong inhibitor for PTOX activity *in vitro* assay (100% at 5 μM, Josse, 2003). As shown in figure A.1a, the positive control treatment with norflurazon (NF), a well known PDS inhibitor, added as 60 μl of a 10 μM of stock solution, readily inhibits carotenoid biosynthesis during 3 days under dim light, when compared to the negative control treatment with 1% DMSO. Evidently, OG (60 μl from a 300 μM stock solution) appears far less efficient. Pigment analysis by HPLC showed that after 20h incubation phytoene accumulation is 5 fold higher in NF-treated samples compared with those treated by OG (data not shown).

In conclusion, OG is not a good *in vivo* inhibitor for PTOX. This conclusion is confirmed by the lack of influence of OG treatment on F_0 level in contrast to what was observed for the PTOX deficient mutant in chapter 3.2 (data not shown).

A.3.2 Bleaching herbicides as potential PTOX inhibitor

Experimental or known herbicides (provided by Syngenta and listed in appendix A.1) were added (from a 250 μM stock solution) to tomato fruit explants at the mature green stage, which were then incubated for 3 days to verify the inhibitory activity on carotenoid biosynthesis (Fig. A.1b).

To determine their inhibitory activity on phytoene desaturase, these herbicides were added to cultures of a recombinant *E. coli* strain expressing a eucaryotic phytoene desaturase type (PDS) and producing ζ-carotene (*cf.* Materials and Methods § 2.2.3, according to Schneider *et al.*, 1997). Accumulation of phytoene was monitored by HPLC (not shown).

To examine the potential inhibitory effect of these compounds on PTOX, typical assays for oxygen consumption in *E. coli* membranes containing the *Arabidopsis* PTOX protein (adapted from Josse, 2003) were performed in the presence of these herbicides (*cf.* Materials and Methods § 2.12.1). As shown in figure A.2a, for certain herbicides, namely D, E, F and diflufeni-

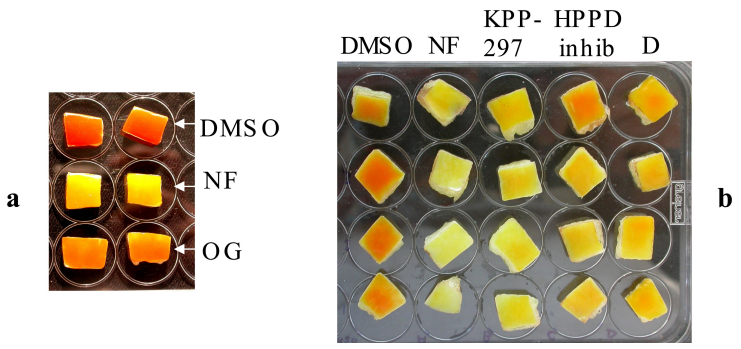

FIGURE A.1 – **The effects of inhibitors on the carotenoid biosynthesis of tomato fruits from SM plants. a. The fruit explants from fruit at 2 DPB were treated with NF (10 μM), OG (300 μM) and DMSO (1%) as a solvent control during 3 days under low light. b. The fruit explants from fruit at mature green stage were treated with 250 μM of NF, KPP-297, HPPD-inhibitor, D and DMSO (1%) as a solvent control during 3 days under low light.**

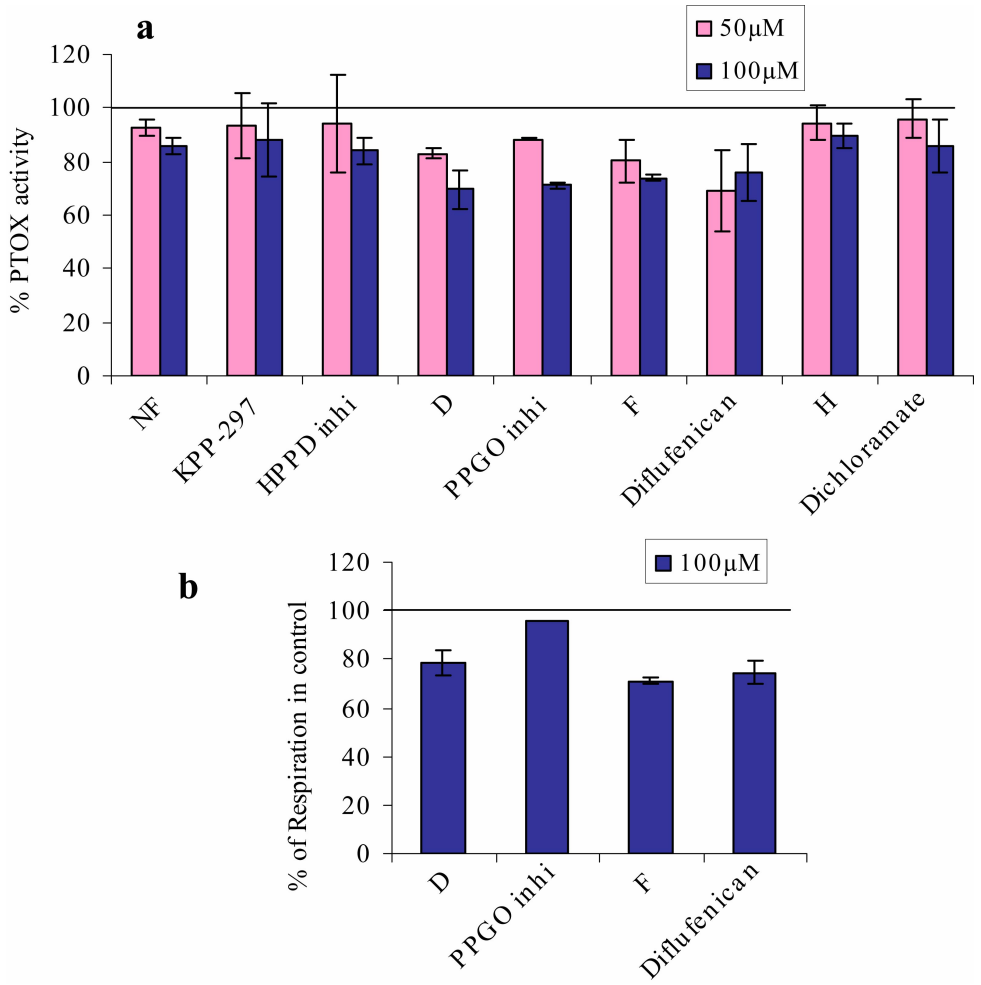

FIGURE A.2 – **The effects of the bleaching herbicides on PTOX activity. a. *In vitro* assay for oxygen consumption in *E. coli* membranes containing the At-PTOX protein in the presence of herbicides (50 and 100 μM). b. Influence of different herbicides (100 μM) on the oxygen consumption in isolated *E. coli* membranes control (with plasmid but without PTOX, *cf.* Materials and Methods § 2.2.1)**

can, respiration rate were reduced to less than 70-80% of the level of non-treated membranes. However, the oxygen consumption rate of *E. coli* control membranes (without PDS) decreased almost in the same range (Fig. A.2b).

In conclusion, none of the tested compounds inhibits PTOX. It appears that experimental herbicides selected on their likely ability to inhibit carotenoid desaturation target preferentially PDS. It seems unlikely that inhibitors for the alternative cofactor for PDS can be identified by this approach.

Appendix B

Publication

Dual Role of the Plastid Terminal Oxidase in Tomato

Maryam Shahbazi, Matthias Gilbert, Anne-Marie Labouré, and Marcel Kuntz*

Centre National de la Recherche Scientifique and Université Joseph Fourier, Laboratory Plastes et Différenciation Cellulaire, 38041 Grenoble, France (M.S., A.-M.L., M.K.); and Institut für Biologie I, Pflanzenphysiologie, Universität Leipzig, D–04103 Leipzig, Germany (M.G.)

The plastid terminal oxidase (PTOX) is a plastoquinol oxidase whose absence in tomato (*Solanum lycopersicum*) results in the *ghost* (*gh*) phenotype characterized by variegated leaves (with green and bleached sectors) and by carotenoid-deficient ripe fruit. We show that PTOX deficiency leads to photobleaching in cotyledons exposed to high light primarily as a consequence of reduced ability to synthesize carotenoids in the *gh* mutant, which is consistent with the known role of PTOX as a phytoene desaturase cofactor. In contrast, when entirely green adult leaves from *gh* were produced and submitted to photobleaching high light conditions, no evidence for a deficiency in carotenoid biosynthesis was obtained. Rather, consistent evidence indicates that the absence of PTOX renders the tomato leaf photosynthetic apparatus more sensitive to light via a disturbance of the plastoquinone redox status. Although *gh* fruit are normally bleached (most likely as a consequence of a deficiency in carotenoid biosynthesis at an early developmental stage), green adult fruit could be obtained and submitted to photobleaching high light conditions. Again, our data suggest a role of PTOX in the regulation of photosynthetic electron transport in adult green fruit, rather than a role principally devoted to carotenoid biosynthesis. In contrast, ripening fruit are primarily dependent on PTOX and on plastid integrity for carotenoid desaturation. In summary, our data show a dual role for PTOX. Its activity is necessary for efficient carotenoid desaturation in some organs at some developmental stages, but not all, suggesting the existence of a PTOX-independent pathway for plastoquinol reoxidation in association with phytoene desaturase. As a second role, PTOX is implicated in a chlororespiratory mechanism in green tissues.

The plastid terminal oxidase (PTOX) is a nucleus-encoded plastid-located plastoquinone (PQ)-O_2 oxidoreductase (plastoquinol oxidase) whose absence gives rise to the *immutans* phenotype in Arabidopsis (*Arabidopsis thaliana*) and in the *ghost* (*gh*) phenotype in tomato (*Solanum lycopersicum*; Carol et al., 1999; Wu et al., 1999; Josse et al., 2000; Carol and Kuntz, 2001; Rodermel, 2001; Aluru et al., 2006). These phenotypes are characterized by variegated leaves consisting of green and bleached sectors and, in addition in tomato, by a yellow-orangey ripe fruit. The latter is characterized by reduced carotenoid content (Barr et al., 2004). In addition, bleached leaf sectors accumulate the carotenoid precursor phytoene, indicating that PTOX functions as a cofactor for the carotenoid dehydrogenases, namely, phytoene desaturase (PDS) and, most likely, ζ-carotene desaturase (ZDS). These conclusions are consistent with the known involvement of quinone as a cofactor for PDS (Mayer et al., 1990; Norris et al., 1995). PDS and ZDS sequentially catalyze the conversion of the colorless phytoene to lycopene (the main pigment in red tomato fruit), which, in turn, is converted to various photoprotective carotenoids. Thus, the phenotype observed in the absence of PTOX can be explained by reduced ability to synthesize carotenoids leading to photobleaching of green tissues.

PTOX shares sequence similarity with the alternative oxidase found in mitochondria of a number of species (Berthold and Stenmark, 2003). In the presence of plastoquinol, PTOX is able to divert the electron flow to O_2 in *Escherichia coli* membranes when the cytochrome path is inhibited by cyanide (Josse et al., 2003). PTOX behaves as an intrinsic membrane protein in the thylakoid lamellae (Lennon et al., 2003). Thus, PTOX possesses all the characteristics expected for a terminal oxidase involved in chlororespiration (Peltier and Cournac, 2002; Kuntz, 2004). Such a role for PTOX is not incompatible with a role in carotenoid desaturation because the latter process is dependent on a redox pathway (Morstadt et al., 2002). Evidence was obtained that seems to confirm a chlororespiratory role for PTOX in algae (Cournac et al., 2000, 2002) and in tobacco (*Nicotiana tabacum*) overexpressing a PTOX gene (Joet et al., 2002). Furthermore, data indicate induction of the PTOX gene and/or an accumulation of the protein under stress conditions in tobacco lacking both ascorbate peroxidase and catalase (Rizhsky et al., 2002) or deficient in PSII (Baena-Gonzalez et al., 2003). Strikingly, the high mountain plant *Ranunculus glacialis*, which has been shown to contain alternative sinks to dissipate photosynthetic electrons, was also found to contain high levels of PTOX (Streb et al., 2005). In contrast, using Arabidopsis lines either deficient in or overexpressing PTOX, Rosso et al. (2006) concluded that this enzyme does not act as a stress-induced safety valve involved in the protection of the photosynthetic

* Corresponding author; e-mail marcel.kuntz@ujf-grenoble.fr.

The author responsible for distribution of materials integral to the findings presented in this article in accordance with the policy described in the Instructions for Authors (www.plantphysiol.org) is: Marcel Kuntz (marcel.kuntz@ujf-grenoble.fr).

www.plantphysiol.org/cgi/doi/10.1104/pp.107.106336

apparatus. These authors stressed that high PTOX levels may simply be correlative and not indicative of an energy-dissipating role for this enzyme.

In this article, various tomato organs were used under experimental conditions leading to photobleaching to examine in the absence of PTOX whether this phenomenon is linked to abnormal carotenoid content or to abnormal photosynthetic electron transport. A potential influence of PTOX on the redox status of the PQ pool was also examined.

RESULTS

Effect of PTOX Deficiency in *gh* Tomato Cotyledons

'San Marzano' (SM) control and *gh* seedlings were grown in darkness for 4 d after seed imbibition (time point T0). These white seedlings were then transferred to either low or high light conditions for 24 h. As shown in Figure 1A, at T0, cotyledons from both SM and *gh* were almost devoid of chlorophyll and carotenoid (mainly lutein and violaxanthin) levels were low, but slightly higher in SM than in *gh*. Within the low light period, both cotyledon types accumulated substantial amounts of chlorophyll *a/b* and carotenoids (including β-carotene and traces of other compounds). All pigment levels in *gh* were reduced to about one-half the amount found in SM.

Under high light conditions (Fig. 1A), a slightly higher level (not statistically significant) of pigments was observed in SM (including the xanthophyll cycle pigments antheraxanthin and zeaxanthin; A + Z) when compared to low light, whereas this increase was not observed in *gh* (chlorophyll content is even reduced in *gh* under high light compared to low light).

The carotenoid precursor phytoene was not detected in SM under any condition, but was present (as two isomers) in *gh* at T0 (Fig. 1A). A rise in phytoene level was observed in *gh* under low light but was not statistically significant. Accumulation of phytoene is most likely the result of two parameters: (1) the activity of the whole biosynthetic pathway; and (2) the limiting rate of PDS activity in the absence of PTOX. However, phytoene levels in *gh* were lower under high light than

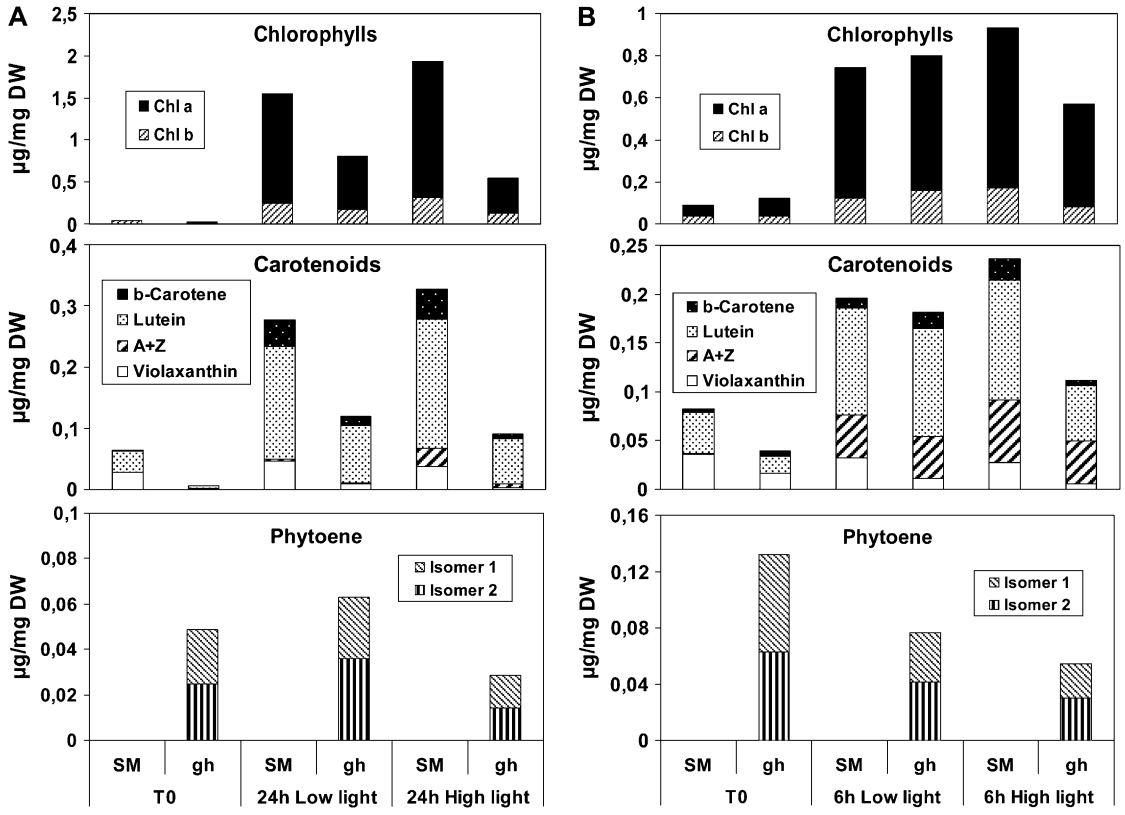

Figure 1. Pigment content of cotyledons from SM and *gh* tomato lines. Seedlings were grown in darkness for 4 and 6 d after seed imbibition to obtain white (A) and pale yellow (B) cotyledons (T0 time point), respectively. Seedlings were then transferred to either low light (20 μmol m^{-2} s^{-1} PAR) or to a higher light intensity (200 μmol m^{-2} s^{-1} PAR). Samples were analyzed after 24 h of light for white cotyledons and after 6 h of light for yellow cotyledons. Eight cotyledons were pooled for a given measurement. Each measurement was repeated three times with a different pool of cotyledons. SES of the mean values were below 12% (data not shown). Whether changes are statistically significant is discussed in the "Results" section. PAR, Photosynthetically active radiation.

under low light (statistically significant; $P < 0.01$), despite the fact that the carotenoid biosynthetic pathway seems active under high light (as deduced from the high levels of colored carotenoid in SM). Because lower levels of colored carotenoids and chlorophyll are also found in *gh* under high light versus low light, the simplest explanation for these observations is increased photodestruction of all these compounds.

Seedlings grown for a longer period (6 d) in darkness (Fig. 1B, time point T0) showed a faint yellow color. Significantly higher carotenoid levels were present in SM than in *gh*. The same low or high light conditions were then applied during 6 h. Low light led to an increase in chlorophyll and carotenoid levels, with no significant difference between SM and *gh*. Compared to low light, high light triggered again a slight increase (not statistically significant) in pigment levels in SM. In *gh*, significantly lower pigment levels were observed under high light compared to SM. In addition, its phytoene levels under high light were lower than at T0 (statistically significant; $P < 0.01$), which can be explained in part by photodestruction. The fact that lower levels of phytoene were also observed in *gh* under low light at 6 h than at T0 (statistically significant; $P < 0.05$) is more surprising and may suggest that carotenoid biosynthesis is less active (because almost-normal carotenoid content was reached; see Fig. 1B).

Taken together, these data suggest that PTOX deficiency leads to photobleaching in cotyledons exposed to high light primarily as a consequence of reduced ability to synthesize colored carotenoids in the mutant, which is fully consistent with the known role of PTOX as a PDS cofactor.

Effect of PTOX Deficiency in Stressed Tomato Leaves

When grown under standard growth chamber conditions, SM and *gh* plants produce green and variegated leaves, respectively. The color aspect of *gh* leaves is decided at a very early leaf developmental stage. Depending on light intensities at an early seedling developmental stage (see "Materials and Methods"), *gh* leaves, which are mainly green, mainly white, or variegated, could be obtained (Fig. 2A, inset). Mainly white leaves (of adult size) showed clear reduction in chlorophyll *a/b* and carotenoids (neoxanthin, violaxanthin, lutein, and β-carotene) when compared to green leaves, whereas this reduction was not as pronounced in variegated leaves (Fig. 2, A and B), as expected. A slight (but significant) trend for higher chlorophyll content was observed in fully green leaves from *gh* versus SM. It is accompanied by a slight increase in carotenoid content (although it does not appear to be statistically significant for all carotenoids). Such an increase was also reported in green sectors of variegated leaves from the *immutans* mutant (Baerr et al., 2005) and is accompanied by an increase in the rate of carbon assimilation (Aluru et al., 2007). These observations were interpreted as the necessity for green sectors to compensate for the limited photosynthetic and metabolic activities of adjacent white sectors. The latter data cannot be compared directly with ours, which were obtained with entirely green tomato leaves. In the *gh* mutant, phytoene was detected in white, but

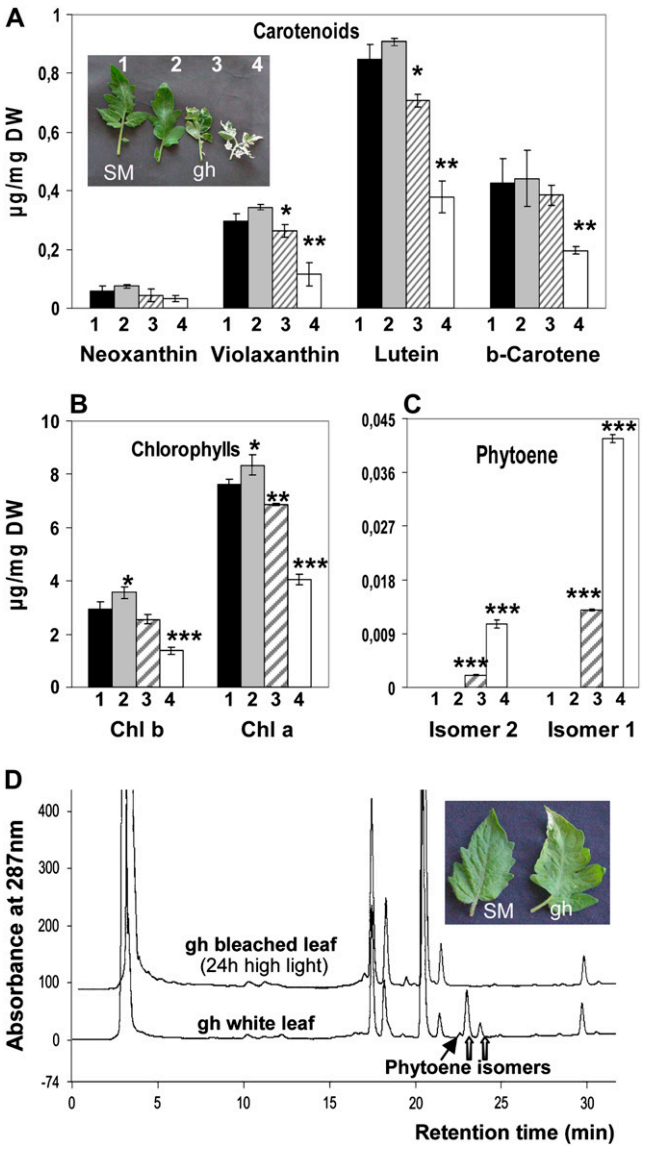

Figure 2. Bleaching of SM and *gh* adult leaves. A, Carotenoid content in SM (1) and different types of *gh* leaves (2–4) as shown in the inserted photograph: 2, green *gh*; 3, variegated; 4, mainly white. For details, see "Materials and Methods." Statistically significant differences are indicated compared to SM leaves: *, $P < 0.05$; **, $P < 0.01$; ***, $P < 0.001$. B, Chlorophyll content in the four leaf types. C, Phytoene content in the four leaf types. D, HPLC elution profiles of pigments (A_{287}). The top trace shows an extract from sectors bleaching after 24 h on green *gh* leaves submitted to high light conditions (1,000 μmol m^{-2} s^{-1}), as shown in the inset photograph. The bottom trace shows an extract from mainly white *gh* leaves, as shown in A. Thick arrows point to the two major phytoene isomers that are quantified in C; the thin arrow points to a minor phytoene isomer.

not in green, leaves (Fig. 2C). This latter observation suggests that, despite the absence of PTOX, PDS activity is not limiting carotenoid biosynthesis in green leaves from *gh*.

Detached fully green leaves (with no visible deficit in pigments, as shown in Fig. 2A, sample 2) were then exposed to high light (1,000 μmol m^{-2} s^{-1}) for long incubation periods. Leaves from both SM and *gh* showed early bleaching symptoms in some sectors after 20 to 24 h. This trend appears earlier and is stronger in *gh* (Fig. 2D, inset) and extends to larger leaf sectors with longer incubation time. Pigments were extracted separately from green and bleaching sectors. As expected, these leaves showed accumulation of the xanthophyll cycle pigments A + Z (data not shown) and bleaching sectors contained reduced chlorophyll and carotenoid content. This reduction was more pronounced in *gh* than in SM. However, an unexpected observation was that phytoene was not detected in any tissues in contrast to what was observed in cotyledons (Fig. 1) or mainly white or variegated leaves (Fig. 2C). Figure 2D compares typical HPLC elution profiles from a bleached sector after 24 h of high light and from a mainly white leaf whose aspect is determined early during leaf development (as shown in Fig. 2A).

To shed more light on changes occurring in chloroplasts under these experimental conditions, a series of experiments were performed at earlier time points (before bleaching was visible). First, pigment analyses (Table I) were performed using plants grown under low light (60 μmol m^{-2} s^{-1}) conditions (T0), and then green leaves were detached and incubated either under low light (60 μmol m^{-2} s^{-1}) or high light (1,000 μmol m^{-2} s^{-1}) for 6 h (T6h) or 16 h (T16h). At T6h under low light, only marginal changes in pigment content were observed with respect to T0 in both SM and *gh* leaves, with the exception of an increase in the levels of xanthophyll A + Z for both SM and *gh*. This increase was unexpected because this light intensity is identical to that experienced by the plants before these experiments and is most likely due to the detachment of leaves. At T6h under high light conditions, higher A + Z levels were observed, as expected, and, interestingly, with a stronger increase in SM versus *gh*. No other significant change in pigment content was observed at T6h under high light, with the exception of a decrease in violaxanthin, the precursor of A + Z during activation of the xanthophyll cycle. Compared to T6h, at T16h under high light conditions, the most notable change was an increase in A + Z levels in *gh*, which equaled the levels in SM (data not shown). No phytoene was detected in any sample.

Proteins were extracted from leaves at T0 and over a time course up to T16h, under either low or high light. Immunodetection did not reveal any signal for PTOX in *gh* (data not shown), as expected, but a 37-kD band was visible in SM (Fig. 3A). High light conditions led to a gradual rise in PTOX level in SM (which is particularly evident at T16h). Under low light, only a slight increase with time is apparent (most likely due to leaf detachment). The PSI-D polypeptide level was not found to change during this time course and can therefore be considered an internal control to ensure equal gel loading. Figure 3B shows the densitometric scanning of the PTOX band from Figure 3A after normalization using the PSI-D band as a standard.

The maximal quantum yield of PSII was estimated from the F_v/F_m ratio. At T6h, under high light (Fig. 4), the F_v/F_m ratio was found to decrease, as expected, under these photoinhibitory conditions in both SM and *gh* leaves (but more in *gh*). The same observations were made when the temperature was shifted to 15°C instead of 24°C: Again, *gh* leaves showed a lower F_v/F_m ratio than SM leaves under high light (Fig. 4). At T16h, the further decrease in F_v/F_m was also stronger in *gh* than in SM leaves (data not shown).

Lipid peroxidation was estimated using the malondialdehyde (MDA) method over a 6-h time course after transfer of leaves to high light. These data (Fig. 5A) suggest an increase in lipid peroxidation in both *gh* and SM, but greater in *gh*.

Thermoluminescence measurements were performed on attached green leaves directly after 6 h of high light

Table I. *Pigment content of SM and gh green leaves*

Plants were grown under low light (60 μmol m^{-2} s^{-1}). At T0, leaves were detached and incubated 6 h under either low (60 μmol m^{-2} s^{-1}) or high (1,000 μmol m^{-2} s^{-1}) light. Values (given as μg mg^{-1} dry weight) are the mean of four measurements. SD is given in brackets. Statistically significant differences under high light compared to low light are indicated: **, $P < 0.01$; ***, $P < 0.001$. V, Violaxanthin; Chl, chlorophyll; n.d., not detected.

	T0		Low Light		High Light	
	SM	*gh*	SM	*gh*	SM	*gh*
Neoxanthin	0.13 (0.02)	0.13 (0.02)	0.12 (0.02)	0.17 (0.03)	0.09 (0.01)	0.14 (0.02)
Violaxanthin	0.53 (0.03)	0.66 (0.13)	0.56 (0.05)	0.61 (0.06)	0.35 (0.03)***	0.55 (0.02)
Z + A	n.d.	n.d.	0.17 (0.01)	0.16 (0.02)	0.39 (0.08)**	0.24 (0.03)**
Lutein	1.60 (0.10)	1.94 (0.17)	1.91 (0.10)	2.21 (0.17)	1.72 (0.22)	2.07 (0.11)
β-Carotene	0.74 (0.04)	0.86 (0.05)	0.72 (0.03)	0.93 (0.08)	0.68 (0.04)	0.85 (0.03)
Total carotenoids	2.90 (0.23)	3.61 (0.35)	3.49 (0.17)	4.09 (0.29)	3.23 (0.34)	3.85 (0.13)
(Z + A)/(Z + A + V)	0	0	23.58 (2.49)	21.14 (0.80)	53.16 (3.61)***	30.03 (1.71)***
Chl *b*	6.52 (0.71)	7.55 (0.30)	6.94 (0.44)	8.51 (0.72)	6.65 (0.74)	8.14 (0.50)
Chl *a*	13.86 (0.70)	14.67 (0.11)	13.76 (0.73)	15.86 (1.71)	12.84 (0.82)	15.47 (0.77)

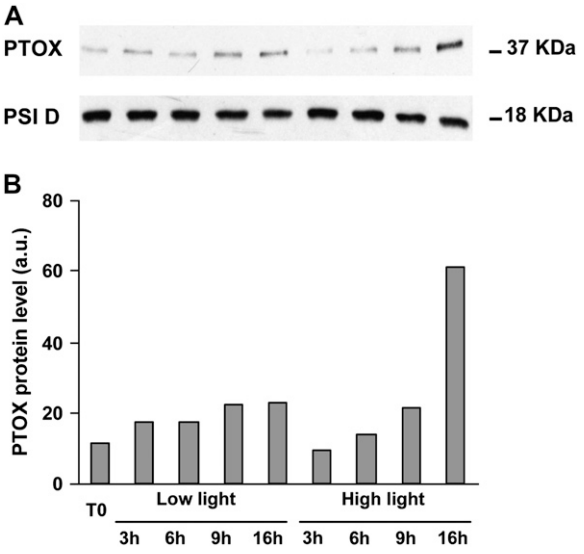

Figure 3. PTOX protein levels in SM leaves. A, Immunodetection of PTOX and PSI-D (a PSI protein used as a control for equal gel loading). Plants were grown under low light (60 μmol m^{-2} s^{-1}) and at T0 detached leaves were incubated during a 16-h time course under low (60 μmol m^{-2} s^{-1}) or high (1,000 μmol m^{-2} s^{-1}) light. Leaf protein samples were separated by gel electrophoresis and immunodetected as described in ''Materials and Methods.'' B, Densitometric scanning values of the PTOX band in A after normalization using the PSI-D values as a standard.

stress and after an additional 24-h recovery period under low light conditions. As controls, leaves maintained for 6 h under low light were used. Thermoluminescence glow curves (Ducruet, 2003) show a B band peaking at 25°C and a high temperature band peaking at 130°C to 140°C (HTL2; representing the oxidative stress of leaves). As shown in Figure 5B (left), the B band is shifted after light stress to a position corresponding to a lower temperature with a 43% decrease in light-stressed SM leaves, indicating photoinhibition and damage to PSII. After 24 h of recovery, the B band resumes its initial amplitude and peak position. In light-stressed *gh* leaves, a decrease of 78% is observed for the B band, also accompanied by a shift to lower temperature, but after 24 h of recovery the B band regenerated only to 70% compared to control leaves and the peak shift was still visible (Fig. 5B, right).

No increase in the HTL2 band was visible after 6 h of light stress in SM leaves (Fig. 5B). In contrast, the HTL2 band was 150% higher in light-stressed *gh* leaves compared to control leaves (significant at $P < 0.01$). After 24 h of recovery, a further increase was observed in *gh*, but an increase was also observed in SM at that time point in comparison to 6 h of light stress (see ''Discussion'').

It therefore appears that the absence of PTOX renders the tomato leaf photosynthetic apparatus more sensitive to extreme conditions (provided here by a transfer to excessive light). This increased sensitivity is observed in the absence of any detectable accumulation of phytoene or decrease in carotenoid content.

Effects of PTOX on the Redox State of the PQ Pool

Fast fluorescence kinetics (OJIP, also called OI_1I_2P; Schreiber, 2004; Strasser et al., 2004) were performed after 5 min, 30 min, or 4 h of dark adaptation and recorded during a light pulse of 1 s (Fig. 6). The O level (0.01 ms), also reflecting F_0, is increased significantly in the *gh* mutant versus SM, after 5 or 30 min of dark adaptation, but not after a longer dark adaptation of 4 h. In addition, for all dark adaptation times, the fluorescence at 2 ms (J level) is strongly increased during the light pulse in *gh* compared to SM. An increased J level is an excellent indicator of a more reduced PQ pool and a more pronounced primary electron acceptor of PSII (Q_A^-) accumulation under light excitation (Haldimann and Strasser, 1999). Whereas the J level decreases continuously with increasing dark adaptation time in SM, it increases in *gh* between 5 to 30 min of dark adaptation and strongly decreases again after 4 h. In parallel to the J level, the I level is also significantly increased after 5 and 30 min of dark adaptation in *gh* versus SM. Strikingly, after 4 h of dark adaptation, the P level in *gh* remains at a similar level compared to that after 5 and 30 min, whereas a significant increase is observed in SM (Fig. 6). These observations are discussed below.

In another set of experiments, induction kinetics of chlorophyll fluorescence were performed over a longer time range after 30-min incubation of leaves in the dark followed by exposure to actinic light (200 μmol m^{-2} s^{-1}) for 10 min (Fig. 7). In this time window, the Kautsky kinetic describes the drop of the fluorescence from the F_m level (P level) to the steady-state level (F_s) and is characterized by the complex superposition of processes, including the light-induced activation of PSI, the Calvin cycle, alternative electron transfer (e.g.

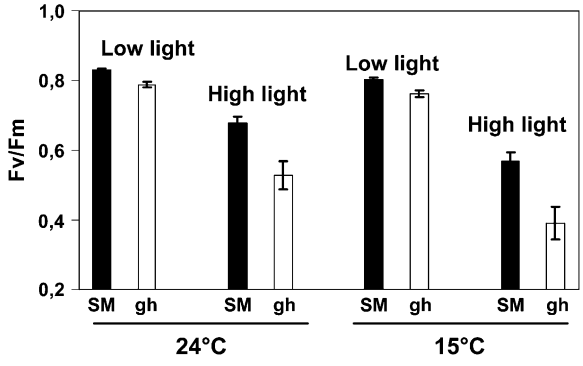

Figure 4. Photoinhibition of SM and *gh* fully green leaves. The maximal quantum yield of PSII is expressed as the F_v/F_m ratio. SM and *gh* leaves were incubated at 24°C or 15°C for 6 h under either low (60 μmol m^{-2} s^{-1}) or high light (1,000 μmol m^{-2} s^{-1}) and then kept for 30 min in the dark before chlorophyll fluorescence measurement. Mean values of six measurements (i.e. six different leaves) are shown.

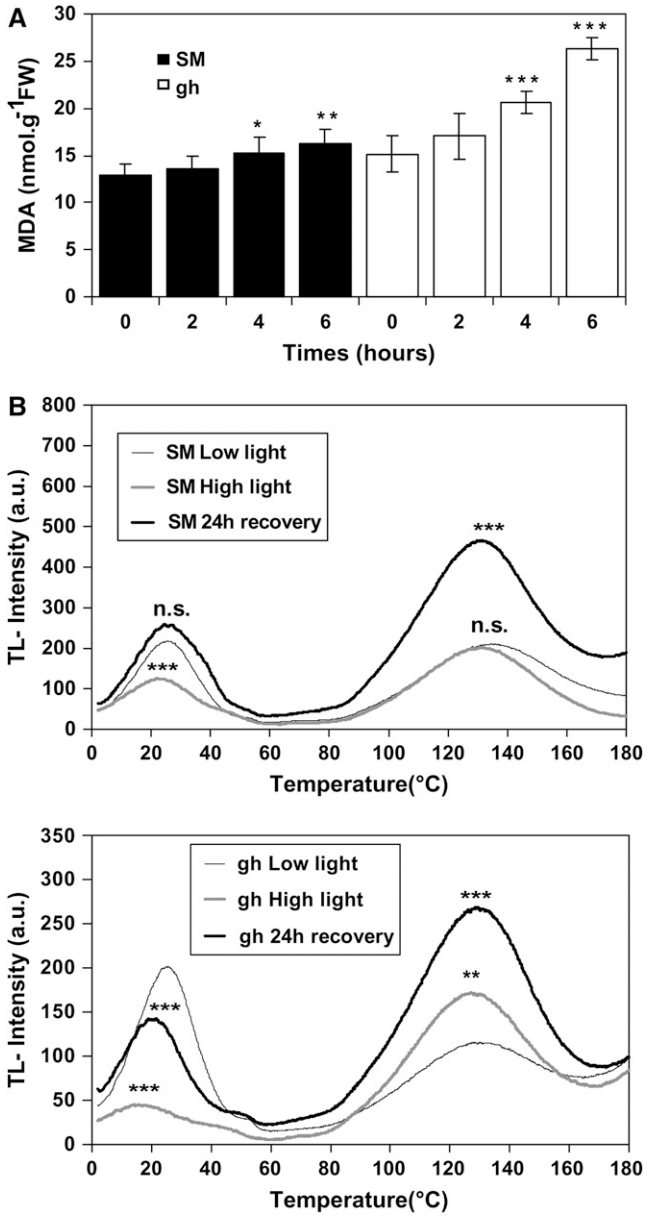

Figure 5. Damage to PSII and oxidative stress in SM and *gh* fully green leaves. A, Lipid peroxidation in SM (black columns) and *gh* (white columns) leaves. Plants were exposed to high light stress (1,000 μmol m^{-2} s^{-1}) for 6 h. Lipid peroxidation was estimated using the MDA method. Data are mean values of a minimum of five experiments. Statistically significant differences are indicated compared to T0: *, $P < 0.05$; **, $P < 0.01$; ***, $P < 0.001$. B, Thermoluminescence (TL) measurements in SM (top) and *gh* (bottom) leaf discs from control leaves (low light) or leaves treated for 6 h under high light (1,000 μmol m^{-2} s^{-1}) or leaves treated under the same high light conditions but allowed to recover for 24 h under the light conditions used for the control leaves. Samples were then treated as described in "Materials and Methods," cooled to 2°C, and flash illuminated to induce charge separation. The samples were then heated to induce charge recombination of PSII radical pairs (2°C–60°C; the B band represents the thermoinduced light emission from the recombination of $S_2Q_B^-$ radical pairs after one light flash) and chemiluminescent reactions (70°C–180°C) representing the chemical stress status (HTL2 band). n.s., Not significant; *, $P < 0.05$; **, $P < 0.01$; ***, $P < 0.001$ (compared to control). TL measurements were performed under N_2 atmosphere to avoid autooxidation at high temperatures. There was no influence on the B band by N_2 flushing compared to air (data not shown).

Mehler reaction), and buildup of ΔpH-dependent nonphotochemical quenching (qN). Consistent results were obtained showing that the effective quantum yield of PSII (ΦPSII) is lower in *gh* versus SM and that the relative reduction state of Q_A (estimated as 1 − photochemical quenching parameter [qP]) is higher in *gh* versus SM. 1 − qP also reflects the overall reduction state of the electron transport chain and therefore the quinone pool. When this parameter was expressed as 1 − qL (Kramer et al., 2004), the same result was obtained (data not shown). In contrast, qN was not found to differ significantly between both leaf types.

Effect of PTOX Deficiency in Tomato Fruit

Young tomato fruit bleach in the *gh* line under standard greenhouse conditions or show a variegated green/white color under shaded conditions (Barr et al., 2004). Using controlled growth chamber conditions, we produced white fruit (termed "*gh* white" in the subsequent experiments) as well as fully green fruit (termed "*gh* green") for *gh*. The latter were obtained by keeping fruit under low light. To avoid plant etiolation under these conditions, only the fruit were kept under low light, which was achieved by wrapping the fruit in a cloth as soon as they started to develop. During ripening, *gh* white fruit become yellow (a color predominantly due to flavonoids), whereas *gh* green fruit become orangey. Under both light conditions, SM fruit are green before ripening and become fully red during ripening. As shown in Figure 8, A and B, SM and *gh* green fruit at the mature green stage (adult size) show only nonsignificant variation in pigment content. As expected, these pigment levels are severely reduced in *gh* white fruit. Whereas phytoene is present in *gh* white fruit, only trace amounts of this pigment are found in *gh* green fruit (Fig. 8C). During ripening, phytoene is present in all fruit types, including SM, but at the highest level in fruit that ripened from the *gh* white type (Fig. 8D). During ripening, the level of the newly accumulating pigments (all-trans lycopene and low amounts of its cis-isomers) is dramatically affected in the *gh* white fruit type and reduced to about 17% of their level in SM in the *gh* green fruit type (Fig. 8E). The latter observation contrasts with the normal carotenoid content of *gh* fruit at the green stage (Fig. 8, A and B).

Explants from mature green fruit were incubated under 1,000 μmol m^{-2} s^{-1} for up to 48 h at 24°C. Bleaching symptoms were observed after approximately 24 h in both SM and *gh* explants, but were stronger in *gh* (data not shown). Analysis of their carotenoid content at various time points (6, 18, 30, and 42 h) revealed no phytoene (data not shown), indicating that the absence of PTOX does not limit

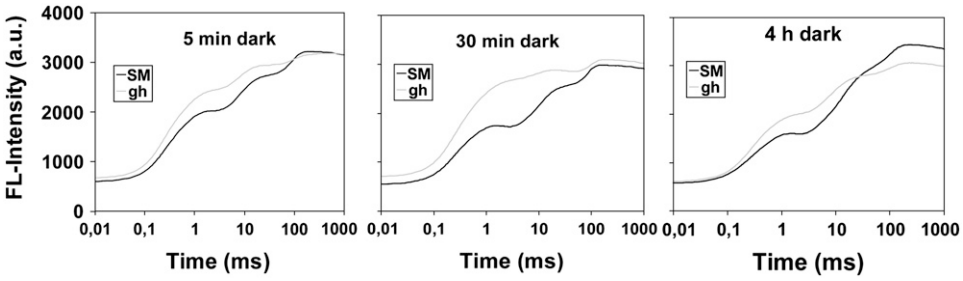

Figure 6. Fast fluorescence kinetics (OJIP) for fully green leaves from *gh* and SM plants pulse illuminated after different times of dark adaptation. The O level at 0.01 ms represents a fluorescence value close to F_0. The fluorescence rise from the O to the J level (2 ms) indicates the reduction of Q_A. The fluorescence rise from the J to the I level (30 ms) indicates the reduction of Q_B and partially of the PQ pool. The rise from the I to the P level (200–300 ms) indicates the electron flow through PSI (PQ pool fully reduced at P level).

carotenoid biosynthesis in these *gh* explants. Estimation of the maximal quantum yield of PSII after 6 h of incubation (Fig. 9) showed that *gh* fruit are more sensitive to photoinhibition than SM fruit under this high light condition at 24°C. At 15°C, both fruit types are fully photoinhibited under these light conditions.

DISCUSSION

Fully Greened Tissues Can Desaturate Carotenoids without PTOX

Our data show that, in the absence of PTOX, the lower capacity to desaturate carotenoids is primarily responsible for the phenotype in cotyledons of dark-grown tomato *gh* seedlings and when these seedlings are transferred to light. These tissues have reduced colored carotenoid levels and accumulate their precursor phytoene. Considering the well-known photoprotective role of carotenoids, this pigment deficiency will lead to bleaching in tissues where assembly of the photosynthetic apparatus is initiated upon transfer to light. Although not studied here, it can be speculated that such a pigment deficit is also (at least partially) responsible for the variegated leaf phenotype that is initiated at an early chloroplast developmental stage (when optimal carotenoid biosynthesis is likely to be important). Consistent with this view, bleached sectors in variegated leaves contain phytoene. However, an additional role for PTOX in photosynthetic electron transport (see below) during the buildup of the photosynthetic apparatus cannot be excluded.

In contrast, when normal chloroplast biogenesis was not impaired (i.e. when excessive light was avoided at an early stage), different observations were made in *gh* green adult leaves: We were unable to detect phytoene (nor a deficit in carotenoid content) even under such excessive light ultimately leading to bleaching. This is highly surprising because the carotenoid biosynthetic pathway is likely to be very active under such conditions to compensate for carotenoid turnover and photodestruction (Simkin et al., 2003). This contrasts with the accumulation of phytoene in adult tomato leaves when PDS is inhibited by the bleaching herbicide norflurazon (Simkin et al., 2003). Thus, the absence of phytoene in leaves bleaching under strong light is not due to its photodegradation, but rather to the fact that the carotenoid biosynthetic pathway is not limited by the lack of PTOX. In other words, PTOX is dispensable as a carotenoid desaturase cofactor in tissues with fully functional photosynthetic apparatus. Because optimal carotenoid desaturation is obtained in the range of the midpoint potential of the PQ/plastoquinol redox couple (Nievelstein et al., 1995), this redox control may be obtained for PQs in the vicinity of the desaturases by a mechanism provided by photosynthetic membranes. Chemical reoxidation of plastoquinol (Khorobrykh and Ivanov, 2002) may also participate.

gh Leaves Are Affected in Photosynthetic Electron Transport under Light Constraints

Our data consistently suggest that PTOX plays a specific role in the protection of the fully assembled photosynthetic apparatus under light constraints. We used adult leaves subjected to severe light conditions, which led to photobleaching after prolonged incubation (24 h) in both *gh* and control SM lines. Such prolonged light exposure and provoked photobleaching are not normal phenomena in nature but were used here to ensure that the applied conditions were creating extreme constraints. We then used earlier time points compatible with a normal photoperiod for detailed investigation. These indicated higher PSII photoinhibition in *gh* versus SM leaves after 6 h (Fig. 4) and 16 h of light stress (data not shown), as well as higher damage level of PSII in *gh* than in SM and only partial recovery in *gh* (thermoluminescence B band; Fig. 5B). High-temperature thermoluminescence measurements (HTL2 band; Vavilin and Ducruet 1998; Vavilin et al., 1998) also point to reduced potential to prevent oxidative damage in *gh* versus SM leaves after 6 h of light stress. Estimation of lipid peroxidation by MDA level measurements (Fig. 5A) is consistent with

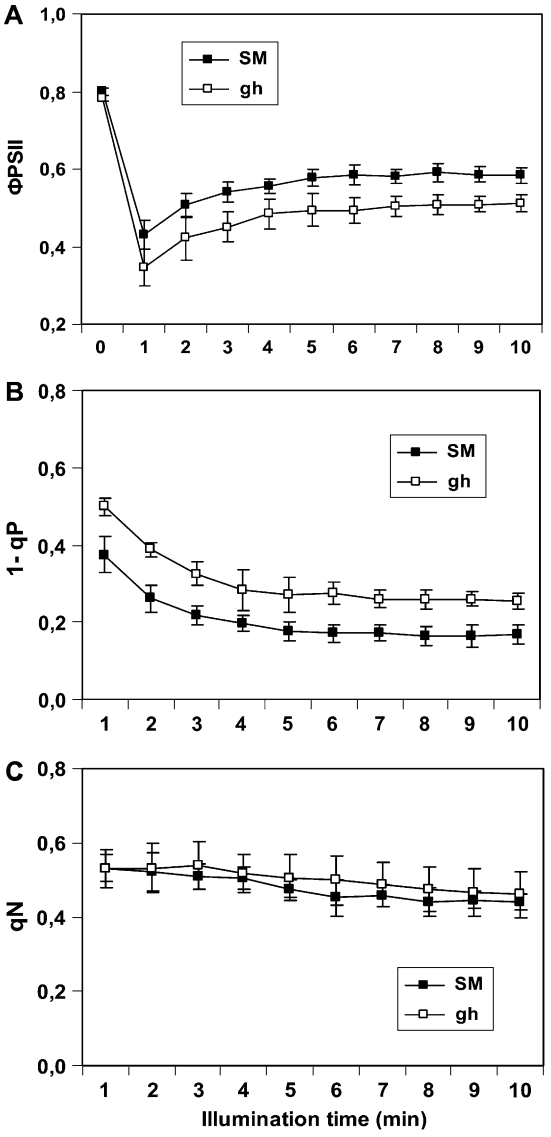

Figure 7. Induction kinetics for the chlorophyll fluorescence parameters ΦPSII (A), 1 − qP (B), and qN (C). SM and green *gh* leaves were dark adapted 30 min and then illuminated with actinic light of 200 μmol m^{-2} s^{-1} for 10 min. Mean values (n = 6) were used.

the latter observations. The observed delayed oxidative damages (occurring poststress; HTL2 band) may appear surprising, but progress of lipid peroxidation (MDA levels) after stress relief has also been observed under low-temperature photoinhibition (Hegedüs et al., 2004) and drought stress (Olsson et al., 1996). What is clear from our observation on this poststress phenomenon (Fig. 5B) is that it affects both the *gh* and control lines and therefore seems independent of PTOX.

In vitro, PTOX is a plastoquinol oxidase (Josse et al., 2000, 2003). Consistent in vivo data were obtained here suggesting that PTOX affects the redox status of PQ in leaves. Under 10 min of actinic illumination, induction kinetics of chlorophyll fluorescence show higher 1 − qP values (lower photochemical quenching) in *gh* consistent with reduced operational quantum yield of PSII. This is indicative of the more reduced status of PSII acceptors (Q_A) in *gh* leaves compared to control SM leaves (Fig. 7), which most likely indicates that the PQ pool is more reduced. Unlike 1 − qP values, the qN parameter was not significantly different in *gh* and control leaves, suggesting that the extent of qN reached similar levels. The higher reduction state of the electron transport chain under steady-state illumination in *gh* versus SM leaves suggests that the lack of PTOX leads to less efficient utilization of photosynthetic and alternative electron sinks (Ort and Baker, 2002).

In addition, fast fluorescence induction kinetics (Fig. 6) show that PTOX regulates the reduction state of the PQ pool in the dark. The increased amplitude of the J level indicates that a more strongly reduced PQ pool is present in *gh*, the extent of which depends on the duration of the dark incubation prior to pulse illumination. The simplest way to interpret these results is to assume that, in the absence of PTOX, the NAD(P)H dehydrogenase (NDH) complex strongly reduces PQs in the first 30 min in the dark. The decrease in the J level after 4 h in *gh* suggests that, over a long period of time, reoxidation of reduced PQs does occur in *gh*, either by pure chemical oxidation with molecular oxygen (Khorobrykh and Ivanov, 2002) or by an alternative mechanism. Inactivation of the NDH complex after long dark adaptation might also contribute to PQH_2 reoxidation. The J-I phase describes the reduction of the PQ pool (Schreiber et al., 1989). Because the PQ pool is more reduced in *gh* than in SM after dark adaptation, the amplitude of this phase is significantly lower in *gh* than in SM (Fig. 6). Recent results indicate that the I-P phase in higher plants is governed by electron transfer beyond the cytochrome b_6/f complex and a transient block at the acceptor side of PSI due to inactive ferredoxin-$NADP^+$-oxidoreductase (Schansker et al., 2005). The increase of the P level after 4 h of dark adaptation in SM indicates the release of yet-unexplained quenching of fluorescence. These observations need further investigation before they can be unambiguously interpreted.

Role of PTOX in Photosynthesis: Safety Valve or Regulatory Adjustment?

Correlative evidence for PTOX as a bona fide safety valve (i.e. allowing the transfer of excess electrons to O_2) is essentially provided for higher plants by gene expression/protein accumulation data (Rizhsky et al., 2002; Baena-Gonzalez et al., 2003; Quiles, 2006). However, PTOX remains a minor constituent of photosynthetic membranes (Lennon et al., 2003) with the notable exception of alpine plants such as *Geum montanum* and *R. glacialis* (Streb et al., 2005), which may have selected natural overexpressers as an additional protection mechanism. We could show here that PTOX protein levels do increase unambiguously (in wild-type

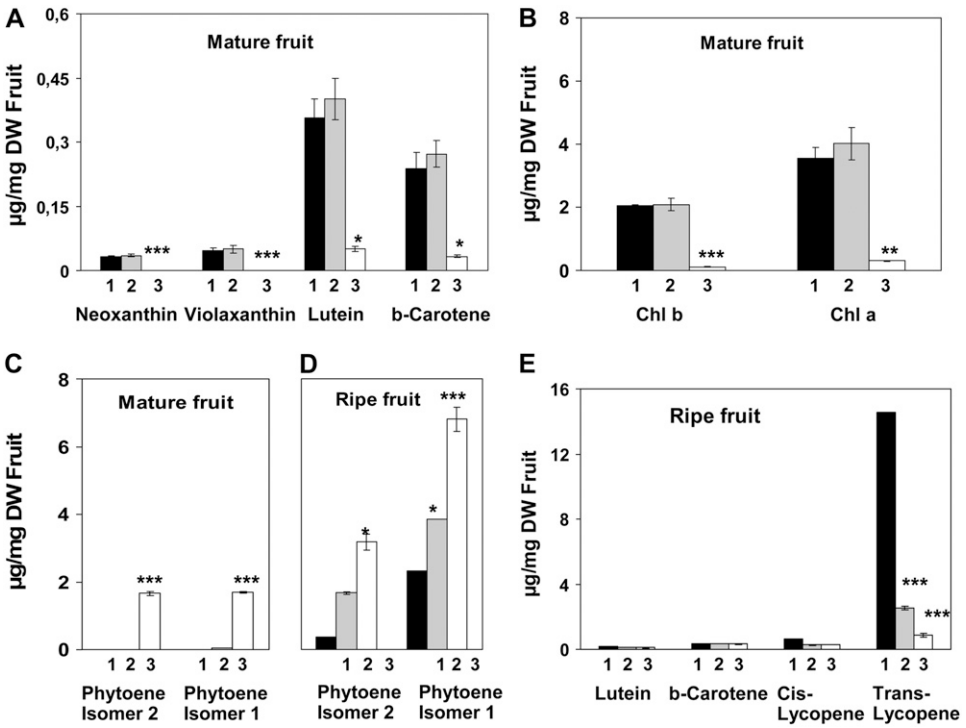

Figure 8. Pigment content of mature and ripe SM and *gh* fruits. The colored carotenoid (A), chlorophyll (B), and phytoene (C) contents were analyzed in mature green (adult size) fruit. The phytoene (D) and colored carotenoid (E) contents were analyzed in ripe fruit (10 d after the breaker stage). Samples were taken from SM green and red fruit (histogram columns indicated by 1), *gh* green and their derived orangey fruit (2), and *gh* bleached and their derived yellow fruit (3). Statistically significant differences are indicated compared to SM fruit: *, $P < 0.05$; **, $P < 0.01$; ***, $P < 0.001$.

control plants) under strong light conditions, but only after a long period (especially after 16 h; Fig. 3). In contrast, after 6 h of illumination, no increase in PTOX level was observed, although we could demonstrate clear involvement of PTOX in photoprotection at that time point. Therefore, it seems difficult to propose a role for PTOX merely as a safety valve allowing massive photosynthetic electron flow toward O_2.

Acclimation of plants to environment and its constantly changing conditions implies a highly sophisticated network of regulation, which seems to involve chlororespiration (Rumeau et al., 2007). Quiles (2006) has shown that in vitro chlororespiratory activity (NADH dehydrogenase and a PTOX-like activity) is stimulated when thylakoids are isolated from heat and high light-treated oat (*Avena sativa*) plants. PTOX activity, rather than directly compensating for an over-reduced PQ status, could be viewed as a fine-tuning device. Together with the NDH complexes and the ferredoxin/PGR5-dependent PQ reductase, PTOX might provide photosynthetic regulatory mechanisms (Rumeau et al., 2007; Shikanai, 2007). A regulatory function for PTOX is suggested by our present data. After 6 h of photostress (but not after 16 h when PTOX protein levels are at their highest in SM), lower levels of de-epoxidated xanthophyll cycle pigments (A + Z; Table I) were observed in *gh* versus SM. Furthermore, the more strongly reduced electron transport chains when dark-to-light transitions are applied to *gh* leaves (Fig. 7) indicate a lack of fine tuning for optimal allocation of electrons to photosynthetic and nonphotosynthetic sinks. This is important in the first minutes of illumination when light activation of the Calvin cycle and the development of ΔpH-dependent qN are critical. The more reduced state of Q_A during this time might also render PSII more sensitive to photobleaching because photoinhibition or photodamage to PSII strongly depends on the redox state of PSII and membrane energization (Ögren, 1991).

A regulatory role for PTOX is also suggested by the slightly higher pigment content of green leaves in *gh* versus SM (Fig. 2, A and B). However, this slight increase in both chlorophyll and carotenoid content is

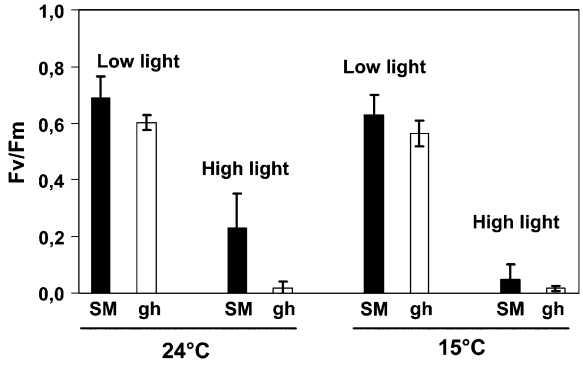

Figure 9. Photoinhibition of SM and *gh* green fruit. The maximal quantum yield of PSII is expressed as the F_v/F_m ratio. Fruit pericarp of SM and *gh* were incubated at 24°C or 15°C for 6 h under either low (60 μmol m^{-2} s^{-1}) or high light (1,000 μmol m^{-2} s^{-1}) and then kept 30 min in the dark before chlorophyll fluorescence measurement. Mean values are shown ($n = 3$).

unlikely to be the causal link between the lack of PTOX and the various effects on photosynthetic electron transport described here. For instance, in *gh* the influence of dark adaptation time on fast fluorescence kinetics (Fig. 6) or delay in full activation of the xanthophyll cycle during long incubation under severe light conditions (Table I) must result from more complex regulatory mechanisms. In addition, a rise in chlorophyll content was observed in quite similar proportions when wild-type and *immutans* Arabidopsis were compared (Rosso et al., 2006), whereas these authors did not report effects on the photosynthetic electron chain for this species. This apparent discrepancy between tomato and Arabidopsis is also, in our opinion, more in favor of a regulatory role for PTOX: In a multicomponent regulatory network, it is conceivable that the relative importance of a given component differs from species to species. This is even more plausible because, within one single species (tomato; our present data), the relative importance of the dual role of PTOX (related to carotenoid biosynthesis and to photosynthesis) differs from organ to organ and also within a given organ (leaf, fruit) from one developmental stage to another.

Changes in PTOX Function during Tomato Fruit Development

As in leaves, bleaching of young *gh* fruit is determined at an early developmental stage. The presence of phytoene in white *gh* fruit suggests it is linked (at least partially) to a deficit in carotenoid biosynthesis. In contrast, the sensitivity to high light conditions of mature *gh* fruit that were maintained green could not be linked to a deficit in carotenoid biosynthesis. We found *gh* green fruit to be more susceptible to photoinhibition than SM control fruit, which again is similar to our observation in adult green *gh* leaves.

In ripening *gh* fruit derived from green fruit, the lycopene-synthesizing capacity of fruit is reduced compared to wild type, but is not zero, which may suggest that, in the absence of PTOX, another cofactor of carotenoid desaturase replaces PTOX. The identity of this cofactor (Carol and Kuntz, 2001) and whether it is identical to the one that operates in green or etiolated (dark-grown cotyledons) tissues remain to be determined. Alternatively, chemical reoxidation of plastoquinol may be sufficient for the low level of phytoene desaturation in *gh* ripening fruit as well as in dark-grown cotyledons.

Bleaching at the green stage in *gh* fruit influences the capacity to synthesize carotenoids during fruit ripening: The amount of lycopene present in ripe fruit derived from white *gh* fruit is decreased 3-fold compared to ripe fruit derived from green *gh* fruit (Fig. 8E). Because carotenoid biosynthesis is catalyzed by membrane-bound enzymes and because bleached *gh* fruit are affected in their plastid ultrastructure (Barr et al., 2004), it seems reasonable to consider that irreversible damage to membranes in bleached tissues will affect this biosynthetic pathway. Because fruit ripening is characterized by the disassembly of photosynthetic membranes to resynthesize new (achlorophyllous) ones, membrane disintegration at an early stage will affect this biosynthetic pathway during ripening. It is also likely that photobleaching will have additional pleiotropic effects that will affect the carotenoid biosynthetic pathway.

MATERIALS AND METHODS

Plant Materials

Tomato (*Solanum lycopersicum*) of SM genotype and its monogenic *gh* mutant (LA0259; Tomato Genetic Stock Center) were grown at 24°C with a 16-h photoperiod (white light, 60 μmol m^{-2} s^{-1}). Seedlings were first grown at low light intensity (10 μmol m^{-2} s^{-1} for 1 week and then 20 μmol m^{-2} s^{-1} for 4 weeks) and then placed under the above-mentioned light conditions to obtain adult plants with green leaves for *gh*. Both white and variegated *gh* leaves were obtained by incubation of seedlings directly at 60 μmol m^{-2} s^{-1}.

For experiments with cotyledons, SM and *gh* seedlings were grown in darkness for 4 and 6 d after seed imbibition to obtain white and pale yellow cotyledons, respectively. Seedlings were then transferred to either low light (20 μmol m^{-2} s^{-1}) or higher light intensities (200 μmol m^{-2} s^{-1}).

For light stress experiments, young (fully elongated) leaves or mature green fruit were harvested 3 to 4 h after the beginning of the photoperiod and incubated at 24°C under 60 μmol m^{-2} s^{-1} (control) and 1,000 μmol m^{-2} s^{-1} (stress).

Chlorophyll Fluorescence

Chlorophyll *a* fluorescence was measured with a pulse-modulated fluorometer (Walz) at room temperature. Leaves and fruits were kept in the dark for 30 min prior to the measurements. Variable fluorescence (F_v) was calculated as $F_m - F_0$, where F_0 is minimal fluorescence (under a weak measuring beam) and F_m maximal fluorescence (determined after an 800-ms saturating pulse of white light at 2,500 μmol m^{-2} s^{-1}). Prior to fluorescence measurements, photoinhibitory conditions were obtained by exposing plant samples to an irradiance of 1,000 μmol m^{-2} s^{-1} for 6 or 16 h at 15°C or 24°C.

For experiments using prolonged illumination, actinic white light (200 μmol m^{-2} s^{-1}) was used and saturating pulses were applied at 1-min intervals for 10 min to determine maximal fluorescence (F'_m), steady-state fluorescence (F_s), and, after actinic light was switched off and a brief far-red pulse was applied, to measure minimal fluorescence (F'_0). The coefficient qP was calculated as $(F'_m - F_s)/(F'_m - F'_0)$ (Schreiber et al., 1989), qN as $1 - (F'_m - F'_0)/(F_m - F_0)$, and ΦPSII as $(F'_m - F_s)/F'_m$.

Fluorescence induction kinetic curves (OJIP) were measured with a Handy-PEA fluorometer (Hansatech) according to Strasser et al. (2004). Plant leaves were dark adapted for 5 min, 30 min, and 4 h in a leaf clip prior to illumination with saturating light of 3,500 μmol m^{-2} s^{-1} from three red LEDs (duration 1 s).

Thermoluminescence and Lipid Peroxidation Measurements

Thermoluminescence measurements were performed on 6-mm leaf discs as described previously (Gilbert et al., 2004). Briefly, leaf discs were preilluminated by two single turnover flashes at 20°C and dark adapted for 5 min to establish a defined ratio of S_0/S_1 states in the water-splitting complex and a defined ratio of Q_B/Q_B^- at the acceptor side of PSII. Samples were then cooled to 2°C and illuminated with one single turnover flash to induce charge separation. Then the samples were heated from 2°C to 180°C at a rate of 20°C min^{-1}. All thermoluminescence steps were performed under N_2 atmosphere to reduce autooxidation by O_2. A change in the intensity of the B band ($S_2Q_B^-$) peaking at 25°C points to damage of PSII. The amplitude of the 130°C thermoluminescence band (HTL2 band) was used as an index of lipid peroxidation.

MDA assays were performed according to Hodges et al. (1999) and Sairam and Srivastava (2001). About 100 mg of fresh tissue were ground in 1 mL of chilled reagent (0.25% [w/v] thiobarbituric acid in 10% [w/v] TCA). After incubation at 95°C for 20 min, extracts were cooled at room temperature and then centrifuged. Thiobarbituric acid reactivity was determined in the supernatant by measuring the A_{532}. Nonspecific turbidy was determined at 600 nm.

Extraction and Immunodetection of Total Proteins

Total protein was extracted from frozen and ground material using the Hurkman and Tanaka method (Hurkman and Tanaka, 1986). Protein samples were fractionated by SDS-PAGE and electroblotted onto nitrocellulose. Membranes were blocked in 5% milk and immunodetected with antibodies. PSI-D antibodies were purchased from Agrisera. Immunodetection was performed using the horseradish peroxidase conjugate substrate kit (Bio-Rad) and ECL western-blotting kit (Amersham) as recommended by the suppliers. Densitometric analysis of the immunoblots was performed using Image J software (Wayne Rasband, National Institute of Mental Health).

Pigment Analysis

Pigments were extracted from lyophilized samples (5-mg leaves or cotyledons, 10-mg fruit pericarp) using methanol (neutralized with 5 mM Tris-HCl, pH 7.0). In addition, fruit methanolic extracts were added with 1 volume of water and then phase partitioned with a volume of chloroform. The aqueous phase was re-extracted twice with chloroform and the pigments dried from the pooled chloroform phases. The HPLC method used to analyze and quantify phytoene, carotenoids, and chlorophylls has been detailed by Fraser et al. (2000). Identification of carotenoids was achieved by comparing retention times and spectral properties of authentic standards. Quantification was achieved from standard curves.

ACKNOWLEDGMENTS

We are grateful to Prof. Dr. C. Wilhelm and Dr. T. Jakob (Leipzig) and Dr. S. Lobréaux (Grenoble) for helpful discussions, and to J.P. Alcaraz (Grenoble) for expert technical assistance. M.S. was supported by the Iranian Ministry of Science, Research, and Technology (Ph.D. scholarship).

Received July 26, 2007; accepted September 10, 2007; published September 14, 2007.

LITERATURE CITED

Aluru MR, Stessman DJ, Spalding MH, Rodermel SR (2007) Alterations in photosynthesis in Arabidopsis lacking IMMUTANS, a chloroplast terminal oxidase. Photosynth Res **91:** 11–23

Aluru MR, Yu F, Fu A, Rodermel S (2006) Arabidopsis variegation mutants: new insights into chloroplast biogenesis. J Exp Bot **57:** 1871–1881

Baena-Gonzalez E, Allahverdiyeva Y, Svab Z, Maliga P, Josse EM, Kuntz M, Maenpaa P, Aro EM (2003) Deletion of the tobacco plastid psbA gene triggers an upregulation of the thylakoid-associated NAD(P)H dehydrogenase complex and the plastid terminal oxidase (PTOX). Plant J **35:** 704–716

Baerr JN, Thomas JD, Taylor BG, Rodermel SR, Gray GR (2005) Differential photosynthetic compensatory mechanisms exist in the immutans mutant of *Arabidopsis thaliana*. Physiol Plant **124:** 390–402

Barr J, White WS, Chen L, Bae CH, Rodermel S (2004) The GHOST terminal oxidase regulates developmental programming in tomato fruit. Plant Cell Environ **27:** 840–852

Berthold DA, Stenmark P (2003) Membrane-bound diiron carboxylate proteins. Annu Rev Plant Biol **54:** 497–517

Carol P, Kuntz M (2001) A plastid terminal oxidase comes to light: implications for carotenoid biosynthesis and chlororespiration. Trends Plant Sci **6:** 31–36

Carol P, Stevenson D, Bisanz C, Breittenbach J, Sandmann G, Mache R, Coupland G, Kuntz M (1999) Mutations in the Arabidopsis gene IMMUTANS cause a variegated phenotype by inactivating a chloroplast terminal oxidase associated with phytoene desaturation. Plant Cell **11:** 57–68

Cournac L, Latouche G, Cerovic Z, Redding K, Ravenel J, Peltier G (2002) In vivo interactions between photosynthesis, mitorespiration, and chlororespiration in *Chlamydomonas reinhardtii*. Plant Physiol **129:** 1921–1928

Cournac L, Redding K, Ravenel J, Rumeau D, Josse EM, Kuntz M, Peltier G (2000) Electron flow between photosystem II and oxygen in chloroplasts of photosystem I-deficient algae is mediated by a quinol oxidase involved in chlororespiration. J Biol Chem **275:** 17256–17262

Ducruet JM (2003) Chlorophyll thermoluminescence of leaf discs: simple instruments and progress in signal interpretation open the way to new ecophysiological indicators. J Exp Bot **54:** 2419–2430

Fraser PD, Pinto ME, Holloway DE, Bramley PM (2000) Technical advance: application of high-performance liquid chromatography with photodiode array detection to the metabolic profiling of plant isoprenoids. Plant J **24:** 551–558

Gilbert M, Wagner H, Weingart I, Skotnica J, Nieber K, Tauer G, Bergmann F, Fischer H, Wilhelm C (2004) A new type of thermoluminometer: a highly sensitive tool in applied photosynthesis research and plant stress physiology. J Plant Physiol **161:** 641–651

Haldimann P, Strasser RJ (1999) Effects of anaerobiosis as probed by the polyphasic chlorophyll a fluorescence rise kinetic in pea (*Pisum sativum* L.). Photosynth Res **62:** 67–83

Hegedüs A, Erdei S, Janda T, Tóth E, Horváth G, Dudits D (2004) Transgenic tobacco plants overproducing alfalfa aldose/aldehyde reductase show higher tolerance to low temperature and cadmium stress. Plant Sci **166:** 1329–1333

Hodges DM, DeLong JM, Forney CF, Prange RK (1999) Improving the thiobarbituric acid-reactive-substances assay for estimating lipid peroxidation in plant tissues containing anthocyanin and other interfering compounds. Planta **207:** 604–611

Hurkman WJ, Tanaka CK (1986) Solubilization of plant membrane proteins for analysis by two-dimensional gel electrophoresis. Plant Physiol **81:** 802–806

Joet T, Genty B, Josse EM, Kuntz M, Cournac L, Peltier G (2002) Involvement of a plastid terminal oxidase in plastoquinone oxidation as evidenced by expression of the *Arabidopsis thaliana* enzyme in tobacco. J Biol Chem **277:** 31623–31630

Josse EM, Alcaraz JP, Laboure AM, Kuntz M (2003) In vitro characterization of a plastid terminal oxidase (PTOX). Eur J Biochem **270:** 3787–3794

Josse EM, Simkin AJ, Gaffe J, Laboure AM, Kuntz M, Carol P (2000) A plastid terminal oxidase associated with carotenoid desaturation during chromoplast differentiation. Plant Physiol **123:** 1427–1436

Khorobrykh SA, Ivanov BN (2002) Oxygen reduction in a plastoquinone pool of isolated pea thylakoids. Photosynth Res **71:** 209–219

Kramer D, Johnson G, Kiirats O, Edwards G (2004) New fluorescence parameters for the determination of Q_A redox state and excitation energy fluxes. Photosynth Res **79:** 209–218

Kuntz M (2004) Plastid terminal oxidase and its biological significance. Planta **218:** 896–899

Lennon AM, Prommeenate P, Nixon PJ (2003) Location, expression and orientation of the putative chlororespiratory enzymes, Ndh and IMMUTANS, in higher-plant plastids. Planta **218:** 254–260

Mayer MP, Beyer P, Kleinig H (1990) Quinone compounds are able to replace molecular oxygen as terminal electron acceptor in phytoene desaturation in chromoplasts of *Narcissus pseudonarcissus* L. Eur J Biochem **191:** 359–363

Morstadt L, Graber P, De Pascalis L, Kleinig H, Speth V, Beyer P (2002) Chemiosmotic ATP synthesis in photosynthetically inactive chromoplasts from *Narcissus pseudonarcissus* L. linked to a redox pathway potentially also involved in carotene desaturation. Planta **215:** 134–140

Nievelstein V, Vanderkerckhove J, Tadros MH, von Lintig J, Nitschke W, Beyer P (1995) Carotene desaturation is linked to a redox pathway in *Narcissus pseudonarcissus* chromoplast membranes. Involvement of a 23 kDa oxygen evolving complex like protein. Eur J Biochem **233:** 864–872

Norris SR, Barrette TR, DellaPenna D (1995) Genetic dissection of carotenoid synthesis in *Arabidopsis* defines plastoquinone as an essential component of phytoene desaturation. Plant Cell **7:** 2139–2149

Ögren E (1991) Prediction of photoinhibition of photosynthesis from measurements of fluorescence quenching components. Planta **184:** 538–544

Olsson M, Nilsson K, Liljenberg C, Hendry GAF (1996) Drought stress in seedlings: lipid metabolism and lipid peroxidation during recovery from drought in *Lotus comiculatrus* and *Cerastium fontanum*. Physiol Plant **96:** 577–584

Ort DR, Baker NR (2002) A photoprotective role for O_2 as an alternative electron sink in photosynthesis. Curr Opin Plant Biol **5:** 193–198

Peltier G, Cournac L (2002) Chlororespiration. Annu Rev Plant Biol **53:** 523–550

Quiles MJ (2006) Stimulation of chlororespiration by heat and high light intensity in oat plants. Plant Cell Environ **29:** 1463–1470

Rizhsky L, Hallak-Herr E, Van Breusegem F, Rachmilevitch S, Barr JE, Rodermel S, Inze D, Mittler R (2002) Double antisense plants lacking ascorbate peroxidase and catalase are less sensitive to oxidative stress than single antisense plants lacking ascorbate peroxidase or catalase. Plant J **32:** 329–342

Rodermel S (2001) Pathways of plastid-to-nucleus signaling. Trends Plant Sci **6:** 471–478

Rosso D, Ivanov AG, Fu A, Geisler-Lee J, Hendrickson L, Geisler M, Stewart G, Krol M, Hurry V, Rodermel SR, et al (2006) IMMUTANS does not act as a stress-induced safety valve in the protection of the photosynthetic apparatus of Arabidopsis during steady-state photosynthesis. Plant Physiol **142:** 574–585

Rumeau D, Peltier G, Cournac L (2007) Chlororespiration and cyclic electron flow around PSI during photosynthesis and plant stress response. Plant Cell Environ **30:** 1041–1051

Sairam RK, Srivastava GC (2001) Water stress tolerance of wheat (*Triticum aestivum* L.): variations in hydrogen peroxide accumulation and antioxidant activity in tolerant and susceptible genotypes. J Agron Crop Sci **186:** 63–70

Schansker G, Tóth SZ, Strasser RJ (2005) Methylviologen and dibromothymoquinone treatments of pea leaves reveal the role of photosystem I in the Chl a fluorescence rise OJIP. Biochim Biophys Acta **1706:** 250–261

Schreiber U (2004) Pulse-amplitude-modulation (PAM) fluorometry and saturation pulse method: an overview. *In* C Papageorgiou, Govindjee, eds, Chlorophyll *a* Fluorescence: A Signature of Photosynthesis. Springer, Dordrecht, The Netherlands, pp 217–319

Schreiber U, Neubauer C, Klughammer C (1989) Devices and methods for room-temperature fluorescence analysis. Philos Trans R Soc Lond B Biol Sci **323:** 241–251

Shikanai T (2007) Cyclic electron transport around photosystem I: genetic approaches. Annu Rev Plant Biol **58:** 199–217

Simkin AJ, Laboure AM, Kuntz M, Sandmann G (2003) Comparison of carotenoid content, gene expression and enzyme levels on tomato (*Lycopersicon esculentum* L) leaves. Z Naturforsch [C] **58c:** 371–380

Strasser RJ, Tsimilli-Michael M, Srivastava A (2004) Analysis of the chlorophyll *a* fluorescence transient. *In* C Papageorgiou, Govindjee, eds, Chlorophyll *a* Fluorescence: A Signature of Photosynthesis. Springer, Dordrecht, The Netherlands, pp 321–362

Streb P, Josse EM, Gallouet E, Baptist F, Kuntz M, Cornic G (2005) Evidence for alternative electron sinks to photosynthetic carbon assimilation in the high mountain plant species *Ranunculus glacialis*. Plant Cell Environ **28:** 1123–1135

Vavilin DV, Ducruet JM (1998) The origin of 115–130°C thermoluminescence bands in chlorophyll-containing material. Photochem Photobiol **68:** 191–198

Vavilin DV, Ducruet JM, Matorin DN, Venediktov PS, Rubin AB (1998) Membrane lipid peroxidation, cell viability and photosystem II activity in the green alga *Chlorella pyrenoidosa* subjected to various stress conditions. J Photochem Photobiol B **42:** 233–239

Wu DY, Wright DA, Wetzel C, Voytas DF, Rodermel S (1999) The immutans variegated locus of *Arabidopsis* defines a mitochondrial alternative oxidase homolog that functions during early chloroplast biogenesis. Plant Cell **11:** 43–55

Résumé : L'oxydase terminale plastidiale (PTOX) est une plastoquinol oxidase. Le mutant *ghost* de tomate, déficient en PTOX, présente un phénotype de feuilles panachées et accumule du phytoène (dans ses secteurs blancs) et montre un déficit en caroténoïdes dans les fruits mûrs. Pour élucider les différents rôles de PTOX, qui ont en commun la modulation de l'état redox de plastoquinones, nous avons utilisé différentes conditions expérimentales. Nous avons montré que l'importance du rôle de PTOX dans la désaturation des caroténoïdes, en tant que cofacteur redox, se limite à certaines étapes développementales comme la différentiation des chloroplastes et des chromoplastes. En effet, en faible lumière, *ghost* peut produire des feuilles adultes et des fruits verts, qui contiennent la même quantité des caroténoïdes que celle de la tomate non-déficiente en PTOX, et qui n'accumulent pas de phytoène. D'autre part, nous avons constaté que des plantes de tomates transgéniques surexprimant PTOX ne surproduisent pas les carotenoides. Tandis que la surexpression de PTOX a un effet minimal sur la photosynthèse, les feuilles et les fruits verts de *ghost* sont moins capables d'éviter des dommages oxydatifs et sont plus sensibles à la photoinhibition et aux dommages de PSII. Cette sensibilité vient d'un niveau élevé de surréduction non-photochimique des plastoquinones à l'obscurité et d'un état réduit plus important de la chaîne de transfert d'électrons photosynthétiques à la lumière. Ainsi, PTOX joue un rôle indispensable et direct dans la photosynthèse, notamment sur l'état redox du pool des plastoquinones entre PSII et PSI. Nous proposons que PTOX a un rôle régulateur dans la distribution des électrons photosynthétiques entre flux linéaire et circulaire, plutôt qu'un rôle de puits d'électrons, et que sa présence est importante dans la transition de l'obscurité à la lumière ainsi que de la faible lumière à la forte lumière.

Mots-clés : caroténoïdes, développement de fruit, électron transfert photosynthétique, plastoquinone, état redox, stress lumineux.

Abstract: The plastid terminal oxidase (PTOX) is a plastoquinol oxidase whose absence in tomato results in the *ghost* (*gh*) phenotype characterized by variegated leaves (with bleached sectors accumulating phytoene) and by a carotenoid deficient ripe fruit. In order to elucidate the different roles of PTOX which have in common the modulation of plastoquinone redox states, various experimental conditions were applied. PTOX function in carotenoid biosynthesis, as a cofactor for phytoene desaturation, is essentially important at some developmental stage such as plastid de-etiolation or chromoplast differentiation. However, in low light, *gh* can produce adult green leaves and fruits containing similar carotenoids contents than in WT, without phytoene accumulation. Over-expression of an *Arabidopsis* PTOX cDNA in tomato did not lead to carotenoid over-production. While PTOX overproduction has minimal effects on photosynthesis, PTOX deficient green leaves and fruits have a reduced potential to prevent oxidative damage, as well as a higher PSII sensitivity to photoinhibition and damage. The absence of PTOX renders the tomato leaf photosynthetic apparatus more sensitive to light due to a nonphotochemical overreduction of plastoquinones in dark and high reduction state of the electron transport chain under steady state illumination. Thus, PTOX has an indispensable and direct role in photosynthesis, namely its influence on the redox status of the plastoquinone pool between PSII and PSI. Rather than contributing to an electron sink, PTOX has a global regulatory role in the distribution of electrons to different linear and alternative electron pathways, which is particularly important during dark to light and low light to high light transitions.

Keywords: carotenoid, fruit development, photosynthetic electron transport, plastoquinone, redox state, photostress.